An investigation into the anti-hypertensive effects of Green Rooibos Tea Extract (GRT)

by

Mignon van Vuuren

Dissertation presented for the degree of Doctor of Philosophy (Medical Physiology)
in the Faculty of Medicine and Health Sciences
at Stellenbosch University

Supervisor: Prof Barbara Huisamen

Co-Supervisors: Dr Shantal Windvogel and Prof Daneel Dietrich

April 2019

DECLARATION

By submitting this dissertation electronically, I declare that the entirety of the work contained therein is my own, original work, that I am the sole author thereof (save to the extent explicitly otherwise stated), that reproduction and publication thereof by Stellenbosch University will not infringe any third-party rights and that I have not previously in its entirety or in part submitted it for obtaining any qualification.

Signature:

Date: **March 2018**

ABSTRACT

Introduction and Aims: Obesity is defined as a primary cause of insulin resistance, hypertension and cardiovascular diseases. Rooibos (*Aspalathus linearis*), an indigenous South African herbal plant, presents with two unique polyphenolic compounds i.e. aspalathin and aspalalinin, which are associated with anti-obesity, anti-diabetic, anti-hypertensive and a lower risk for developing cardiovascular diseases. Green “unfermented” rooibos is dried directly after harvesting thereby preserving its polyphenolic compounds. Afriplex GRT™ is an aspalathin-rich spray-dried powder prepared from green rooibos under Good Manufacturing Practice (GMP) standards, thus ensuring high quality products. To date, the potential anti-hypertensive abilities of Afriplex GRT™ have not yet been investigated. We aimed to (i) monitor blood pressure changes in animals on a high fat diet (HFD) and determine whether the Afriplex GRT™ extract modulates diet-induced blood pressure changes within 6 weeks and (ii) elucidate mechanisms responsible for any changes induced by Afriplex GRT™.

Methods: *In vivo* model: Adult male Wistar rats were randomly divided into a control (n=40) and HFD group (n=48) which respectively received rat chow and HFD food for 16 weeks. The HFD was specifically developed to induce obesity, insulin resistance and hypertension. After 10 weeks, 20 rats of each group received aspalathin-rich Afriplex GRT™ (60 mg/kg/day) and 8 HFD animals received Captopril (positive control for blood pressure lowering effects of Afriplex GRT™) (50 mg/kg/day) for the last 6 weeks of the 16-week diet regimen. Food and water intake, body weight, intraperitoneal fat (IP-fat), liver weight, insulin sensitivity, blood pressure and urine parameters were determined**. *Ex vivo* model:** Vascular reactivity (contraction and relaxation of aorta with perivascular adipose tissue (PVAT)) were determined using phenylephrine, acetylcholine and sodium nitroprusside respectively. Expression and activation of enzymes in the nitric oxide (NO)- synthesis pathway such as AMPK, eNOS and PKB was determined by Western blotting using aortas with PVAT. Serum was collected at sacrifice for determination leptin, adiponectin and endothelin-1 (ET-1). ***In vitro* model:** Aortic endothelial cells (AECs) were cultured to determine the effect of Afriplex GRT™ on cellular apoptosis, cellular metabolic activity and NO production. Angiotensin converting enzyme (ACE)-inhibitor activity was determined using a Fluorescence resonance energy transfer (FRET) assay in AECs in response to treatment with Afriplex GRT™ extract or with non-fasting serum (collected previously from the experimental animals).

Results: HFD (vs control) animals presented with increased: food intake ($p<0.0001$), bodyweight ($p<0.0001$), IP-fat accumulation ($p<0.0001$); liver weight ($p<0.0001$), leptin levels ($p<0.01$), adiponectin levels ($p<0.01$) and decreased glucose clearance ($p<0.0001$). Treatment with Afriplex GRT™ attenuated food intake ($p<0.01$), body weight ($p<0.0001$) liver weight ($p<0.05$)

and increased glucose clearance ($p<0.001$). Furthermore, the HFD (vs control) reduced water intake ($p<0.0001$), urine excretion ($p<0.05$), vascular contraction ($p<0.05$), vascular relaxation ($p<0.0001$), and increased systolic ($p<0.001$) and diastolic ($p<0.001$) blood pressure; whereas treatment with Afriplex GRT™ reduced water intake ($p<0.05$), improved vascular relaxation ($p<0.001$), decreased systolic ($p=0.0348$) and diastolic ($p=0.0434$) blood pressure and interestingly, increased glucose excretion via the urine. In addition the HFD downregulated AMPK expression ($p<0.0001$), increased AMPK activation according to the AMPK phosphorylated(P):total(T) ratio ($p<0.001$), increased eNOS expression ($p<0.01$), decreased eNOS activation according to the P:T ratio ($p<0.01$), and lastly decreased PKB activation ($p<0.05$). Treatment with Afriplex GRT™ increased AMPK phosphorylation ($p<0.05$) as well as PKB expression ($p<0.05$) and phosphorylation ($p<0.05$). Afriplex GRT™ treatment did not result in cellular apoptosis, NO production or ACE inhibition according to *in vitro* studies, however cellular metabolic activity was increased at a high Afriplex GRT™ concentration ($p<0.001$).

Conclusion: Treatment with Afriplex GRT™ in this animal model was closely associated with anti-obesogenic, anti-diabetic and anti-hypertensive effects and improved vascular function. Increased glucose excretion via the urine is indicative of sodium-glucose co-transporter (SGLT2) inhibition and we therefore conclude that the associated health benefits of Afriplex GRT™ can amongst other, be ascribed to SGLT2 inhibition.

OPSOMMING

Inleiding en doelwitte: Vetsug word beskou as ‘n primêre oorsaak van insulienweerstandigheid, hipertensie en kardiovaskulêre siektes. Rooibos (*Aspalathus linearis*) is ‘n inheemse Suid-Afrikaanse kruieplant en bevat twee unieke polifenoliese komponente, naamlik aspalatien en aspalalinien. Hierdie twee komponente word hoofsaaklik geassosieer met rooibos se anti-vetsug, anti-diabetiese, anti-hipertensiewe en verlaagde risiko vir die ontwikkeling van kardiovaskulêre siektes. Groen ongefermenteerde rooibos word dadelik gedroog nadat dit geoes is, wat gevolglik die polifenoliese komponente van hierdie rooibos bewaar. Afriplex GRT™ is ‘n aspalatien-ryke gedroogde poeier ekstrak afkomstig vanaf groen rooibos en voorberei onder Goeie Vervaardigingspraktyk (GMP) standaarde wat goeie produksgehalte verseker. Tot op hede is hierdie ekstrak nog nie ondersoek vir moontlike anti-hipertensiewe potensiaal nie. Die doel van hierdie navorsing was om (i) die bloeddruk veranderinge in hoë vet dieet (HFD) diere te monitor en ook te bepaal of behandeling met Afriplex GRT™ dieet-geïnduseerde bloeddruk veranderinge binne 6 weke kan reguleer en (ii) die meganismes wat verantwoordelik is vir hierdie bloeddruk veranderinge te identifiseer.

Metodes: *In vivo* model: Volwasse manlike Wistar-rotte is lukraak verdeel in 'n kontrole (n = 40) en HFD groep (n = 48) wat onderskeidelik standaard rot kos en HFD-voedsel ontvang het. Die HFD is spesifiek ontwikkel om vetsug, insulienweerstandigheid en hipertensie te induseer. Na 10 weke het 20 rotte van elke groep aspalatien-ryke Afriplex GRT™ (60 mg/kg/dag) ontvang en 8 HFD-diere het Captopril (positiewe kontrole vir bloeddruk verlagende effekte van Afriplex GRT™) (50 mg/kg/dag) ontvang. Behandeling was toegedien vir die laaste 6 weke van die 16-week dieetprogram. Voedsel- en waterinname, liggaamsgewig, intraperitoneale vet (IP-vet), lewermassa, insulien sensitiwiteit, bloeddruk en urine parameters is bepaal. ***Ex vivo* model:** Vaskulêre reaktiwiteit (sametrekking en verslapping van die aorta met perivaskulêre vetweefsel (PVAT)) is bepaal deur gebruik te maak van fenielefrien, asetielkolien en natrium nitroprussied. Die uitdrukking en aktivering van proteïene wat betrokke is in die stikstofoksied (NO)-sintese padweg (AMPK, eNOS en PKB) is bepaal deur gebruik te maak van aortas met PVAT en Westerse klad tegnieke. Serum is versamel tydens opoffering van die diere en gebruik ter bepaling van leptien, adiponektien en endotelin-1 (ET-1) vlakke. ***In vitro* model:** Aorta endoteel-selle (AECs) is gekweek om die effek van Afriplex GRT™ op sellulêre apoptose, sellulêre metaboliese aktiwiteit en NO produksie te bepaal. Angiotensien-omskakelingsensiem (ACE)-inhibitor aktiwiteit is bepaal deur gebruik te maak van ‘n Fluorosensie resonansie energie oordrag (FRET) metode in AEC's wat behandel is met die Afriplex GRT™ of met nie-vastende serum wat voorheen versamel is vanaf die eksperimentele diere.

Resultate: HFD (vs. kontrole) diere het verhoogde voedselinname ($p<0.0001$), liggaamsgewig ($p<0.0001$), IP-vet ($p<0.0001$); lewermassa ($p<0.0001$), leptienvlakke ($p<0.01$), adiponektienvlakke ($p<0.01$) en verlaagde glukose-opruiming ($p<0.0001$) getoon; terwyl die behandeling met Afriplex GRT™ die voedselinname ($p<0.01$), liggaamsgewig ($p<0.0001$) en lewermassa ($p<0.05$) verlaag het asook glukose-opruiming ($p<0.001$) verhoog het. Verder het die HFD (vs kontrole) waterinname ($p<0.0001$), urienuitskeiding ($p<0.05$), vaskulêre kontraksie ($p<0.05$) en vaskulêre verslapping ($p<0.0001$) verlaag asook sistoliese ($p<0.001$) en diastoliese ($p <0.001$) bloeddruk verhoog. Behandeling met Afriplex GRT™ het waterinname ($p<0.05$) verder verlaag, vaskulêre verslapping verbeter ($p <0.001$), sistoliese ($p=0.0348$) en diastoliese ($p =0.0434$) bloeddruke verlaag asook glukose-uitskeiding in die urine verhoog. Daarbenewens het die HFD AMPK-uitdrukking ($p<0.0001$) afgereguleer, AMPK-aktivering volgens die AMPK gefosforileerde (P):totale (T) verhouding ($p<0.001$) verhoog, eNOS-uitdrukking ($p<0.01$) verhoog, eNOS-aktivering volgens die P:T-verhouding ($p<0.01$) verlaag, en laastens PKB-aktivering ($p<0.05$) verlaag. Behandeling met Afriplex GRT™ het AMPK-fosforilering ($p<0.05$) asook PKB-uitdrukking ($p<0.05$) en fosforilering ($p<0.05$) verhoog.
Afriplex GRT™ behandeling het nie tot sellulêre apoptose, NO produksie of ACE inhibisie volgens *in vitro* studies gelei nie, alhoewel die sellulêre metaboliese aktiwiteit verhoog het met die hoogste konsentrasie Afriplex GRT™ toediening ($p<0.001$).

Gevolgtrekking: Behandeling met Afriplex GRT™ in hierdie spesifieke HFD diere model was geassosieer met anti-vetsug, anti-diabetiese, anti-hipertensiewe effekte en verbeterde vaskulêre funksie. Verhoogde glukose uitskeiding via die urine is 'n aanduiding van natrium-glukose transporter (SGLT2) inhibisie. Ons lei dus af dat die gepaardgaande gesondheidsvoordele van Afriplex GRT™ gedeeltelik ook aan SGLT2-inhibisie toegeskryf kan word.

ACKNOWLEDGEMENTS

- Firstly, I would like to acknowledge the Division of Medical Physiology for the privilege to partake in this research project.

- To Professor Barbara Huisamen, I would like to express my sincerest appreciation for all the guidance, help, encouragement, advice and continuous support throughout my PhD. I am really honoured to have worked with her for the last 6 years.

- A special thanks to my co-supervisors, Dr Shantal Windvogel and Prof Daneel Dietrich for their guidance and advice throughout this study.

- I would like to thank all my colleagues in the Department of Medical Physiology, especially for Marlouw Engelbrecht, Zimvo Maqeda, Sybrand Smit, Clara Marincowitz and Marguerite Blignaut for their wonderful friendship, encouragement and assistance in the lab.

- Thank you to Dr John Lopes for his assistance with cell culture related work.

- A special thanks to Dr Carl Lombard of the Division of Epidemiology and Biostatistics, Stellenbosch University, for the statistical analyses of the blood pressure data.

- Thank you to the Harry Crossley Foundation, National Research Foundation, Medical Research Council and the University of Stellenbosch for funding throughout my PhD studies. Also, to the Medical Research Council for supplying the Afriplex GRT™.

- My sincere gratitude to all the staff members of the animal unit – it was an absolute pleasure working with you throughout this study.

- Thank you to my family and friends for their continuous support and love.

- Lastly, I would like to thank my Heavenly Father for giving me the ability to complete my PhD degree.

DISCLOSURE OF INTEREST

Signed on March 2019

at Tygerberg Campus.

……..…….. **……..……...**

(Prof. Barbara Huisamen) **(Mignon van Vuuren)**

TABLE OF CONTENTS

LIST OF FIGURES

LIST OF TABLES

LIST OF ABBREVIATIONS

(3-(4,5-dimethylthiazol-2-yl)-2,5-diphenyltetrazolium bromide	MTT
2,4-dinitrophenyl	Dnp
4E-binding protein 1	4EBP1
5-diaminofluorescein-2/diacetate	DAF-2/DA
6-phosphofructo-2-kinase	PFK-2
Acetylcholine	ACh
Adapter molecule crk	Crk
Adaptor protein 1	Nck
Adenosine diphosphate	ADP
Adenosine monophosphate	AMP
Adenosine triphosphate	ATP
Adenylyl cyclase	AC
Adipocyte-derived relaxing factor	ADRF
Advanced glycation endproduct	AGE
Akt substrate of 160 kDa	AS160
AMP-activated protein kinase	AMPK
Analysis of Variance	ANOVA
Angiotensin converting enzyme	ACE
Angiotensin II receptor type 1	AT1
Angiotensin II receptor type 2	AT2
Angiotensin receptor type 4	AT4
Anti-diuretic hormone	ADH
Aortic endothelial cells	AECs
Area under curve	AUC
Blank	Bs

Body Mass Index	BMI
Bovine Serum Albumin	BSA
Breakpoint-cluster region homology	BH
Ca^{2+}/CaM- dependent protein kinase II	CaMKII
Calcium calmodulin-dependent protein kinase kinase β	CAMKKβ
Calmodulin	CaM
Carboxyl	COOH
Casein kinase II	CK2
Casitas B-lineage Lymphoma	Cbl
Catalase	CAT
Catalytic/kinase	cat
Cbl associated protein	CAP
Colony stimulating factor	CSF
C-Src kinase	Csk
Cyanidin 3-glucoside	C3G
Cyclic guanosine monophosphate	cGMP
Cystathionine β-synthase	CBS
Diacylglycerol	DAG
Diaminofluorescein-2	DAF-2
Diethylamine NONOate diethylammonium salt	DEA/NO
Dimethyl sulfoxide	DMSO
DNA-activated protein kinase	DNA-PK
Endothelial cell growth medium	EGM
Endothelial surface layer	ESL
Endothelial-derived constricting factors	EDCF
Endothelin-1	ET-1

Endothelins	ET
Endothelium-derived hyperpolarizing factors	EDHF
Endothelial nitric oxide synthase	eNOS
Enzyme-linked immunosorbent assay	ELISA
Ethylene glycol-bis(β-aminoethylether)-N,N,N',N'-tetraacetic acid	EGTA
Ethylenediaminetetraacetic acid	EDTA
Extracellular signal-regulated kinases	ERK
Fatty acid translocase	FAT/CD36
Fetal Bovine Serum	FBS
Flavin adenine dinucleotide	FAD
Flavin mononucleotide	FMN
Fluorescence resonance energy transfer	FRET
Forkhead box protein O1	FOXO
Free fatty acids	FFAs
Fructose 2,6-bisphosphate	Fru-2,6-P2
G protein-coupled receptor	GPCR
Gastric inhibitory polypeptide	GIP
Glucagon-like peptide-1	GLP-1
Glucose oxidase	GOD
Glucose transporter 2	GLUT2
Glucose transporter 4	GLUT4
Glucose-6 phosphatase	G6Pase
Glucose-6-phosphate	G6P
Glucose-dependent insulinotropic polypeptide	GIP
Glutathione peroxidase	GPx
Glycogen synthase	GS

Glycogen synthase kinase 3β	GSK-3β
Good Manufacturing Practice	GMP
Grams	g
Green rooibos extract	GRE
Growth factor receptor-bound protein 2	Grb2
Hanks balanced salt solution	HBSS
Helical domain	HD
High fat diet	HFD
High-density lipoprotein	HDL
High-performance liquid chromatography	HPLC
Horse Radish Peroxidase	HRP
Hydrochloric acid	HCl
Hydrogen peroxide	H_2O_2
Hydroxyl radicals	OH·
Hypochlorite	ClO−
Iinositol 1,4,5-triphosphate	IP3
Inducible NOS	iNOS
Insulin degrading enzyme	IDE
Insulin receptor	IR
Insulin receptor substrates	IRS
Integrin-linked kinase	ILK
Interleukin-6	IL-6
Intra-peritoneal fat	IP-fat
Kilo Dalton	kDa
Kilograms	kg
Kinase regulatory loop binding	KRLB

Krebs Henseleit	KH
Liver kinase B1	LKB1
Long chain fatty acids	LCFA
Low-density lipoprotein	LDL
Low-density lipoprotein cholesterol	LDL-C
Mammalian target of rapamycin	mTOR
Matrix metalloproteinase	MMP
Messenger ribonucleic acid	mRNA
Meter	m
Microliter	µl
Milligram	mg
Millilitre	ml
Millimetre	mm
Millimetres of mercury	mm Hg
Minutes	min
Mitogen-activated protein kinase	MAPK
Mitogen-activated protein kinase	MEK
Monocyte chemoattractant protein-1	MCP-1
Neuronal NOS	nNOS
Nicotinamide adenine-dinucleotide phosphate	NADPH
Nitric oxide	NO
NO synthase	NOS
Non-alcoholic fatty liver disease	NAFLD
Non-specific binding	NSB
N-terminal adaptor-binding domain	ABD
Nuclear factor-κB	NF-κB

O-aminobenzoic acid	Abz
Optical density	OD
Oral glucose tolerance tests	OGTT
Oxidised LDL	oxLDL
Oxygen singlet	$^1O_2$
p70 ribosomal protein S6 kinase	p70S6K
Parent	P
Perivascular adipose tissue	PVAT
Peroxidise	POD
Peroxisome proliferator-activated receptor-gamma	PPAR-γ
Peroxynitrite	$ONOO^-$
PH-domain leucine-rich-repeat protein phosphatase	PHLPP
Phenylephrine	Phe
Phenylmethylsulfonyl Fluoride	PMSF
Phosphatase-2A	PP2A
Phosphate-buffered saline	PBS
Phosphatidylinositol-3,4,5-trisphosphate	PIP3
Phosphatidylinositol-4,5-bisphosphate	PIP2
Phosphofructokinase-1	PFK-1
Phosphoinositide 3-kinase	PI3K
Phosphoinositide-dependent kinase 1	PDK1
Phosphoinositide-dependent kinase 2	PDK2
Phospholipase Cγ	PLC
Phosphotyrosine-binding	PTB
Pituitary adenylate cyclase-activating polypeptide	PACAP
Pleckstrin homology domain	PH

Polyvinylidene fluoride	PVDF
Propidium iodide	PI
Prostacyclin	PGI2
Prostaglandin F2	PGF2
Protein kinase A	PKA
Protein Kinase B	PKB
Protein Kinase C	PKC
Proto-oncogene tyrosine-protein kinase Fyn	Fyn
Rapidly Accelerated Fibrosarcoma	Raf
Ras binding domain	RBD
Ras homologue enriched in brain	Rheb
Reactive nitrogen species	RNS
Reactive oxygen species	ROS
Receptor for advanced glycation endproducts	RAGE
Regulatory	reg
Renin-angiotensin system	RAS
Revolutions per minute	rpm
SH2-containing collagen-related proteins	SHC
SHC-transforming protein 1	Shc
Sodium chloride	NaCl
Sodium Fluoride	NaF
Sodium nitroprusside	SNP
Sodium orthovanadate	Na_3VO_4
Sodium-glucose co-transporter-2	SGLT2
Sodium-glucose co-transporter-1	SGLT1
Son of sevenless homolog 1	SOS

S-phase kinase-associated protein 2	SKP2
Src homology 2	SH2
Src Homology 3	SH3
Src-homology-2 domain-containing inositol phosphatase-2	SHIP2
Standard deviation	SD
Standard Error	SE
Sulfate–polyacrylamide gel electrophoresis	SDS-PAGE
Superoxide anions	O_2•-
Superoxide dismutase	SOD
Tensin homolog phosphatase	PTEN
Tetrahydrobiopterin	BH4
Tetramethylbenzidine	TMB
Thiobarbituric acid reactive substance	TBARS
Thromboxane A2	TXA2
Total activity	TA
Triazolofluorescein	DAF-2T
Tuberous sclerosis 1/2	TSC1/2
Tumour necrosis factor alpha	TNF-α
Tyrosine-protein phosphatase non-receptor type II	SHP2
Vascular adhesion molecule-1	VCAM-1
Vascular endothelial growth factor	VEGF
Vascular smooth muscle cells	VSMCs
Very low-density lipoprotein	VLDL
Volume pressure recording	VPR
von Willebrand factor	VWF
Weibel-Palade bodies	WPBs

World Health Organization	WHO
Zero standard	B0

CHAPTER 1: LITERATURE REVIEW

1.1. Introduction

Obesity is classified as a major health problem and is gradually affecting more individuals globally. According to 2016 data, the incidence of obesity more than tripled since the year 1975 ('WHO | Obesity and overweight', 2018). Obesity is a major risk factor for hypertension, insulin resistance, coronary disease, hyperlipidemia, heart failure (Strumpf, 2004; Bloomgarden, 2006), and endothelial dysfunction (Park and Park, 2015). Hypertension is considered to be a key risk factor for cardiovascular diseases, heart failure and stroke (Vasan et al., 2002; Chobanian et al., 2003; Duckitt and Harrington, 2005). Cardiovascular diseases are identified as the leading cause of deaths globally with more than 17.7 million deaths in the year 2015 (World Health Organization, 2017). Taken together, obesity is a complex disorder increasing the risk of several health problems and diseases, such as hypertension, diabetes and cardiovascular diseases.

The consumption of polyphenols have been linked to a reduction in the development of coronary heart disease (Arts and Hollman, 2005) and the incidence of cardiovascular disease related mortality (Mink *et al.*, 2007).

Rooibos (*Aspalathus linearis*), a well-known South African fynbos plant has several health promoting properties which initiate anti-hypertensive (Persson *et al.*, 2010), anti-diabetic (Muller *et al.*, 2012) and anti-atherosclerotic (Canda, Oguntibeju and Marnewick, 2014) effects. These health benefits can be ascribed to the rich phenolic compounds present in rooibos (Joubert and De Beer, 2011), such as aspalathin (Koeppen and Roux, 1965), aspalalinin (Shimamura *et al.*, 2006) and nothofagin (Hillis and Inoue, 1967). Once harvested, rooibos leaves are processed to fermented rooibos or unfermented rooibos. Fermented rooibos is associated with a substantial reduction in aspalathin content (Joubert, 1996) due to oxidation. The processing method of unfermented rooibos excludes oxidation, thus preserving its phenolic content (Schulz, Joubert and Schütze, 2003; Joubert and De Beer, 2011). Spray-dried powders prepared from fermented rooibos and unfermented rooibos are respectively known as fermented rooibos extract (FRE), and green rooibos extract (GRE).

In the current study, we used a Good Manufacturing Practice (GMP) laboratory standardized aspalathin-rich GRE, namely Afriplex GRT™. To date, no prior studies have been done to determine if there is an ameliorative relationship between Afriplex GRT™ and obesity-induced hypertension, which is the main reason for this research.

1.2. Insulin resistance

Insulin resistance, a pathological condition, refers to the inability of cells such as liver, muscle and fat cells to respond to the hormone insulin. Previously, obesity, particularly that associated with the presence of additional fat around the waist, has been described as the primary cause of insulin resistance, high blood pressure, imbalanced cholesterol and cardiovascular diseases. Development of these conditions are mainly ascribed to several hormones and adipokines which are produced in the stomach fat, and consequently secreted in to circulation (Hardy, Czech and Corvera, 2012).

1.2.1. Link between obesity and insulin resistance

Obesity is a clinical condition that refers to excessive fat accumulation (Garrow, 1988) leading to a state of abnormally high body weight compared to predetermined standardized anthropometric cut-off values. Obesity may be the consequence of the imbalance between energy intake and energy expenditure. To store the excess energy in the form of fat, the adipose tissue increase in size (hypertrophy) and in the number of cells (hyperplasia) (Goedecke, Jennings and Lambert, 2006). According to previous studies, a healthy diet can decrease adipocyte size, whereas the number of adipocytes remain constant during adulthood (Arner and Spalding, 2010).

Once fat cells are enlarged, they activate several macrophage-attracting chemokines, followed by the recruitment of macrophages. The macrophages in turn, secrete the cytokines interleukin-6 (IL-6) and tumour necrosis factor alpha (TNF-α), thereby inducing insulin resistance in the mature adipocytes (Skurk *et al.*, 2007; Hammarstedt, Graham and Kahn, 2012; Lee, 2013). The insulin resistant adipocytes form a vicious loop by increasing the release of free fatty acids (FFAs), followed by additional macrophage activation (Smith, 2002; Virtue and Vidal-Puig, 2010) ***(Figure 1.1).***

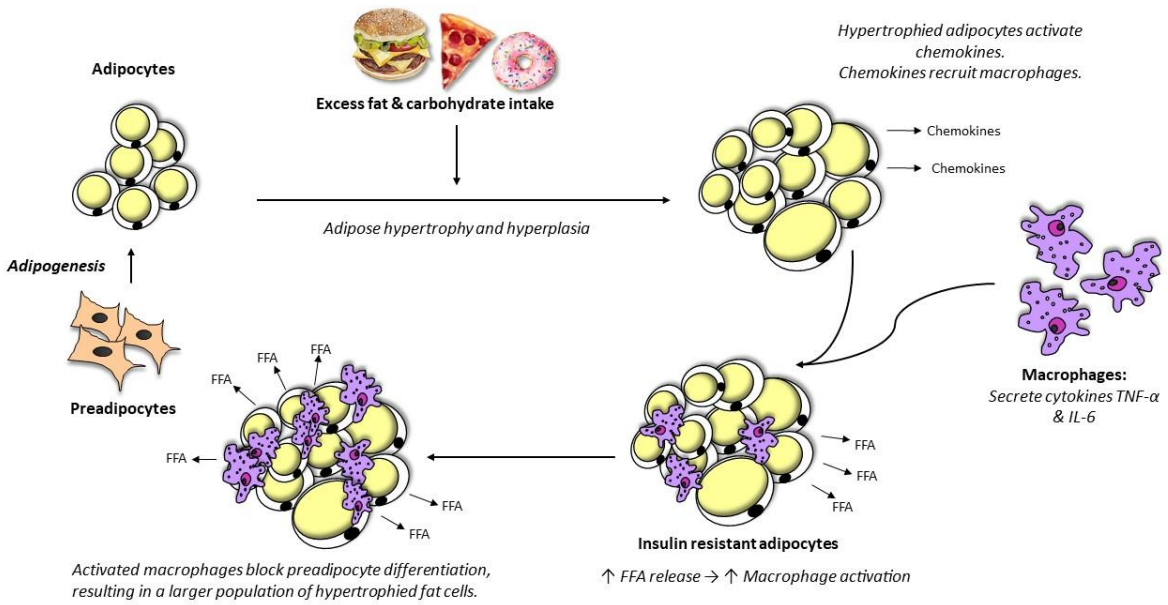

Figure 1.1: *Adipocyte differentiation. Image adapted from (Virtue and Vidal-Puig, 2010) and composed using Microsoft PowerPoint.*

The World Health Organization (WHO) stated that a Body Mass Index (BMI) greater than or equal to 25, is considered as overweight and a BMI greater than or equal to 30, is considered as obese (WHO:Global Database on Body Mass Index, 2018). The BMI is calculated according to the following equation: a person's weight in kilograms (kg), divided by the square of the individual's height in meters (m) (WHO:Global Database on Body Mass Index, 2018).

According to the WHO (2016), the incidence of obesity more than tripled since the year 1975. In 2016, the number of overweight adults, aged 18 years and older, totalled more than 1.9 billion (39 %), with 650 million of these adults classified as obese. Overall, women were more likely to be overweight and obese when compared to men ('WHO | Obesity and overweight', 2018).
Given that the incidence of individuals classified as obese, is still markedly increasing, it can therefore be classified as a global epidemic.

1.2.2. Obesity in South Africa

South Africa is a country undergoing epidemiological transition, involving both dietary and physical activity changes. Dietary changes refer to the shift from undernutrition and malnutrition to overnutrition, and from traditional diets to more energy-dense diets, whereas changes in physical activity refers to the shift from high occupation-and transport-based activity to a sedentary lifestyle (Broyles *et al.*, 2015). As a result, these individuals are more likely to develop obesity and consequently also become more prone to develop metabolic related diseases (Goedecke,

Jennings and Lambert, 2006). According to Baleta and Mitchell (2014), South Africa has the highest obesity rate in sub-Saharan Africa. In 2014, 40 % of South African men and 70 % of South African women were either overweight or obese (Baleta and Mitchell, 2014).

1.2.3. Link between obesity, insulin resistance and the metabolic syndrome

Obesity is associated with enhanced lipolytic activity within the visceral fat cells. As a result, insulin resistance develops due to high quantities of non-esterified fatty acids, glycerol, pro-inflammatory cytokines and hormones which are released from these adipocytes into the portal (hepatic insulin resistance) and systemic (muscle insulin resistance) circulation (DeFronzo, 2004; Kahn, Hull and Utzschneider, 2006).

During insulin resistance, the myocytes, adipocytes and hepatocytes are unresponsive to the hormone, insulin, and therefore glucose is unable to enter these cells as easily. Consequently, the pancreatic β-cells sense the high circulating glucose levels and compensate by releasing more insulin into circulation. Due to the increased demand on the pancreas and the high FFA levels present, β-cell failure in the pancreas develops, resulting in decreased insulin secretion, increased glucose levels and consequently type II diabetes (Kahn, Hull and Utzschneider, 2006).

The elevated FFAs are furthermore also responsible for the downregulation of high-density lipoproteins (HDL) and the increase in triglyceride levels (Borggreve, de Vries and Dullaart, 2003). Together, these changes act as precursors for the development of several cardiovascular diseases including: ischemic heart disease, atherosclerosis, and stroke (Diabetes, Heart Disease, and Stroke | NIDDK, 2017).

The metabolic syndrome develops due to a cluster of conditions. These conditions include: obesity, dyslipidemia, insulin resistance and hypertension which is in turn, associated with the development of non-alcoholic fatty liver disease (NAFLD), thrombosis, reproductive disorders and atherosclerosis. Of all these conditions, insulin resistance and obesity seem to be central to the development of metabolic syndrome, and would therefore be the target in treating or preventing the metabolic syndrome (Cornier et al., 2008). Furthermore, individuals diagnosed with the metabolic syndrome are more susceptible to develop type II diabetes and cardiovascular diseases (Cornier et al., 2008), than those without the metabolic syndrome.

Recently, a new theory on obesity and weight reduction, namely the carbohydrate-insulin model was proposed. Ludwig and Ebbeling (2018) reported that the consumption of processed high-glycemic load carbohydrates results in hormonal changes (increased insulin secretion (Brotman,

2002), which in turn increases calorie deposition in the adipose tissue, decreases energy expenditure and aggravates hunger, therefore obesity. Long term calorie restriction was also shown to be unsuccessful in treating obesity, since the energy balance theory was inadequate. According to Ludwig and Ebbeling (2018), the consumption of a low-glycemic load diet might be a practical and more sufficient alternative when compared to the conventional focus on calorie restriction and dietary fat (Ludwig and Ebbeling, 2018) .

1.3. Insulin

1.3.1. Synthesis and structure of insulin

The synthesis and the progression of pre-proinsulin to insulin occurs within the β-cells of the pancreatic islets of Langerhans (Wilcox, 2005).

Pre-proinsulin is the first precursor in the formation of insulin. This insulin-like structure containing a signal peptide, A-chain, B-chain and a C-peptide, is synthesised from mRNA present in the rough endoplasmic reticulum. Once the signal peptide from pre-proinsulin is cleaved in the endoplasmic reticulum, proinsulin is formed. Proinsulin is then transported via the secretory vesicles to the Golgi apparatus, where type I and type II endoproteases cleave the C-peptide, thus generating mature insulin and a free C-peptide. The secretion rate of insulin and free C-peptides via exocytosis are believed to be equivalent (Wilcox, 2005).

Insulin is a dipeptide, containing two chains, referred to as chain A (21 amino acids) and chain B (30 amino acids). These chains are linked by two disulphide bridges, resulting in the connection of the N-and C-terminal helices of chain A, to the central helix of chain B (Wilcox, 2005) ***(Figure 1.2).***

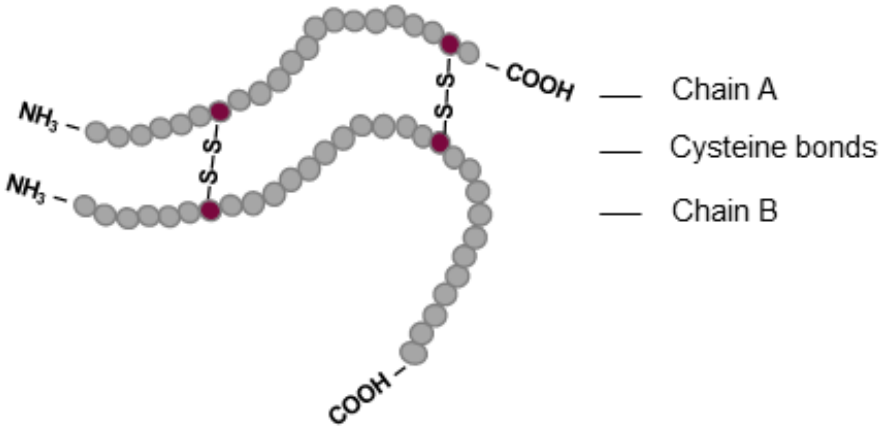

Figure 1.2: *Insulin structure. Image adapted from (Weiss, Steiner and Philipson, 2000) and composed using Microsoft PowerPoint.*

1.3.2. Insulin secretion and mechanism

Glucose is the main factor influencing the biosynthesis and the secretion of insulin (Wilcox, 2005); however, several other factors can also influence insulin release. These factors include: amino acids, pituitary adenylate cyclase-activating polypeptide (PACAP), fatty acids, glucose-dependent insulinotropic polypeptide (GIP), acetylcholine (ACh), glucagon-like peptide-1 (GLP-1), and many other agonists (Bratanova-Tochkova *et al.*, 2002).

Once glucose enters the β-cells via the Glucose transporter 2 (GLUT2), it is phosphorylated by the glucokinase enzyme, consequently generating glucose-6-phosphate (G6P) which is in turn metabolized to adenosine triphosphate (ATP) (De Lonlay and Saudubray, 2012). An increase in the ATP: adenosine diphosphate (ADP) ratio results in the closure of potassium (K^+)- ATP-dependent channels subsequently triggering membrane depolarization together with voltage-dependent calcium channel activation (Soria *et al.*, 2004). Consequently, intracellular calcium causes the activation of insulin containing vesicles, and stored insulin is released into circulation via exocytosis. The release of insulin in response to glucose is augmented by both the K^+- ATP-independent calcium- independent pathway as well as the K^+- ATP-independent calcium-dependent pathway (Bratanova-Tochkova *et al.*, 2002).

The first phase of insulin secretion in response to increased glucose levels is rapid, whereas over time the secretion becomes less intense, but more sustained (second phase) (Bratanova-Tochkova *et al.*, 2002). In addition, it is thought that other mediators might also be responsible for

the second phase of insulin secretion. These mediators include: phospholipases, protein kinase C (PKC), adenylyl cyclase (AC) and protein kinase A (PKA), which are all activated by intestinal hormones (Bratanova-Tochkova *et al.*, 2002).

The insulin receptor (IR) is a well-known tyrosine kinase receptor located on the surface of the cell membrane. It is comprised of two extracellular α-subunits, which are linked by disulphide bonds, to two transmembrane β-subunits (Kido, Nakae and Accili, 2001; Yanagita *et al.*, 2013) ***(Figure 1.3).***

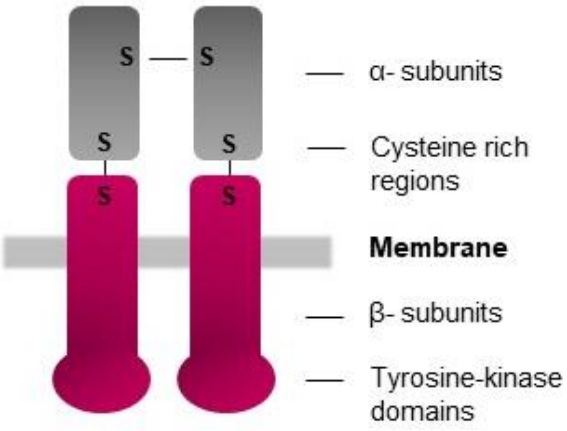

Figure 1.3: *The insulin receptor. Image adapted from (Horton et al., 2006) and composed using Microsoft PowerPoint.*

Once the insulin molecules are in circulation, it binds to the extracellular α-subunits causing autophosphorylation of the intracellular β-subunits (tyrosine residues) (Wolever, 1990). Since proteins containing phosphotyrosine-binding (PTB) and Src homology 2 (SH2) domains are able to identify these phosphorylated tyrosine residues, they are rapidly recruited, and phosphorylated (Yanagita *et al.*, 2013). Previous studies indicated that insulin receptor substrates (IRS), specifically IRS1 and IRS2, as well as SH2-containing collagen-related proteins (SHC), are the two proteins which are most likely to be recruited to the IR (Wada *et al.*, 2005; van der Heide, Ramakers and Smidt, 2006).

Once recruited, these scaffold proteins will be phosphorylated, consequently initiating further cellular actions via the stimulation of the following two parallel downstream signal transduction pathways: phosphoinositide 3-kinase (PI3K) pathway and the mitogen-activated protein kinase (MAPK) pathway (Wada *et al.*, 2005; van der Heide, Ramakers and Smidt, 2006). The PI3K pathway is activated via IRS, whereas the Ras-MAPK pathway is activated via SHC (Godsland, 2009).

In the next section, the four identified IRS proteins and their role in insulin signalling and basic cellular functions, will only be briefly described as it is not the main focus of the thesis.

(a) IRS1

IRS1 is an adaptor protein responsible for the modulation of normal growth, survival, differentiation and metabolism (Dearth *et al.*, 2007). This protein contains 21 tyrosine phosphorylation sites located in amino acid sequence motifs. Therefore, when IRS1 is activated in response to insulin stimulation, it acts as a docking site to bind and phosphorylate SH2 domain proteins (White, 1997). The most well-known SH2 domain protein is the p85 regulatory subunit of PI3K. Other SH2 proteins include: growth factor receptor-bound protein 2 (Grb2), C-Src kinase (Csk), adapter molecule crk (Crk), tyrosine-protein phosphatase non-receptor type II (SHP2), proto-oncogene tyrosine-protein kinase Fyn (Fyn), phospholipase Cγ (PLC), and adaptor protein 1 (Nck) (White, 1997; Mardilovich, Pankratz and Shaw, 2009).

It was previously highlighted that IRS1 has 30 Ser/Thr phosphorylation sites in motifs. These motifs are recognized by the following kinases: Protein Kinase B (PKB), PKC, MAPK and casein kinase II (CK2) (Sun *et al.*, 1991; White, 1997).

When insulin binds to the IR, IRS1 serves as the main docking protein for the phosphorylation/activation of PI3K, consequently increasing glucose uptake in the cell (Rondinone *et al.*, 1997). Furthermore, previous studies using human and mouse samples (muscle and adipose), found that IRS1 can also mediate metabolic as well as mitogenic effects in response to insulin (Sesti *et al.*, 2001). It was furthermore discovered that when IRS1 expression was supressed in mice, insulin secretion from pancreatic β-cells were insufficient to decrease raised glucose levels (Kulkarni *et al.*, 1999).

(b) IRS2

The IRS2 and IRS1 proteins are functionally and structurally similar, although IRS2 is more pronounced in the liver and IRS1 in the skeletal muscle (Sun *et al.*, 1995; Kido, Nakae and Accili, 2001). In size, the IRS2 protein is bigger (100 residues) than IRS1 with similarity in the protein sequences (43 %), PTB domain (75 %) and the Pleckstrin homology domain (PH) (65 %) (Sun *et al.*, 1995). The PH domain allows binding of phosphatidylinositol lipids within biological membranes. One major difference between the IRS1 and IRS2 protein is the unique middle region present in IRS2. This region gives IRS2 the ability to specifically bind to the kinase regulatory loop

binding (KRLB) domain of the intracellular IR β-subunit (Sawka-Verhelle *et al.*, 1996), thereby mediating the peripheral actions of insulin and the growth of pancreatic β-cells (Kido, Nakae and Accili, 2001).

According to previous research, the IRS2 protein possesses the ability to initiate the activation of PI3K more rapidly, when compared to IRS1. This difference in the activation speed plays a crucial role in insulin signalling (Ogihara *et al.*, 1997; Inoue *et al.*, 1998).

Lastly, IRS1 and IRS2 are both able to bind to the following downstream proteins: PI3K, Grb2, PLC, Fyn as well as Crk, although SHP-2 binding is restricted to IRS1 only (Sun *et al.*, 1997; White, 1997).

(c) IRS3

The IRS3 protein is less well characterized and only expressed in rodents (Sesti *et al.*, 2001; Mardilovich, Pankratz and Shaw, 2009). This protein is mainly present in the adipose tissue and is also present in the liver and in the pancreatic β-cells (Withers and White, 2000; Burks and White, 2001). The IRS3 protein is specifically located in the plasma membrane, where it can sense insulin (Anai *et al.*, 1998).

The IRS3 protein is shorter (700-800 residues) in size when compared to the IRS1 and IRS2 protein (Sesti *et al.*, 2001). When comparing the similarity of the three IRS proteins in terms of the three domains, it was found that the PH domain of IRS3 was similar to IRS1 and the PTB domain similar to IRS2 (Lavan, Lane and Lienhard, 1997). The carboxyl (COOH) terminal domain of the IRS3 protein comprises of almost half (13) of the tyrosine phosphorylation sites when compared to those present in the IRS1 (30) and IRS2 (22) proteins.

Once the IRS3 protein is activated, it can effectively bind to the following SH2 domain containing proteins: PI3K, SHP-2, Nck, SHC-transforming protein 1 (Shc) and less effectively to Grb2 and PLC (Xu, Jacobs and Taylor, 1999).

Studies performed on rat adipocytes reported that the overexpression of IRS3 (with or without insulin stimulation) resulted in a significant increase in Glucose transporter 4 (GLUT4) vesicle translocation to the cell membrane for glucose uptake (Zhou *et al.*, 1999). In addition, when these cells were exposed to insulin, the IRS3 protein was the speediest to associate and activate PI3K, when compared to IRS1 and IRS2 (Smith-Hall *et al.*, 1997).

(d) IRS4

IRS4 is the last identified IRS protein. This protein is believed to be associated with the brain, hypothalamus, kidney, heart, skeletal muscle and the thymus (Fantin *et al.*, 1999; Giovannone *et al.*, 2000; Uchida, Myers and White, 2000; Withers and White, 2000; Burks and White, 2001). More specifically, the IRS4 protein is the most abundant in the cell membrane (Tsuruzoe *et al.*, 2001).

The functions of the IRS4 protein include: increased GLUT4 vesicle translocation (adipose tissue), cell differentiation (Zhou *et al.*, 1999), and increased cell proliferation (fibroblasts and hematopoietic cells) (Fantin *et al.*, 1999; Qu *et al.*, 1999).

Like the other IRS proteins, IRS4 also contains a PH domain, PTB domain and a COOH-terminal domain (Lavan *et al.*, 1997). The IRS4 protein sequence is 27 % similar to IRS1 and 29 % similar to IRS2 (Sesti *et al.*, 2001).

Like IRS3, the IRS4 protein also contains much less tyrosine phosphorylation sites (12) than IRS1 and IRS2. Of the 12 potential sites, 7 sites are associated with the YXXM (Tyrosine- XX-Methionine where X is any amino acid) motif, consequently giving IRS4 the ability to bind to PI3K. Interestingly, the IRS4 protein has two extra tyrosine phosphorylation sites. These sites specifically bind to the SH2 domain of the Grb protein and to the NH2-terminal domain of SHP-2 and PLC (Sesti *et al.*, 2001). According to previous studies, IRS3 and IRS4 control the activation/suppression of IRS1 and IRS2 (Tsuruzoe *et al.*, 2001).
Thus, from the detailed description above it is evident that the IRS proteins influence one another, but also work in conjunction to deliver a maximum response.
The two most well-known insulin-dependent signalling pathways are the **PI3K-dependent pathway** and the **PI3K-independent pathway**. In the next section, a detailed description of both pathways will follow.

1.4. Insulin-dependent signalling pathways

1.4.1. PI3K-dependent pathway

The PI3K-dependent pathway ***(Figure 1.4)*** is one of the most important signalling pathways specifically triggered in response to increased circulating insulin (Cho and Park, 2008).

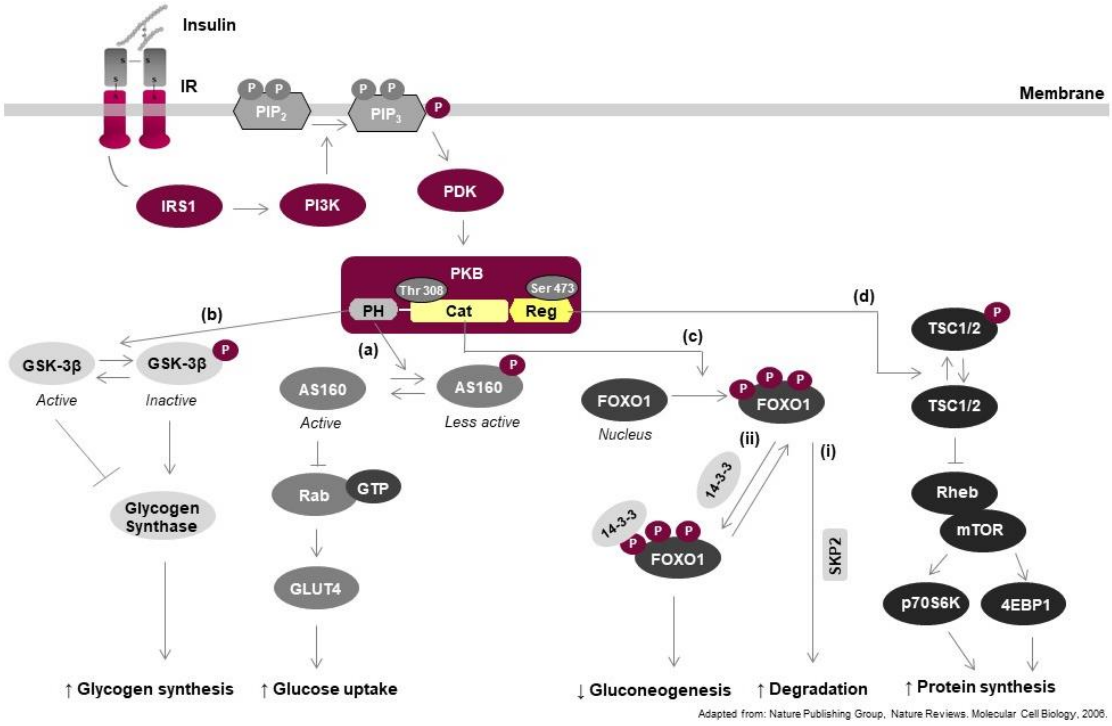

Figure 1.4: *PI3K-dependent pathway. Image adapted from (Nature, 2006) and composed using Microsoft PowerPoint.*

The PI3K protein is a regulated tyrosine kinase, containing an 85 kilo Dalton (kDa) regulatory subunit (p85) and a 110 kDa catalytic subunit (p110) (Hoedemaeker *et al.*, 1999).
The p85 regulatory subunit consists of a Src Homology 3 (SH3) domain, two C-terminal SH2 domains (separated by an inter-SH2 region (i-SH2)), and a breakpoint-cluster region homology (BH) domain (present between the two proline-rich regions). These domains/regions are responsible for p85 and p110 subunit binding (Otsu *et al.*, 1991).

The p110 catalytic subunit has several isoforms which enables it to associate with different classes of PI3Ks. The p110α, p110β and p110δ associate with Class IA PI3Ks, whereas p110γ associates with Class 1B PI3Ks (Wymann and Pirola, 1998). Like the p85 subunit, p110α also contains several domains including a Ras binding domain (RBD), a helical domain (HD), an N-terminal adaptor-binding domain (ABD), a C2 domain and most important, a catalytic kinase domain (Mandelker *et al.*, 2009). The actions of these domains are dependent and coordinated by the SH2 domain present in the p85 subunit (Canner *et al.*, 2013).

Once IRS1 is activated in response to insulin stimulation, it acts as a docking site and phosphorylates the SH2 domain of the PI3K p85 subunit (White, 1997). The active p85 subunit results in the activation of the p110 subunit (von Willebrand *et al.*, 1998).

Activated PI3K is known for its ability to phosphorylate specifically the 3 position hydroxyl group of the inositol ring of phosphatidylinositol-4,5-bisphosphate (PIP_2), consequently resulting in phosphatidylinositol-3,4,5-trisphosphate (PIP_3) generation (Giese, 2009). PIP_3 is a phospholipid and resides in the cell membrane where it creates docking sites for proteins containing a PH domain. These proteins include: phosphoinositide-dependent kinase 1 (PDK1), mammalian target of rapamycin (mTOR) c2 and most importantly for the current study, PKB (Scheid and Woodgett, 2003).

Inactive PKB, located in the cytosol, translocates to the plasma membrane in response to cell stimulation. As mentioned, due to the PH domain present in PKB, its affinity for PIP_3 binding is instantly increased (Miao *et al.*, 2010). Since PIP_3 activation is dependent on PI3K activation, PI3K can be seen as crucial for PKB translocation to the plasma membrane.

The interaction of PKB with PIP_3 initiates a conformational change in the PKB protein, resulting in the exposure of PKBs catalytic phosphorylation sites. These sites include: Thr308 in the catalytic (cat) domain and Ser473 in the C-terminal regulatory (reg) domain (Hemmings and Restuccia, 2012).

Since PDK1 also contains a PH domain, it allows binding to PIP_3, consequently initiating PDK1 to partially phosphorylate PKB at T308 (Dinitto and Lambright, 2006; Bozulic and Hemmings, 2009). The activation of PKB at Ser473 can be catalysed by multiple proteins including: phosphoinositide-dependent kinase 2 (PDK2), mTORc2, integrin-linked kinase (ILK), and DNA-activated protein kinase (DNA-PK) (Vanhaesebroeck and Alessi, 2000; Osaki, Oshimura and Ito, 2004; Hemmings and Restuccia, 2012). Ser473 phosphorylation is crucial for optimal enzymatic activity (Alessi *et al.*, 1996) and is seen as the final step in PKB activation (Bevan, 2001).

According to a previous study, PKB also presents with a third phosphorylation site, namely T450 (Alessi *et al.*, 1996). Originally, this site was thought to be a consequence of autophosphorylation, however recently it was shown that the activation of this site is rather controlled by mTORc2 (Facchinetti *et al.*, 2008; Ikenoue *et al.*, 2008). The role of T450 phosphorylation in PKB signalling remains unclear.

The **PH domain** of the active PKB initiates the downstream (a) activation of the Rab pathway and (b) inhibition of the glycogen synthase kinase 3β (GSK-3β) pathway, whereas the **catalytic subunit** of PKB is responsible for the activation of (c) forkhead box protein O1 (FOXO) pathway and (d) mTOR pathway (Taniguchi, Emanuelli and Kahn, 2006).

(a) Rab pathway

PKB phosphorylates the Akt substrate of 160 kDa (AS160) protein, which in turn inhibits the AS160 associated GTPases-activating domain. Consequently, the less active AS160 protein looses its inhibitory effect on Rab. The Rab protein switches between a GDP bound state to an active GTP bound state, which enables Rab to increase GLUT4 vesicle translocation to the plasma membrane (Guo, 2014).

(b) GSK-3β pathway

GSK-3β is a direct target of PKB. Once phosphorylated, GSK-3β becomes inactive, increases glycogen synthase (GS) activity, and consequently the conversion of glucose to glycogen (Guo, 2014).

(c) FOXO pathway

FOXO1 is located in the liver and regulates the transcription of glucose-6 phosphatase (G6Pase). Once PKB is active, it enters the nucleus and phosphorylates FOXO1 at several phosphorylation sites (Ser256, Ser319 and Thr24) (Rena *et al.*, 1999). Consequently, FOXO1 translocates to the cytoplasm where it (i) interacts with S-phase kinase-associated protein 2 (SKP2) which induces ubiquitination and subsequently proteasome degradation of FOXO1 or (ii) is sequestered in the cytoplasm by binding to 14-3-3 proteins, consequently decreasing gluconeogenesis (Huang and Tindall, 2011).

(d) mTOR pathway

Tuberous sclerosis ½ (TSC1/2) is responsible for the inhibition of GTPase Ras homologue enriched in brain (Rheb). Once the inactive TSC1/2 is phosphorylated by PKB, it becomes active, decrease Rheb suppression, and consequently stimulates the downstream protein, mTOR. Activated mTOR induces protein synthesis by the phosphorylation of 4E-binding protein 1 (4EBP1) and p70 ribosomal protein S6 kinase (p70S6K) (Haar *et al.*, 2007; Hemmings and Restuccia, 2012).

According to previous research, when PI3K was inhibited with Wortmannin and simultaneously activated with insulin, glucose uptake was similar as with insulin stimulation only (Khan and Pessin, 2002), suggesting that an additional pathway functioning independently from PI3K is present (PI3K-independent pathway).

1.4.2. PI3K-independent pathway

The PI3K-independent pathway can be subdivided in to (a) Grb pathway and (b) Cbl (named after Casitas B-lineage Lymphoma) pathway ***(Figure 1.5)***.

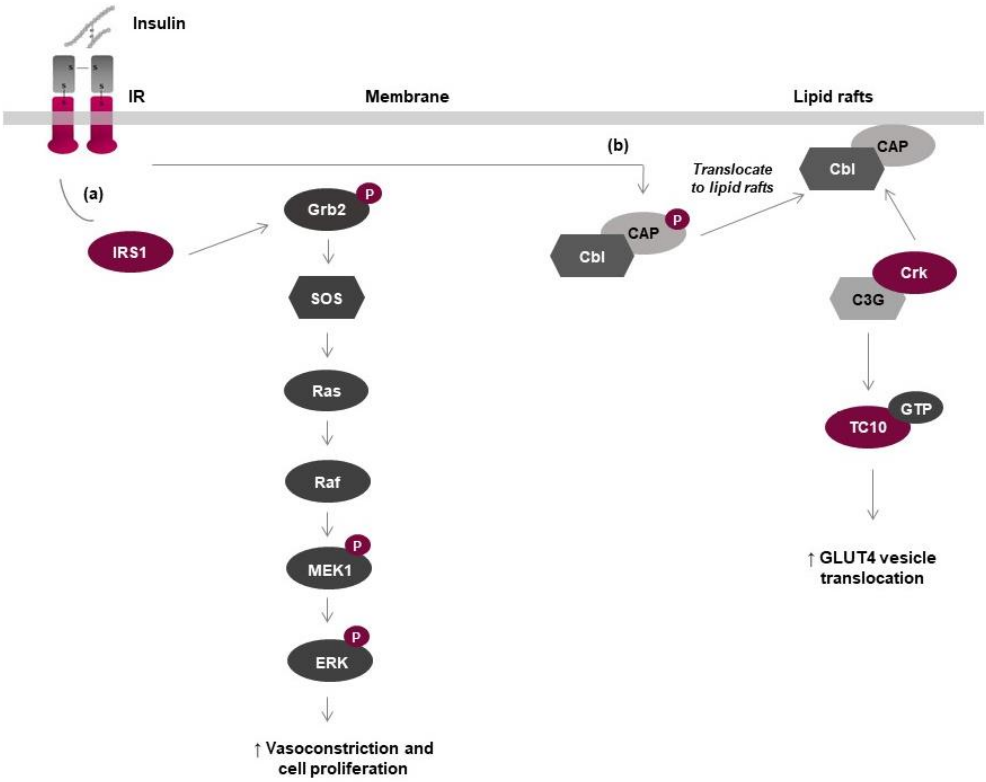

Figure 1.5: *PI3K-independent pathway. Image adapted from (Shaikh, Dadachanji and Mukherjee, 2014) and composed using Microsoft PowerPoint..*

(a) Grb pathway

This pathway is beyond the scope of this thesis and will therefore only be briefly described. Once IRS1 is activated in response to insulin stimulation, the SH2 domain of IRS1 phosphorylates Grb2. Consequently, Grb2 binds to the Son of sevenless homolog 1 (SOS) protein, which in turn acts as a guanine nucleotide exchange factor for Ras. The activated Ras protein will initiate a phosphorylation cascade including rapidly accelerated fibrosarcoma (Raf), mitogen-activated protein kinase (MEK) and extracellular signal-regulated kinases (ERK). Active ERK is pro-atherosclerotic since it increases vasoconstriction and proliferation (King, Park and Li, 2016).

(b) Cbl pathway

This pathway results in the ultimate activation of a small G-protein, TC10, which increases GLUT4 vesicle translocation. Once insulin binds to the IR, the receptor dimerizes, followed by the autophosphorylation of its tyrosine residues. The active IR recruits and phosphorylates the Cbl-associated protein (CAP) complex (Liyasova, Ma and Lipkowitz, 2015). This is followed by the translocation of Cbl-CAP to the lipid rafts present in the cell membrane. The active phosphotyrosine residues on Cbl acts as docking sites for Crk/cyanidin 3-glucoside (C3G) complex (Tanaka et al., 1994). Crk is an adaptor protein and therefore responsible for linking Cbl to C3G, whereas C3G acts as a guanine nucleotide exchange factor for TC10 (Saltiel et al., 2000; Chiang et al., 2001). The GTP-bound TC10 will initiate GLUT4 vesicle translocation, however the exact mechanism still remains unclear (Chiang et al, 2001). Since TC10 is believed to have profound effects on the structure and maintenance of actin (3T3-L1 adipocytes), and transcripts CAP and TC10 are both enriched in cardiac and skeletal muscle, PI3K-independent signalling is proposed to link actin dynamics to GLUT4 translocation (Khan and Pessin, 2002).

Insulin and its associated effects vary according to the physiological function of the specific organs and tissues, together with their dependence on insulin to perform important metabolic processes (Wilcox, 2005). Muscle and adipose tissue are both identified as primary insulin-dependent tissues since they are responsible for intracellular glucose transport. It is important to note that insulin's actions are pleotropic (Reaven, 2004), and therefore it is also associated with the gonads, bone, kidney, pancreas, pituitary, brain, endothelium and vasculature (Wilcox, 2005).

In the next section, the relationship between insulin and the muscle, adipose tissue, endothelium/vasculature and the heart will be briefly described as it is most relevant to the study.

1.5 Relationship between insulin and the muscle, adipose tissue, endothelium and heart

1.5.1. Insulin and the skeletal muscle

The muscle is responsible for 60-70 % of whole-body insulin-mediated glucose uptake via GLUT4 (Smith, 2002). In the fed state, insulin-activated PKB stimulates glycogen synthase and consequently initiates glycogen synthesis (Pessin and Saltiel, 2000). Glycogen synthesis enables the anaerobic release of energy during intense muscular activity. During the basal state when insulin levels are low, the muscle cells are independent of glucose and glycogen as a source of

energy (Wilcox, 2005), as it has already stored glycogen molecules, from the fed state, in granular form.

Furthermore, insulin also increases protein synthesis by activating mTOR, whereas insulin deficiency promotes protein catabolism by releasing amino acids for gluconeogenesis (glucose formation) (Rask-Madsen and Kahn, 2012). In the fasting state, protein synthesis is believed to be reduced by 50 % (Giorgino, Laviola and Eriksson, 2005). According to previous studies, the dosage of insulin to induce protein synthesis is significantly greater than the dosage needed to suppress proteolysis (Giorgino, Laviola and Eriksson, 2005).

1.5.2. Insulin and the adipose tissue

The adipose tissue is only responsible for about 10 % of the insulin stimulated glucose uptake (Smith, 2002). Once an increase in insulin levels are sensed, GLUT4 vesicle translocation in adipocytes are triggered and the absorption of glucose by the fat cells are elevated. Simultaneously, insulin also stimulates fatty acid uptake by the adipocytes, which then convert these molecules to triglycerides, the storage form of fat (Czech *et al.*, 2013).
During fasting, triglycerides in the adipocytes are converted to FFA via a process called lipolysis. Intracellular energy is supplied by the release of these FFAs from the adipocytes into circulation for direct energy utilization by organs such as the liver, muscle and heart. The liver and the heart also convert the FFAs to ketone bodies, which in turn plays an important role in providing the brain with energy during prolonged fasting (Denton and Tavaré, 1997).

1.5.3. Insulin and the endothelium and vasculature

Endothelial cells, the physical lining of the blood vessels, secrete several factors which in turn, influence platelet function, vessel tone, fibrinolysis and coagulation. Nitric oxide (NO), is responsible for inducing endothelial relaxation and inhibiting cell adhesion, platelet aggregation and proliferation of vascular smooth muscle cells (VSMCs). The enzyme endothelial nitric oxide synthase (eNOS) and its cofactors flavin adenine dinucleotide (FAD), flavin mononucleotide (FMN) and tetrahydrobiopterin (BH4), are responsible for the conversion of L-arginine, nicotinamide adenine-dinucleotide phosphate (NADPH) and molecular oxygen to NO. L-arginine is believed to be a potent secretagogue for insulin. The mechanism however still remains unknown. Insulin also increases NO production via the calcium-independent phosphorylation of eNOS by PKB and PIP_3. Lastly, insulin can directly stimulate GTP cyclohydrolase, resulting in BH4 production which in turn, increases vasodilation in the endothelium (Reaven, 2004).
In Chapter 1, Section 1.8, the endothelium will be discussed in more detail.

1.5.4. Insulin and the heart

Under basal conditions, the heart is dependent on fatty acids to produce ATP. When glucose and insulin levels are increased, the heart switches from oxidizing fatty acids to oxidizing glucose for energy production (Bertrand *et al.*, 2008).

In the heart, insulin potently stimulates PKB (Deprez *et al.*, 2000) and PDK1. In addition, PDK1 was also shown to be responsible for the activation of PKB in the cardiac tissue (Mora *et al.*, 2003). Activated PKB increases GLUT4 vesicle translocation and consequently glucose uptake. Furthermore, insulin-stimulated cardiomyocytes showed increased mTOR activation (Rolfe *et al.*, 2005), followed by increased protein synthesis. According to previous studies, insulin prevents the development of atrophy in the cardiac muscle via the inhibition of FOXO1 and FOXO3a through PKB (Liu *et al.*, 2007; Skurk *et al.*, 2007).

Insulin also regulates cardiac glycogen levels by activating 6-phosphofructo-2-kinase (PFK-2) via the PI3K-dependent pathway (Mora *et al.*, 2003). PFK-2 synthesizes fructose 2,6-bisphosphate (Fru-2,6-P_2) (Rider and Hue, 1984), which, in turn activates phosphofructokinase-1 (PFK-1) (Rider *et al.*, 2004). PFK-1 results in the breakdown of glucose into pyruvate and is therefore central in regulating glycolytic flux in the cardiac muscle (Rider *et al.*, 2004).

Lastly, insulin also stimulates the translocation of fatty acid translocase (FAT/CD36) via the PI3K-dependent pathway, to the cell membrane (Luiken *et al.*, 2002). As a result, long chain fatty acid (LCFA) uptake is increased and stored in the intracellular pool of lipids (Dyck, Steinberg and Bonen, 2001).

1.6. Attenuation of insulin signalling

Insulin signalling is attenuated via negative regulators including the Src-homology-2 domain-containing inositol phosphatase-2 (SHIP2), tensin homolog phosphatase (PTEN), phosphatase-2A (PP2A), PH-domain leucine-rich-repeat protein phosphatase (PHLPP) (Taniguchi, Emanuelli and Kahn, 2006), SHP2 (Luo et al., 2014) and the insulin degrading enzyme (IDE) (Pivovarova *et al.*, 2016).

Both SHIP2 and PTEN act by degrading PIP_3 to PIP_2 (Lazar and Saltiel, 2006). PHLPP and PP2A are both known to directly dephosphorylate/inactivate PKB (Cazzolli *et al.*, 2001; Gao, Furnari and Newton, 2005). SHP2 inhibits insulin signalling by dephosphorylating IRS1, consequently supressing PI3K activation (Luo *et al.*, 2014). Finally, the zinc endopeptidase, IDE, further

attenuates insulin signalling by degrading biologically active insulin peptides (Pivovarova *et al.*, 2016).

Insulin-independent signalling via the AMP-activated protein kinase (AMPK) pathway can also mediate glucose uptake and induce vasorelaxation, an important aspect of the current study. In the next section, the AMPK pathway will be discussed.

1.7. Insulin-independent pathway: AMPK

1.7.1. AMPK signalling

AMPK is a fuel-sensing enzyme activated by changes in the adenosine monophosphate (AMP)/ATP ratio. This kinase can increase the generation of cellular ATP (fatty acid oxidation) or diminish the use of ATP for less important processes such as triglyceride, fatty acid and protein synthesis (Carling, Zammit and Hardie, 1987). Additionally, AMPK can also control glucose transport and factors that have been linked to insulin resistance such as increasing glucose uptake via GLUT4 and regulating autophagy, inflammation and endoplasmic reticulum stress (Ruderman *et al.*, 2013).

AMPK consists of two regulatory subunits (γ and β) and a single catalytic subunit (α). These subunits are further divided into three γ isoforms and two α and β isoforms. In the regulatory γ-subunit, four cystathionine β-synthase (CBS) domains are present, acting as adenine nucleotide-binding sites (site 1, 3, 4) (Ruderman *et al.*, 2013).

AMP binds at site 4 in a nonexchangeable manner where site 1 and 3 are exchangeable nucleotide-binding sites. Increased AMP (due to cell stress) is associated with the displacement of ATP from the exchangeable sites, thus resulting in the allosteric activation of AMPK. The activity of AMPK is further increased when ATP displacement via AMP also prevents the dephosphorylation of the phosphorylated Thr 172 residue on the α-subunit (Xiao *et al.*, 2011). Interestingly, recent studies proposed that ATP displacement by ADP instead of AMP is responsible for the secondary activation (Xiao *et al.*, 2011). Both AMP and ADP also increase the phosphorylation of Thr 172, and is thus seen as additional regulators of AMPK (Oakhill *et al.*, 2011).

The β-subunit contains a glycogen-binding domain which is involved in carbohydrate metabolism. When glycogen and branched-chain sugars bind to this domain, the activity of AMPK is inhibited (Ruderman *et al.*, 2013), whereas binding of small molecule activators such as tumor suppressor

liver kinase B1 (LKB1) and calcium calmodulin (CaM)-dependent protein kinase kinase β (CAMKKβ) phosphorylate AMPK on Thr 172. LKB1 is activated in response to energy state changes whereas CAMKKβ is activated when intracellular calcium increases (Stahmann *et al.*, 2006; Racioppi and Means, 2012).

The current study will only focus on AMPK and its role in the vascular endothelium.

1.7.2. AMPK in the vascular endothelium

Within vascular endothelial cells, the catalytic α1-subunit of AMPK is dominant when compared to α2 (Evans *et al.*, 2005; Rubin *et al.*, 2005; Davis *et al.*, 2006). Once AMPK is activated in response to nutrient starvation (particularly glucose), hypoxia and the inhibition of the mitochondrial respiratory chain complex via toxins (Mihaylova and Shaw, 2011; Hardie, Ross and Hawley, 2012), AMPK phosphorylates eNOS on Ser 1179 (Hu *et al.*, 2008) and Ser 633 (Chen *et al.*, 2009). In turn, the active eNOS enzyme converts L-arginine, to NO. NO initiates endothelial relaxation by inhibiting cell adhesion, platelet aggregation and proliferation of smooth muscle cells (Reaven, 2004).

In addition, AMPK can also be activated via LKB1 in response to increased generation of ROS (Zou *et al.*, 2004). As a result, AMPK will prevent oxidative stress induced apoptosis (Ido, Carling and Ruderman, 2002). Taken together, the AMPK pathway acts as an important protection mechanism within endothelial cells.

1.7.3. Link between AMPK, obesity, hypertension and insulin resistance

Obesity is associated with increased insulin resistance and decreased AMPK levels, which in turn results in the development of hypertension (Ruderman *et al.*, 2013).

Previous studies suggested a link between insulin resistance and AMPK in the vascular endothelium (Ido, Carling and Ruderman, 2002). Insulin resistant endothelial cells are associated with decreased mitochondrial membrane potential which can be alleviated when AMPK phosphorylation is stimulated (Ido, Carling and Ruderman, 2002; Hattori *et al.*, 2006; Kukidome *et al.*, 2006). The activation or overexpression of AMPK in insulin resistant endothelial cells is in addition, also linked to the prevention of oxidative stress, inflammation (nuclear factor-κB (NF-κB) pathway transactivation) and apoptosis (Ruderman *et al.*, 2003; Cacicedo *et al.*, 2004). Furthermore, AMPK in insulin resistant endothelial cells can elevate the phosphorylation of eNOS on Ser 1177 (Chen *et al.*, 1999) as a compensatory mechanism, consequently synthesizing NO,

which in turn diminishes oxidative stress and aortic atherogenesis (Cai and Harrison, 2000). *Oxidative stress is described in Chapter 1, Section 1.8.6.2.*

1.8. Vascular endothelium

The endothelium, a thin single layer of endothelial cells lining the interior surface of all blood vessels (Xu and Si, 2010), maintains vascular homeostasis by releasing vasoactive factors in response to hormonal and physical stimuli (Navar, 2014). Vascular homeostasis which forms an important part of the current study, is crucial in preventing the development of cardiovascular-related diseases, such as atherosclerosis (Anderson *et al.*, 1995). In the following sections, the vascular endothelium, and the link between the vascular endothelium and blood pressure regulation, will be discussed.

1.8.1. Arterial wall structure

A normal arterial wall is composed of three distinct layers; tunica intima (endothelial cells), tunica media (vascular smooth muscle cells) and the adventitia (fibroblasts, perivascular adipocytes, collagen fibers and nerve endings (Zhao, Vanhoutte and Leung, 2015) ***(Figure 1.6).***

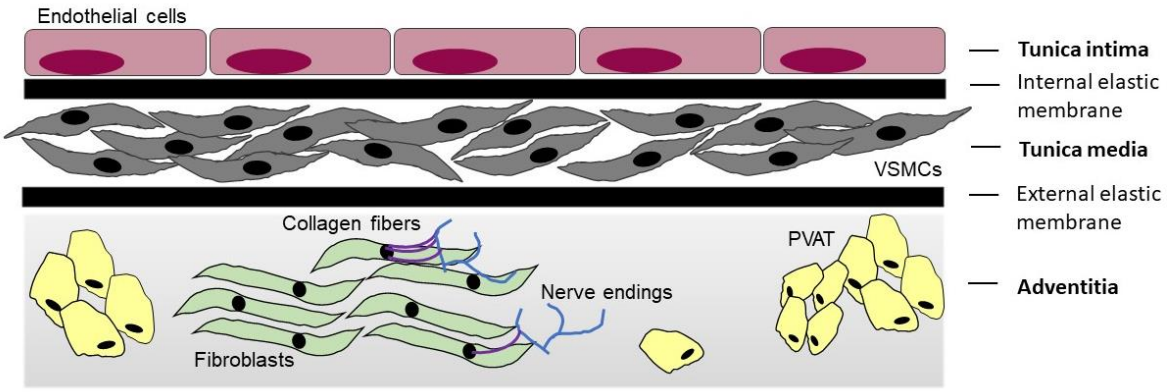

Figure 1.6: *Arterial wall structure. Image adapted from (Zhao, Vanhoutte and Leung, 2015) and composed using Microsoft PowerPoint.*

The endothelium refers to a thin single layer of endothelial cells, connected via intercellular junctions, which covers the interior surface of all blood vessels (Xu and Si, 2010). These junctional complexes include tight junctions, adherens junctions and gap junctions (Bazzoni and Dejana, 2004). The organization and the expression of the junctional complexes are dependent on the vessel type and the permeability related necessities of the perfused organs (Bazzoni and Dejana, 2004). Endothelial cells are separated via the glycocalyx layer from the vascular lumen. The

glycocalyx layer refers to carbohydrate-rich chains which are anchored to the endothelial cells (via transmembrane protein domains) and projects into the vessel lumen (Pries, Secomb and Gaehtgens, 2000; Tarbell and Pahakis, 2006). Consequently, a network is formed in which soluble molecules (endothelium or plasma-derived) are incorporated (Reitsma *et al.*, 2007). The last layer identified is the endothelial surface layer (ESL) which is known to restrict plasma flow by excluding red blood cells and macromolecular solutes (Pries, Secomb and Gaehtgens, 2000).

Furthermore, endothelial cells are flat, with a central nucleus bulging into the vascular lumen. The appearance of the endothelial cells is location-dependent, being round in the venules and capillaries, and more spindle-shaped in the arterioles and arteries. Like other cell types, endothelial cells present with plenty of caveolae (Mas, 2009) and mitochondria (Weibel and Palade, 1964), vesicular membrane invaginations, and a Golgi apparatus (Mas, 2009). Interestingly, endothelial mitochondria obtain most of their energy via anaerobic glycolysis, and is therefore associated with a low oxygen consumption profile (Davidson and Duchen, 2007). According to previous studies, endothelial mitochondria rather act as signalling organelles through regulatory reactive oxygen species (ROS) production (Quintero *et al.*, 2006). A distinct structural feature of endothelial cells is the presence of electron-dense structures, known as Weibel-Palade bodies (WPBs) (Weibel and Palade, 1964). These WPBs contain von Willebrand factor (VWF), together with several other proteins which contributes to angiogenesis, inflammation and tissue repair (Valentijn *et al.*, 2011).

1.8.2. Function of the endothelium

Endothelial cells respond to several hormonal (insulin, bradykinin, thrombin) and physical (shear stress) stimuli which initiate the release of vasoactive factors to maintain vascular homeostasis (Navar, 2014). These factors are subdivided into vasodilators and vasoconstrictors which are respectively responsible for blood vessel relaxation and contraction (Rubanyi, 1991) depending on the type of stimulus.

Under normal physiological conditions, the endothelial-derived vasodilator/vasoconstrictor ratio is delicately balanced, but can be disrupted by cardiovascular risk factors (Mas, 2009). An unbalanced endothelial-derived vasodilator/vasoconstrictor ratio results in local (vasospasm) and generalized (hypertension) vascular tone increase together with thrombus (blood clot) formation (Rubanyi, 1991).

Vasodilatory agents include NO, endothelium-derived hyperpolarizing factors (EDHF) and prostacyclin (PGI_2), whereas the endothelial-derived constricting factors (EDCF) include

thromboxane A_2 (TXA_2), endothelin-1 (ET-1), prostaglandin F_2 (PGF_2) (Navar, 2014) and angiotensin II (Mudau *et al.*, 2012).

NO, ET-1 and angiotensin II will be discussed in more detail as these endothelium-derived factors are most relevant to our study. The other vasoactive agents with their specific physiological effects, enzymatic source and mechanism of action are summarized in ***Table 1.1***.

Table 1.1: *Endothelium-derived factors. Table adapted from (Wong et al., 2009; Mudau et al., 2012)*.

Endothelium-derived factors	Physiological effect	Enzymatic source and mechanism of action
NO	• Vigorous vasodilator • Inhibits VSMC proliferation and migration, inflammation, leukocyte adhesion, platelet aggregation and adhesion • Regulates myocardial contractility • Regulates cardiac metabolism • Cardio-protective during ischaemia-reperfusion injury	• Synthesized by the enzymes, eNOS, nNOS and iNOS, with eNOS being the main source of NO production during physiological conditions. • Diffuses from endothelial cells to underlying VSMCs, followed by binding to soluble guanylyl cyclase, consequently initiating a cascade of events that ultimately result in vascular relaxation.
EDHF	• Initiates vasodilation specifically in small arteries (≤300 µm)	• Unknown identity with proposed candidates such as K^+ and hydrogen peroxide. • Initiates VSMCs relaxation via membrane hyperpolarisation.
PGI_2	• Inhibits platelet aggregation • Initiates vasodilation	• Derived from arachidonic acid via cyclooxygenase-2.
TXA_2	• Vigorous vasoconstrictor	• Derived from arachidonic acid via cyclooxygenase-2.
ET-1	• Vigorous vasoconstrictor	• Synthesised via endothelin-converting enzyme. • Exerts its effects via receptor ET_A (expressed on endothelial cells) and ET_B (expressed on VSMCs). • ET_A receptors promote vasoconstriction while ET_B promote NO generation and ultimately reduced ET-1 production.
PGF_2	• Vigorous vasoconstrictor	• Derived from cyclooxygenase-2. • Exerts its effects via the activation of the F prostanoid receptor.
Angiotensin II	• Vigorous vasoconstrictor	• Synthesised via ACE. • Exerts its effects via AT_1 (promote cell proliferation and vasoconstriction) or AT_2 (antagonises the effects of AT_1).

1.8.3. NO

1.8.3.1. NO background

NO, a diatomic gas, plays a crucial role in the physiological regulation of the cardiovascular system, since defective NO production accompany or in some cases even precede diseases such as atherosclerosis (Anderson *et al.*, 1995), hypertension (Herrmann and Dzau, 1983) and angiogenesis-associated disorders (Cooke, 2002).

NO is intracellularly synthesized by a family of NO synthase (NOS) enzymes. These enzymes are responsible for the electron oxidation of L-arginine's guanidine-nitrogen terminal, consequently releasing NO (Achan *et al.*, 2003). To date, three NOS isoforms have been identified including: neuronal NOS (nNOS), eNOS and inducible NOS (iNOS) (Ignarro *et al.*, 1999). These NOS enzymes require several cofactors to produce NO from L-arginine. Cofactors include NADPH, FAD, FMN, BH4 (Ignarro *et al.*, 1999) iron protoporphyrin IX (haeme) and calmodulin (Alderton, Cooper and Knowles, 2001; Förstermann and Münzel, 2006). All three NOS isoforms are synthesized as monomers and need to dimerize for optimal BH4 and L-arginine binding (Förstermann and Münzel, 2006). NOS monomers generate superoxide anions (O_2•-) instead of NO, a mechanism known as uncoupling (Higman *et al.*, 1996; Stroes *et al.*, 1997). In addition, NOS uncoupling also refers to the oxidation of BH4 to BH3 via ROS, resulting in attenuated NO production (Zhao, Vanhoutte and Leung, 2015).

Both nNOS and eNOS are produced in relatively constant amounts in the endothelium and are regulated by calmodulin and calcium. The last isoform, iNOS is calcium-independent and mainly regulated by inflammatory cytokines to produce NO. The production rate of NO by iNOS is up to 1000-fold more than the rate of NO produced by nNOS and eNOS (Johanning *et al.*, 2001). Surplus NO out-competes superoxide dismutases (SOD) for increased O_2•-, consequently generating the highly reactive pro-oxidant, peroxynitrite ($ONOO^-$) (Moulian *et al.*, 2001). $ONOO^-$ results in the oxidation and nitration of proteins, consequently initiating protein damage and cytotoxic events (Radi, 2013).
All mammalian cells (including endothelial cells) can generate O_2•-. These anions are inactivated by SOD (Rubbo, Darley-Usmar and Freeman, 1996).

For the current study, we are specifically interested in vascular NO production, and therefore only eNOS will be described in depth.

1.8.3.2. NO formation via eNOS

Several stimuli, such as shear stress (Andrews *et al.*, 2010; Kolluru *et al.*, 2010), ACh (Kellogg *et al.*, 2005), histamine (Li *et al.*, 2003; Mondillo *et al.*, 2009), and bradykinin (Coppo and Amore, 2000; Bae *et al.*, 2003) can initiate the activation of eNOS in a calcium-dependent and independent manner (Zhao, Vanhoutte and Leung, 2015) ***(Figure 1.7)***.

ACh, histamine and bradykinin bind to specific receptors on the endothelial cell membrane to initiate biological responses. As a result, the concentration of intracellular calcium increases, followed by binding to CaM which in turn activates the CaM-binding domain of eNOS (Kuchan and

Frangos, 1994; Hall, 1997; Walch, Brink and Norel, 2000; Parsons and Ganellin, 2009). NADPH provides an electron flux through FAD, FMN, CaM and lastly protoporphyrin IX (haeme Fe), and is subsequently used for NO generation (Sessa, 2004). Calcium-independent phosphorylation enables the active flux of electrons from the reductase to the oxygenase domain (Sessa, 2004). The activity of eNOS can also be altered when phosphorylated at either Ser 1177 (activation site) or Thr 495 (inhibitory site) (Kolluru, Siamwala and Chatterjee, 2010). Under unstimulated conditions, Thr 495 is phosphorylated (probably by PKC), which prevents the binding of CaM to the CaM-binding domain (Förstermann and Sessa, 2012). Once dephosphorylated, intracellular calcium is elevated, eNOS activity is increased and CaM binding to eNOS is amplified (Fleming and Busse, 2003). Dephosphorylated Thr 495 can also favour eNOS uncoupling (Lin *et al.*, 2003).

Oestrogen, vascular endothelial growth factor (VEGF) and insulin (Förstermann and Sessa, 2012) phosphorylate PKB which in turn phosphorylates/activates eNOS at Ser 1177 (Chen *et al.*, 1999; Dimmeler *et al.*, 1999). Insulin can also phosphorylate AMPK (Förstermann and Sessa, 2012), which in turn phosphorylates eNOS at Ser 1177 (Hu *et al.*, 2008) and Ser 633 (Chen *et al.*, 2009). Bradykinin induced phosphorylation of Ser 1177 is initiated via the Ca^{2+}/CaM- dependent protein kinase II (CaMKII) (Förstermann and Sessa, 2012). Furthermore, shear stress phosphorylates eNOS via a PKA-dependent manner at Ser 1177, and at an additional site, i.e. Ser 635 (Boo, Hwang, *et al.*, 2002; Boo, Sorescu, *et al.*, 2002).

Cardiovascular risk factors such as diabetes, hypertension, or hypercholesterolemia result in L-arginine and BH4 depletion, consequently promoting NOS-mediated ROS formation which increase $ONOO^-$ formation (Cai and Harrison, 2000; Ignarro and Napoli, 2004).

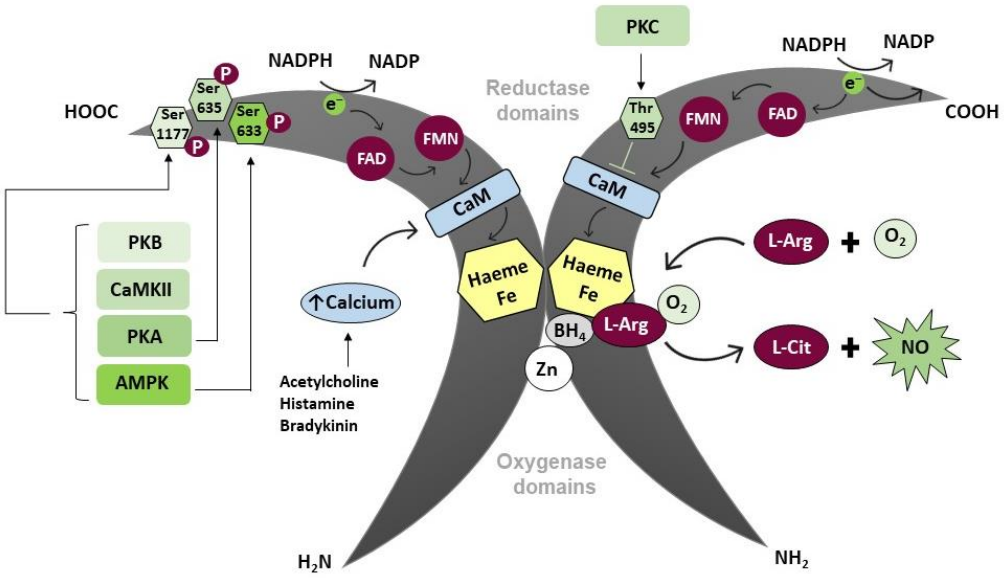

Figure 1.7: *Generation of NO via the two eNOS monomers. Image adapted from: (Förstermann and Sessa, 2012; Zhao, Vanhoutte and Leung, 2015) and composed using Microsoft PowerPoint.*

1.8.3.3. Physiological functions of eNOS-derived NO

NO, derived specifically from eNOS, has been proposed to play an important role in the regulation of essential cardiovascular functions. These include the inhibition of (a) vasoconstriction and platelet adhesion and aggregation, (b) leukocyte adhesion and inflammation, (c) VSMC proliferation (Förstermann and Sessa, 2012), and (d) low-density lipoprotein (LDL) oxidation (Rubbo *et al.*, 1994).

(a) Vasodilation and platelet aggregation/adhesion

NO, generated by eNOS, stimulates soluble guanylyl cyclase in smooth muscle cells, consequently increasing cyclic guanosine monophosphate (cGMP), resulting in the vasodilation of all blood vessel types (Rapoport, Draznin and Murad, 1983; Förstermann *et al.*, 1986; Ignarro *et al.*, 1986). Defective eNOS is associated with blood pressure elevation (Huang *et al.*, 1995; Shesely *et al.*, 1996).

Furthermore, NO also inhibits the aggregation and adhesion of platelets to the vascular wall (Alheid, Frölich and Förstermann, 1987) thereby preventing blood clot formation (thrombosis) and the release of platelet-derived growth factors (smooth muscle proliferators) (Rudic *et al.*, 1998).

(b) Leukocyte adhesion and inflammation

Monocyte chemoattractant protein-1 (MCP-1) is released by endothelial cells and smooth muscle cells to initiate macrophage and monocyte recruitment to the subendothelial layer. Once recruited, lipids within these macrophages and monocytes are released, resulting in the development or enlargement of atherosclerotic lesion (Gu *et al.*, 1998). NO derived from eNOS downregulates MCP-1 expression (Zeiher *et al.*, 1995), thus preventing the development of atherosclerosis.

In addition, NO also plays a protective role against the development of atherosclerosis by either interfering with the binding of the leukocyte adhesion molecule (CD11/CD18) to the endothelial cell surface, or by supressing the expression of CD11/CD18 on leukocytes (Kubes, Suzuki and Granger, 1991; Arndt, Smith and Granger, 1993).

The endothelial monolayer barrier is capable of initiating proinflammatory ations, subsequently inducing apoptosis. These apoptotic actions initiated by proinflammatory cytokines and pro-atherosclerotic factors (ROS and angiotensin II) can be supressed by eNOS-derived NO (Dimmeler and Zeiher, 1999).

(c) VSMC proliferation

VSMCs proliferation promotes plaque formation, consequently increasing the susceptibility for atherosclerosis development (Bennett, Sinha and Owens, 2016).

NO mediates the inhibition of VSMCs proliferation via cGMP (Garg and Hassid, 1989; Nakaki, Nakayama and Kato, 1990; Southgate and Newby, 1990), and has also been shown to inhibit mitogenesis and DNA synthesis of the VSMCs (Garg and Hassid, 1989; Nakaki, Nakayama and Kato, 1990; Hogan, Cerami and Bucala, 1992; Nunokawa and Tanaka, 1992).

As mentioned, NO prevents platelet aggregation and adhesion, therefore protecting the smooth muscle from exposure to platelet-derived growth factors. Thus, NO averts the development of fibrous plaque formation, which can later result in atherogenesis (Förstermann, 2008).

(d) LDL oxidation

NO can exhibit dual effects on the oxidation of LDL. During macrophage-dependent LDL oxidation, NO has been shown to be protective (Hogg *et al.*, 1993) when reacting with lipid peroxyl radicals (Rubbo *et al.*, 1994); however the simultaneous occurrence of LDL and O_2•- results in pro-oxidant

formation. This may contribute to LDL modification resulting in foam cell formation and atherogenesis (*Described in Chapter 1, Section 1.8.6.3*).

1.8.4. ET-1

Endothelins (ET) are well-known potent endogenous vasoconstrictors with three distinct isoforms: ET-1, ET-2 and ET-3 (Kowalczyk *et al.*, 2015). The most abundant and well-studied isoform is ET-1 (Yanagisawa *et al.*, 1988; Motte, McEntee and Naeije, 2006). Cells producing ET-1 include the endothelium, cardiomyocytes, VSMCs (Hynynen and Khalil, 2006; Ohkita *et al.*, 2012), renal medulla (Endo *et al.*, 1992) and several other cells which are unrelated to the current study.

Once ET-1 is released in response to low shear stress or stimulation via angiotensin II, free radicals, IL-6 and TNF-α, it acts through two types of G protein-coupled receptors: ETA and ETB. The ETA receptors are located in the VSMCs and mainly responsible for initiating vascular contraction, pro-inflammation and cell proliferation. The ETB receptors are subdivided into ETB_1 and ETB_2. ETB_1 receptors are expressed on endothelial cells and initiates NO-mediated vasodilation, whereas ETB_2 receptors are present in VSMCs, but initiates vasoconstriction (Yanagisawa *et al.*, 1988; Hynynen and Khalil, 2006). ETB_1 receptor stimulation can also result in the release of vasodilators, PGI_2 and EDHF. In addition, ETB receptors have been suggested to take part in the clearance of ET-1, however to date these findings are not yet elucidated (Hynynen and Khalil, 2006; Kawanabe and Nauli, 2011; Ohkita *et al.*, 2012).

Binding of ET-1 to the ETA or the ETB_2 receptor stimulates PLC activation. Activated PLC converts PIP_2 to inositol 1,4,5-trisphosphate (IP_3) and diacylglycerol (DAG). IP_3 stimulates the release of stored Ca^{2+} from the sarcoplasmic reticulum into the cytoplasm of the VSMC. The ETA receptor also stimulates the inflow of Ca^{2+} from the extracellular space into the VSMC. As a result, the increased intracellular Ca^{2+} leads to VSMC contraction. DAG activates PKC, which in turn induce Ca^{2+}-independent VSMC contraction via calponin phosphorylation. In addition, DAG also affects gene transcription via Ras/Raf/MEK/MAPK activation. MAPK activates caldesmon, consequently increasing VSMC contraction (Hynynen and Khalil, 2006; Lima *et al.*, 2011).

Binding of ET-1 to the ETB_1 receptors, located on the endothelium, stimulates NO production and vasodilator cyclooxygenase metabolites, which causes vasodilation of the VSMCs (Kedzierski and Yanagisawa, 2001).

Cardiovascular risk factors, such as obesity, the metabolic syndrome and type II diabetes are associated with increased ET-1 levels and decreased NO levels when compared to healthy

individuals, suggesting that the ETB_2 receptors are upregulated and the ETB_1 receptors are downregulated (Böhm and Pernow, 2007).

1.8.5. Angiotensin II

Angiotensin II (1-8) is the end-product of angiotensin I (1-10) cleavage by the angiotensin converting enzyme (ACE), or alternatively due the action of chymase and cathepsins (present in local Renin-angiotensin system (RAS) (Schmieder et al., 2007). This octapeptide hormone is a potent vasoconstrictor and specifically responsible to increase blood pressure.

Blood pressure is defined as the pressure of systemic circulating blood on the arterial walls and is influenced by cardiac output (amount of blood pumped by the heart per minute) and systemic vascular resistance (resistance that must be overcome for the blood to easily flow through the circulatory system) (Foëx and Sear, 2004).

Since the release of angiotensin II (1-8) is dependent on activation the RAS, the system will be discussed in the following section, including a more detailed description of angiotensin II.

1.8.5.1. RAS: Blood pressure regulation

The RAS is a physiological system specifically responsible for blood pressure regulation together with electrolyte and fluid balancing (Kalupahana and Moustaid-Moussa, 2012). Primarily, it consists of angiotensinogen, renin, ACE, angiotensin II, and angiotensin receptors (Griendling, Murphy and Alexander, 1993) ***(Figure 1.8).***

Angiotensinogen is a globular protein with a molecular weight of 60 kDa (*Angiotensinogen | definition of angiotensinogen by Medical dictionary*, 2012). In lean individuals, this protein is mainly secreted by the liver, whereas in obese individuals, the adipose tissue is suggested to be responsible as an additional source of angiotensinogen secretion (Kalupahana and Moustaid-Moussa, 2011). To date, not much is known about the hepatic synthesis and release of angiotensinogen. In a study performed by Herrmann & Dzau (1983), rat livers were harvested and subjected to components of the RAS to determine the possible RAS feedback mechanism. They found that the inhibition of renin increased angiotensinogen release, whereas the inhibition of angiotensin II (1-8) decreased the release rate of angiotensinogen (Herrmann and Dzau, 1983). Once angiotensinogen is secreted by the liver, it serves as the substrate for renin, thus making it the main precursor peptide of the RAS (Griendling, Murphy and Alexander, 1993).

Prorenin, the inactive precursor of renin, is synthesized in the submandibular gland, mast cells, collecting duct, zona glomerulosa, adrenal, Müller cells, ovary, thecal cells, uterus, placenta, chorionic cells, myometrium/decidual cells, testis and Leydig cells (Krop and Danser, 2008). Prorenin is released from these tissues into the blood, and the level of circulating prorenin is ten times higher than mature renin (Luetscher *et al.*, 1985; Leckie, Birnie and Carachi, 1994). Prorenin was previously associated with no specific function, but when it was discovered that individuals suffering from diabetes present with increased prorenin: renin levels, it was speculated that prorenin may have some function after all (Luetscher *et al.*, 1985; Danser *et al.*, 1989; Danser and Deinum, 2005).

After many years of research, it seems that the inactive prorenin precursor becomes activated proteolytically (proteases) or non-proteolytically (low temperature or pH) which allows binding to the renin/prorenin receptor, consequently generating angiotensin I (1-10) (Danser, Batenburg and van Esch, 2007).

Chronic stimulation of the RAS increases the conversion of prorenin to **renin**. Renin, a glycoproteolytic enzyme with a molecular weight of 37-40 kDa, is synthesized only in the granular cells of juxtaglomerular apparatus, in the kidney (Gomez et al., 1990). This enzyme is secreted into the blood when the stretch receptors in the vascular walls sense an increase in serum sodium (hypernatremia) or a decrease in blood pressure (hypotension) (Wong, 2016). Renin is highly specific for its substrate, angiotensinogen, and has maximum activity at a pH of 7 (Dzau, Burt and Pratt, 1988). Once in circulation, renin is responsible for the enzymatical cleavage and proteolytical conversion of angiotensinogen, to the decapeptide, angiotensin I (1-10) (Kalupahana and Moustaid-Moussa, 2011). The release of renin is attenuated when intracellular Ca^{2+} is increased (Persson, 2003).

ACE is a dipeptidyl carboxypeptidase with a molecular weight ranging between 140-160 kDa for endothelial ACE (Ehlers and Riordan, 1990). This metalloenzyme comprises of a C- and N-domain, each containing a catalytic Zn^{2+} atom. ACE is located primarily in the vascular endothelium of the lungs and in the kidney epithelial cells (Forslund, Kouvonen and Fyhrquist, 1984; Griendling, Murphy and Alexander, 1993; Kierszenbaum, 2007). Four isoforms of ACE have been identified: plasma ACE, tissue ACE, testicular ACE (Ehlers *et al.*, 2012) and the newly discovered ACE2 (Warner *et al.*, 2005). The majority of ACE is membrane bound within tissue, although when cleaved near the C-terminus, the ACE released into circulation is known as plasma ACE (Sadhukhan *et al.*, 1998). Testicular ACE will not be discussed since it is not relevant to the current study.

The main functions of ACE are to: (a) convert angiotensin I (1-10) to the potent vasoconstrictor, angiotensin II (1-8) and (b) degrade the vasodilator, bradykinin (Griendling, Murphy and Alexander, 1993).

The C-domain of **tissue ACE** is specifically responsible for cleaving the terminal dipeptides from the substrate, angiotensin I (1-10) (Ehlers and Riordan, 1990; van Esch *et al.*, 2005; Fuchs *et al.*, 2008), whereas both the C- and the N-domains of **plasma ACE** contribute to the conversion of angiotensin I (1-10) to angiotensin II (1-8) together with bradykinin degradation at tissue sites (van Esch *et al.*, 2005). For cleavage via ACE, it is an absolute necessity that the C-terminus of the substrate lacks a second last proline residue (Ehlers and Riordan, 1990). The rate of substrate hydrolysis via ACE is also dependent on the presence of chloride anions (Cushman and Ondetti, 1980), as it induces a conformational change in the enzyme itself, thus increasing substrate binding. The presence of chloride is therefore crucial for angiotensin I (1-10) cleavage (Griendling, Murphy and Alexander, 1993).

ACE 2, a Captopril-insensitive ACE homologue, is abundant in the kidney and heart (Warner *et al.*, 2005) and has been shown to convert angiotensin I (1-10) to angiotensin (1-9) and angiotensin II (1-8) to angiotensin (1-7). The secreted angiotensin (1-9) is cleaved by ACE, resulting in additional angiotensin (1-7) formation (Schmieder *et al.*, 2007). The properties of angiotensin (1-7) are mediated by the Mas receptor (Santos *et al.*, 2003), resulting in NO (Almeida *et al.*, 2000) release and vasodilation (Paizis *et al.*, 2005). Interestingly, in animals suffering from diabetes, ACE2 expression was increased in early and decreased in late diabetes (Bindom *et al.*, 2010). Thus, ACE2 plays a crucial role in controlling the balance between vasoconstriction and vasodilation.

Angiotensin II (1-8) is the end-product of angiotensin I (1-10) cleavage by ACE, or alternatively due the action of chymase and cathepsins (present in local RAS) (Schmieder et al., 2007).
Angiotensin II (1-8) is the main effector peptide of the RAS acting on the kidneys, adrenal glands, hypothalamus and the arterioles to elicit specific responses (Kalupahana and Moustaid-Moussa, 2011, 2012; Yvan-Charvet and Quignard-Boulangé, 2011). These biological responses are mainly mediated through two G-protein coupled receptors, angiotensin II (1-8) receptor type 1 (AT_1) and angiotensin II (1-8) receptor type 2 (AT_2) (Ramalingam et al., 2017). Angiotensin II (1-8) can also be cleaved by aminopeptidase A to angiotensin III (2-8). The latter follows a second round of cleavage via aminopeptidase B, to form angiotensin IV (3-8). Angiotensin IV (3-8) acts on the angiotensin receptor type 4 (AT_4) which is widely distributed in the brain and peripheral organs including the vessels, kidney, heart, prostate and the adrenals (de Gasparo *et al.*, 2000).

Angiotensin II has a dual role and can induce vasoconstriction or vasodilation, depending on its receptor specificity. Signalling via the AT_1 is mediated by protein kinases, G-protein derived second messengers and small G-proteins such as Rho, Ras and Rac (Higuchi *et al.*, 2007). In contrast, AT_2 signalling is mediated via sphingolipid signalling, protein tyrosine phosphorylation and NO production (Lemarié and Schiffrin, 2010). Literature suggests that AT_1 is more abundant than AT_2 and therefore AT_1 will dominate (Kalupahana and Moustaid-Moussa, 2011). Activation of AT_1 by angiotensin II (1-8) induces (a) vasoconstriction, (b) the release of aldosterone from the adrenal cortex in the kidneys, (c) sympathetic nervous system activation, and lastly (d) the release of the anti-diuretic hormone (ADH) from the pituitary gland (Schmieder *et al.*, 2007; Schlaich *et al.*, 2009). In contrast to AT_1, binding of angiotensin II (1-8) to AT_2 stimulates vasodilation, thus decreasing blood pressure (Schmieder *et al.*, 2007). Binding of angiotensin IV (3-8) to AT_4 is speculated to be responsible for the release vasodilators such as NO, increasing collagen accumulation in the heart (hypertrophied) and controlling the transport of Na^+ in the kidney (Sasaki *et al.*, 1991).

In the next section, the four most important mechanisms initiated in response to binding of angiotensin II (1-8) to AT_1, will be discussed.

(a) Vasoconstriction

Angiotensin II (1-8) can directly or indirectly induce vasoconstriction to elevate blood pressure. When angiotensin II (1-8) binds to AT_1 receptors located on the vascular smooth muscle cell surface, vasoconstriction is directly initiated. Indirectly, angiotensin II (1-8) binds to several brain structures (specifically those lacking a blood-brain barrier), thereby inducing the release of sympathetic discharge. In addition, angiotensin II (1-8) can initiate the release of norepinephrine from adrenergic varicosities present in the peripheral tissues (Montani and van Vliet, 2004). Once the baroreceptors sense that the blood pressure is adequately increased, the sympathetic nerve activity is decreased (Lohmeier *et al.*, 2000).

(b) Aldosterone

Aldosterone, is synthesized by the zona glomerulosa of the adrenal cortex (in the adrenal gland) and is released in response to angiotensin II (1-8) stimulation (Booth, Johnson and Stockand, 2002). This mineralocorticoid, is a well-known steroid hormone responsible for regulating the body's fluid and electrolyte balance in the kidneys, sweat glands, salivary glands and in the colon (Goodfriend, 2006). Aldosterone acts by binding to mineralocorticoid receptors present in the distal

tubules and collecting ducts of the nephron which increases the production of ion channels, thus elevating the excretion of K^+ into the urine, and the reabsorption of Na^+ and water into the kidney (Booth, Johnson and Stockand, 2002). As a result, the blood volume, and consequently the blood pressure, is increased.

(c) Sympathetic nervous system

Angiotensin II stimulates α1-adrenergic receptors which form part of the G protein-coupled receptor family. According to a molecular cloning study, the α1-adrenergic receptors can be subdivided into α1A, α1B and α1D (Zhong and Minneman, 1999). Once stimulated, all three α1-adrenergic receptor subtypes activate the Gq/11 signalling pathway. The Gq/11 signalling pathway entails the activation of PLC, generation of DAG and IP3 and consequently the acceleration of calcium inflow into the cell (Piascik and Perez, 2001; Pupo and Minneman, 2001).
The α1A adrenergic receptor is expressed in the prostate, controlling benign prostatic hypertrophy (Nagarathnam *et al.*, 1998) and the α1D receptor is expressed in the aorta regulating aortic contraction (Fan *et al.*, 2009). The definite location of the α1B adrenergic receptor is still unclear.
In addition, α2 adrenergic receptors are known to regulate blood pressure, and are subdivided into α2A/D, α2B and α2C. Signalling via the α2 receptors is mostly mediated via the pre-synaptic α2A receptors, which is known to specifically decrease blood pressure by inhibiting norepinephrine release. Contradictory to the α2A receptors, the α2B receptors are mostly present at the postsynaptic sites, where they increase blood pressure via vasoconstriction. Lastly, the α2C adrenergic receptors are responsible for hypothermic regulation and are not associated with any cardiovascular related effects (Joyner, Charkoudian and Wallin, 2010).

(d) ADH

ADH, also known as vasopressin, is synthesized in the hypothalamus and stored in the posterior pituitary. Angiotensin II (1-8), which is activated amongst others, in response to increased blood osmolarity, stimulates the release of ADH. ADH in turn initiates the reabsorption of water into the renal tubules, consequently increasing the fluid volume, cardiac output, vascular resistance and arterial pressure. Together all these changes result in blood pressure increase (Navar, 2014).

Negative feedback: The baroreceptors present in the blood vessels act as sensors whereby they detect the increase in the blood pressure induced by vasoconstriction, aldosterone, sympathetic activation and ADH. Consequently, a signal is sent to the hypothalamus, which in turn signals to the blood pressure effector organs including the kidneys and the heart. Vasodilation is initiated, the heart rate is decreased, and less water is reabsorbed by the kidneys (Torday, 2015).

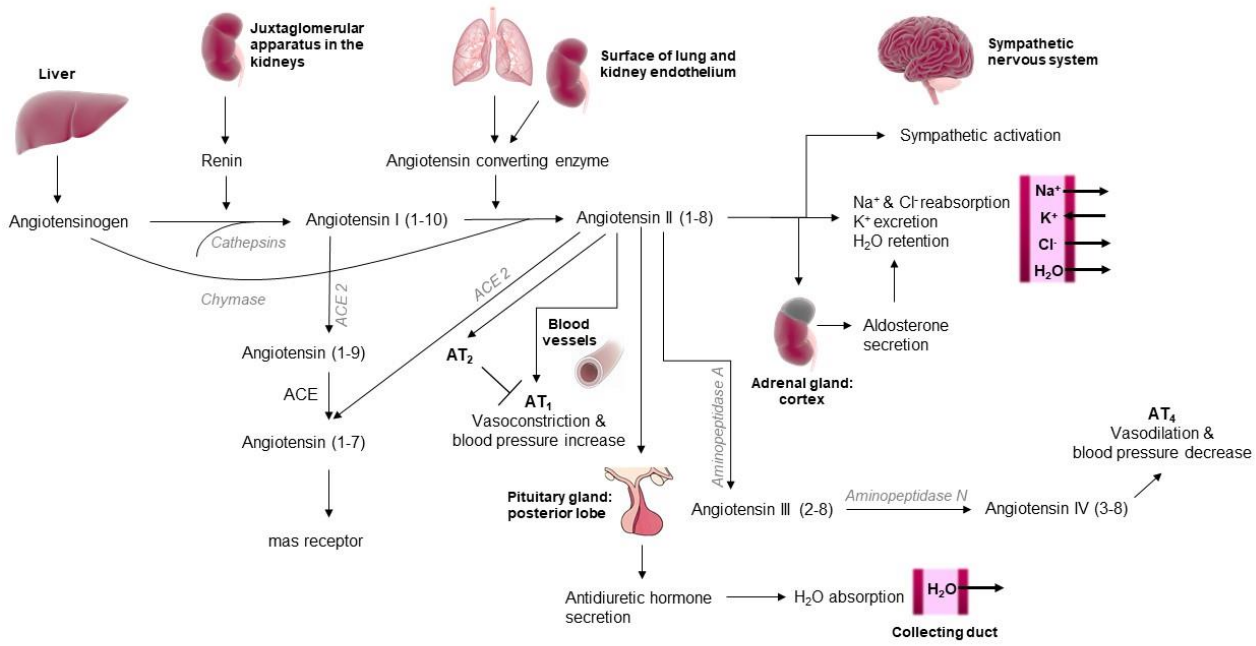

Figure 1.8: *The Renin-angiotensin system. Image adapted from:* (Rad, 2006; Kalupahana and Moustaid-Moussa, 2011) *and composed using* (*Library of Science & Medical Illustrations*, 2018)*.*

1.8.6. Endothelial dysfunction

Endothelial dysfunction refers to decreased bioavailability of vasodilators (predominantly NO) and/or increased EDCF (Lerman and Burnett, 1992) ***(Table 1.1)***. This imbalance results in impaired endothelium-dependent vasodilation and increased vasoconstriction, a known functional characteristic associated with endothelial dysfunction (Hadi, Carr and Al Suwaidi, 2005). Furthermore, endothelial dysfunction is characterized by the stimulation of pro-coagulatory, proinflammatory and proliferative conditions, thereby supporting all stages of atherogenesis (Anderson, 1999). If left untreated, endothelial dysfunction can progress to atherosclerosis, a condition associated with increased plaque formation together with elevated atherosclerotic complications (Anderson *et al.*, 1995).

1.8.6.1. Pathophysiology of endothelial dysfunction

Chronic exposure to cardiovascular risk factors such as obesity, hypertension, aging, smoking and diabetes, result in altered endothelial function (Reddy *et al.*, 1994; Bonetti, Lerman and Lerman, 2003) ***(Figure 1.9).*** Although the development of endothelial dysfunction is multifactorial,

oxidative stress appears to be most common mechanism responsible for the development of endothelial dysfunction (Park and Park, 2015).

Altered endothelial function results in elevated leukocyte adhesion and inflammation, lipid deposition, VSMCs proliferation, release of vasoconstrictors, platelet aggregation and thrombosis, all resulting in the progression of atherosclerosis and cardiovascular associated diseases (Park and Park, 2015). *These mechanisms were described in Chapter 1, Section 1.8.3.3.*

Early detection of endothelial dysfunction may be crucial in the prevention of atherosclerosis and cardiovascular associated diseases, since early identified endothelial dysfunction can still be reversed (Park and Park, 2015).

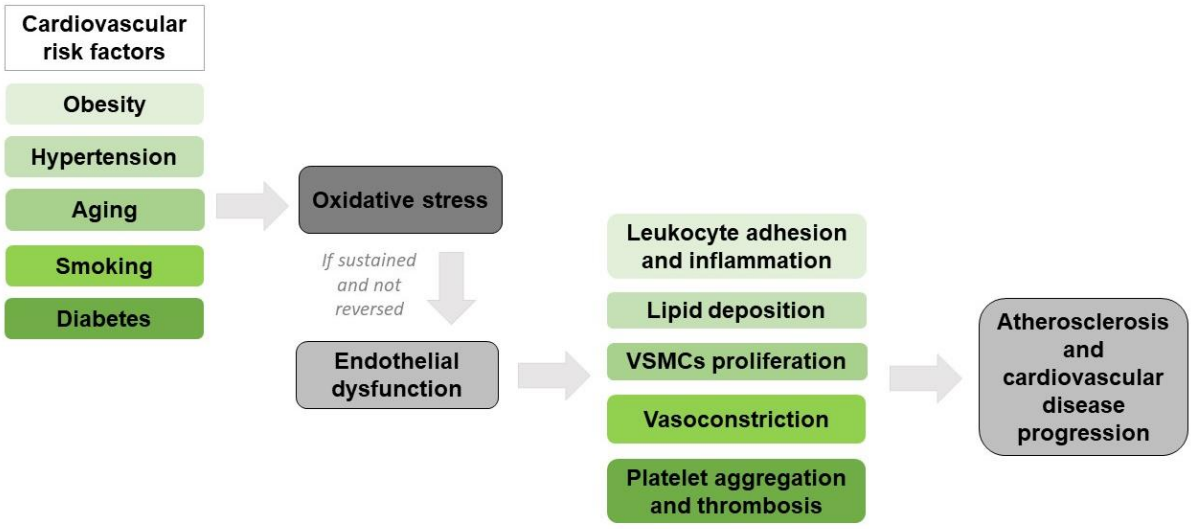

Figure 1.9: *Pathophysiology of endothelial dysfunction. Image adapted from (Park and Park, 2015) and composed using Microsoft PowerPoint.*

In the next section, the link between oxidative stress and endothelial dysfunction will be discussed since oxidative stress appears to be the most common mechanism responsible for the development of endothelial dysfunction (Park and Park, 2015).

1.8.6.2. Oxidative stress and endothelial dysfunction

Oxidative stress, in the context of endothelial dysfunction, refers to the imbalance between NO and ROS levels (Higashi *et al.*, 2014). Under normal physiological and tightly regulated conditions, endothelial cells produce ROS (O_2•- and hydrogen peroxide (H_2O_2)) to act as second messengers in redox signalling (de Dios, Sobey and Drummond, 2010). Endogenous defence mechanisms regulating ROS under normal conditions include SOD, which catalyses the dismutation of O_2•- into

H_2O_2 and water, glutathione peroxidase (GPx) which reduces H_2O_2 to water, and catalase (CAT) which elevates the decomposition of H_2O_2 to oxygen and water (Fridovich, 1975).

Cardiovascular risk factors are, however, associated with the activation of xanthine oxidase, NADPH oxidase, cyclooxygenase and mitochondrial electron transport, the inactivation of antioxidant production and increased eNOS uncoupling, all resulting in elevated ROS production (Higashi *et al.*, 2014).

As a result, O_2•- and H_2O_2 escape detoxification via the antioxidant cellular pathways. O_2•- rather directly interacts with NO to form $ONOO^-$, and H_2O_2 with O_2 to generate hydroxyl radicals (OH·). Both OONO- and OH· are associated with the development of endothelial dysfunction via increased oxidative damage to cellular macromolecules, initiation of pro-inflammatory signalling pathways and NO signalling impairment (de Dios, Sobey and Drummond, 2010).

1.8.6.3. Atherosclerosis

Atherosclerosis is a chronic disease characterized by hardened blood vessels due to plaque build-up within the arterial walls. As a result, blood vessels are narrowed and blood flow is restricted. Classical risk factors associated with atherosclerosis development include diabetes, hypertension, dyslipoproteinaemia, smoking and genetic abnormalities (Bergheanu, Bodde and Jukema, 2017).

Elevated cholesterol (hypercholesterolaemia) is considered to be one of the main causes of atherosclerotic plaque formation and can therefore serve as a model of atherosclerosis. Increased plasma cholesterol levels are associated with increased arterial endothelial permeability, consequently allowing the passive migration of low-density lipoprotein cholesterol (LDL-C) into the arterial wall (Bergheanu, Bodde and Jukema,2017) ***(Figure 1.10***).

Once in the intima, LDL is oxidised (oxLDL) by ROS and reactive nitrogen species (RNS) (Navab *et al.*, 1996; Madamanchi, Vendrov and Runge, 2005). OxLDL stimulates the release of MCP-1 from both the endothelial cells and VSMCs, which in turn increases the recruitment of monocytes to the adhesion proteins (selectins and vascular adhesion molecule-1 (VCAM-1) (Madamanchi, Vendrov and Runge, 2005). Once adhered, monocytes travel via diapedesis into the subendothelial space (Sakakura *et al.*, 2013), where they obtain macrophagic characteristics (Naseem, 2005) via oxLDL. This transformation is typical of an inflammatory phase (Naseem, 2005). Macrophages release several ROS, which convert oxLDL into highly oxidised LDL (Madamanchi, Vendrov and Runge, 2005). oxLDL also increases the release of macrophage

colony stimulating factor (CSF), a known growth factor (Rajavashisth *et al.*, 1990). CSF initiates the expression of a scavenger receptor on the macrophage, which allows the absorption of the highly oxidised oxLDL to form foam cells (Lusis, 2000; Sakakura *et al.*, 2013). Foam cells refers to macrophages containing high levels of cholesterol lipids (Fielding and Fielding, 1995). These cells, in turn, increase the release of cytokines which subsequently induce VSMC proliferation. Due to collagen deposition from the VSMC, a so-called fibrous cap develops. Atherosclerotic plaques differ in fibrous cap thickness and the number of macrophages and lipids present. Plaques with a thin cap are more susceptible to small tears. Pro-thrombotic protein leakage will result in the activation of blood platelets via the initiation of a coagulation cascade. Elevated blood platelets form a thrombus, consequently restricting blood flow (Naseem, 2005).

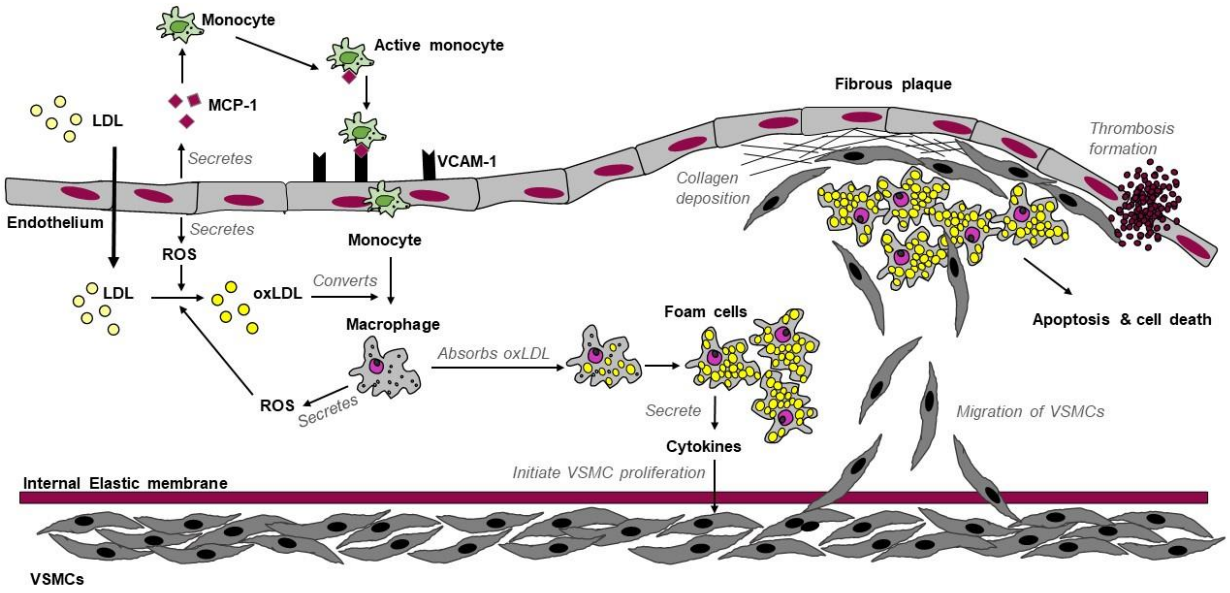

Figure 1.10: *Atherosclerotic plaque formation. Image adapted from (Madamanchi, Vendrov and Runge, 2005; Naseem, 2005) and composed using Microsoft PowerPoint.*

From all the cardiovascular risk factors associated with the development of endothelial dysfunction and atherosclerosis, we are specifically interested in obesity-induced insulin resistance and hypertension, therefore the link between these risk factors will be discussed in the following section.

1.9. Hypertension

1.9.1. Overview of hypertension

Hypertension is a condition characterized by a systolic blood pressure reading higher than or equal 140 mm Hg or a diastolic blood pressure reading higher than or equal to 90 mm Hg (Russo *et al.*, 2018).

Blood pressure is defined as the force (pressure) of systemic circulating blood on the arterial walls (Foëx and Sear, 2004). Blood pressure is recorded as two measurements, the systolic measurement (top measurement) which refers to the amount of pressure against the arterial wall when the blood is pumped from the contracting heart, whereas the diastolic measurement (bottom measurement) refers to the amount of pressure against the arterial wall when the heart is resting between every heartbeat (American Heart Association, 2017). According to the WHO, a typical blood pressure measurement in humans is 120/80 millimetres of mercury (mm Hg) (World Health Organization, 2015).
When a sustained increase in blood pressure is left untreated, the severity of hypertension will progress resulting in the development of structural and functional vascular and cardiac abnormalities. In turn, these abnormalities can result in premature morbidity or even death (Giles *et al.*, 2005).

Specifically important for the current study, hypertension is globally a key risk factor for cardiovascular diseases, heart failure and stroke (Vasan *et al.*, 2002; Chobanian *et al.*, 2003; Duckitt and Harrington, 2005). According to previous studies, low-and middle-income countries have more than two-thirds of people suffering from hypertension (Lim *et al.*, 2012).

In 2014, 22 % of adults (aged 18 and above) were globally suffering from hypertension (*WHO | World Health Organization*, 2015) and since the prevalence of hypertension is still markedly increasing, it is estimated that in the year 2025, more than 500 million people will globally be affected (Fuentes *et al.*, 2000; Kearney *et al.*, 2005).

In South Africa, 28 % of the adult population presents with hypertension (*WHO | World Health Organization*, 2015), with a higher prevalence in women compared to men (Steyn *et al.*, 2001). Since South Africa is classified as a country undergoing epidemiological transition, with a shift to more energy-dense diets and sedentary lifestyles, this subsequent increase in the prevalence of hypertension is expected (Thorogood *et al.*, 2007; Gómez-Olivé *et al.*, 2013; Peltzer and Phaswana-Mafuya, 2013; Lloyd-Sherlock *et al.*, 2014).

Hypertension can be subdivided into essential (primary) or secondary hypertension. More than 95 % of adults are diagnosed with essential hypertension – hypertension without an identifiable cause (Gupta-Malhotra *et al.*, 2015). Although the exact cause of essential hypertension is still unidentified, several non-modifiable and modifiable risk factors can be associated with the condition. Non-modifiable risk factors include: sex, age, family history, race, and genetic composition whereas modifiable risk factors include: high fat diet, obesity, excessive salt intake, smoking, alcohol consumption and inactivity (Ibekwe, 2015).

Secondary hypertension occurs only in a small number of adult patients and refers to high blood pressure caused by an additional medical condition such as obstructive sleep apnoea, aldosteronism and renal artery stenosis (Puar *et al.*, 2016).

1.9.2. Stages of hypertension

The severity of changes in diastolic and systolic blood pressure together with the presence or absence of potential cardiovascular disease markers are used as an indicator for hypertension stage categorization; whereas priority is given to cardiovascular status. The progression of hypertension from early to advanced is characterized as hypertension stage 1, stage 2 and stage 3 (Giles *et al.*, 2009) ***Table 1.2***.

Table 1.2: *Stages of hypertension. Table adapted from (Giles et al., 2009; Whelton et al., 2018).*

	Normal	Hypertension Stage 1	Hypertension Stage 2	Hypertensive Crisis Stage 3
Blood pressure	< 120/80 mm Hg	130-139/80-89 mm Hg	140/90 mm Hg	> 180/120 mm Hg
Description	Well balanced blood pressure Absence of cardiovascular diseases	Occasional blood pressure increase Early cardiovascular diseases are present	Sustained blood pressure increase or Increasing cardiovascular disease development	Marked blood pressure increase or Advanced cardiovascular diseases present
Cardiovascular associated risk factors	None or very little	A few risk factors are present	Many risk factors are present	Many risk factors are present
Target organ tissue	None	None	Early signs	Openly present with or without cardiovascular disease events
Presence of early disease markers	None	Normally present	Openly present	Openly present with gradual movement towards a more advanced state

1.9.3. Pathophysiology of hypertension

1.9.3.1. Link between obesity and hypertension

Obesity is a major risk factor for type II diabetes, hypertension, coronary disease, hyperlipidemia, heart failure and several cancers (Strumpf, 2004; Bloomgarden, 2006).

To date, the exact mechanism by which obesity causes hypertension remains unclear (Jiang *et al.*, 2016); however the pathogenesis of obesity-related hypertension is speculated to be closely associated with sympathetic nervous system and RAS activation, the amount of intra-vascular and intra-abdominal fat and sodium retention (Jiang *et al.*, 2016).
A diet high in fat and carbohydrates increases the stimulation of norepinephrine release, which in turn binds to peripheral α1 and β-adrenergic receptors. Once activated, the sympathetic activity is increased, vasoconstriction is initiated, and the blood pressure is increased (Rocchini, Yang and Gokee, 2004).

Individuals suffering from obesity have increased plasma renin, angiotensinogen, ACE and angiotensin II levels (Hall, 2003). Increased angiotensin II is associated with increased sodium reabsorption and renal-pressure natriuresis (increased sodium loss) impairment, causing hypertension (Segura and Ruilope, 2007). The adipose tissue serves as an important site for the production of angiotensinogen (Ailhaud *et al.*, 2000). The overexpression of angiotensinogen in the adipose tissue results in adipocyte hypertrophy, the development of hypertension via angiotensin II, increased systemic vasoconstriction, sodium and water retention and elevated aldosterone levels (Massiéra *et al.*, 2001; Yiannikouris *et al.*, 2012).

Angiotensin II overexpression is also linked to adipocyte proliferation and differentiation (Ailhaud, 1999), increased leptin (Cassis *et al.*, 2004) and decreased adiponectin (Ran *et al.*, 2006) secretion from adipocytes and enhanced sympathetic activity. Elevated leptin and decreased adiponectin is associated with decreased insulin sensitivity and atherosclerosis development (Okamoto *et al.*, 2002; Osegbe, Okpara and Azinge, 2016). Aldosterone is implicated in the development of hypertension due to obesity (Rahmouni *et al.*, 2005). Obesity-induced hypertension is associated with increased aldosterone levels, especially in individuals who present with visceral obesity (Goodfriend and Calhoun, 2004). To date, the exact mechanisms whereby obesity increases aldosterone levels is still unknown; but it is suggested to relate to potent mineralocorticoid releasing factor production from the adipocytes (Ehrhart-Bornstein *et al.*, 2003)

or to the synthesis of aldosterone via linoleic acid (specifically the oxidised derivatives) (Goodfriend *et al.*, 2004).

Excess visceral fat may result in physical renal compression, thereby increasing tubular reabsorption and intrarenal pressures. Sustained obesity in response to insulin resistance (specifically due to elevated angiotensin II and insulin), results in glomerular hyperfiltration (Gallagher, 2005), subsequently changing the structure of the kidneys (focal segmental glomerulosclerosis and glomerular hypertrophy (Naumnik and Myśliwiec, 2010). Once the kidneys are injured (due to cytokines released from the adipose tissue), the glomerular filtration rate is continuously decreased, resulting in additional arterial pressure which escalates cardiovascular-related morbidity and mortality (Naumnik and Myśliwiec, 2010).

Lastly, obesity also results in hypercholesterolemia and the release of FFAs into the blood (Kwok *et al.*, 2010). The FFAs are released from phospholipids where after they can directly act on membrane located ion channels of smooth muscle cells (Ordway, Singer and Walsh, 1991) or phosphorylate the calcium-independent isoenzyme of PKC (Khan *et al.*, 1993). When FFAs bind to Na/K-ATPase, the activation of the epidermal growth factor is initiated, which in turn increase ROS production (Oishi, Zheng and Kuo, 1990). Increased ROS production is associated with endothelial dysfunction.

In obese subjects, endothelial dysfunction is mainly the result of decreased NO generation, increased oxidative stress or the result of increased pro-inflammatory cytokines (Ferrario and Schiavone, 1989). Endothelial dysfunction results in vasoconstriction and vascular resistance, which are closely associated with the development of hypertension (Poirier *et al.*, 2006).

1.9.3.2. Link between insulin resistance and hypertension

The co-occurrence of insulin resistance together with hypertension can be seen (a) as a cause effect relationship, thus insulin resistance results in hypertension or vice versa, or (b) as a non-directional association. There are several mechanisms identified whereby insulin resistance results in blood pressure elevation. These mechanisms include: sympathetic nervous system activation, amplified renal sodium reabsorption, hypertrophy of resistance vessels and transmembrane ion transport alterations (Salvetti *et al.*, 1993).

On the other hand, hypertension results in insulin resistance when it alters insulin and glucose delivery to the skeletal muscle cells, thereby preventing adequate glucose uptake by the cells.

Hypertension also causes vascular structural changes, such as thickening of artery walls, reducing vessels in microcirculation, lengthening of small arteries, and remodelling of small muscular arteries consequently increasing the wall to lumen ratio (Thom, 1997). Together these changes increase vasoconstriction and decrease vasodilation.

Non-directionally, both insulin resistance and hypertension represent with two independent consequences of a similar metabolic disorder, that is, accumulation of intracellular free calcium, which can result in both impaired insulin action and vasoconstriction (Salvetti *et al.*, 1993; Soleimani, 2015).

1.9.4. Hypertension treatment

The first step in treating hypertension would be the implementation of lifestyle modifications. These modifications include bodyweight reduction, limited sodium intake, increased exercise and decreased alcohol consumption. If the above-mentioned measures were unsuccessful in lowering blood pressure, or if hypertension stage 3 is already diagnosed, drug therapy would immediately be prescribed (Foëx and Sear, 2004).

Anti-hypertensive drugs act by decreasing peripheral vascular resistance, cardiac output, or both. The most common anti-hypertensive drugs used are: β-blockers, ACE inhibitors, diuretics, angiotensin II receptor antagonists, calcium channel blockers, direct vasodilators and α1-adrenergic blockers (Foëx and Sear, 2004). Anti-hypertensive drugs with their specific target and mechanism are summarized in ***Table 1.3.***

Table 1.3: *Anti-hypertensive drugs. Table composed using the following references: (Foëx and Sear, 2004; Beta-Blockers: Function and Effects | MU Science Blog, 2010; Klabunde, 2017).*

	Treatment	Mechanism
β-blockers	• Angina • High sympathetic tone • Previously diagnosed myocardial infarction	• Inhibit binding of the hormone epinephrine, which in turn reduces heart rate, increases vasodilation and decreases blood pressure.
ACE inhibitors	• Diabetes-associated hypertension • Hypertension together with heart failure	• Inhibit the conversion of angiotensin I to angiotensin II, thus decreasing vasoconstriction and blood pressure.
Loop Diuretics	• Heart failure • High blood pressure • Liver disease • Kidney disease	• Inhibit the Na^+-K^+-Cl^- co-transporter present in the thick ascending loop. Once inhibited, sodium concentration in the distal tubular is increased, hypertonicity in the surrounding interstitium is reduced and water reabsorption in the collecting duct is reduced. The Na^+ and water alterations results in increased water loss (diuresis) together with increased natriuresis.
Thiazide diuretics		• Inhibit the Na^+-Cl^- transporter present in the distal tubule. Less efficient than loop diuretics.
K^+- sparing diuretics		• Acts as an aldosterone receptor antagonists, consequently increasing the amount of Na^+ and water entering the collecting duct, which in turn is excreted into the urine.
Angiotensin II receptor blockers	• Stroke-related incidents • Hypertrophy of the left ventricle	• Preventing the binding of angiotensin II to AT_1.
Calcium channel blockers	• Vascular resistance	• Disrupt the movement of calcium through calcium channels, consequently relaxing blood vessels.
α1-Adrenergic blockers	• Peripheral vascular resistance • Elevated cholesterol levels	• Inhibit the α1-adrenergic receptors present in the smooth muscle, central nervous system and the arteries, thus preventing norepinephrine binding.

1.10. Rooibos (*Aspalathus linearis*)

1.10.1. Background and composition of rooibos

Rooibos is a well-known South African fynbos plant, growing predominantly in the Cederberg region of the Western Cape Province of South Africa (McKay and Blumberg, 2007; van Niekerk and Viljoen, 2008), with most of its commercial production conducted in the Clanwilliam, Cederberg and Cirtusdal areas (Joubert, 1996). The rooibos plant is also present, and cultivated, in the Niewoudtville area, situated in the Northern Cape. Since the temperatures in Clanwilliam and Citrusdal are higher when compared to Nieuwoudtville, the product quality from the regions can differ as rooibos processing is an open-air process (Joubert, 1996).

Rooibos is a popular caffeine-free and low tannin (Canda, Oguntibeju and Marnewick, 2014) herbal tea (van Wyk and Verdoorn, 1989), consumed in more than 37 countries (Joubert and De Beer, 2011). Tannins, water-soluble polyphenols, are present in numerous plant foods, and responsible for decreases in feed efficacy, feed intake, growth rate, net metabolizable energy and protein digestion. Thus, food with high tannin levels are associated with low nutritional capabilities (Chung *et al.*, 1998).

Rooibos contains two unique phenolic compounds, namely aspalathin (Koeppen and Roux, 1965), a C-linked dihydrochalcone glucoside and aspalalinin (Shimamura *et al.*, 2006), a cyclic dihydrochalcone. Another rare C-linked dihydrochalcone glucoside, nothofagin, is also identified in rooibos, where it was previously only identified in the heartwood of Nothofagus fusca (Hillis and Inoue, 1967) ***(Figure 1.11)***. Additional major phenolic compounds present in rooibos include flavones (chrysoeriol, vitexin, isovitexin, orientin, isoorientin and luteolin), flavanones (dihydro-isoorientin, hemiphlorin and dihydro-orientin) and flavonols (quercetin, isoquercitrin, hyperoside and rutin) (Koeppen, Smit and Roux, 1962; Rabe, Joubert and Ferrema, 1994; Ferreira *et al.*, 1995; Marais *et al.*, 2000; Shimamura *et al.*, 2006).

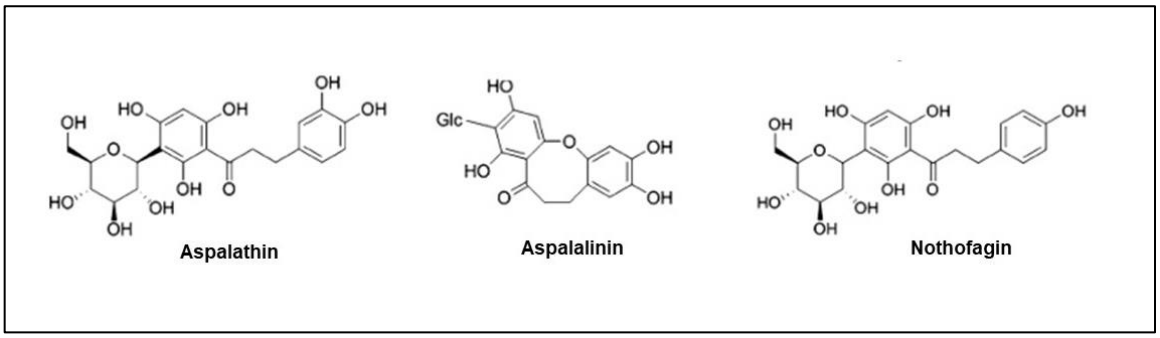

Figure 1.11: *Chemical structures of specific flavonoids present in rooibos, namely aspalathin, aspalalinin and nothofagen. Image adapted from (Joubert et al., 2008).*

1.10.2. Processing of rooibos – "fermented" versus "unfermented"

After the young stems and cut leaves are harvested and bruised, a "fermentation" process is conducted. "Fermentation" refers to the oxidative process where green rooibos is degraded to a red-brown "fermented" product, via two identified mechanisms (Krafczyk *et al.*, 2009).

The first proposed mechanism involves the oxidation of aspalathin to dihydro-isoorientin ((R)- and (S)-eriodictyol-6-C-glucoside) and dihydro-orientin ((R)- and (S)-eriodictyol-8-C-glucoside) respectively. Dihydro-isoorientin can be directly oxidized to the flavone, isoorientin, whereas dihydro-orientin is dependent on the formation of isoorientin's intermediate chalcone to generate orientin (Krafczyk and Glomb, 2008; Krafczyk *et al.*, 2009).

The second mechanism entails the formation of colourless aspalathin dimers (Krafczyk *et al.*, 2009) together with coloured substances i.e. dibenzofurans (Heinrich, Willenberg and Glomb, 2012). The colourless substances degrade over time, whereas the dibenzofurans result in the typical red-brown colour associated with fermented rooibos.

Fermented rooibos is associated with a substantial reduction in aspalathin content (Joubert, 1996) and accordingly anti-oxidative capabilities (Joubert *et al.*, 2008). More specifically, previous research reported that green rooibos presents with roughly forty-five times more aspalathin when compared to fermented rooibos (Schulz, Joubert and Schütze, 2003). Due to the latter, interest in green rooibos was and is still of major interest.

The processing method of unfermented rooibos is adapted in such a manner that the leaves are immediately dried after harvesting, thus minimizing the oxidation (fermentation) of its polyphenols. As a result, the green colour is retained; and therefore, termed as green rooibos (Schulz, Joubert

and Schütze, 2003; Joubert and De Beer, 2011). Since green rooibos is associated with a higher phenolic content when compared to fermented rooibos, it is the most commonly used rooibos to produce aspalathin-rich extracts for the nutraceutical market and the food industry.

Green rooibos extract (GRE) refers to a aspalathin-rich spray-dried powder prepared from green rooibos (Kamakura *et al.*, 2015). The GRE used in our study, namely Afriplex GRT™ extract, was specifically developed by the Medical Research Council in collaboration with Afriplex for research purposes.

According to high-performance liquid chromatography (HPLC) analysis (Beelders, 2011), also conducted by the Medical Research Council, the Afriplex GRT™ extract presented with the following phenolic compounds in g/100g soluble solids: phenyl pyruvic acid glucoside (0.42), aspalathin (12.78), nothofagin (1.97), isoorientin (1.43), orientin (1.26), vitexin (0.34), isovitexin (0.30), Q-3 ROB (1.04), hyperoside (0.40), rutin (0.50) and isoquercetin (0.57).

In the next section, polyphenols, the benefits of polyphenols and polyphenolic-related antioxidant actions will be discussed since the majority of rooibos' effects can be ascribed to its high polyphenolic content.

1.10.3. Polyphenols

Polyphenols are defined as naturally occurring chemical compounds which are predominantly found in vegetables, fruits, beverages and cereals (Pandey and Rizvi, 2009). Moreover, polyphenols are classified as secondary metabolites of plants, where they act in a defensive manner against ultraviolet radiation or pathogen aggression (Beckman, 2000). The bitterness, odour, colour, and oxidative stability of foods are closely related to the polyphenols present within the food (Pandey and Rizvi, 2009). A diet rich in plant polyphenols is associated with increased protection against the development of several diseases, such as diabetes, cardiovascular diseases, osteoporosis, cancers and neurodegenerative diseases (Arts and Hollman, 2005; Graf, Milbury and Blumberg, 2005).

Polyphenols can be subdivided into several subgroups, depending on the number of their phenolic rings and the foundation of the structural elements present to ensure binding between these rings. The main classes of polyphenols are: phenolic acids, flavonoids, lignans and stilbenes (Spencer *et al.*, 2008) ***(Figure 1.12)***.

Phenolic acids are abundant in foods and can be subdivided into derivatives of cinnamic acid and derivatives of benzoic acid. Hydroxycinnamic acid levels are more pronounced in food when compared to the hydroxybenzoic acid content. Known hydroxycinnamic acids include: ferulic, p-coumaric, caffeic, and sinapic acids (Pandey and Rizvi, 2009).

Flavonoids are to date the best studied group of polyphenols with more than 4000 identified varieties. Characteristic to flavonoids is their ability to give plants, flowers and fruits their attractive colours (de Groot and Rauen, 1998). Furthermore, flavonoids also have a unique basic structure with two aromatic rings linked by three carbon atoms, thus forming an oxygenated heterocycle. Depending on the heterocyclic composition of the flavonoid, it can be subdivided into six different classes namely: flavonols, flavanols, flavones, isoflavones, flavanones and anthocyanins (Pandey and Rizvi, 2009) ***(Figure 1.12)***. Variation in the subgroups is associated with the number and arrangement of hydroxyl groups together with their degree of glycosylation and/or alkylation (Spencer *et al.*, 2008). Common flavonoids include: myricetin, catechins, quercetin (Pandey and Rizvi, 2009) and rutin (Panche, Diwan and Chandra, 2016).

Lignans are defined as bioactive, non-caloric, and non-nutrient phenolic plant compounds predominantly present in sesame and flax seeds (Peterson *et al.*, 2010). Furthermore, lignans are classified as diphenolic compounds containing a 2,3-dibenzylbutane structure, which is formed in response to the dimerization of two cinnamic acid residues (Pandey and Rizvi, 2009).

Stilbenes are formed by two phenyl parts which are linked by a two-carbon methylene bridge. The occurrence of stilbenes in the human diet is relatively small. Overall, most plant stilbenes are associated with the generation of antifungal phytoalexins specifically in response to an infection or injury. The most well-known and best studied stilbene is resveratrol (3,4′,5-trihydroxystilbene), found abundantly in grapes (Pandey and Rizvi, 2009).

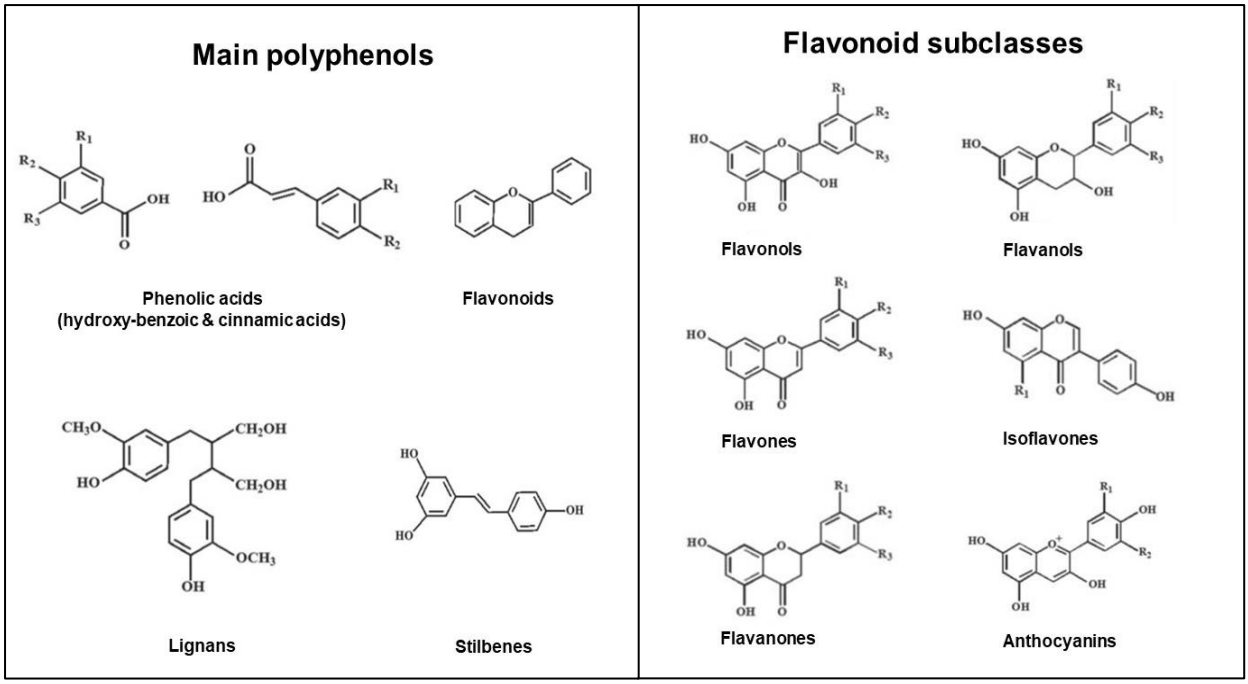

Figure 1.12: *Chemical structures of main polyphenols and flavonoid subclasses. Image adapted from (Pandey and Rizvi, 2009).*

1.10.3.1. Benefits of polyphenols

Several epidemiological studies suggested that a diet rich in polyphenols, such as vegetables, tea, wine and cocoa may result in cardiovascular protection (Renaud and de Lorgeril, 1992; Hertog *et al.*, 1993, 1995; Knekt *et al.*, 1996; Hertog, Feskens and Kromhout, 1997; Yochum *et al.*, 1999; Rein, Paglieroni, *et al.*, 2000(a); Nakachi *et al.*, 2000; Arts *et al.*, 2001; Arts and Hollman, 2005; Mink *et al.*, 2007).

Flavonol, flavanol and flavone intake was shown to reduce the development of coronary heart disease (Arts and Hollman, 2005), whereas the consumption of flavanones reduced the incidence of cardiovascular disease related mortality (Mink *et al.*, 2007). Several studies performed on animals, humans and cells, showed that polyphenols contain antioxidant properties (Stein *et al.*, 1999; Rein, Lotito, *et al.*, 2000; Wan *et al.*, 2001) which lowers blood pressure (Taubert, Roesen and Schömig, 2007; Erlund *et al.*, 2008; Hooper *et al.*, 2008; Desch *et al.*, 2010), inhibits platelet aggregation (Rein, Paglieroni, *et al.*, 2000(b); Keevil *et al.*, 2000; Pearson *et al.*, 2002; Erlund *et al.*, 2008) and LDL oxidation (Mathur *et al.*, 2002), improves endothelial function (Heiss *et al.*, 2003, 2005, 2007; Grassi *et al.*, 2005, 2009; Schroeter *et al.*, 2006; Wang-Polagruto *et al.*, 2006; Widlansky *et al.*, 2007), and reduce inflammation (Mao *et al.*, 2002; Schramm *et al.*, 2003). Together, these improvements may be beneficial in terms of the vascular system (Vauzour *et al.*, 2010).

One of the mechanisms whereby polyphenols act on the vascular system involve the modulation of eNOS, and consequently the bioavailability of NO to the endothelium (Fitzpatrick *et al.*, 1995; Leikert *et al.*, 2002; Wallerath *et al.*, 2002; Heiss *et al.*, 2003; Appeldoorn *et al.*, 2009; Schmitt and Dirsch, 2009). This regulation of NO production is speculated to be the result of polyphenols interacting with several signalling pathways such as the PI3K-dependent pathway and intracellular calcium, which in turn, activates eNOS (Lorenz *et al.*, 2004; Stoclet *et al.*, 2004). Furthermore, many polyphenols also increase the expression of eNOS and PGI_2 production and inhibit NADPH oxidase, ET-1 (Corder *et al.*, 2001; Wallerath *et al.*, 2002; Steffen, Schewe and Sies, 2007; Steffen *et al.*, 2008), vascular cell migration/proliferation, angiogenesis, matrix metalloproteinase (MMP) activation (Stoclet *et al.*, 2004) and platelet aggregation (Pignatelli *et al.*, 2000; Freedman *et al.*, 2001).

Lastly, both flavanols and flavonols are suggested to prevent advanced glycation end product (AGE) related vascular-injury (Schramm and German, 1998; Peppa and Raptis, 2008) by (a) regulating the MAPK signalling pathway via the receptor for advanced glycation end products (RAGE) (Huang, Wu and Yen, 2006) and (b) by reducing NF-kB, thus suppressing NADPH oxidase (Kim *et al.*, 2010).

1.10.3.2. Polyphenolic-related antioxidant actions

(a) Radical scavenging

Free radicals are defined as extremely unstable and highly reactive atoms or molecules containing one or more unpaired electron in an atomic orbital. Due to the presence of unpaired electrons, these molecules are capable of donating or accepting an electron to or from other molecules, thus acting as oxidants or reductants (Cheeseman and Slater, 1993).

In humans, free radicals and ROS are formed in response to normal essential metabolic processes, or in response to external factors such as smoking, x-rays, industrial chemicals, ozone and air pollutants (Bagchi and Puri, 1998). Free radical generation is enzymatic and non-enzymatic related (Lobo *et al.*, 2010), and has both beneficial as well as deleterious effects (Valko *et al.*, 2006). Enzymatic reactions include prostaglandin synthesis, phagocytosis and the involvement in respiratory chain and the cytochrome P-450 system (Liu *et al.*, 1999). Non-enzymatic reactions include the binding of oxygen with organic compounds as well as ionizing reactions (Lobo *et al.*, 2010).

During disease states, the following highly reactive oxygen-containing free radicals are produced, O_2•-, OH·, H_2O_2, $ONOO^-$, NO, hypochlorite (ClO−) and singlet oxygen ($^1O_2$). Reactions with free

radicals, usually branched chain reactions, damage biologically relevant molecules such as proteins, lipids, DNA and carbohydrates (Young and Woodside, 2001).

Antioxidants are defined as stable molecules which are capable of donating an electron to a free radical, thus reducing its deleterious effects. The delay in cellular and vital molecule damage can be ascribed to the free radical scavenging properties of antioxidants (Halliwell, 1995). During normal metabolism in the body, several antioxidants including ubiquinol, glutathione and uric acid are generated (Shi, Noguchi and Niki, 1999). Since the body is unable to produce additional antioxidants, a diet rich in antioxidants is crucial. Key micronutrient antioxidants include vitamin C, vitamin E and B-carotene (Levine *et al.*, 1999).

(b) Flavonoids: Antioxidant activity and interaction with cell membranes

Flavonoids compete with natural ligands for binding to the active sites of nitrogen and oxygen producing enzymes, such as lipoxygenases, NOS, oxidoreductases, xanthine oxidase and NADPH-oxidase. Binding to these enzymes results in optimal antioxidant activity (Korkina *et al.*, 2009).

Furthermore, hydrophobic flavonoids (flavonoids with fewer OH· groups) can interact with the hydrophobic core of cell membranes. This interaction results in the modulation of the membrane's physical properties to increase free radical scavenging and to some extent also inhibit the lipid oxidation chain reaction. Hydrophilic flavonoids (flavonoids with more OH· groups) interact with the polar head groups at the lipid-water border of cell membranes, thus providing a level of protection against the movement of free radicals into the cell (Oteiza *et al.*, 2005).

(c) Metal chelation

Structurally, flavonoids present with detailed coordination sites within its core, which allows the formation of complexes with metal ions. This process is termed metal chelating (Symonowicz and Kolanek, 2012). The newly formed flavonoid-metal complexes are associated with higher radical scavenging abilities (Kostyuk *et al.*, 2001), whereas the antioxidant activity is dependent on the transfer potential of the electron or the ease in which the molecule can accept or transfer electrons from/to another molecule (Fraga *et al.*, 2010).

1.10.4. Health benefits of Rooibos

The potential health benefits of rooibos are mainly ascribed to its phenolic content (Joubert and De Beer, 2011). According to Marnewick et al. (2011), the daily consumption of 6 cups of rooibos within a period of 6-weeks resulted in optimal rooibos-related health benefits (Marnewick *et al.*, 2011).Some of these benefits include anti-carcinogenic, anti-mutagenic, anti-inflammatory and anti-viral properties (Marnewick *et al.*, 2005, 2009; Joubert *et al.*, 2008; Fukasawa, Kanda and Hara, 2009). Specifically of interest for the current study, rooibos was also shown to induce anti-hypertensive (Persson *et al.*, 2010), anti-diabetic (Muller *et al.*, 2012) and anti-atherosclerotic (Canda, Oguntibeju and Marnewick, 2014) effects, and decrease lipid peroxidation (Marnewick *et al.*, 2011) and blood glucose levels (Muller *et al.*, 2012).

In streptozotocin induced diabetic rats, treatment with fermented rooibos extract (**FRE**) has been shown to reduce diabetic-mediated H_2O_2 levels as well as ischemia-induced oxidative stress (Ulicná *et al.*, 2006). Furthermore, FRE increased oxygen radical absorbance capacity (indicative of increased antioxidant capacity), liver SOD levels and decreased plasma thiobarbituric acid reactive substances in the same animal model (Ayeleso, Brooks and Oguntibeju, 2014), suggesting that treatment with FRE has anti-oxidative potential.

Acute and sub-chronical oral administration of **GRE** has been shown to significantly decrease glucose levels in diabetic animals (Muller *et al.*, 2012). The mechanism whereby acute GRE improves insulin sensitivity might be due to improved glucose uptake in the liver (Muller *et al.*, 2012) and muscle (Muller *et al.*, 2012; Kamakura *et al.*, 2015), in response to increased AMPK and PKB activation, which in turn increase GLUT4 vesicle translocation to the plasma membrane (Kamakura *et al.*, 2015). Treatment with GRE is furthermore associated with reduced H_2O_2-induced oxidative stress and AGE in the pancreatic β-cells (Kamakura *et al.*, 2015). The reduction in oxidative stress has been shown to exert protective effects against DNA damage, which in turn inhibits lipid oxidation (Gelderblom *et al.*, 2017).
In addition, GRE also had the ability to reverse palmitate-induced insulin resistance and to suppress inflammation via the inhibition of NF-κB in 3T3-L1 adipocytes (Mazibuko *et al.*, 2015). It is suggested that the total antioxidant activity of GRE can be ascribed to its aspalathin content and that the glucose lowering benefits of GRE are resultant of its involvement in several organs such as the liver, pancreas, muscle and adipose tissue (Joubert *et al.*, 2008).

Health benefits of **aspalathin** is positively correlated to its bioavailability or to the way in which it is metabolised by the body (Snijman *et al.*, 2007). Treatment of streptozotocin induced diabetic rats with only aspalathin was less effective in lowering glucose levels when compared to treatment

with GRE (Muller *et al.*, 2012). This observation is most probably due to the presence of additional polyphenols in the GRE, such as vitexin/isovitexin (Choo *et al.*, 2012; Nurdiana *et al.*, 2017) and rutin (Kamalakkannan and Prince, 2006; Prince and Kannan, 2006; Fernandes *et al.*, 2010; Panchal *et al.*, 2011; Lee *et al.*, 2016; Yuan *et al.*, 2017), which previously decreased glucose levels in the same animal model.

Furthermore, aspalathin treatment was capable of supressing elevated fasting blood glucose levels and/or improving glucose tolerance in two different obesogenic animal models (Kawano *et al.*, 2009; Son *et al.*, 2013). *In vitro* studies suggested that these effects were most probably mediated by increased AMPK activation, GLUT4 vesicle translocation and consequently increased glucose uptake in the muscle (Kawano *et al.*, 2009; Son *et al.*, 2013; Kamakura *et al.*, 2015). Additional aspalathin benefits include a reduction in pancreatic AGE-mediated ROS (Son *et al.*, 2013) and increased pancreatic insulin secretion (Kawano *et al.*, 2009).

Aspalathin is associated with two anti-diabetic pharmacological properties. Firstly, it inhibits the sodium-glucose co-transporter-2 (SGLT2) and α-glucosidase (degrades glycogen to glucose), and secondly, it lowers glucose levels by targeting the muscle (Sasaki, Nishida and Shimada, 2018).

1.11. Study motivation

Cardiovascular diseases are identified as the leading cause of deaths globally. In the year 2015, more than 17.7 million individuals died from cardiovascular diseases, whereas 7.4 million of these deaths were due to coronary heart disease and 6.7 million were due to stroke (World Health Organization, 2017). Obesity is a major risk factor for type II diabetes, hypertension, coronary disease, hyperlipidemia, heart failure, several cancers (Strumpf, 2004; Bloomgarden, 2006) and endothelial dysfunction (Park and Park, 2015). In South Africa, obesity is markedly increasing due to epidemiological transition (Goedecke, Jennings and Lambert, 2006). Data obtained from Baleta and Mitchell (2014), indicated that South Africa presents with the highest obesity rate in the sub-Saharan Africa with more than 40 % of South African men and 70 % of South African women being either overweight or obese (Baleta and Mitchell, 2014).

The indigenous South African plant, Rooibos, has several health promoting properties such as anti-carcinogenic, anti-mutagenic, anti-inflammatory and anti-viral effects (Marnewick *et al.*, 2005, 2009; Joubert *et al.*, 2008; Fukasawa, Kanda and Hara, 2009). Specifically of interest to the current study, rooibos has also been shown to induce anti-hypertensive (Persson *et al.*, 2010), anti-diabetic (Muller *et al.*, 2012) and anti-atherosclerotic (Canda, Oguntibeju and Marnewick, 2014) effects, and also decrease lipid peroxidation (Marnewick *et al.*, 2011) and blood glucose levels (Muller *et al.*, 2012). These health benefits are suggested to be closely related to the phenolic compounds present in rooibos (Joubert and De Beer, 2011), such as aspalathin (Koeppen and Roux, 1965), aspalalinin (Shimamura *et al.*, 2006) and nothofagin (Hillis and Inoue, 1967). Previous research reported that green rooibos presents with roughly forty-five times more aspalathin when compared to fermented rooibos (Schulz, Joubert and Schütze, 2003). Due to the higher aspalathin content, it is speculated that green rooibos might be associated with more health benefits.

Spray-dried powders prepared from fermented rooibos and unfermented rooibos are known as fermented rooibos extract (FRE), and green rooibos extract (GRE) respectively. According to previous research, GREs present with higher (three times) total phenolic compounds when compared to FREs (Sasaki, Nishida and Shimada, 2018). In the current study, we used a specific aspalathin-rich GRE, namely Afriplex GRT™ extract. This extract was standardized by the Afriplex (Pty) Ltd pharmaceutical company in Paarl, South Africa.

To date, information regarding the effects of Afriplex GRT™ extract on obesity-induced cardiovascular risk factors such as insulin resistance, hypertension and vascular function, is limited.

We therefore propose to study the role of Afriplex GRT™ extract in the development of the cardiovascular pathology associated with the metabolic syndrome.

1.12. Aims and Objectives

Aim 1: To monitor blood pressure increase in an established obesity-induced hypertensive animal model and to determine whether Afriplex GRT™ lowers diet-induced hypertension within 6 weeks.

(i) To induce obesity and hypertension in half of the experimental animals by feeding an HFD for 16 weeks compared to age-matched chow fed controls. Half of each group will be treated with Afriplex™ GRT extract for the last 6 weeks of the 16-week diet regimen. An additional HFD group will be treated with the ACE inhibitor, Captopril, (a known anti-hypertensive medication) which will serve as a positive control in the study.

(ii) To monitor food and water intake, body weight, glucose levels and blood pressure for 16 weeks to determine whether obesity/hypertension was successfully induced in response to the HFD and whether Afriplex GRT™ has any ameliorative effects.

(iii) To determine whether obesity or treatment with Afriplex GRT™ has any effect on water retention/diuresis by measuring urine excretion volume and to analyse the chemical compounds of the urine to determine the presence of any disorders induced by obesity or Afriplex GRT™.

(iv) To determine vascular reactivity, in response to obesity and treatment with Afriplex GRT™, using thoracic aortas (with PVAT) and to measure intermediates of NO production (AMPK, eNOS, PKB) using the same aortas.

Aim 2: To elucidate the mechanisms responsible for any changes induced by Afriplex GRT™.

(i) Blood will be analysed for aldosterone, an intermediate of the RAS system.

(ii) Serum levels of insulin, leptin, adiponectin, and ET-1 will be determined.

Aim 3: To determine whether Afriplex GRT™ has any effect on NO production, cell apoptosis and cell viability using aortic endothelial cells (AECs).

(i) AECs will be cultured *in vitro* and will be subjected to three different Afriplex GRT™ concentrations to determine the effect of Afriplex GRT™ on NO production, cell apoptosis and cell viability using the 5-diaminofluorescein-2/diacetate (DAF-2/DA), propidium iodide (PI) and (3-(4,5-dimethylthiazol-2-yl)-2,5-diphenyltetrazolium bromide (MTT) assays respectively.

(ii) The possibility of ACE-inhibitor activity will be determined using a Fluorescence Resonance Energy Transfer (FRET) technique. FRET will be performed using the Afriplex GRT™ extract itself as well as non-fasting blood serum collected from the experimental animals at sacrifice.

CHAPTER 2: METHODS

2.1. Animals

Eighty-eight age-matched (7-8 weeks old) male Wistar rats with initial body weights of 180 ± 10 grams (g) were used in the study. The animals were randomly allocated to four animals per cage. 48 animals (12 cages) were assigned to the high fat diet (HFD) group and 40 animals (10 cages) to the control group ***(Figure 2.1)***.

Figure 2.1: *Animal treatment groups.*

The HFD group was only fed a HFD made up of 390 g Epol™ rat pellets, 200 millilitre (ml) water, 400 g holsum cooking fat, 100 g fructose, 100 g casein and 10 g cholesterol for 16 weeks, while the age-matched control group only received Epol™ pellets over the same period (Huisamen *et al.*, 2013). HFD food was prepared every second day, but the animals were fed daily. The composition of the diets **(*Table 2.1*)** were analysed by Microchem Lab Sciences (Pty) Ltd. Cape Town, South Africa.

Table 2.1: *Diet compositions.*

	Fat (g/100g)	Cholesterol (mg/100g)	% Protein	% Carbohydrates	Sugar (g/100g)	Fructose	kJ/100g
Control	4.8	-	17.1	34.6	6.6	-	1272
HFD	27.9	6.4	14.6	29.5	13.3	11	1829

Treatment started after 10 weeks on the respective diets and continued for the last 6 weeks of the 16-week diet programme. Treatment groups included 20 control and 20 HFD animals treated with Afriplex GRT™ extract and 8 HFD animals treated with Captopril, a well-known anti-hypertensive drug ***(Figure 2.1)***. A control group treated with Captopril was not included as it would have resulted in hypotension.

All animals had *ad libitum* access to water and food and were kept on a 12-hour day/night cycle at 24-25°C in the Central Research Facility of the Faculty of Health Sciences, University of Stellenbosch.

The study was registered with the Committee for the use of animals in research of the University of Stellenbosch (Project Number SU-ACUD15-00102) and conducted under the revised South African National Standard for the Care and Use of Animals for Scientific Purposes (South African Bureau of Standards, SANS 10386, 2008).

2.2. Treatment: Concentrations and administration

The Afriplex GRT™ extract was supplied by the South African Medical Research Council (SAMRC), and the Captopril was purchased from Sigma Aldrich®. For 6 weeks, Afriplex GRT™ extract was administered on a daily basis at a dosage of 60 mg/kg/rat, and Captopril at a dosage of 50 mg/kg/rat. Both drugs were diluted in a strawberry jelly/gelatine and water mixture, and aliquoted into ice cube trays. Gelatine has a very distinct taste, and we therefore used a strawberry jelly/gelatine mixture to ensure highly palatable jelly blocks. Each rat daily received one jelly block containing Afriplex GRT™ extract or Captopril calculated according to the rat's body weight determined weekly. To control for the sugar present in the jelly blocks, the untreated groups received drug-free jelly blocks.

2.3. Afriplex GRT™ extract and Captopril dosage

Due to a lack of evidence with regards to an exact optimal dosage of Afriplex GRT™ extract for rats, a dosage from the available literature on similar extracts was chosen. A study performed by Muller et al. (2012) at the SAMRC indicated that a GRE prepared in the same way at a dosage of 30 mg/kg, potentially lowered plasma glucose levels (Muller *et al.*, 2012). The same GRE was also used in a mouse study at a dosage of 0.3% and 0.6% of the diet (Kamakura *et al.*, 2015). Thus, for a rat weighing 250 g and consuming ~20 g of food daily, it corresponded to a GRE dosage of roughly 250 mg/kg/day – a very high dose. In a personal communication with the SAMRC, it was mentioned that the Afriplex GRT™ extract was administered at a dosage of 90

mg/kg/day in non-human primates, corresponding to 180 mg/kg/day in a rat. Consequently, a slightly higher starting dose was used in this study than the initial dose used by Muller et al. (2012) in rats (Muller *et al.*, 2012), but lower than that used in mice or non-human primates. Captopril was administered at the same dosage that was previously used in our laboratory as a positive control in the same animal model (Huisamen *et al.*, 2013).

2.4. Biometric data and sacrificing of animals

Throughout the 16-week period, the food and water consumption per cage was measured thrice weekly and the body weight of each animal once weekly. The animal's general health (posture, coat, vocalization and deaths) was also recorded daily.

Food and water intake as well as body weight data were statistically analysed by means of a two-way Analysis of Variance (ANOVA), followed by a Bonferroni post-hoc multiple comparison test. Data are expressed as Mean ± Standard deviation (SD), $p < 0.05$ was considered significant.

In week 17, rats were sacrificed by an injection with 0.5 ml Eutha-naze (265 mg/kg Sodium pentobarbital). Before opening the chest cavity, several reflex tests were performed to assure that the animals were unresponsive to any stimuli. The first test entailed a foot-pinch test (pedal reflex) followed by an eye-blinking test (corneal reflex). After opening the chest cavity, the blood, aorta with perivascular adipose tissue (PVAT), liver, and intra-peritoneal fat (IP-fat) of each animal were removed. The IP-fat and livers were weighed, snap frozen in liquid nitrogen and stored at -80°C. The aortas were immediately used for experimentation. Processing of non-fasting blood is described in *Chapter 2, Section 2.9*

The IP-fat weight and liver weight data are respectively presented as total weight and as a ratio of total body weight. IP-fat weight data were statistically analysed by means of a one-way ANOVA since the Captopril group was included in this analysis. The liver weight data were statistically analysed by means of a two-way ANOVA since only the control and HFD Afriplex GRT™ treated and untreated groups were compared. Both the one-way ANOVA and two-way ANOVA were followed by a Bonferroni post-hoc multiple comparison test. Data are expressed as Mean ± SD, $p < 0.05$ was considered significant.

2.5. Insulin sensitivity

2.5.1. Oral glucose tolerance tests (OGTT)

An OGTT is a well-known medical test which determines the body's sensitivity to glucose. In the current study, OGTTs were performed on randomly selected groups of animals in week 10 (1 week prior to commencement of treatment) and in week 16 (1 week prior to sacrificing). Animals were fasted overnight, followed by the injection of Eutha-naze (53 mg/kg Sodium pentobarbital). The administration of Eutha-naze created an anaesthetised and more relaxed environment throughout the 2-hour procedure. Each rat was tail pricked, a droplet of blood was collected, and the baseline fasting glucose level was determined using a GlucoPlus™ glucometer. Following this, a 50 % sucrose solution was gavaged to each animal at a dosage of 1 milligram (mg)/kg per animal. Using the GlucoPlus™ glucometer and the same tail prick, the blood glucose level of each animal was measured at 3 minutes (min), 5 min, 10 min, 15 min, 20 min, 25 min, 30 min, 45 min, 60 min, 90 min and 120 min respectively. Animals were left for one week to recover from the metabolic insult before treatment (week 11) or experimentation (week 17) commenced.

OGTT data were statistically analysed by means of a two-way ANOVA, followed by a Bonferroni post-hoc multiple comparison test. Data are expressed as Mean ± SD, $p < 0.05$ was considered significant.
The Area Under the Curve (AUC) was determined using GraphPad Prism® 6. AUC values obtained were statistically analysed by means of a t-test (Week 10 data - only control versus HFD group) and a two-way ANOVA followed by a Bonferroni post-hoc multiple comparison test (Week 16 data - Control and HFD untreated and treated groups). Data are expressed as Mean ± SD, $p < 0.05$ was considered significant.

2.5.2. Fasting and non-fasting glucose levels

Fasting glucose levels were determined in conjunction with the OGTTs performed in week 10 and in week 16, whereas non-fasting glucose levels were determined in week 17 at sacrifice. Both measurements were obtained in anesthetised animals (53 mg/kg Sodium pentobarbital in week 10 and 265 mg/kg Sodium pentobarbital in week 16) via a tail prick and a GlucoPlus™ glucometer.

Fasting and non-fasting glucose levels were respectively analysed by means of a two-way ANOVA (4 groups - Control and HFD Afriplex GRT™ treated and untreated groups) and a one-way ANOVA (5 groups - Control and HFD Afriplex GRT™ treated and untreated groups and HFD

+ Captopril), both followed by a Bonferroni post-hoc multiple comparison test. Data are expressed as Mean ± SD, $p < 0.05$ was considered significant.

2.5.3. Insulin assay

In week 16, a group of animals, excluding those that were part of the OGTTs, were sedated with 2 % isoflurane to induce general anaesthesia. Fasting blood (1-2 ml) was drawn from the carotid artery and placed on ice for 20 min. Thereafter, the samples were centrifuged for 10 min at 3000 revolutions per minute (rpm) and 4°C. The serum was collected, aliquoted and kept at -80°C.

Serum insulin was determined using the RayBio® Rat Insulin Enzyme-linked immunosorbent assay (ELISA) kit (Catalog #: ELR-Insulin). Before assaying, all the reagents and serum samples were pre-warmed to room temperature (18-25°C). The serum samples were diluted (1:1) with diluent buffer prior to experimentation. This *in vitro* enzyme-linked immunosorbent assay included a 96-well plate pre-coated with an antibody specific for insulin as well as all the required reagents to perform the assay. 100 microliter (µl) of each standard (1400 µlU/ml, 300 µlU/ml, 150 µlU/ml, 75 µlU/ml, 37.5 µlU/ml, 18.75 µlU/ml, 9.38 µlU/ml, 4.69 µlU/ml and 0 µlU/ml) and serum sample were loaded in duplicate to the appropriate wells, where diluent buffer served as the zero standard. This was followed by an incubation period of 2.5 hours at room temperature on a slow rotator (400-500 rpm). The solution was decanted, and each well was washed four times with 300 µl 1X Wash buffer. After the last wash, any remaining washing buffer or bubbles were aspirated. Following this, 100 µl 1X insulin antibody was added to each well and incubated for 1 hour at room temperature on a slow rotator (400-500 rpm) to allow binding to the antigen. After 1 hour, the antibody was discarded, and the same washing procedure was conducted. To detect and visualize insulin, 100 µl Horse Radish Peroxidase (HRP)-Streptavidin solution was pipetted to each well and incubated for 45 min at room temperature on a slow rotator (400-500 rpm). After the HRP-Streptavidin solution was discarded, the same washing procedure was conducted and 100 µl 3,3',5,5'-Tetramethylbenzidine (TMB) One-Step Substrate Reagent was added to each well for 30 min at room temperature (in the dark). TMB acts as a hydrogen donor in response to the reduction of H_2O_2 (electron acceptor) to O_2 and H_2O via HRP. As a result, the remaining diimine causes a blue colour which is directly proportional to the amount of insulin present in the standards/samples (Martin, Mufson and Mesulam, 1984). The reaction was stopped by the addition of 50 µl stop solution (sulfuric acid) to each well which turned the TMB colour from blue to yellow. The absorbance was immediately measured at 450 nm using the FLUOstar Omega plate reader.

The mean absorbance of each standard and serum sample was calculated, where after the zero standard was subtracted from all these values. A log-log standard curve was set-up by plotting the

standard concentrations (µlU/ml) on the x-axis with the corresponding optical density (OD) values on the y-axis. The best-fitted linear regression line was drawn through the standard points and an equation was generated. Using this equation, the insulin present in the serum samples were determined.

Insulin levels were analysed by means of a two-way ANOVA (4 groups - Control and HFD Afriplex GRT™ treated and untreated groups), followed by a Bonferroni post-hoc multiple comparison test. Data are expressed as Mean ± SD, $p < 0.05$ was considered significant.

2.5.4. Homeostasis Model Assessment of insulin resistance (HOMA-IR)

The HOMA-IR, an insulin resistance evaluation model, was used to determine whether the treated and untreated animals presented with insulin resistance after 16 weeks. The HOMA-IR was calculated by means of the following equation:

HOMA-IR = Fasting glucose levels (mmol/L) x Fasting insulin levels (mIU/ml)/22.5 (Matthews *et al.*, 1985).

HOMA-IR data were analysed by means of a two-way ANOVA (4 groups - Control and HFD Afriplex GRT™ treated and untreated groups), followed by a Bonferroni post-hoc multiple comparison test. The control + Afriplex GRT™ group initially had a n-value of 3, but since the one animal had an insulin value higher than the accepted 57.6 uUl/ml, it was excluded. Data are expressed as Mean ± SD, $p < 0.05$ was considered significant.

2.6. Blood pressure related markers

2.6.1. Blood pressure

The blood pressure of each animal was determined using a non-invasive computerized CODA® tail-cuff blood pressure system (Kent Scientific). The tail-cuff consisted of the occlusion (O)-cuff and the volume pressure recording (VPR)-cuff. From week 9 to the end of week 10 (14 days), the animals were introduced and acclimatized to the warming platform, restraining holder and the tail-cuff.

The actual blood pressure readings were taken after 10 weeks and the CODA® tail-cuff blood pressure system was set-up as follows: acclimation cycles: 1, interval between cycles: 5 seconds, number of sets: 2, and reading cycles: 5. Thus, in one session, 10 diastolic and 10 systolic readings (excluding the acclimation cycle) were recorded for each rat; whereas only the cycles accepted by the CODA® tail-cuff system were averaged and statistically analysed. Blood pressure values were also excluded if the rats' heart rate was above normal (330-480 beats per minute).

Blood pressure data were analysed by Dr Lombard from the Division of Epidemiology and Biostatistics, Stellenbosch University. Baseline adjusted analyses were performed before actual statistical analyses, as the blood pressures of the untreated and treated groups differed before treatment commenced. Data are expressed as Mean ± SD, $p < 0.05$ was considered significant.

2.6.2. Urine volume and chemical composition

The urine volume (ml) and its chemical composition were determined in week 10 and again in week 16. These measurements were conducted prior to the OGTTs to compensate for any possible effect the 18-hour fast might have had on these parameters.

Animals were placed separately into metabolic cages for a 24-hour period while having *ad libitum* access to food and water. The urine excreted from each animal was collected in a plastic measuring cylinder attached to the cage and the volume was recorded.
A Test-it™ 10 dipstick was inserted into the urine to determine bilirubin, blood (erythrocytes, haemoglobin), glucose, leukocyte, protein, ketone, nitrite and urobilinogen levels as well as the pH. The principle of each test is described in ***Table 2.2.***

Table 2.2: *Principle of urine parameters. Information obtained from (Test-it Urinalysis, 2010).*

	Indicates	Principle of test
Bilirubin	Certain liver and bile diseases	The test is based on the coupling of bilirubin with a diazonium salt under acidic conditions. Discoloration of the reagent suggests liver disease (+ or ++ or +++).
Blood	Urological or kidney diseases	The test is based on the pseudoperoxidative activity of myoglobin and haemoglobin, which catalyze the oxidation of an indicator by an organic hydroperoxide and a chromogen to produce a green colour. Intact erythrocytes are visualized as spots on the test pad (ca.5-10, ca.50, ca.250 Ery/µl), and myoglobin/haemoglobin and by increasing green coloration (+ca.5-10, ++ca.50, +++ca.250 Ery/µl).
Glucose	Hyperglycaemia and diabetes	This pH and ketone independent test are based on the reaction of glucose oxidase (GOD) – peroxidise (POD) with a chromogen.
Leukocytes	Kidney or urinary tract inflammation	The test is based on the release of leukocyte esterase from lysed neutrophils, which reacts with an ester to produce a pyrrole. When the pyrrole reacts with a diazo salt, a violet colour is observed.
Protein	Renal diseases	The test is based on the "protein error" principle of the indicator and especially sensitive to albumin.
Ketones	Acidosis or ketosis	This test is based on the principle of Legal's test, referring to the interaction of the acetoacetic acid and acetone in the alkaline solution, which consequently results in the formation of a violet coloured complex.
Nitrite	Urinary tract infections of bacterial origin	The test is specific for nitrite and based on the principle of Griess's test. Nitrite-forming (Gram Negative) bacteria can be identified by a pink discoloration on the test patch. Even a slight pink coloration is indicative of significant bacteriuria.
Urobilinogen	Liver diseases and haemolytic disorders	The test is based on the coupling of a stabilised diazonium salt with urobilinogen resulting in the formation of a red azo compound.
pH	Acidity or alkalinity	This test is based on an indicator that changes colour from 5 to 9.

We only had two animal groups before treatment and therefore the urine volume prior to treatment was analysed by means of an unpaired t-test. After treatment, urine volume was analysed by means of a one-way ANOVA, followed by a Bonferroni post-hoc multiple comparison test. Data are expressed as Mean ± SD, $p < 0.05$ was considered significant. Each urine parameter for each group was interpreted on a majority basis.

2.7. Vascular Endothelium

After the animals were sacrificed as previously described, their aortas with surrounding PVAT were removed and placed in ice-cold Krebs-Henseleit (KH) buffer (119 mM NaCl; 24.9 mM NaHCO3; 4.74 mM KCl; 1.19 mM KH2PO4; 0.6 mM MgSO4.7H2O; 0.59 mM Na2SO4; 1.25 mM

CaCl2.12H2O and 10 mM glucose). A small section from each aorta was removed for aortic ring studies, and the remaining aortic tissue was snap-frozen and stored at -80°C for Western blotting.

2.7.1. Vascular contraction and relaxation: Aortic ring isometric tension studies

Vascular contraction and relaxation studies were performed using the aortic rings of the control and HFD treated and untreated animals.

2.7.2. Aortic ring removal and mounting

The experimental system consisted of a Powerlab data acquisition system, isometric force transducer with stainless steel mounting hooks and a 25 ml organ bath (AD Instruments, Bella Vista, New South Wales, Australia). The system was connected to a computer to monitor contraction and relaxation throughout the experiment. Prior to experimentation, the organ bath, with steel mounting hooks inside, was rinsed four times with boiling water. The organ bath was filled with pre-warmed (37°C) KH buffer and gassed with 5 % carbon dioxide and 95 % oxygen. The tension of the aorta was determined by the isometric force transducer and recorded as grams of tension (g) on the LabChart 7 software (Dunedin, New Zealand). The system was calibrated at 0 g and 2 g prior to experimentation.

As mentioned, the thoracic aortas with surrounding PVAT were gently removed from the proximal aortic opening (open end of the aorta where the heart was cut off). To grab hold of this open end, tweezers were used, and the aorta was gradually removed by cutting horizontally, as close as possible, to the spine. The aorta was placed in a petri dish containing ice-cold KH buffer. The clotted blood from the lumen was removed and a 3-4 mm segment from the centre of the aorta was used in experiments ***(Figure 2.2 a)***. The segment was carefully mounted on the two steel hooks and immersed in the organ bath filled with the pre-warmed KH buffer ***(Figure 2.2 b-c)***. To prevent the aortic ring from sliding off, the tension was increased from 0 g to 0.2 g prior to submerging.

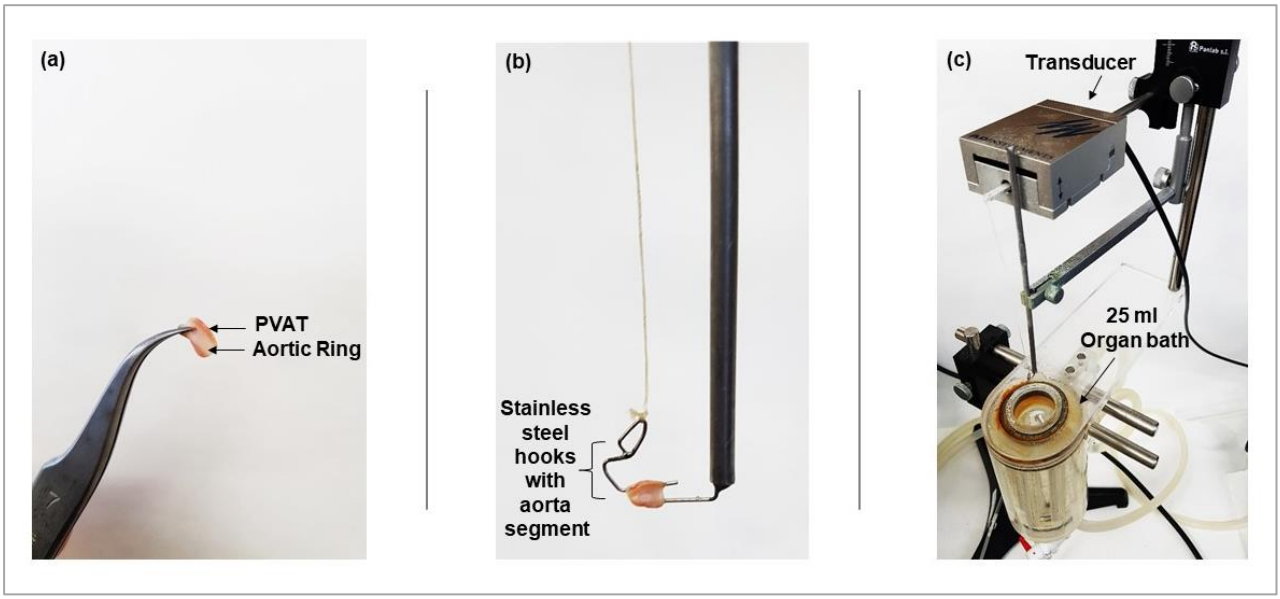

Figure 2.2: (a) *Aortic ring with PVAT,* ***(b)*** *aortic ring mounted on two steel hooks,* ***(c)*** *the organ bath in which the aortic ring was submerged.*

2.7.3. Experimental protocol - Isometric tension study

The aortic ring experimental protocol, modified from Privett et al. (2004) (Privett, Kunert and Lombard, 2004), was divided into four phases: initial stabilization, initial contraction and relaxation, second stabilization, and second cumulative contraction and relaxation. Phenylephrine (Phe) was used as a VSMC vasoconstrictor, where after **endothelium-dependent** vasodilation or **endothelium-independent** vasodilation was initiated. These experiments are summarized in ***Figure 2.3 - 2.5.***

Endothelium-dependent vasodilation: Phenylephrine (Phe) and Ach

Initial stabilization: The resting aortic ring was stabilized for 40 min in the organ bath, changing the buffer at 10 min, 20 min and 30 min. During the first 20 min of stabilization, the tension was gradually increased from 0.2 g to 0.8 g and then again to 1.5 g in the remaining 20 min.

Initial contraction and relaxation: To determine endothelium functionality, the aortic rings were subjected to an initial round of contraction and relaxation. After 40 min, the KH buffer in the organ bath was adjusted to exactly 25 ml, where after 100 nM Phe (Sigma-Aldrich, St. Louis, MO, USA) and then 10 µM ACh (Sigma-Aldrich, St. Louis, MO, USA) were directly added to induce contraction and relaxation respectively. Both drugs were prepared in 0.9 % saline solution prior to addition.

Phe acts as an α-adrenergic receptor agonist which induces vasoconstriction of the smooth muscle cells, whereas ACh binds to specific receptors on the endothelial cell membrane which consequently initiates eNOS activation and NO production leading to vasodilation of the smooth muscle.

When the Phe-induced contraction plateaued and maximum contraction was reached, ACh was added to the organ bath. Only the aortic rings that showed at least 70 % relaxation in response to the Phe-induced contraction, were used for experimentation.

Second stabilization: To flush out the Phe and ACh, the organ bath with the aortic ring inside, was rinsed three times with pre-warmed KH buffer. The organ bath was refilled up to 25 ml and the aortic rings were stabilized at 1.5 g for 30 min. The buffer was changed with pre-warmed KH buffer at 10 min and 20 min respectively.

Second cumulative contraction and relaxation: After 30 min, the KH buffer in the organ bath was adjusted to exactly 25 ml. Cumulatively, the concentration of Phe was increased as follows: 100 nM, 300 nM, 500 nM, 800 nM, 1µM. Once the maximum Phe-induced contraction was reached, the concentration of ACh was cumulatively increased as follows: 30 nM, 100 nM, 300 nM, 1 µM, 10 µM ***(Figure 2.3)***. The data were saved, and the aortic rings were weighed and measured. The organ bath, with the steel hooks inside, was thoroughly rinsed with boiling water.

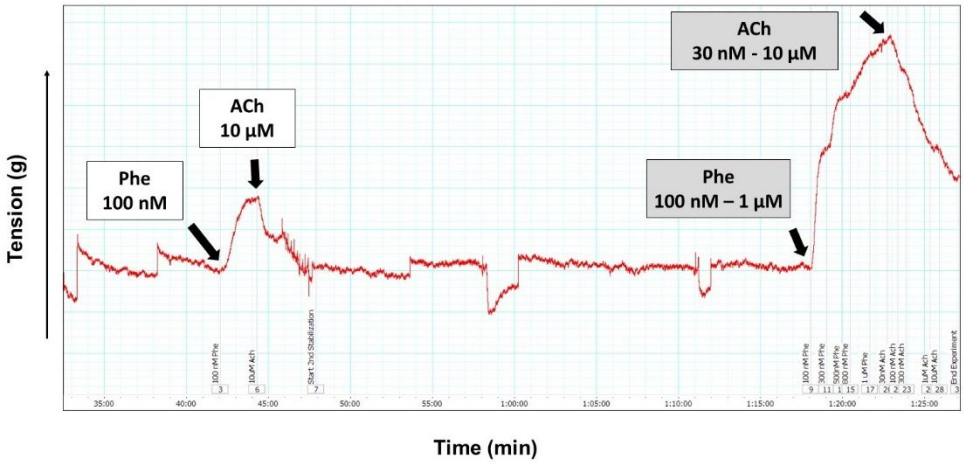

Stabilization (40 min)	Phe (100 nM)	ACh (10 µM)	Stabilization (30 min)	Phe (100 nM – 1 µM)	ACh (30 nM - 10 µM)

Figure 2.3: *Summary of Phe and ACh aortic ring experimental protocol.*

Endothelium-independent vasodilation: Phe and Sodium nitroprusside (SNP)

SNP: SNP is an exogenous NO donor which induces relaxation of the VSMCs independently of the endothelium. The same initial stabilization, initial contraction and relaxation steps, as in the endothelium-dependent vasodilation experiment, were performed. After the second cumulative Phe-induced contraction, SNP instead of ACh was cumulatively added to the aortic rings (1.2 nM, 20 nM, 70 nM, 100 nM, 750 nM) and maximum endothelium-independent relaxation was determined ***(Figure 2.4)***. The data were saved, and the aortic rings were weighed and measured. The organ bath, with the steel hooks inside, was thoroughly rinsed with boiling water.

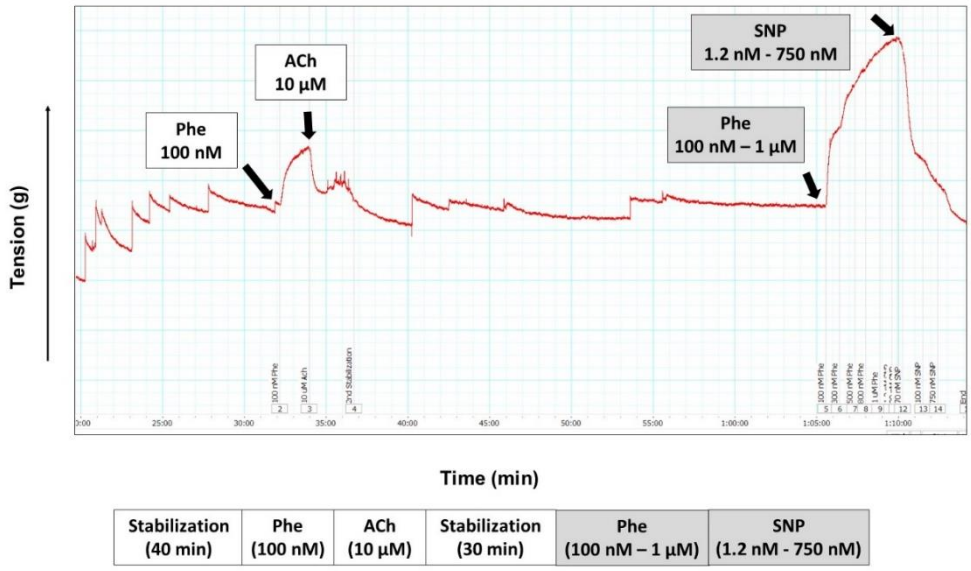

Figure 2.4: *Summary of Phe and SNP aortic ring experimental protocol.*

Additional aortic ring experiment using KCl as vasoconstrictor:

A few stabilized (1.5 g) aortic rings of both the control and HFD Afriplex GRT™ treated and untreated groups were exposed twice to 75 mM KCl to determine maximum smooth muscle contractility (Xavier *et al.*, 2003) via a different VSMC mechanism. Unlike Phe, KCl bypasses the G-coupled protein receptor to stimulate calcium release and consequently vasoconstriction. Since the rings were unable to relax to baseline (1.5 g) when SNP was cumulatively added to the aortic rings (1.2 nM, 20 nM, 70 nM, 100 nM, 750 nM, 1.5 µM) or after washing the ring four times with pre-warmed KH buffer **(*Figure 2.5 a-b*)**, KCl was no longer used for experimentation, and therefore the low n-value. The data were saved, and the aortic rings were weighed and measured.

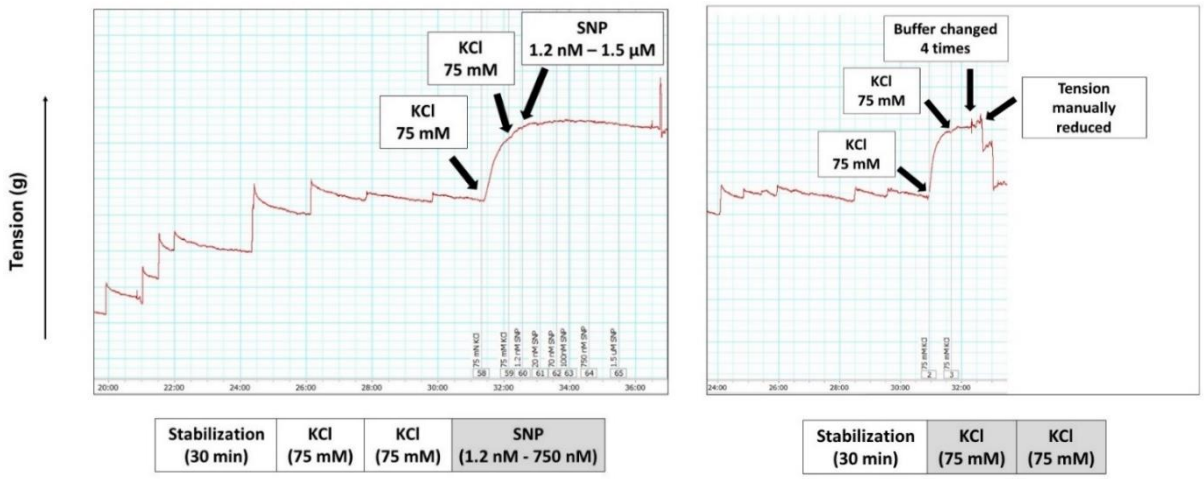

Figure 2.5: *Summary of* ***(a****) KCl and SNP and* ***(b)*** *KCl and buffer changing aortic ring experimental protocol.*

Phe/KCl-induced vasoconstriction are expressed as an increase in gram tension from a resting tension of 1.5 g, while ACh/SNP relaxation are expressed as % relaxation of the maximum contraction. All isometric tension data were analysed by means of two-way ANOVA, followed by a Bonferroni post-hoc multiple comparison test, except for the comparison between KCl and Phe. The effect on maximum contraction between these two vasoconstrictors were analysed by a one-way ANOVA followed by a Bonferroni post-hoc multiple comparison test. Data are expressed as Mean ± SD; $p < 0.05$ was considered significant.

LogEC50 values were generated by log-transforming the data, followed by non-linear regression. Data are expressed as Mean ± Standard Error (SE), $p < 0.05$ was considered significant.

2.7.4. Western blotting

Western blotting was performed on aortic tissue from both the control and HFD untreated and treated animals to determine the expression (total) and activation (phosphorylation) of the following proteins: AMPK, eNOS and PKB.

2.7.4.1. Tissue homogenate preparation (lysates)

For each rat, 40-50 mg frozen aortic tissue was pulverized using a pre-cooled mortar and pestle. The aortic tissue was transferred to an Eppendorf tube containing 600 µl lysis buffer (20 mM Tris-hydrochloric acid (HCl) (pH 7.5), 1 mM Ethylene glycol-bis (β-aminoethylether)-N,N,N',N'-tetraacetic acid (EGTA), 1 mM Ethylenediaminetetraacetic acid (EDTA), 150 mM Sodium chloride (NaCl), 1 mM β-glycerophosphate, 2.5 mM tertasodiumpyrophosphate, 1 mM Sodium orthovanadate (Na_3VO_4), 1% Triton X-100, 10 µg/ml leupeptin, 10 µg/ml aprotinin, 50 nM Sodium Fluoride (NaF), 0.1% Sodium dodecyl sulphate (SDS) and 50 µg/ml Phenylmethylsulfonyl Fluoride (PMSF).

To disrupt the cells, 7-8 Next Advance stainless-steel beads (1.6 millimetre (mm)) were added to each tube, where after the tubes were homogenised three times in the Bullet Blender® (Next Advance) at speed 8 for 1 min (4°C). In between the first two homogenizations, the samples were allowed to rest for 5 min at 4°C. After the last homogenization, the samples were placed on ice for 20 min to ensure optimal tissue lysis.

Next, the samples were centrifuged (SIGMA® 1-14K) at 15000 rpm for 20 min at 4°C, where after the supernatant of each sample was transferred into a new Eppendorf tube. The Bradford method was used to determine the protein quantity in these samples (Bradford, 1976).

For the Bradford assay, the supernatant of each sample was diluted (A) 1:9 (10 µl supernatant in 90 µl dH_2O) to dilute the amount of detergent that may interfere with the assay. This was followed by dilution (B) 1:4 (20 µl of the first dilution (A) in 80 µl dH_2O). A standard curve was set up by adding increasing volumes of 1:4 diluted Bovine Serum Albumin (BSA) (100 µl BSA + 400 µl dH_2O) to decreasing volumes of dH_2O **(*Table 2.3*)**. dH_2O served as the zero standard (blank). Standards and samples were prepared in duplicate.

Table 2.3: *Bradford standard curve.*

BSA protein concentration	1:4 Diluted BSA	dH_2O
0 µg	0 µl	100 µl
1.25 µg	5 µl	95 µl
2.5 µg	10 µl	90 µl
5.0 µg	20 µl	80 µl
10.0 µg	40 µl	60 µl
15.0 µg	60 µl	40 µl
20.0 µg	80 µl	20 µl

The Bradford solution (0.6 mM Coomassie Brilliant Blue G-250, 50 % (v/v) phosphoric acid and 95 % ethanol) was diluted five times with dH_2O (20 ml Bradford solution + 80 ml dH_2O) and filtered through a double layer of Whatman cellulose filter paper. Next, 900 µl of the Bradford solution was added to all the standards and samples, followed by an incubation period of 15 min at room temperature. During this time, the colour changed from red to blue, in response to the acidity of the Bradford solution. The absorbance of the standards and samples were read at 595 nm in the GENESYS™ 20 Visible spectrophotometer. The Coomassie blue colour is directly proportional to the amount of protein present in the standards/samples.

The mean absorbance of each standard and sample was calculated. Using Microsoft® Excel the standard curve was set up by plotting the standard concentrations (µg protein) on the x-axis with the corresponding mean OD values on the y-axis. The best-fitted straight line was drawn through the standard points and an equation was generated. Using this equation, the amount of sample protein and lysis buffer was specifically calculated to ensure equal protein loading per volume unit. We aimed to load between 15 µg- 20 µg protein sample per well.

After protein loading, 850 µl of a 2X Laemmli sample buffer (0.125 M Tris-HCl (pH 6.8), 20 % Glycerol, 4 % SDS, 5 % β-mercaptoethanol (2-ME), 0.03 % Bromophenol Blue) was mixed with 150 µl 2-ME, and added to each sample in a 1:2 ratio where 1 = sample buffer and 2 = sample + lysis buffer combination (Laemmli, 1970). After the samples were prepared, they were boiled for 5 min and stored at -80°C overnight.

2.7.4.2. Protein separation and transfer

For protein separation and transfer, 4-20 % 26 well Bio-Rad Criterion™ TGX Stain-Free™ Precast gels, a Bio-Rad Criterion™ Midi Electrophoresis system, and a Bio-Rad Criterion™ Blotter were used.

Samples were re-boiled for 5 min, followed by centrifugation at 5000 rpm for 5 min. An equal volume (25 µl) containing equal protein of each sample was loaded in to the respective wells of the gel using a Hamilton® syringe (Sigma-Aldrich, St. Louis, MO, USA). To detect the molecular weight of the proteins of interest at the end of the experiment, 5 µl PageRuler™ Prestained Protein Ladder (ThermoFisher Scientific) was loaded in the first well. Once the samples were loaded sequentially in the remaining wells, the electrophoresis tank was filled with running buffer (25 mM Tris, 192 mM glycine and 0.1 % SDS) and the system was connected to a power source. For 60 min at 200 V, 200 mA, the gel was exposed to sodium dodecyl sulfate–polyacrylamide gel electrophoresis (SDS-PAGE). After the proteins were separated, the polyacrylamide gel was activated using the Bio-Rad ChemiDoc™ MP system. An image was acquired and stored.
Prior to protein transfer, the polyvinylidene fluoride (PVDF) (ImmobilonTM P, Millipore) membrane was activated for 5 min in methanol where after it was soaked in transfer buffer (25 mM Tris, 192 mM glycine and 20 % (v/v) methanol) at 4°C until used. For 60 min at 200 V, 200 mA the proteins on the activated gel was transferred to the PVDF membrane, using the Bio-Rad Criterion™ Blotter system as power source. The system was filled with cold transfer buffer and an ice-pack to ensure optimal transfer.

After the transfer, each membrane was visualized on the Bio-Rad ChemiDoc™ MP system to determine if the proteins successfully transferred onto the membrane. An image was acquired and stored for normalization purposes.

The proteins on the PVDF membrane was fixed by immersing the membrane for 30 seconds in undiluted methanol. Following this, the membrane was left on the bench to air dry for 15 min.

2.7.4.3. Protein immunodetection

To compensate for non-specific binding, the air-dried membranes were placed in 5 % fat free milk (5 ml fat free milk in 95 ml TBS-Tween (Tris-buffered saline + 0.1 % Tween® 20)) for 2 hours at room temperature on a slow rotator. After the blocking period, membranes were thoroughly washed with TBS-Tween for 30 min (3 x 10 min) on a lab rotator (FMH instruments) at room temperature. Following this, each membrane was allocated to a specific rabbit polyclonal primary

antibody prepared in TBS-Tween or primary SignalBoost™ Immunoreaction Enhancer (7.5 µl primary antibody + 5 ml TBS-Tween/ primary SignalBoost™) (***Table 2.4***). After the membranes were subjected overnight (4°C) to the primary antibody solutions, the membranes were washed with TBS-Tween for 30 min (3 x 10 min) on a lab rotator (FMH instruments).

The secondary antibody was prepared in TBS-Tween or secondary SignalBoost™ Immunoreaction Enhancer (1.25 µl secondary antibody in 5 ml TBS-Tween/secondary SignalBoost™) ***(Table 2.4)***. Membranes were individually immersed for 1 hour in these secondary antibody dilutions at room temperature. During the 1-hour period, the secondary antibody bound to the primary antibody consequently initiating a signal. To remove the excess secondary antibody, all the membranes were washed again with TBS-Tween for 30 min (3 x 10 min) on a lab rotator (FMH instruments).

Table 2.4: *Specifications of proteins of interest.*

Protein	Molecular Size	Gel type	Primary antibody	Secondary antibody
Total-AMPK	62 kDa	4-20 % Precast (26 wells)	7.5 µl/5 ml TBS-Tween	1.25 µl/5 ml TBS-Tween
Phosphorylated-AMPK (Thr 172)				
Total-eNOS	140 kDa	4-20 % Precast (26 wells)	7.5 µl/5 ml primary SignalBoost™	1.25 µl/5 ml secondary SignalBoost™
Phosphorylated-eNOS (Ser 1177)				
Total-PKB	56 kDa	4-20 % Precast (26 wells)	7.5 µl/5 ml TBS-Tween	1.25 µl/5 ml TBS-Tween
Phosphorylated-PKB (Ser 473)				

The proteins of interest were visualized by adding Bio-Rad Clarity™ enhanced chemiluminescence (ECL) detection reagent to the membranes (1:1 ratio of the black and white ECL) for 5 min. Using the Bio-Rad ChemiDoc™ MP system, the membranes were exposed one-by-one for the pre-selected time. During the exposure time, any bands coloured red by the Image Lab™ program, were indicative of overexposure, and was therefore not used for further analysis. The best image of each antibody was stored for normalisation purposes.

The density of each exposed band on the PVDF membrane was normalized against the total amount of protein in the first band, in our case, the same Captopril sample. Control values were adjusted to 1. The total protein expression and phosphorylation of AMPK, eNOS and PKB were calculated as a ratio of the control. This was followed by a two-way ANOVA and Bonferroni post-hoc multiple comparison test. The P:T ratio of each protein was also analysed by a two-way ANOVA followed by a Bonferroni post-hoc multiple comparison test. For the AMPK P:T ratio, an additional t-test was performed to point out the difference specifically between the control and

control + Afriplex GRT™ group. Data are expressed as Mean ± SD, $p < 0.05$ was considered significant.

2.7.4.4. Stripping of membranes

After the membranes were probed in total primary antibody, they were stripped to remove any of the previous bound antibody. Following this, the same membranes were re-probed with the phosphorylated antibody, thus each membrane was used for its total and phosphorylated counterpart. The stripping procedure entailed: incubation of the membranes 2 x 5 min in dH_2O, 1 x 7 min in 0.2 NaOH stripping solution and again 2 x 5 min in dH_2O. Subsequently, membranes were immersed for 2 hours at room temperature in 5 % fat free milk and the same procedures as described in *Chapter 2, Section 2.7.4.3* were followed.

2.8. Aortic endothelial cells (AECs)

In vitro experimentation was performed using adult rat AECs, purchased commercially from VEC Technologies (Rensselaer, New York, USA). Once these cells were received in 75 cm^2 culture flasks, they were supplemented with fresh sterile all-in-one ready-to-use rat endothelial cell growth medium (EGM) (Cell Applications, Inc, San Diego) and placed in the NuAire™ tissue culture incubator (Minnesota, USA) pre-set at the following atmospheric composition: 21 % O_2, 5 % CO_2, 40-60 % humidity and a temperature of 37°C. The EGM consists of a combination of endothelial cell basal medium, Fetal Bovine Serum (FBS), growth supplements and antibiotics which guarantees ideal cell health, physiology, morphology, viability, performance and consistency.
Cells received fresh EGM every second day and were grown until 80 % confluent. The cells were grown into different 'Parent (P)-generations' (P1, P2 and P3), transferred to multiple Cryotubes each containing 5 % EGM, 90 % FBS and 5 % Dimethyl sulfoxide (DMSO) and stored in liquid nitrogen (-196°C) for future use. In the current study, we used only P3 generation cells.

2.8.1. Seeding of cells

Prior to experimentation, Gibco™ attachment factor protein (Thermo Fisher Scientific, Waltham, USA) was added to two 35x10 mm cell culture dishes and placed in the tissue culture incubator (1 hour). The attachment factor contains gelatine which enhances microvascular endothelial cell growth. A P3 cell line was thawed and resuspended in fresh EGM. Once the excess attachment factor was removed, the resuspended cell mixture was equally split between the plates. Confluency was microscopically determined when the growth area of the tissue cultured dishes were 80 % covered with cells.

2.8.2. Passaging of cells

When the cells were 80 % confluent, cell culture dishes were washed twice with pre-warmed phosphate-buffered saline (PBS) (137 mM NaCl, 2.68 mM KCl, 8.33 mM Na_2HPO_4, 1.47 mM KH_2PO_4, pH 7.4) followed by a 3 min incubation period with pre-warmed (37°C) 0.25 % Gibco™ trypsin (Thermo Fisher Scientific, Waltham, USA). Trypsin is an irradiated mixture of proteases which results in cell dissociation/detachment. Using a 1000 µl pipette, the detached cell-trypsin mixture was rapidly transferred to 15 ml conical tubes containing fresh EGM to prevent cell lysing. These tubes were centrifuged at 1000 rpm for 3 min (4°C) followed by supernatant removal. The remaining pellet was resuspended in fresh EGM and split between new 35x10 mm cell culture dishes (pre-coated with attachment factor as described above). Passaging to the next generation was performed at a 1:2 ratio.
In the current study, cells were passaged from the P3 generation to the P7 generation before experimentation. All culture dishes were randomly assigned to control and treatment groups.

Experiments were performed in black 24-well plates (Vision Plate™ 24, 4titude® Limited, UK) with 2-4 technical repeats of each sample per plate. All experiments were repeated thrice, each time using a new P3 cell line, thus 3 biological repeats. The passaging process of the current study is summarized *in* ***Figure 2.6***.

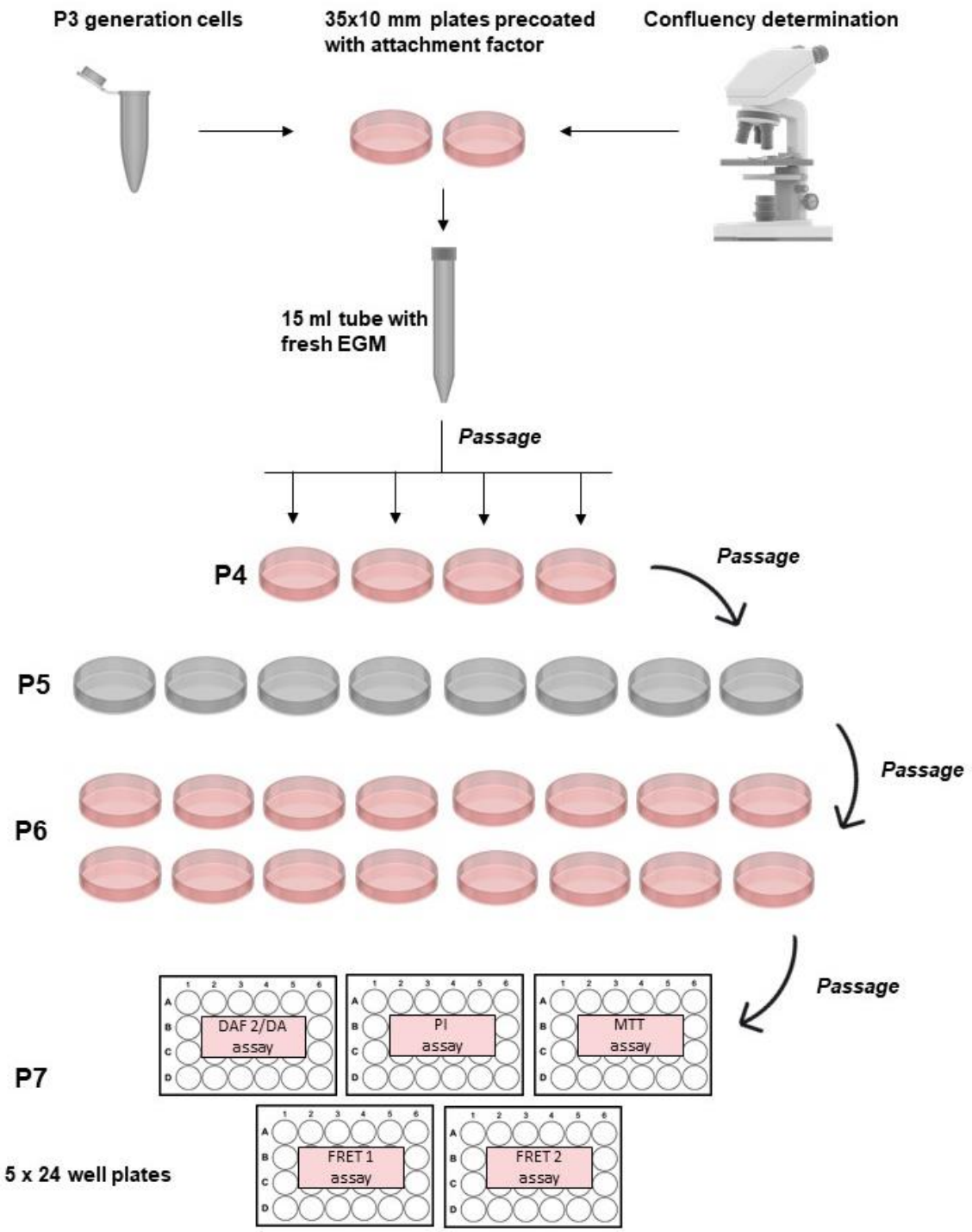

Figure 2.6: *Passaging of cells from the P3 generation to the P7 generation. Image composed using* (*Library of Science & Medical Illustrations*, 2018).

2.8.3. Treatment preparation and experimental protocols

Experiments were conducted once the cells in the wells were 80 % confluent. Prior to treatment, cells were serum starved to synchronize them to similar cell cycle phase, which in turn removes the impact the cell cycle might have in response to treatment (Russell and Hamilton, 2014). Serum starvation entailed the incubation of cells for 24 hours in rat endothelial cell basal medium (Cell Applications, Inc, San Diego) containing 0 % FBS. After the aspiration of the FBS-free medium, cells were treated for a 24-hour period with either an Afriplex GRT™ solution or non-fasting serum collected from the animals at sacrifice.

2.8.3.1. Afriplex GRT™ solution and vehicle control

Three concentrations (1 mg/ml; 10 mg/ml; 100 mg/ml) of Afriplex GRT™ were prepared in PBS. Following this, 10 µl of each solution was further dissolved in a total volume of 9.990 ml EGM (1000X dilution). The final concentrations of Afriplex GRT™ used for treatment were thus: 1 µg/ml; 10 µg/ml or 100 µg/ml. Since the PBS was also diluted 1000X, the amount of PBS present in the 10 ml Afriplex GRT™-EGM solution was 1 µl (vehicle control) (***Figure 2.7***).

2.8.3.2. Non-fasting serum and vehicle control

Non-fasting serum collected from Afriplex GRT™ treated and untreated animals were thawed prior to experimentation. The serum was diluted 4X with EGM (vehicle) (***Figure 2.7***).

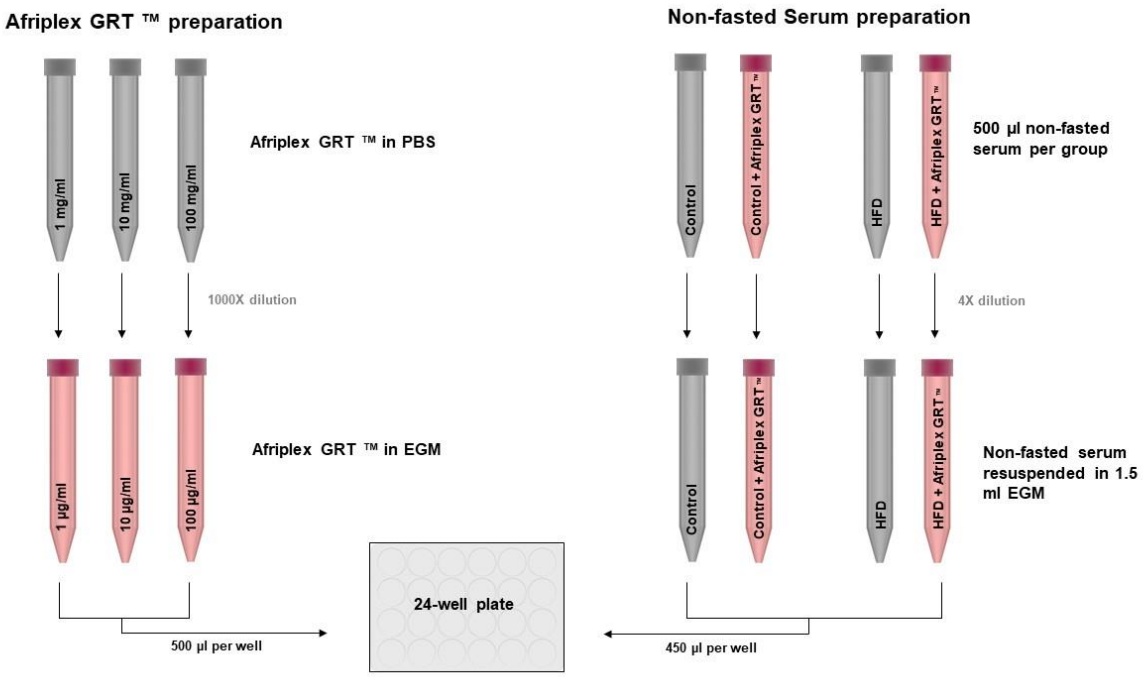

Figure 2.7: *Preparation of Afriplex GRT™ solutions and non-fasting serum. Image composed using* (*Library of Science & Medical Illustrations*, 2018)*.*

2.8.3.3. Experimental protocol: Plate Reader Analyses

After the 24-hour treatment period, we performed five analyses including: (a) 5-diaminofluorescein-2/diacetate (DAF-2/DA), (b) Propidium Iodide (PI), (c) MTT (3-(4,5-dimethylthiazol-2-yl)-2,5-diphenyltetrazolium bromide) and (d) two FRET assays.

(a) DAF-2/DA

DAF/DA is a well-known technique which measures NO levels in living cells and tissues (Zhou and He, 2011). The principle of this method entails the permeation of DAF-2/DA through the cell membrane. Once inside, DAF-2/DA is hydrolysed by intracellular esterases, consequently generating the impermeable Diaminofluorescein-2 (DAF-2). The amino groups of DAF-2 intracellularly reacts with NO, which in turn yields the highly fluorescent green light, Triazolofluorescein (DAF-2T) (***Figure 2.8***).

.

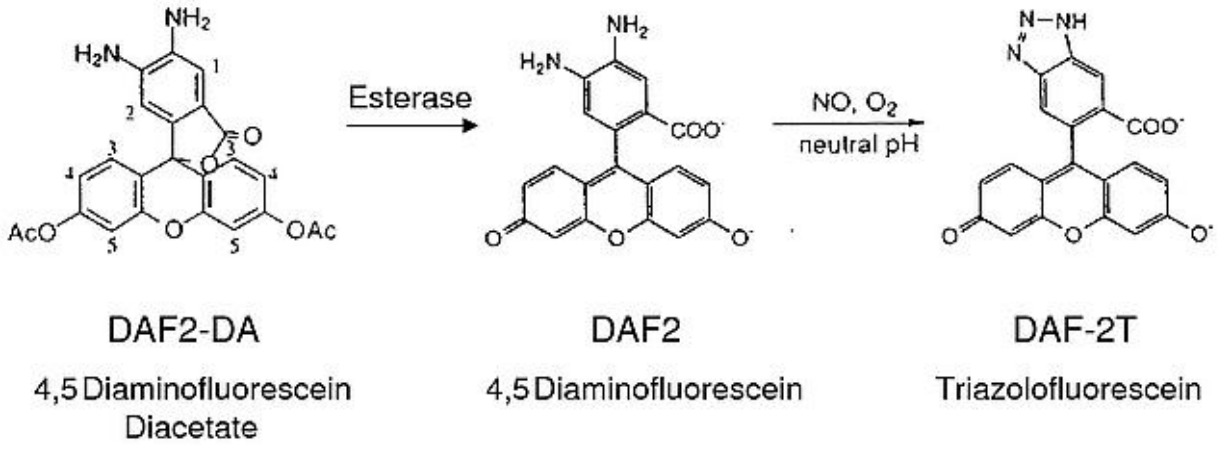

Figure 2.8: *Principle of DAF-2/DA. Image from Sigma-Aldrich (Sigma-Aldrich, 2018a).*

The entire DAF-2/DA experiment was repeated 3 times (3 biological repeats) using freshly prepared Afriplex GRT™ solution. Each sample was loaded 4 times in one experiment (4 technical repeats).

DAF-2/DA assay included:

- 4 x **positive control** technical repeats
- 4 x **vehicle control** technical repeats
- 4 x **1 µg/ml Afriplex GRT™** technical repeats
- 4 x **10 µg/ml Afriplex GRT™** technical repeats
- 4 x **100 µg/ml Afriplex GRT™** technical repeats

After treatment, cells in the 24-well plates were washed with PBS followed by incubation with 10 µM DAF-2/DA (25 µl DAF-2/DA in 12.475 ml PBS) (Calbiochem San Diego, CA, USA) for 2 hours at 37°C. For the final 30 min, 100 µM Diethylamine NONOate diethylammonium salt (DEA/NO) (Sigma-Aldrich, St. Louis, MO, USA) was added to the positive control wells. DEA/NO is a known NO donor with a high success rate in our laboratory.

After 2 hours, the DAF-2/DA solution was aspirated, cells were resuspended in 500 µl fresh PBS and the fluorescence was immediately read on the FLUOstar Omega plate reader at 485/520 nm.

Fluorescence values from the positive control and treatment groups were divided by the average fluorescence of the vehicle control. All values are expressed as a % of the vehicle control. One-way ANOVA, followed by a Bonferroni post-hoc multiple comparison test, was performed to determine any differences between the groups. Data are expressed as Mean ± SD, $p < 0.05$ was considered significant.

(b) PI

PI, a fluorescent intercalating agent, is widely used for evaluating cellular apoptosis and/or cell death. Apoptotic or necrotic cells are characterized by DNA fragmentation, and consequently, nuclear DNA content loss. PI is incapable to cross the cell membrane of viable cells, and will therefore only bind to the DNA released from the apoptotic cells (Riccardi and Nicoletti, 2006) (***Figure 2.9***).

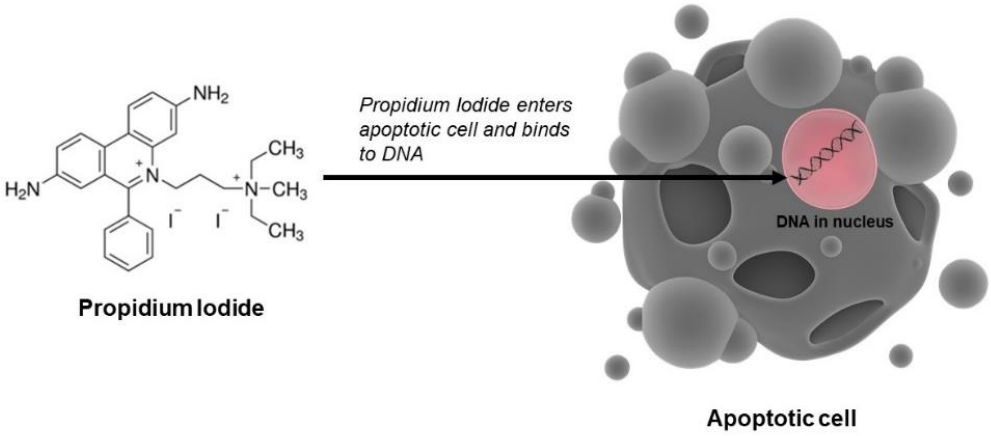

Figure 2.9: *Principle of PI staining. Image adapted from: Sigma-Aldrich and Alpha Laboratories (AlphaLaboratories, 2018; Sigma-Aldrich, 2018b) and composed using* (*Library of Science & Medical Illustrations*, 2018)*.*

The entire PI experiment was repeated 3 times (3 biological repeats) using freshly prepared Afriplex GRT™ solution. Each sample was loaded 4 times in one experiment (4 technical repeats).

PI assay included:
- 4 x **positive control** technical repeats
- 4 x **vehicle control** technical repeats
- 4 x **1 µg/ml Afriplex GRT™** technical repeats
- 4 x **10 µg/ml Afriplex GRT™** technical repeats
- 4 x **100 µg/ml Afriplex GRT™** technical repeats

After treatment, cells in the 24-well plates were washed with PBS. Following this, all the cells were resuspended in PBS, except for the positive control cells which were resuspended in dH_2O. Since dH_2O can cross the semi-permeable membrane via diffusion, the cells will experience osmotic stress, which will eventually result in cell swelling and bursting. The ruptured cell membranes will allow PI to bind to the released DNA.

Next, 5 µM PI (100 µl PI in 200 µl dH_2O) (Sigma-Aldrich, St. Louis, MO, USA) was added to each well for 15 min at 37°C. After the 15 min incubation period, the PI probe was left in the wells and the fluorescence was immediately measured on the FLUOstar Omega plate reader at 544/640 nm.

Fluorescence values from the positive control and treatment groups were divided by the average fluorescence of the vehicle control. All values are expressed as a % of the vehicle control. One-way ANOVA, followed by a Bonferroni post-hoc multiple comparison test, was performed to determine any differences between the groups. Data are expressed as Mean ± SD, $p < 0.05$ was considered significant.

(c) MTT

MTT, is a sensitive colorimetric assay which measures cellular metabolic activity and is thus often used as a test for cell viability. The principle of this technique entails the reduction of MTT, a yellow water-soluble tetrazolium dye, by mitochondrial dehydrogenases, to purple insoluble formazan crystals. These crystals are usually dissolved in DMSO where after the absorbance is measured at 570 nm (Patravale *et al.*, 2012) (***Figure 2.10***).

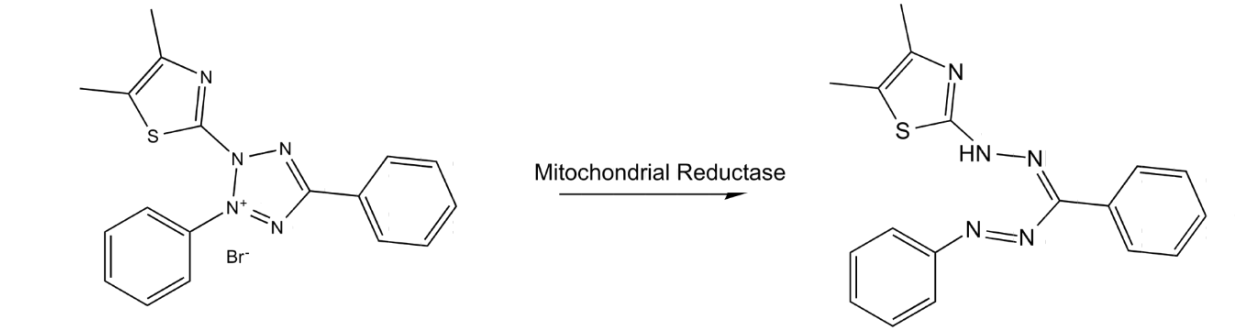

Figure 2.10: *Principle of MTT. Image adapted from (Grant, 2014).*

The entire MTT experiment was repeated 3 times (3 biological repeats), using freshly prepared Afriplex GRT™ solution. Each sample was loaded 4 times in one experiment (4 technical repeats).

MTT assay included:

- 4 x **vehicle control** technical repeats
- 4 x **1 µg/ml Afriplex GRT™** technical repeats
- 4 x **10 µg/ml Afriplex GRT™** technical repeats
- 4 x **100 µg/ml Afriplex GRT™** technical repeats

After treatment, cells in the 24-well plates were washed with PBS. Following this, 2 mg/ml MTT prepared in PBS was added to each well for 2.5 hours at 37°C. After incubation, the MTT solution was aspirated and the purple formazan crystals in each well was dissolved by the addition of 50 µl Sorenson's buffer (0.1 M Glycine, 0.1 M NaCl, 50 ml sterile water; pH 10.5) and 400 µl DMSO. Once dissolved, the absorbance was immediately read on the FLUOstar Omega plate reader at 570 nm.

Absorbance values from the treatment groups were divided by the average absorbance of the vehicle control. All values are expressed as a % of the vehicle control. One-way ANOVA, followed by a Bonferroni post-hoc multiple comparison test, was performed to determine any differences between the groups. Data are expressed as Mean ± SD, $p < 0.05$ was considered significant.

(d) FRET

FRET refers to the distance dependant radiationless transfer of energy between two light-sensitive molecules known as fluorophores. The principle of this technique involves the transfer of energy from an excited donor fluorophore to an acceptor fluorophore via a dipole-dipole interaction (Hussain, 2009). This transfer only occurs when the emission spectrum of the donor fluorophore overlaps the absorption spectrum of the acceptor fluorophore (Sapsford, Berti and Medintz, 2006). Fluorescence is generated and detected when a peptide bond between the donor/acceptor pair is hydrolyzed (Carmona *et al.*, 2006) (***Figure 2.11***).

Using FRET substrates containing o-aminobenzoic acid (Abz) as the fluorescent group and 2,4-dinitrophenyl (Dnp) as the acceptor, both the non-fasting serum collected from the animals and the aqueous Afriplex GRT™ extract were examined for ACE inhibitor activity.

ACE is composed of two homologous domains, i.e. C-domain and N-domain, which differs in substrate specificity. Commercially available ACE fluorescent peptides for the C-domain (Abz-LFK(Dnp)-OH and N-domain (Abz-SDK(Dnp)P-OH) were used (Purchased from Sigma-Aldrich, St. Louis, MO, USA). Captopril was used as the positive control.

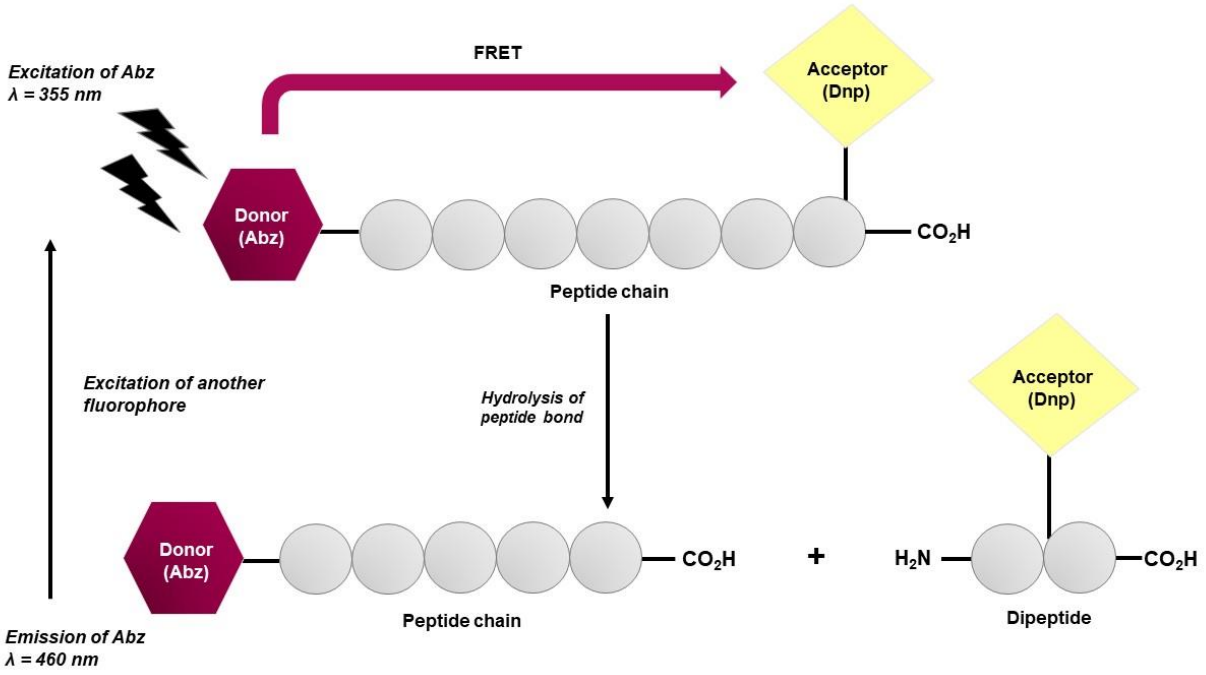

Figure 2.11: *Principle of FRET. Image adapted from (Carmona et al., 2006) and composed using Microsoft PowerPoint.*

For both FRET assays (Non-fasting serum and aqueous Afriplex GRT™), the entire experiment was repeated 3 times (3 biological repeats), using fasting serum from different animals, and freshly prepared Afriplex GRT™ solution. Each sample was loaded twice in one experiment (2 technical repeats).

	Abbreviation	Function
Hanks balanced salt solution	HBSS	Buffer containing Mg and Zn required for FRET
Dimethyl sulfoxide	DMSO	Vehicle control
Abz-LFK(Dnp)-OH	LFK	Fluorescent peptide: ACE C-domain
Abz-SDK(Dnp)P-OH	SDK	Fluorescent peptide: ACE N-domain

Insert: *Summary of specific substrates used in the FRET assay*

FRET 1 assay included:

2 x **HBSS + DMSO** (**vehicle control)** technical repeats
2 x **HBSS only** (**background)** technical repeats
2 x **LFK (C-domain)** technical repeats
2 x **SDK (N-domain)** technical repeats
2 x **LFK + Captopril (C-domain positive control** technical repeats
2 x **SDK + Captopril (N-domain positive control)** technical repeats
2 x **1 µg/ml Afriplex GRT™ LFK** technical repeats
2 x **1 µg/ml Afriplex GRT™ SDK** technical repeats
2 x **10 µg/ml Afriplex GRT™ LFK** technical repeats
2 x **10 µg/ml Afriplex GRT™ SDK** technical repeats
2 x **100 µg/ml Afriplex GRT™ LFK** technical repeats
2 x **100 µg/ml Afriplex GRT™ SDK** technical repeats

FRET 2 assay included:

2 x **LFK (C-domain)** technical repeats
2 x **SDK (N-domain)** technical repeats
2 x **LFK + Captopril (C-domain positive control)** technical repeats
2 x **SDK + Captopril (N-domain positive control)** technical repeats
2 x **LFK + Control serum** technical repeats
2 x **SDK + Control serum** technical repeats
2 x **LFK + Control + Afriplex GRT™ serum** technical repeats
2 x **SDK + Control + Afriplex GRT™ serum** technical repeats
2 x **LFK + HFD serum** technical repeats
2 x **SDK + HFD serum** technical repeats
2 x **LFK + HFD + Afriplex GRT™ serum** technical repeats
2 x **SDK + HFD + Afriplex GRT™ serum** technical repeats

After treatment, cells in the 24-well plates were washed with Hanks balanced salt solution (HBSS). The HBSS buffer contained: 140 mM NaCl, 5mM KCl, 0.1 mM $CaCl_2$, 0.63 mM $MgSO_4$, 1 mM Na_2HPO_4, 6.1 mM glucose and 10 µM $ZnSO_4$; pH 7.4. We used the HBSS buffer as a substitute for PBS, since the FRET assay requires Mg and Zn which were not present in PBS. Following this, HBSS, HBSS+DMSO (990 µl HBSS + 10 µl DMSO), 10 µM LFK, 10 µM SDK, 10 µM LFK + 0.5 µM Captopril and 10 µM SDK + 0.5 µM Captopril were added to the respective wells for 90 min at 37°C.

DMSO was used to prepare the 1 mM LFK and 1 mM SDK peptide stocks. Due to the latter, DMSO diluted in HBSS was included as the vehicle control. For the assay, all stocks were further diluted with HBSS. To prevent a drop in the pH, cells were placed in a O_2 incubator instead of in a CO_2 incubator. The reason for this decision was that the HBSS does not contain any bicarbonate to balance the protons coming from a CO_2 regulated incubator. After 90 min, the fluorescence was measured at 355/460 nm using the FLUOstar Omega plate reader.

Data are expressed as fluorescence intensity (arbitrary units). One-way ANOVA, followed by a Bonferroni post-hoc multiple comparison test, was performed to determine any differences between the groups. Data are expressed as Mean ± SD, $p < 0.05$ was considered significant.

2.9. Biochemical analysis

Non-fasting blood was collected at sacrifice, left on ice for 20 min and spun down at 3000 rpm for 10 min (4°C). The serum was removed and stored at -80°C for the determination of leptin, adiponectin, aldosterone and ET-1 levels in both the control and HFD untreated and Afriplex GRT™ treated animals.

2.9.1. Leptin ELISA

For the determination of serum leptin levels, the Abcam® leptin rat ELISA kit was used (ab100773). This *in vitro* ELISA included a leptin pre-coated 96-well plate together will all the necessary reagents to perform the assay. Before experimentation, all the materials, prepared reagents and serum samples were equilibrated to room temperature (18-25°C). The serum samples were diluted (1:2) with assay diluent D.

Control, standard and serum samples were loaded in duplicate. Of each standard (8000 pg/ml, 2667 pg/ml, 888.9 pg/ml, 296.3 pg/ml, 98.77 pg/ml, 39.92 pg/ml, 10.97 pg/ml and 0 pg/ml) and serum sample, 100 µl were loaded to the appropriate wells, where assay diluent D served as the zero standard. After an incubation period of 2.5 hours at room temperature on a slow rotator (400-500 rpm), the solution was discarded, and each well was washed four times with 300 µl 1X wash buffer. After the final wash, any remaining solution or bubbles were aspirated, where after 100 µl biotinylated leptin antibody solution was added to each well and incubated for 1 hour at room temperature on a slow rotator. After 1 hour, the solution was discarded, and the same washing procedure was conducted. This was followed by the addition of 100 µl TMB one-step substrate reagent to each well. After incubating for 30 min at room temperature on a slow rotator, 50 µl stop solution was added to each well which turned the TMB colour from blue to yellow, and the absorbance was immediately read at 450 nm.

After the OD readings were obtained, the mean absorbance for each set of duplicate controls, standards and samples were calculated, followed by subtracting the average zero standard OD. A log-log standard curve was set-up by plotting the standard concentrations (pg/ml) on the x-axis with the corresponding OD values on the y-axis. The best-fitted linear regression line was drawn through the standard points and an equation was generated. Using this equation, the leptin (pg/ml) present in the serum samples were determined.

Leptin values generated from the graph were statistically analysed by means of two-way ANOVA (4 groups - Control and HFD Afriplex GRT™ treated and untreated groups), followed by a Bonferroni post-hoc multiple comparison test. Data are expressed as Mean ± SD, $p < 0.05$ was considered significant. Leptin levels were converted from pg/ml to ng/ml for graphical purposes.

2.9.2. Adiponectin ELISA

Serum adiponectin levels were determined using the Abcam® adiponectin rat ELISA kit (ab108784). This *in vitro* ELISA included an adiponectin microplate (96-wells) as well as all the required reagents to perform the assay. Prior to experimentation, all the materials, prepared reagents and serum samples were equilibrated to room temperature (18-25°C). The serum samples were diluted (1:400) with assay diluent N.

Control, standard and serum samples were loaded in duplicate. Of each standard (100 ng/ml, 50 ng/ml, 25 ng/ml, 12.5 ng/ml, 6.250 ng/ml, 3.125 ng/ml, 1.563 ng/ml and 0 pg/ml) and serum sample, 50 µl were loaded to the appropriate wells and incubated at room temperature for 1 hour on a slow rotator (400-500 rpm). Assay diluent N served as the zero standard. After incubation,

the solution was discarded, and each well was washed five times with 200 µl 1X wash buffer. After the final wash, any remaining solution or bubbles were aspirated. This was followed by the addition of 50 µl 1X biotinylated adiponectin antibody to each well. After an incubation period of 1 hour at room temperature on a slow rotator, the solution was discarded, and the same washing procedure was conducted. Next, 50 µl Streptavidin conjugate was added to each well and incubated for 30 min at room temperature on a slow rotator. The solution was discarded, the same washing procedure was conducted and 50 µl of the chromogen substrate was added to each well and incubated for 10 min at room temperature (or till an optimal blue colour developed). Stop solution (50 µl per well) was added to each well, and absorbance was immediately read at 450 nm and 570 nm on the FLUOstar Omega plate reader.

Once the OD values obtained at 570 nm were subtracted from the 450 nm readings, the mean absorbance for each set of duplicate standards and samples were calculated. A log-log standard curve was set-up by plotting the standard concentrations (ng/ml) on the x-axis with the corresponding OD values on the y-axis. The best-fitted linear regression line was drawn through the standard points and an equation was generated. Using this equation, the adiponectin present in the serum samples were determined.

Adiponectin values generated from the graph were statistically analysed by means of two-way ANOVA (4 groups - Control and HFD Afriplex GRT™ treated and untreated groups), followed by a Bonferroni post-hoc multiple comparison test. Data are expressed as Mean ± SD, $p < 0.05$ was considered significant.

2.9.3. Aldosterone ELISA

For serum aldosterone determination, the Abcam® aldosterone ELISA kit was used (ab136933). Before experimentation, all the materials, prepared reagents and serum samples were equilibrated to room temperature (18-25°C). Controls, standards and serum samples were loaded in duplicate. This *in vitro* competitive assay included a 96-well donkey anti-sheep IgG pre-coated plate together with all the required reagents to perform the assay.

Of each standard (250 pg/ml, 125 pg/ml, 62.5 pg/ml, 31.3 pg/ml, 15.6 pg/ml, 7.8 pg/ml, 3.9 pg/ml and 0 pg/ml) and serum sample (diluted 1:2 with assay buffer), 100 µl were loaded to the appropriate wells, where assay buffer served as the zero standard (B_0). The non-specific binding (NSB) wells received 150 µl assay buffer. Following this, 50 µl of the aldosterone alkaline phosphatase conjugate was added to the B_o, NSB, standard and sample wells (excluding total activity (TA), and blank (B_s) wells), consequently labelling the standards/samples. Next, 50 µl of

the aldosterone antibody was added to the B_o, standard and sample wells (excluding the NBS, B_s, and TA wells) and incubated overnight (4°C) without shaking. After the incubation period, each well was washed three times with 400 µl 1X wash buffer. After the final wash, any remaining solution or bubbles were aspirated and 5 µl aldosterone alkaline phosphatase (diluted 1:5) was added to the TA wells. This was followed by the addition of 200 µl substrate solution to each well. After incubating for 1 hour without shaking, 50 µl stop solution was added to each well and absorbance read immediately at an OD of 405 nm on the FLUOstar Omega plate reader.

The mean OD of the B_s wells were subtracted from all the readings. The average net OD for each standard and sample was calculated by subtracting the average NBS reading from the average standard/sample OD measurement. The standard curve was set up by calculating the binding of each standard (in duplicate) as a percentage of the maximum binding wells (B_o):

Percentage bound = (average net OD of standard/average net B_o OD) x 100

The percentage bound was plotted on the y-axis and the concentration of the standards on the x-axis. The best-fitted linear regression line was drawn through the data points and the unknown samples were determined via interpolation.

No statistical analyses were performed because the aldosterone assay failed the required minimum threshold.

2.9.4. ET-1 assay

The Abcam® ET-1 ELISA kit was used to determine the serum ET-1 levels in the control and HFD treated and untreated animals. The kit included a 96-well mouse monoclonal ET-1 microplate together with all the necessary reagents to perform the assay. Prior to experimentation, all the materials, prepared reagents and serum samples were equilibrated to room temperature (18-25°C). The serum samples were diluted (1:2) with assay buffer. All the standards, controls and samples were loaded in duplicate.

Of each standard (50 pg/ml, 25 pg/ml, 12.5 pg/ml, 6.25 pg/ml, 3.13 pg/ml, 1.56 pg/ml, 0.78 pg/ml and 0 pg/ml) and serum sample, 100 µl were loaded to the appropriate wells and incubated on a slow rotator (400-500 rpm) for 1 hour at room temperature. Assay buffer served as the zero standard. After 1 hour had elapsed, the contents were emptied, and each well was washed five times with 400 µl 1X wash buffer. After the final wash, any remaining solution or bubbles were aspirated, where after 100 µl ET-1 antibody was added to each well and incubated for 30 min at

room temperature on a slow rotator. After 30 min, the solution was discarded, the same washing procedure was conducted and 100 µl TMB one-step substrate reagent was added to each well and incubated for 30 min at room temperature on a slow rotator. Following this, 100 µl stop solution was added to each well which turned the TMB colour from blue to yellow. The absorbance was read immediately at 450 nm.
The average net OD bound for each standard and sample were calculated as follows:

Average net OD = Average bound OD – Average blank OD

A standard curve was set-up by plotting the standard concentrations (pg/ml) on the x-axis with the corresponding OD values on the y-axis. The best-fitted linear regression line was drawn through the standard points and an equation was generated. Using this equation, ET-1 present in the serum samples were determined.

ET-1 values generated from the graph were statistically analysed by means of two-way ANOVA (4 groups - Control and HFD Afriplex GRT™ treated and untreated groups), followed by a Bonferroni post-hoc multiple comparison test. Data are expressed as Mean ± SD, $p < 0.05$ was considered significant.

2.10. Statistical analysis

Data were statistically analysed using GraphPad Prism® 6 (GraphPad Software, San Diego, CA, USA). All statistical analyses performed are described at the end of each respective section. Data are, if not stated otherwise, expressed as the Mean ± SD. A p-value of < 0.05 was considered statistically significant.
The overall effect of Afriplex GRT™ or the HFD according to the two-way ANOVA are indicated at the bottom of the graph and the multiple comparison data according to the two-way ANOVA are indicated between the bars.

CHAPTER 3: RESULTS

For 16 weeks, half of the animals were fed an HFD to induce a hypertensive phenotype, compared to the remaining age-matched chow-fed controls. Using both animal models, the relationship between Afriplex GRT™, obesity, insulin resistance and hypertension were investigated.

Significance found using a one-way ANOVA is showed in black, two-way ANOVA in green, and a Student's t-test in grey. All data are expressed as Mean ± SD.

3.1. Biometric data and insulin sensitivity

Food and water intake, body weight, fasting glucose and insulin sensitivity were determined before and after treatment. Prior to sacrifice, non-fasting glucose was determined. After sacrificing the IP-fat and livers of the animals were removed and weighed. The HFD + Captopril group served as a positive control for the putative blood pressure lowering effects of Afriplex GRT™ and therefore the biometric measurements for this group is limited.

3.1.1. Food and water intake

Over the 16-week period, the HFD animals, as expected, daily consumed significantly more food when compared to the control animals (**Before treatment HFD vs control:** 19.9 ± 4.7 g vs 17.2 ± 2.8 g; $p < 0.0001$; **After treatment HFD vs control:** 21.3 ± 4.9 g vs 17.3 ± 5.9 g; $p < 0.0001$). Treatment with Afriplex GRT™ and Captopril significantly decreased daily food consumption in the HFD animals when compared to the HFD untreated animals (**HFD + Afriplex GRT™ vs HFD:** 19.5 ± 4.2 vs 21.3 ± 4.9 g; $p < 0.01$; **HFD + Captopril vs HFD:** 18.0 ± 4.7 vs 21.3 ± 4.9 g; $p < 0.001$). Daily food consumption in the control animals were unaffected by treatment with Afriplex GRT™ (***Figure 3.1***).

Throughout the 16-week period, the HFD animals daily consumed significantly less water when compared to the control animals (**Before treatment HFD vs control:** 16.5 ± 4.7 ml vs 25.2 ± 5.2 ml; $p < 0.0001$; **After treatment HFD vs control:** 15.0 ± 4.8 ml vs 23.3 ± 4.3 ml; $p < 0.0001$). Treatment with Afriplex GRT™ significantly increased daily water intake in the control animals when compared to the untreated controls (**Control + Afriplex GRT™ vs control:** 25.4 ± 6.1 ml vs 23.3 ± 4.3 ml; $p < 0.01$). HFD animals treated with Afriplex GRT™ presented with a significant decrease in daily water intake (**HFD + Afriplex GRT™ vs HFD:** 13.5 ± 5.0 ml vs 15.0 ± 4.8 ml; $p < 0.05$) whereas HFD animals treated with Captopril displayed with a significant increase in daily

water intake when compared to HFD untreated animals (**HFD + Captopril vs HFD** 17.5 ± 4.3 ml vs 15.0 ± 4.8 ml; $p < 0.01$) ***(Figure 3.2)***.

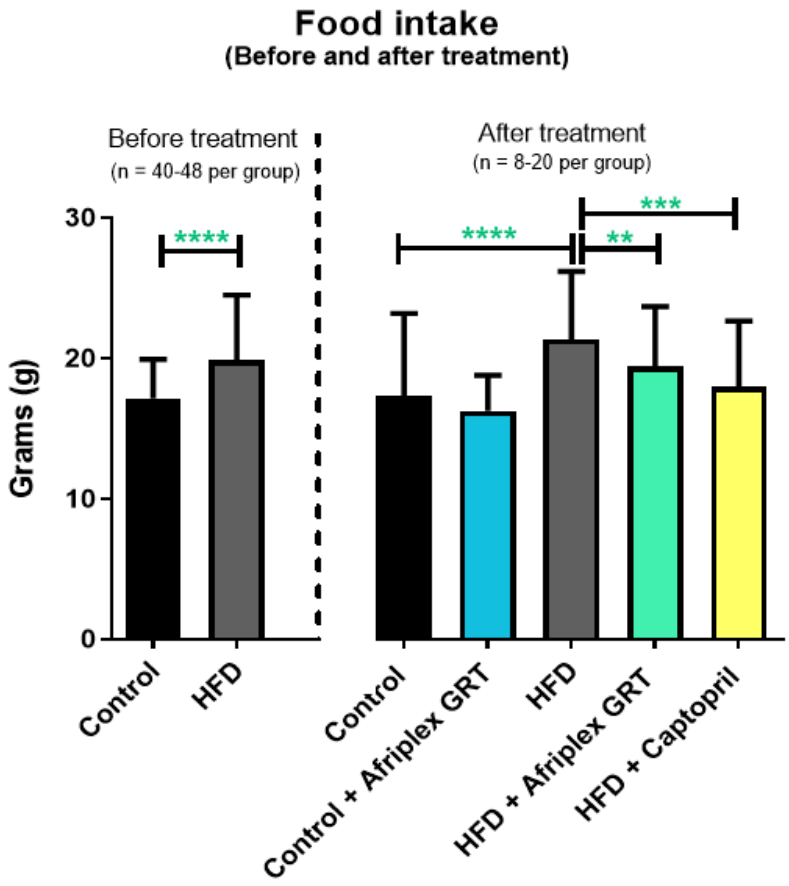

Figure 3.1: *Food intake (g) of the control and HFD animals before (Week 1-10) and after treatment (Week 11-16). ** p < 0.01, *** p < 0.001, **** p < 0.0001 (Before treatment: Control n = 40, HFD n = 48; After treatment: HFD + Captopril n = 8, all other groups n = 20).*

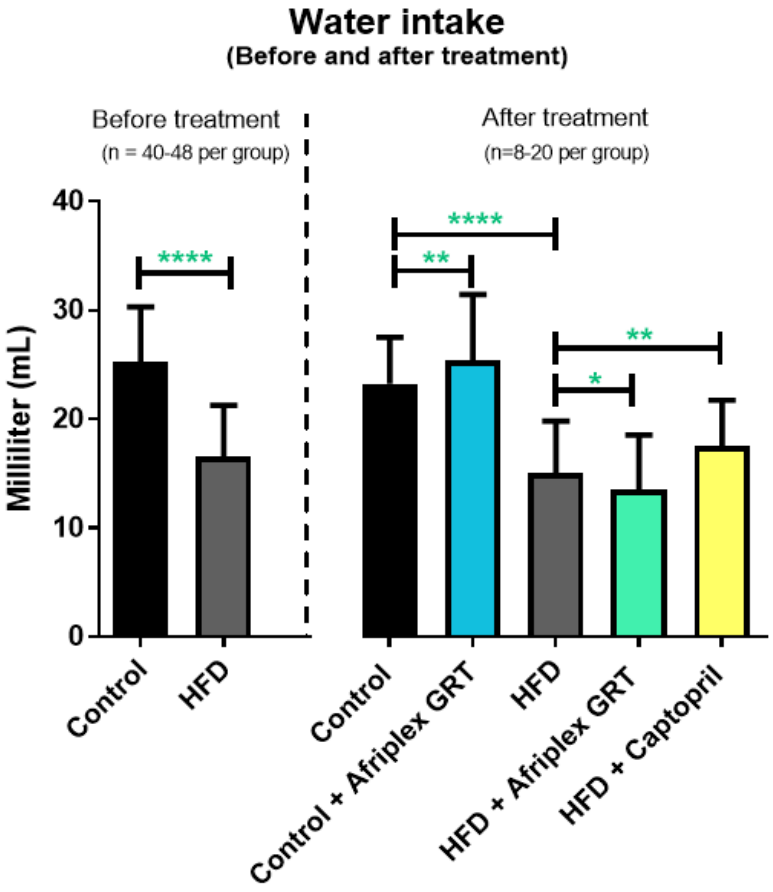

Figure 3.2: *Water intake (ml) of the control and HFD animals before (Week 1-10) and after (Week 11-16) treatment. * $p < 0.05$, ** $p < 0.01$, **** $p < 0.0001$ (Before treatment: Control n = 40, HFD n = 48; After treatment: HFD + Captopril n = 8, all other groups n = 20).*

3.1.2. Body weight

Consumption of the HFD was associated with a significant increase in body weight when compared to the consumption of normal rat-chow (**Before treatment HFD vs control:** 263.8 ± 50.1 g vs 246.0 ± 43.5 g; $p < 0.0001$; **After treatment HFD vs control:** 356.9 ± 46.9 g vs 321.9 ± 32.2 g; $p < 0.0001$). Control animals treated with Afriplex GRT™ presented with a significant decrease in body weight when compared to the untreated controls (**Control + Afriplex GRT™ vs control:** 311.4 ± 25.8 g vs 321.9 ± 32.2 g; $p < 0.01$). Treatment with Afriplex GRT™ and Captopril significantly decreased body weight in the HFD animals when compared to the HFD untreated animals (**HFD + Afriplex GRT™ vs HFD:** 330.9 ± 34.1 g vs 356.9 ± 46.9 g; $p < 0.0001$; **HFD + Captopril vs HFD:** 266.0 ± 22.7 g vs 356.9 ± 46.9 g; $p < 0.0001$) **(*Figure 3.3*)**.

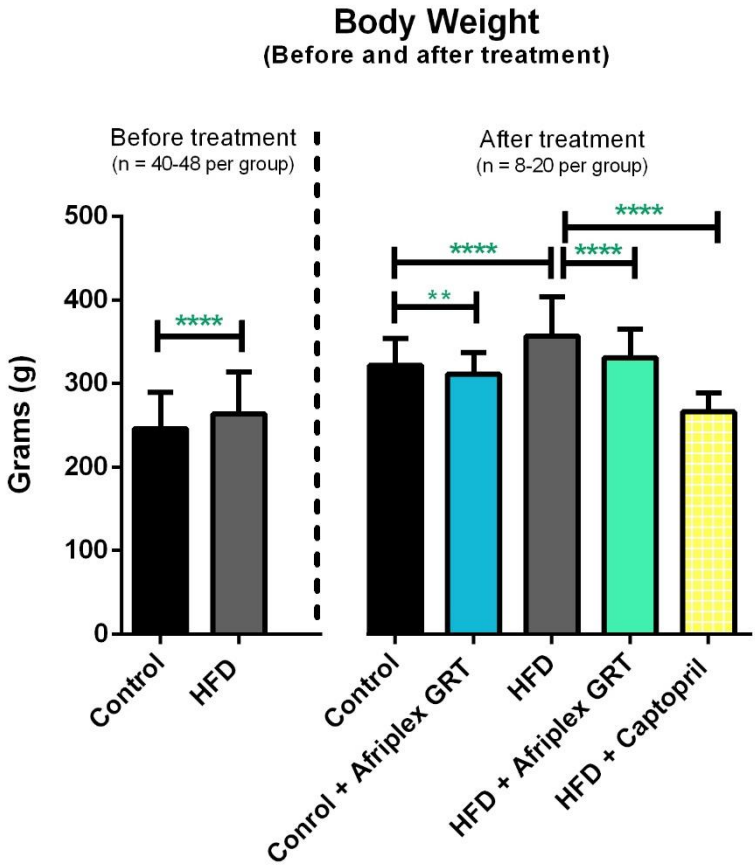

Figure 3.3: *Body weight (g) of the control and HFD animals before (Week 1-10) and after (Week 11-16) treatment. ** $p < 0.01$, **** $p < 0.0001$ (Before treatment: Control n = 40, HFD n = 48; After treatment: HFD + Captopril n = 8, all other groups n = 20).*

3.1.3. Weekly body weight

Analyses showed that over the 16-week period, the HFD animals weighed significantly more, specifically from week 7-15, when compared to the controls (**Week 1-16 HFD vs control:** 303.2 ± 64.8 g vs 274.5 ± 54.2 g; $p < 0.0001$).

Afriplex GRT™ significantly decreased the overall body weight of the control animals when compared to the untreated controls (**Week 1-16 Control + Afriplex vs control:** 267.3 ± 48.9 g vs 274.5 ± 54.2 g; $p < 0.001$). HFD animals treated with Afriplex GRT™ presented with a significant overall body weight decrease (**Week 1-16 HFD + Afriplex GRT™ vs HFD:** 286.7 ± 55.2 g vs 303.2 ± 64.8 g; $p < 0.0001$), specifically in week 16, when compared to the HFD untreated animals.

Treatment with Captopril significantly decreased the body weight, specifically from week 11-16, when compared to the HFD untreated animals (**Week 1-16 HFD + Captopril vs HFD:** 253.1 ± 35.0 g vs 303.2 ± 64.8 g; $p < 0.0001$) (***Figure 3.4***).

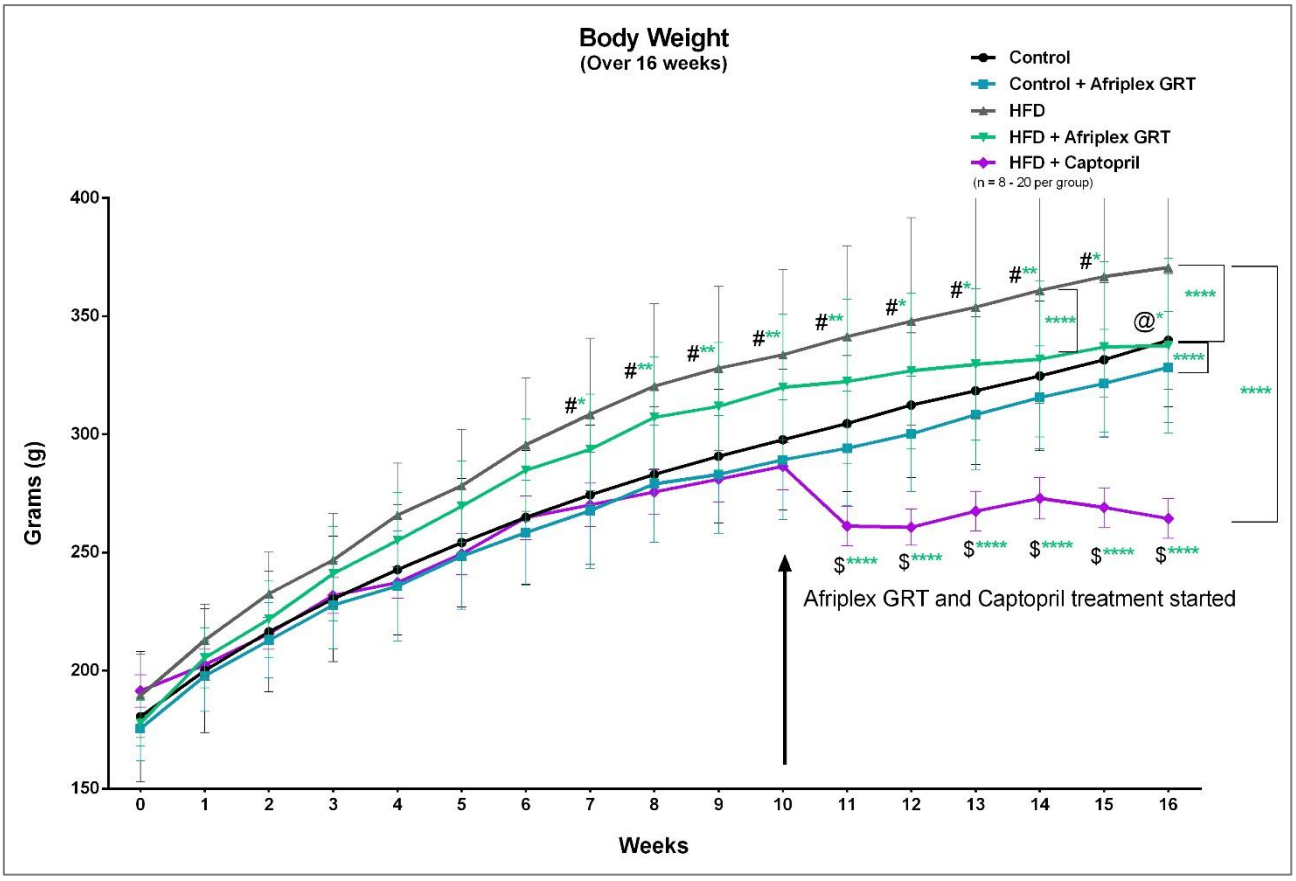

Figure 3.4: *Weekly body weight (g) of the control and HFD before and after treatment. * p < 0.05, ** p < 0.01, *** p < 0.001, **** p < 0.0001; n = 8-20 per group.*
***#:** HFD vs control, **@:** HFD vs HFD + Afriplex GRT™, **$:** HFD vs HFD + Captopril*

3.1.4. IP-fat weight

After 16 weeks, the HFD animals presented with significantly more IP-fat when compared to the controls (**HFD vs control:** 20.4 ± 9.9 g vs 8.7 ± 3.7 g; p < 0.0001). HFD animals treated with Captopril presented with a significant decrease in total IP-fat weight when compared to the HFD untreated animals (**HFD + Captopril vs HFD:** 7.2 ± 2.6 g vs 20.4 ± 9.9 g; p < 0.0001) ***(Figure 3.5 a)***.

When the IP-Fat Weight was calculated as a ratio of the total body weight, the same results were obtained. The HFD animals presented with significantly more IP-fat when compared to the controls (**HFD vs control:** 4.9 ± 1.7 % vs 2.5 ± 0.9 %; p < 0.0001). HFD animals treated with Captopril presented with a significant decrease in total IP-fat weight when compared to the HFD untreated animals (**HFD + Captopril vs HFD:** 2.7 ± 0.8 % vs 4.9 ± 1.7 %; p < 0.001) ***(Figure 3.5 b)***.

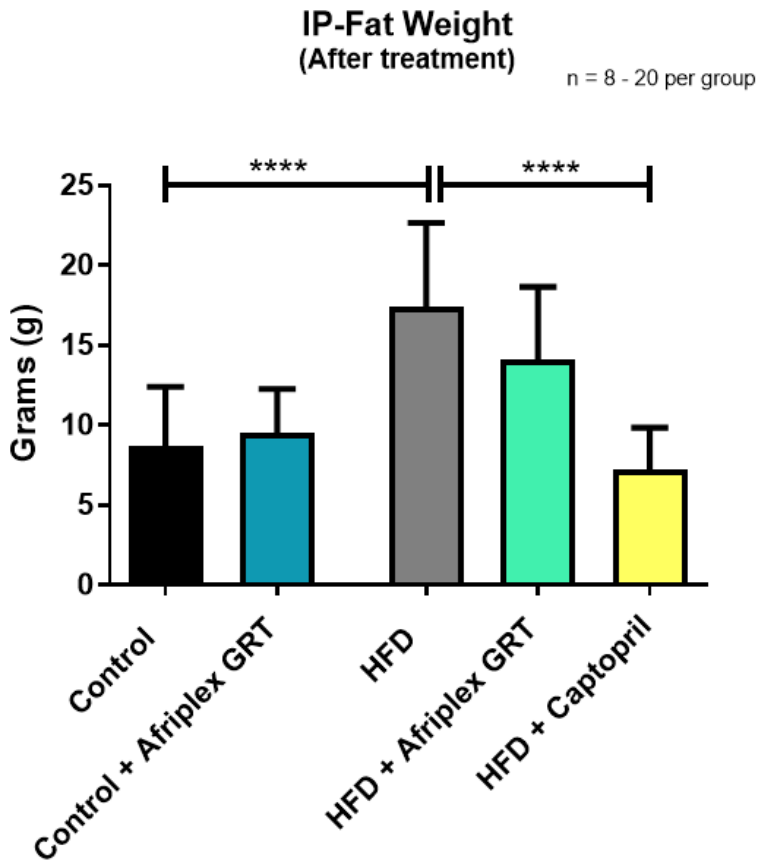

Figure 3.5 (a): *IP-fat weight (g) of the control and HFD animals after treatment. **** p < 0.0001; n = 8-20 per group.*

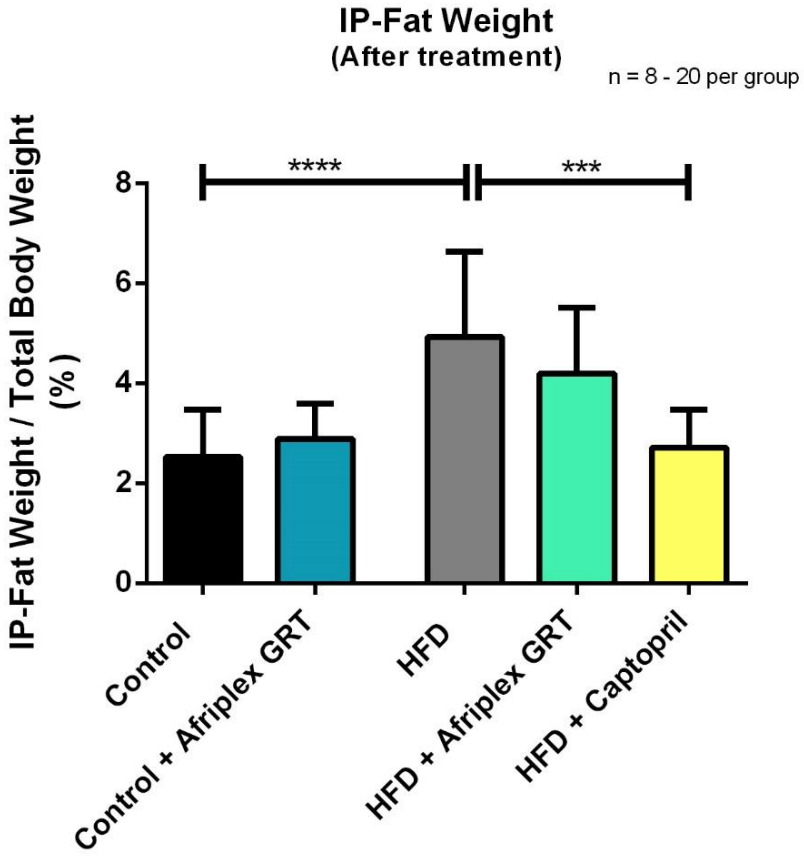

Figure 3.6 (b): *IP fat weight (%) of the control and HFD animals after treatment., *** $p < 0.001$; **** $p < 0.0001$; n = 8-20 per group.*

3.1.5. Liver weight

After 16 weeks, the HFD animals presented with a significant increase in liver weight when compared to the controls (**HFD vs control:**.14.9 ± 3.1 g vs 10.5 ± 1.4 g; $p < 0.0001$).
The overall effect of Afriplex GRT™ treatment was significant in decreasing the liver weight of both the control and HFD animals when compared to their untreated counterparts (**Control + Afriplex GRT™ vs control:** 10.2 ± 1.3 g vs 10.6 ± 1.5 g; $p < 0.05$, **HFD + Afriplex GRT™ vs HFD**: 12.7 ± 1.9 g vs 14.9 ± 3.1 g; $p < 0.05$) ***– indicated at the bottom of the graph (Figure 3.6a)***.
After 16 weeks, the HFD animals presented with a significant increase in liver weight when compared to the controls (**HFD vs control:**.4.0 ± 0.5 % vs 3.1 ± 0.3 %; $p < 0.0001$).

When the liver weight was calculated as a ratio of the total body weight, only the HFD animals presented with a significant increase in liver weight when compared to the controls (**HFD vs control:**.4.0 ± 0.5 % vs 3.1 ± 0.3 %; $p < 0.0001$) ***(Figure 3.6b)***.

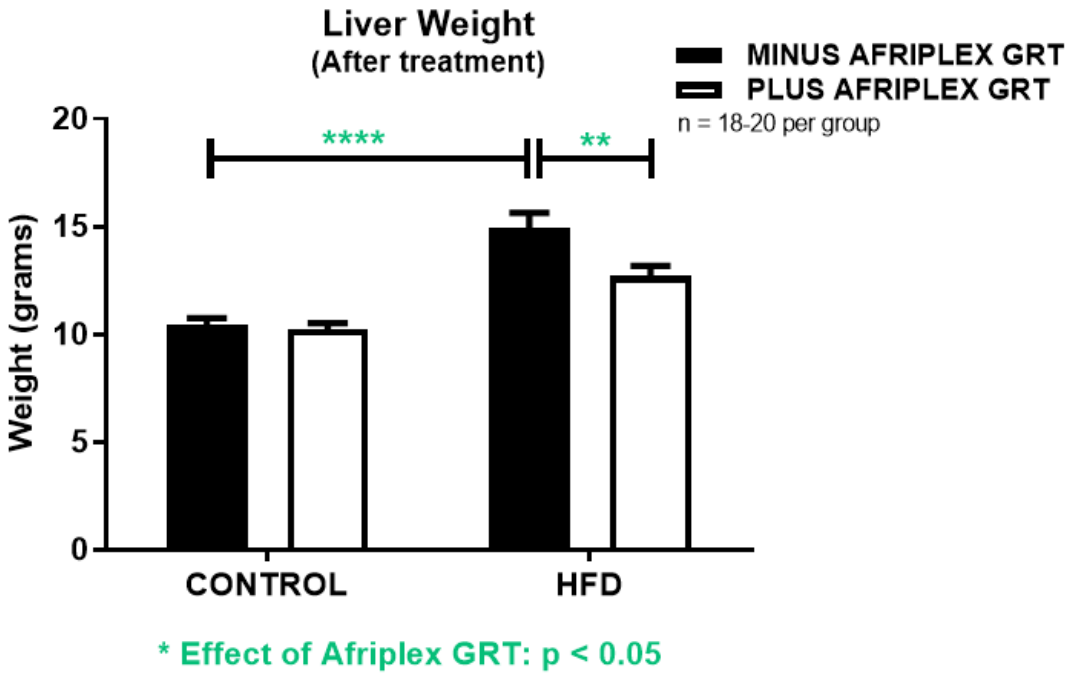

Figure 3.7 (a): *Liver weight (g) of the control and HFD animals after treatment. * $p < 0.05$, ** $p < 0.01$, **** $p < 0.0001$; n = 18-20 per group.*

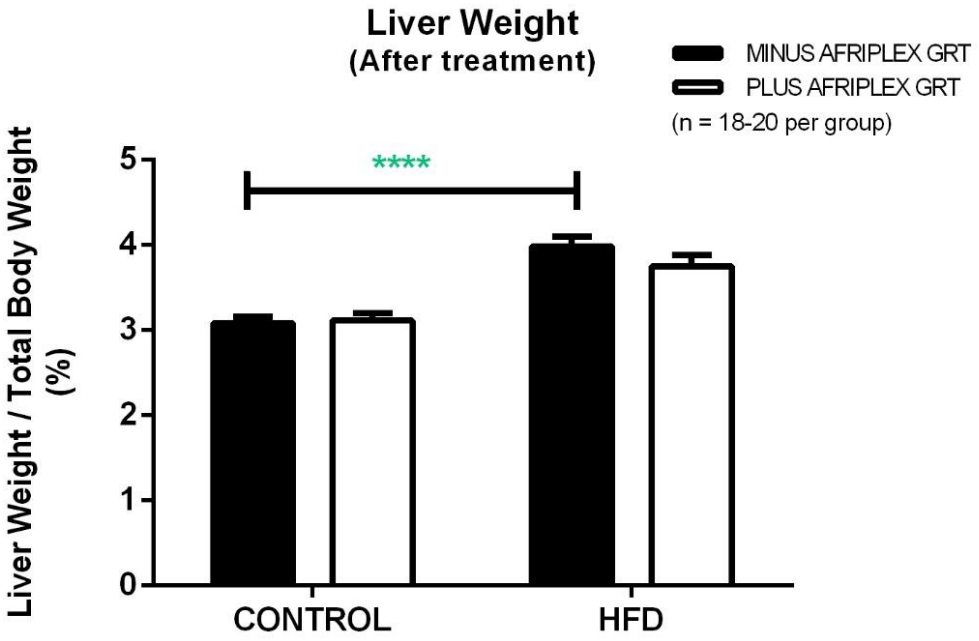

Figure 3.8 (b): *Liver weight (%) of the control and HFD animals after treatment. **** $p < 0.0001$; $n = 18$-20 per group.*

3.1.6. OGTT: Before and after treatment

In week 10 and 16, animals were fasted overnight, followed by the determination of their glucose tolerance using an OGTT. After the fasting (baseline) measurement was obtained (0 min), animals were gavaged with 1 g/kg 50 % sucrose solution and the plasma glucose levels were monitored for 2 hours.

Prior to treatment (Week 10), the overall plasma glucose levels of the HFD animals were significantly higher when compared to the control animals (**HFD vs control:** 6.2 ± 0.7 mmol/L vs 5.6 ± 0.8 mmol/L; $p < 0.0001$). Specifically, 15 min after sucrose administration, the plasma glucose levels of the HFD and control animals differed significantly (**HFD vs control:** 7.3 ± 1.0 mmol/L vs 6.0 ± 1.2 mmol/L; $p < 0.05$) **(*Table 3.1 & Figure 3.7a*)**. The AUC analysis showed no significant differences (**Control vs HFD:** 544.8 ± 233.3 arbitrary units vs 644.5 ± 209.5 arbitrary units) (***Figure 3.7b)***.

After the 16-week treatment period, two-way analyses of variance indicated that the overall plasma glucose levels of the HFD animals were still significantly higher when compared to the control animals (**HFD vs control:** 6.6 ± 0.8 mmol/L vs 5.9 ± 0.8 mmol/L; $p < 0.0001$). This difference was specifically seen after 10-15 min of sucrose administration (**10 min:** 7.5 ± 0.9 mmol/L vs 6.3 ± 0.7 mmol/L; **15 min:** 7.5 ± 0.9 mmol/L vs 6.3 ± 0.8 mmol/L; $p < 0.01$). No significant differences were observed between the control and HFD animals after 20 min to 120 min ***(Table 3.1 & Figure 3.8a)***.

Treatment with Afriplex GRT™ significantly decreased the plasma glucose levels of both the control and HFD animals, when compared to their respective untreated controls (**Control + Afriplex GRT™ vs control:** 5.6 ± 0.7 mmol/L vs 5.9 ± 0.8 mmol/L; $p < 0.001$; **HFD + Afriplex GRT™ vs HFD:** 6.3 ± 0.8 mmol/L vs 6.6 ± 0.8 mmol/L; $p < 0.001$) **(*Figure 3.8a)***.

The AUC analysis showed no significant differences between the groups after treatment (**Control:** 696.7 ± 86.4 arbitrary units, **HFD:** 703.1 ± 202.5 arbitrary units, **Control + Afriplex GRT™:** 565.8 ± 213.6 arbitrary units, **HFD + Afriplex GRT™:** 707.3 ± 86.4 arbitrary units) ***(Figure 3.8b)***.

Table 3.1: *Plasma glucose values (mmol/L) of the control and HFD animal before and after treatment.*

Before treatment - Week 10			After treatment - Week 16			
	Control	HFD	Control	HFD	Control + Afriplex GRT™	HFD + Afriplex GRT™
Time (min)	Mean ± SD		Mean ± SD			
0	4.7 ± 0.3	5.3 ± 0.7	5.1 ± 0.6	5.6 ± 0.9	4.7 ± 0.3	5.6 ± 0.7
3	5.0 ± 0.9	5.9 ± 0.6	5.7 ± 0.7	6.3 ± 0.9	5.2 ± 0.6	6.2 ± 0.7
5	5.4 ± 0.9	6.5 ± 0.4	5.7 ± 0.7	6.7 ± 1.0	5.4 ± 0.7	6.2 ± 0.7
10	6.0 ± 1.0	7.0 ± 1.3	6.3 ± 0.7	7.5 ± 0.9 #**	5.9 ± 0.8	6.7 ± 1.0
15	6.0 ± 1.2	7.3 ± 1.0 #*	6.3 ± 0.8	7.5 ± 0.9 #**	6.1 ± 0.8	6.9 ± 0.8
20	6.4 ± 0.6	7.1 ± 0.9	6.6 ± 0.8	7.5 ± 0.9	6.3 ± 0.6	7.0 ± 0.8
25	6.2 ± 0.6	6.8 ± 0.6	6.5 ± 1.0	7.2 ± 0.7	6.0 ± 0.6	7.0 ± 0.9
30	6.1 ± 1.0	6.6 ± 0.6	6.4 ± 1.3	7.1 ± 0.7	6.2 ± 0.7	6.9 ± 1.1
45	5.8 ± 0.7	6.0 ± 0.6	6.0 ± 1.2	6.6 ± 0.6	5.7 ± 0.7	6.1 ± 0.9
60	5.2 ± 0.8	5.7 ± 0.7	5.8 ± 0.9	6.2 ± 0.8	5.3 ± 0.8	5.7 ± 0.9
90	5.1 ± 0.8	5.1 ± 0.5	5.3 ± 0.7	5.7 ± 0.7	4.8 ± 0.7	5.3 ± 0.7
120	4.8 ± 0.5	5.0 ± 0.5	5.1 ± 0.5	5.6 ± 0.6	5.0 ± 0.4	5.5 ± 0.4
Average (Overall difference)	5.6 ± 0.8	6.2 ± 0.7 #****	5.9 ± 0.8	6.6 ± 0.8 #****	5.6 ± 0.7 &***	6.3 ± 0.8 @***

*OGTT data are expressed as Mean ± SD, * p < 0.05; ** p < 0.01; *** p < 0.001; **** p < 0.0001; n = 11-12 per group.*

***#:** control vs HFD, **&:** control vs control + Afriplex GRT™, **@:** HFD vs HFD + Afriplex GRT™*

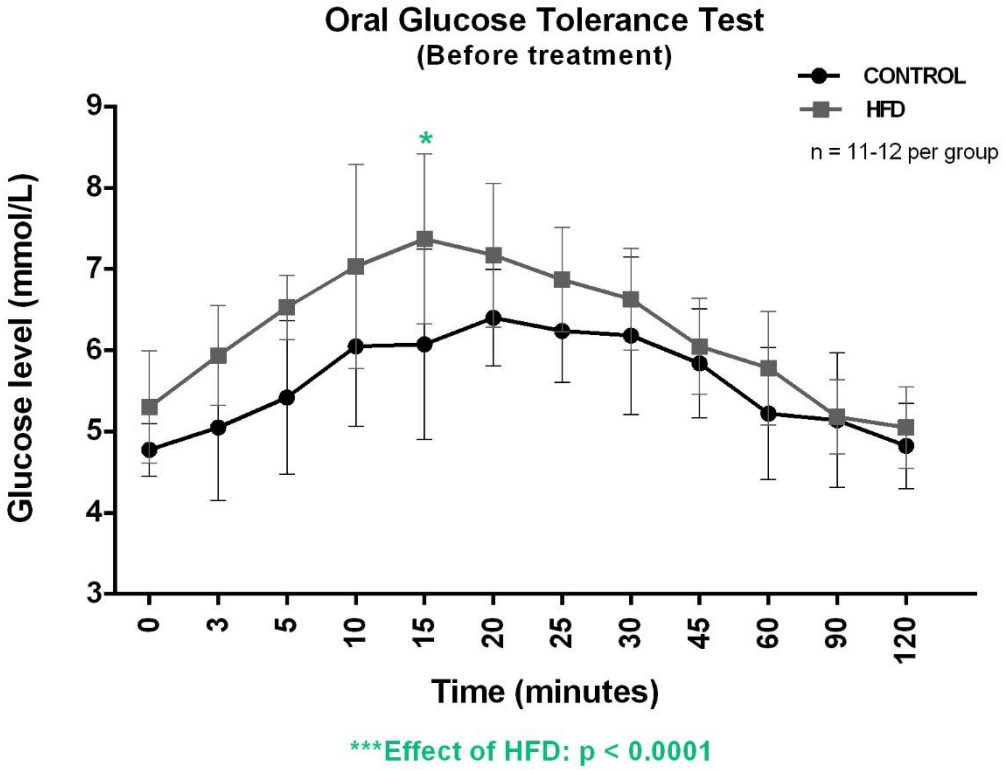

Figure 3.9 (a): *Determination of glucose tolerance in the control and HFD untreated animals (mmol/L). * p < 0.05, **** p < 0.0001; n = 11-12 per group.*

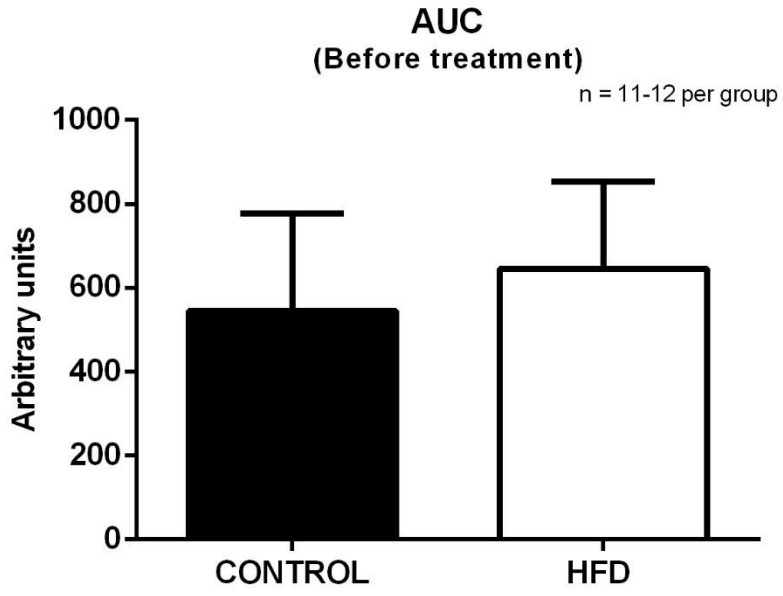

Figure 3.10 (b): *AUC representation of the OGTT's before treatment, n = 11-12 per group.*

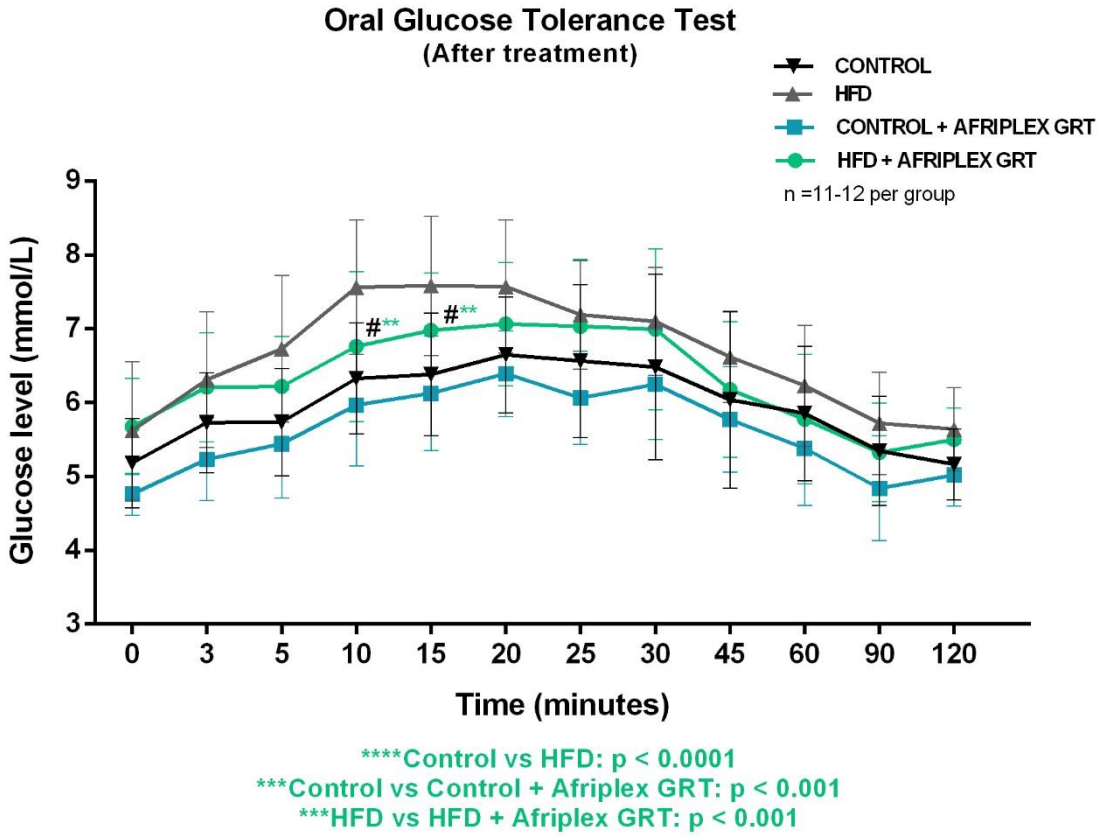

Figure 3.11 (a): *Determination of glucose tolerance in the control and HFD animals after treatment (mmol/L). ** p < 0.01, *** p < 0.001, **** p < 0.0001, n = 11-12 per group.*

#: control vs HFD

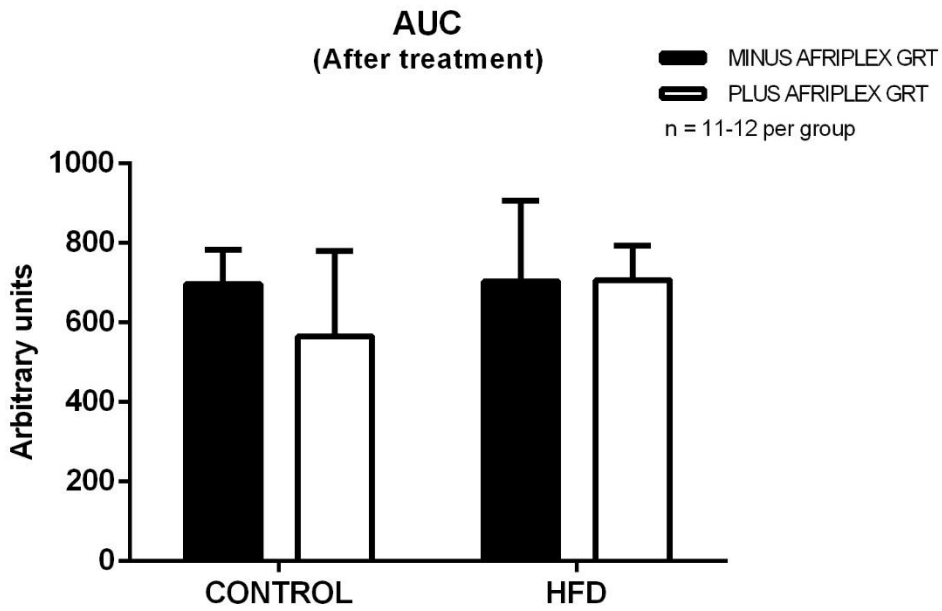

Figure 3.8 (b): *AUC representation of the OGTT's after treatment, n = 11-12 per group.*

3.1.7. Non-fasting blood glucose levels

Prior to sacrifice (Week 16), the HFD animals presented with significantly higher non-fasting blood glucose levels when compared to the control animals (**HFD vs control:** 8.0 ± 1.3 mmol/L vs 7.0 ± 0.9 mmol/L; $p < 0.05$) (***Figure 3.9***).

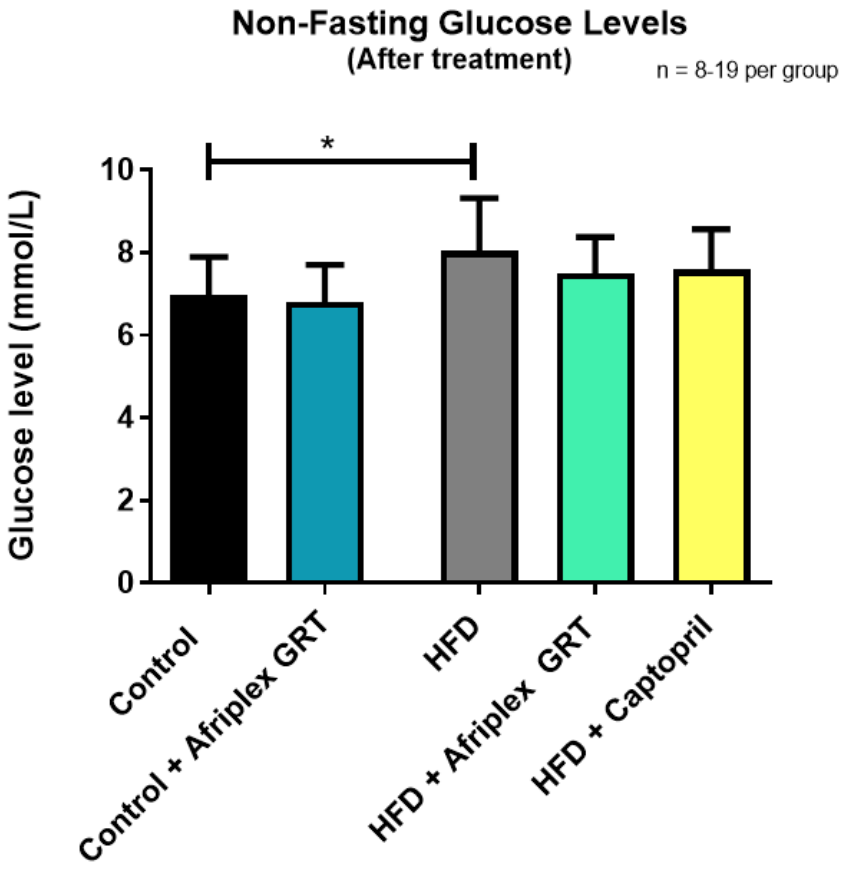

Figure 3.12: *Non-fasting blood glucose levels (mmol/L) of the control and HFD animals after treatment. * $p < 0.05$; n = 8-19 per group.*

3.1.8. Fasting blood glucose levels

After 16 weeks on the respective diets, the fasting glucose levels of the HFD animals were significantly increased when compared to the control animals (**HFD vs control:** 5.6 ± 0.9 mmol/L vs 5.2 ± 0.6 mmol/L; $p < 0.01$). In both groups, treatment with Afriplex GRT™ had no significant effect on the fasting glucose levels (***Figure 3.10***).

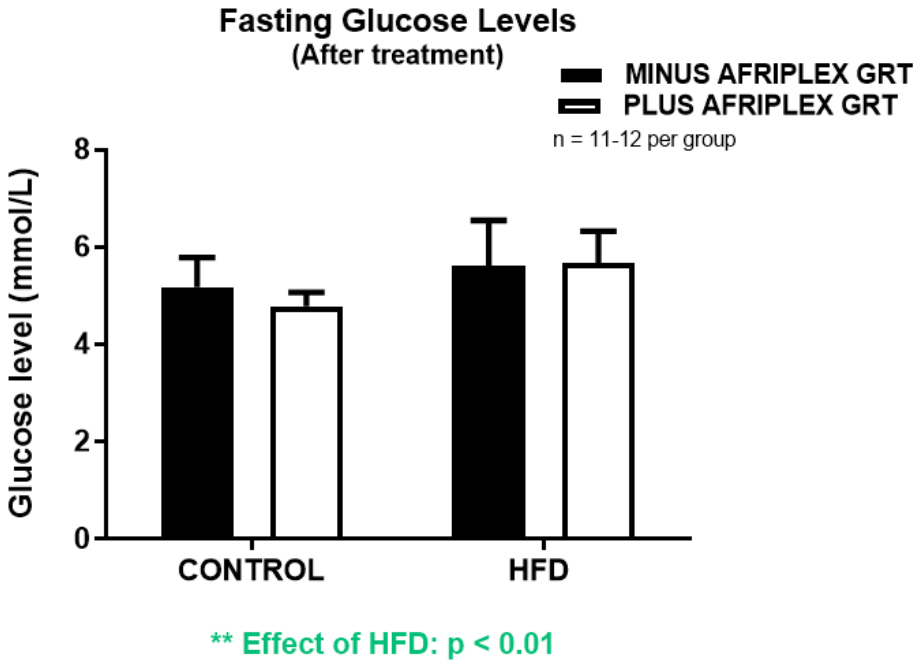

Figure 3.13*: Fasting blood glucose levels (mmol/L) of the control and HFD animals after treatment. ** p < 0.01; n = 11-12 per group.*

3.1.9. Insulin levels

Fasting insulin levels of the HFD animals were significantly decreased when compared to the control animals (**HFD vs control:** 41.0 ± 11.9 µlU/ml vs 54.5 ± 12.6 µlU/ml; $p < 0.01$). Treatment with Afriplex GRT™ significantly decreased the fasting insulin levels in both the control and HFD animals, when compared to their respective controls (**HFD + Afriplex GRT™ vs HFD:** 27.4.8 ± 10.8 µlU/ml vs 41.0 ± 11.9 µlU/ml; $p < 0.05$; **control + Afriplex GRT™ vs control:** 39.8 ± 15.0 µlU/ml vs 54.5 ± 12.6 µlU/ml; $p < 0.05$) ***(Figure 3.11).***

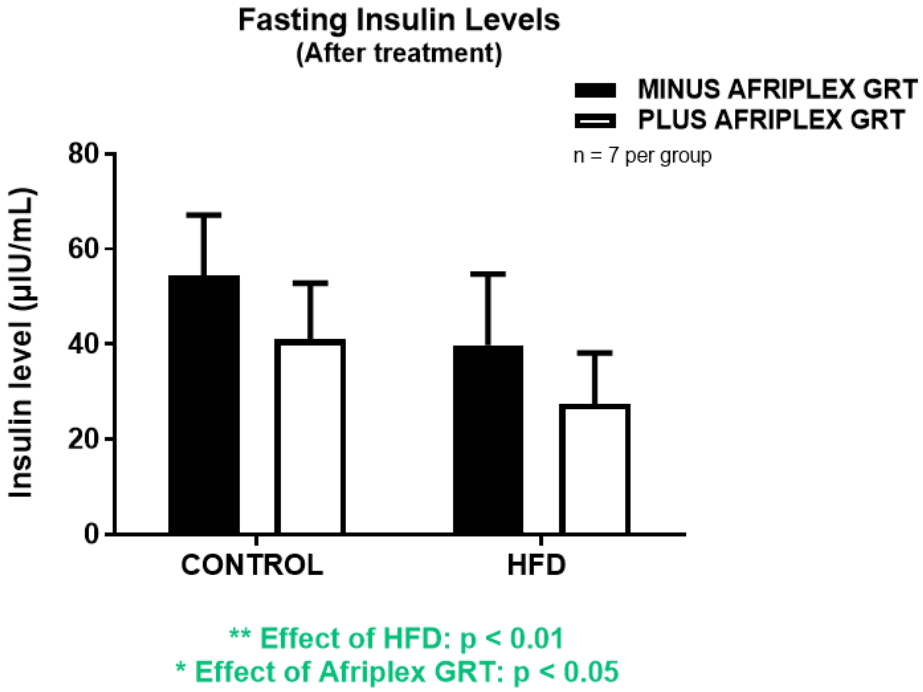

Figure 3.14: *Insulin levels (µlU/mL) of the control and HFD animals after treatment. * $p < 0.05$, ** $p < 0.01$; n = 7 per group*.

3.1.10. HOMA–IR

The HFD had no effect on the HOMA-IR when compared to the controls. Treatment with Afriplex GRT™ significantly decreased the HOMA-IR in both the control and HFD animals when compared to their respective controls (**HFD + Afriplex GRT vs HFD:** 4.2 ± 0.1 vs 6.0 ± 0.5; $p < 0.001$; **Control + Afriplex GRT vs control:** 4.9 ± 0.9 vs 6.2 ± 0.5, $p < 0.001$) (***Figure 3.12).***

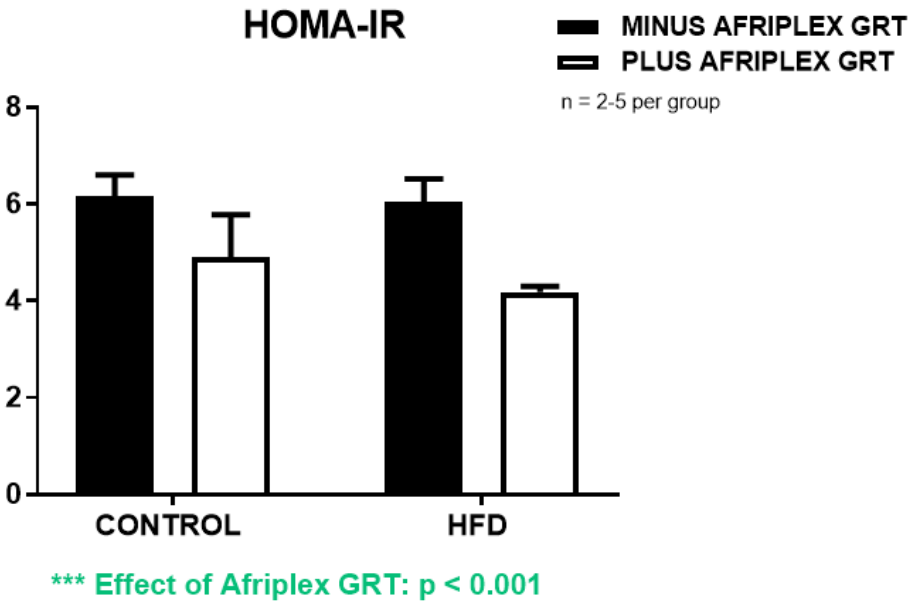

Figure 3.15: *HOMA-IR of the control and HFD animals after treatment. *** $p < 0.001$; n = 2-5 per group.*

3.2. Blood pressure related markers

The data below reflect the blood pressure recordings, urine volume and urine parameters measured before (Week 8-10) and during/after treatment (Week 11-16). Statistical analyses of all blood pressure data were performed by Dr Carl Lombard of the Division of Epidemiology and Biostatistics, Stellenbosch University.

3.2.1. Blood pressure: Before treatment

Systolic pressure: Before treatment, the HFD animals had significantly higher mean baseline systolic blood pressure readings when compared to the controls (**HFD vs control:** 135.4 ± 6.9 mm Hg vs 123.2 ± 5.1 mm Hg; $p < 0.001$). Within the control groups, the mean baseline systolic blood pressure was similar before treatment (**control vs control + Afriplex GRT™:** 123.2 ± 5.1 mm Hg vs 120.9 ± 3.8 mm Hg; $p = 0.1195$). The HFD groups presented with a significant difference in mean baseline systolic blood pressure before treatment (**HFD vs HFD + Afriplex GRT™:** 135.4 ± 6.9 mm Hg vs 129.9 ± 7.2 mm Hg; $p = 0.0176$) ***(Table 3.2 & Figure 3.13)***

Diastolic pressure: The mean baseline diastolic blood pressure readings of the control and HFD animals differed significantly prior to treatment (**control vs HFD:** 84.5 ± 5.2 mm Hg vs 93.6 ± 7.5 mm Hg; $p < 0.001$). Within the control and HFD groups respectively, the mean baseline diastolic blood pressure readings also significantly differed before treatment (**control vs control + Afriplex GRT™:** 84.5 ± 5.2 mm Hg vs 80.0 ± 4.1 mm Hg; $p = 0.0045$; **HFD vs HFD + Afriplex GRT™:** 93.6 ± 7.5 mm Hg vs 89.0 ± 5.5 mm Hg; $p = 0.0303$) ***(Table 3.2 & Figure 3.14)***.

Due to the differences in baseline measurements within the control and HFD groups before treatment, the mean individual baseline value for each one of the four groups was subtracted from the corresponding blood pressure measurements at week 11-16. A linear mixed effects model was then fitted to these baseline adjusted measurements.

Table 3.2: *Systolic and Diastolic Blood pressure (mm Hg) before treatment.*

Blood Pressure: Before treatment						
	Systolic blood pressure (mm Hg)			Diastolic blood pressure (mm Hg)		
	Mean	SD	p-value	Mean	SD	p-value
Control	123.2	5.1	p < 0.001***	84.5	5.2	p < 0.001***
HFD	135.4	6.9		93.6	7.5	
Control	123.2	5.1	p = 0.1195	84.5	5.2	p = 0.0045**
Control + Afriplex GRT™	120.9	3.8		80.0	4.1	
HFD	135.4	6.9	p = 0.0176*	93.6	7.5	p = 0.0303*
HFD + Afriplex GRT™	129.9	7.2		89.0	5.5	

*Data are expressed as Mean ± SD. * p < 0.05; ** p < 0.01; *** p < 0.001; n = 20 per group.*

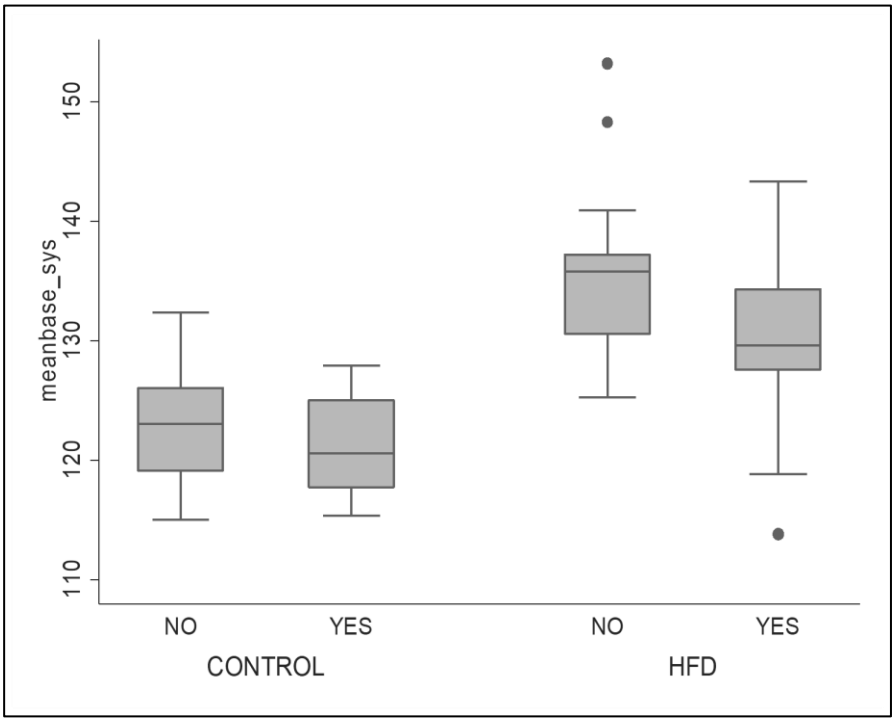

Figure 3.16: *Mean baseline systolic blood pressure (mm Hg) of the control and HFD animals before treatment. At this point Afriplex GRT™ was not administered. NO: Groups who will not receive treatment; YES: Groups who will receive Afriplex GRT™; n = 20 per group.*

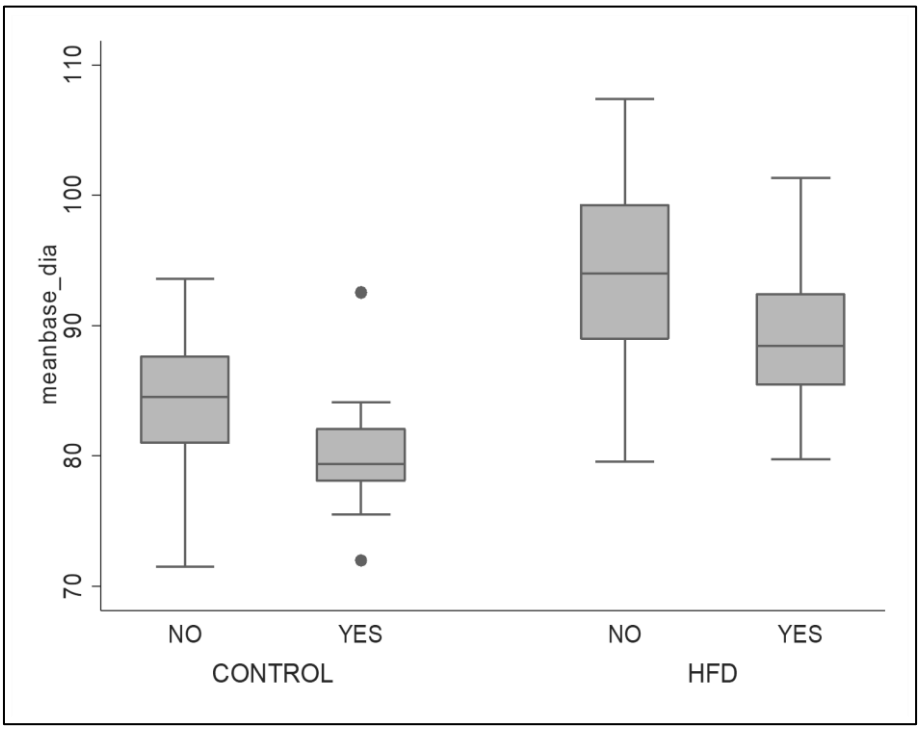

Figure 3.17: *Mean baseline diastolic blood pressure (mm Hg) of the control and HFD animals before treatment. At this point Afriplex GRT™ was not administered. NO: Groups who will not receive treatment; YES: Groups who will receive Afriplex GRT™; n = 20 per group.*

3.2.2. Blood pressure: After treatment

Systolic pressure: In week 13, the control + Afriplex GRT™ group had significantly lower systolic blood pressure readings (p = 0.023); however the overall effect of Afriplex GRT™ on the systolic blood pressure of the control animals was not significant (p = 0.0872). The systolic blood pressure of the HFD + Afriplex GRT™ group was overall significantly lower when compared to the HFD untreated animals from week 11-16; p = 0.0348 ***(Figure 3.15)***. In the HFD animals, Afriplex GRT™ resulted in a quick systolic blood pressure drop, with significant differences at week 13 (p = 0.033) and week 14 (p = 0.048) when compared to the HFD untreated animals. However, this trend was not continuous as treatment with Afriplex GRT™ was completely insignificant in week 15 (p = 0.506) and in week 16 (p = 0.707) **(*Table 3.3*)**.

Table 3.3: *Baseline Adjusted Systolic Blood Pressure (mm Hg): After Treatment*

Baseline adjusted systolic blood pressure: After treatment										
	Control		Control + Afriplex GRT™		Control vs control + Afriplex GRT™	HFD		HFD + Afriplex GRT™		HFD vs HFD + Afriplex GRT™
	Mean	SD	Mean	SD	p-value	Mean	SD	Mean	SD	p-value
Week 11	-0.4	6.5	-2.1	6.9	p = 0.456	-1.1	11.5	2.5	11.2	p = 0.231
Week 12	-2.0	8.8	-3.1	6.1	p = 0.605	-3.2	12.2	-8.9	10.3	p = 0.086
Week 13	0.9	7.8	-3.9	6.9	p = 0.023*	-3.1	11.0	-9.9	8.3	p = 0.033*
Week 14	-6.0	6.7	-2.6	4.7	p = 0.096	-2.7	7.6	-9.1	6.3	p = 0.048*
Week 15	-5.8	6.6	-4.6	6.5	p = 0.573	-5.3	7.2	-7.5	9.7	p = 0.506
Week 16	-2.4	5.7	-2.4	6.7	p = 0.989	-6.6	11.0	-7.8	9.3	p = 0.707

*Data are expressed as Mean ± SD. * p < 0.05; n = 20 per group.*

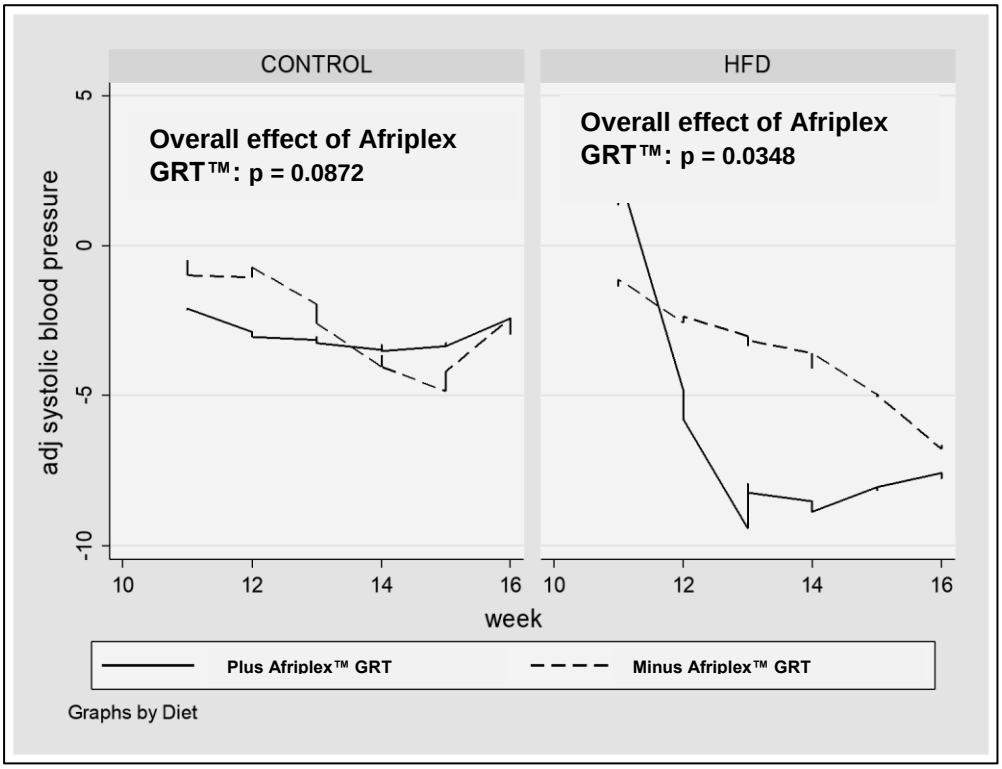

Figure 3.18: *Baseline adjusted systolic blood pressure (mm Hg) of the control and HFD animals after treatment with Afriplex GRT™; n = 20 per group.*

Diastolic pressure: In week 14, the control + Afriplex GRT™ group had significantly lower diastolic blood pressure readings (p = 0.003); however the overall effect of Afriplex GRT™ on the diastolic blood pressure of the control animals was not significant (p = 0.253). Overall the diastolic blood pressure readings of the HFD untreated and HFD + Afriplex GRT™ group did not significantly differ from week 11-16 (borderline significance: p = 0.0589) **(*Table 3.4 & Figure 3.16*)**.

Table 3.4: *Baseline Adjusted Diastolic Blood Pressure (mm Hg): After Treatment*

Baseline adjusted diastolic blood pressure: After treatment										
	Control		Control + Afriplex GRT™		Control vs control + Afriplex GRT™	HFD		HFD + Afriplex GRT™		HFD vs HFD + Afriplex GRT™
	Mean	SD	Mean	SD	p-value	Mean	SD	Mean	SD	p-value
Week 11	-1.1	7.6	1.5	8.1	p = 0.292	-1.0	8.7	2.2	10.6	p = 0.285
Week 12	-4.7	9.5	-2.6	6.1	p = 0.382	-2.4	11.7	-8.5	8.7	p = 0.085
Week 13	1	8.4	1.6	8.9	p = 0.829	0.3	12.4	-5.0	8.6	p = 0.083
Week 14	-7.9	6.8	-0.7	8.2	p = 0.003**	-1.4	9.9	-6.4	7.6	p = 0.109
Week 15	-8.1	6.3	-4.2	8.2	p = 0.109	-8.8	9.6	-8.0	8.0	p = 0.722
Week 16	-3.2	5.1	-0.3	8.3	p = 0.253	-5.0	10.1	-6.2	8.4	p = 0.689

*Data are expressed as Mean ± SD. ** p < 0.01; n = 20 per group.*

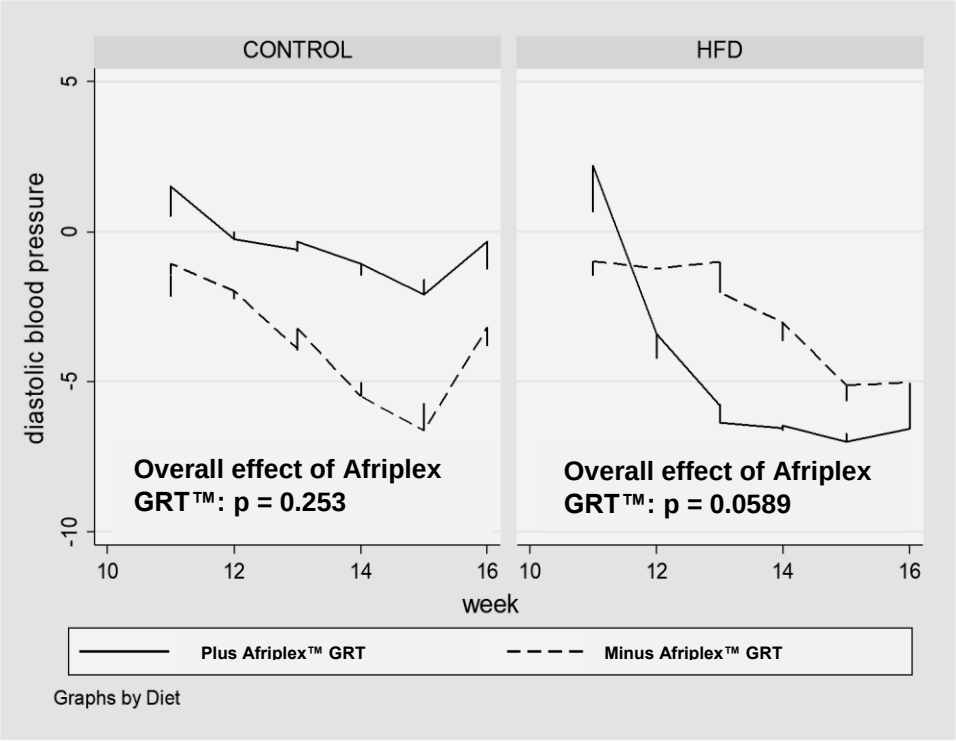

Figure 3.19: *Baseline adjusted diastolic blood pressure (mm Hg) of the control and HFD animals after treatment with Afriplex GRT™; n = 20 per group.*

3.2.3. Blood pressure: Captopril comparison

In this section, the HFD, HFD + Afriplex GRT™ and HFD + Captopril groups were compared. Due to baseline differences, the same baseline adjusted analyses were conducted for both the systolic and diastolic blood pressure readings, bearing in mind that the n-value for this baseline adjusted analyses was increased as the Captopril group was included.

Systolic pressure: The systolic blood pressure of the HFD + Afriplex GRT™ group was overall significantly lower when compared to the HFD untreated animals from week 11-16; p = 0.0277.

No significant differences were observed between the HFD and HFD + Captopril group; p = 0.8108, as well as between the HFD + Afriplex GRT™ and HFD + Captopril group; p = 0.5206. These results are indicative of similar systolic blood pressure profiles **(*Table 3.5 & Figure 3.17*)**.

Table 3.5: *Baseline Adjusted Systolic Blood Pressure (mm Hg): After Treatment*

Baseline adjusted systolic blood pressure: After treatment									
	HFD		HFD + Afriplex GRT™		HFD + Captopril		HFD vs HFD + Afriplex GRT™	HFD vs HFD + Captopril	HFD + Afriplex GRT™ vs HFD + Captopril
	Mean	SD	Mean	SD	Mean	SD	p-value	p-value	p-value
Week 11	-1.1	11.5	2.5	11.2	-12.5	10.4	p = 0.0277*	p = 0.8108	p = 0.5206
Week 12	-3.2	12.2	-9.0	10.3	-15.4	11.8			
Week 13	-3.1	11.0	-9.9	8.3	-20.5	11.7			
Week 14	-2.7	7.6	-9.1	6.3	-17.7	7.6			
Week 15	-5.3	7.2	-7.5	9.7	-18.7	8.2			
Week 16	-6.6	11.0	-7.8	9.3	-21.2	9.6			

*Data are expressed as Mean ± SD. * p < 0.05; n = 8-20 per group.*

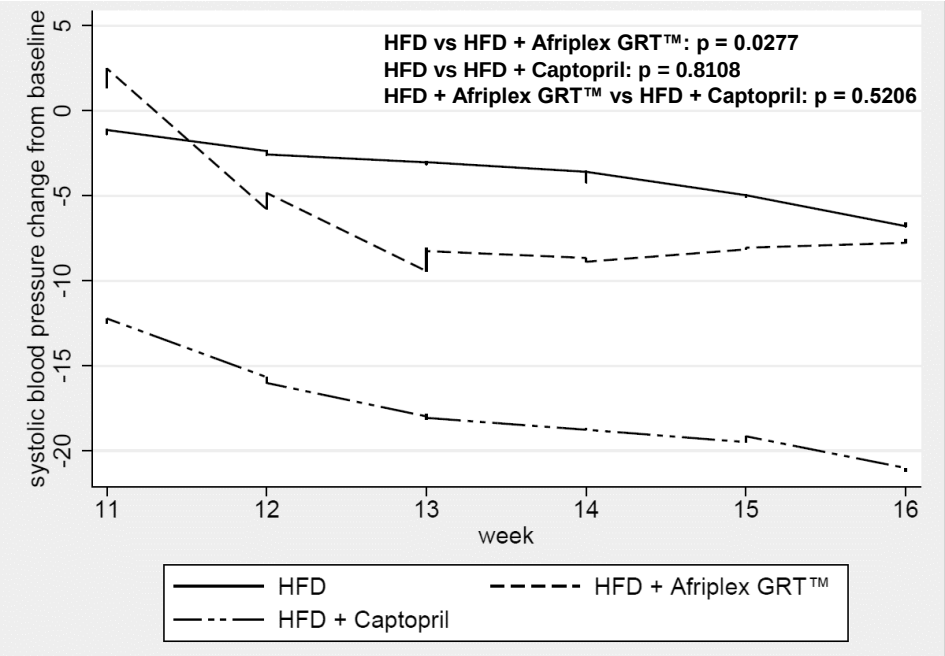

Figure 3.20: *Baseline adjusted systolic blood pressure (mm Hg) of the HFD animals after treatment with Afriplex GRT™ and Captopril; n = 8-20 per group.*

Diastolic pressure: Interestingly according to this diastolic blood pressure analysis, the HFD + Afriplex GRT™ group presented with a significantly lower diastolic blood pressure when compared to the HFD untreated animals from week 11-16; p = 0.0434. Previously, the diastolic pressure between the same groups only differed with borderline significance ***(Figure 3.16)***.

No significant differences were observed between the HFD and HFD + Captopril group; p = 0.3076 as well as between the HFD + Afriplex GRT™ and HFD + Captopril group; p = 0.7945. These results are indicative of similar diastolic blood pressure profiles **(*Table 3.6 & Figure 3.18*)**.

Table 3.6: *Baseline Adjusted Diastolic Blood Pressure (mm Hg): After Treatment*

Baseline adjusted diastolic blood pressure: After treatment									
	HFD		HFD + Afriplex GRT™		HFD + Captopril		HFD vs HFD + Afriplex GRT™	HFD vs HFD + Captopril	HFD + Afriplex GRT™ vs HFD + Captopril
	Mean	SD	Mean	SD	Mean	SD	p-value	p-value	p-value
Week 11	-1.0	8.7	2.2	10.6	-7.9	9.1	p = 0.0434*	p = 0.3076	p = 0.7945
Week 12	-2.4	11.7	-8.5	8.7	-12.9	5.9			
Week 13	0.3	12.4	-5.0	8.6	-14.5	10.9			
Week 14	-1.4	9.9	-6.4	7.6	-11.5	7.0			
Week 15	-8.8	9.6	-8.0	8.0	-13.9	4.7			
Week 16	-5.0	10.1	-6.2	8.4	-12.0	8.4			

*Data are expressed as Mean ± SD. * p < 0.05; n = 8-20 per group.*

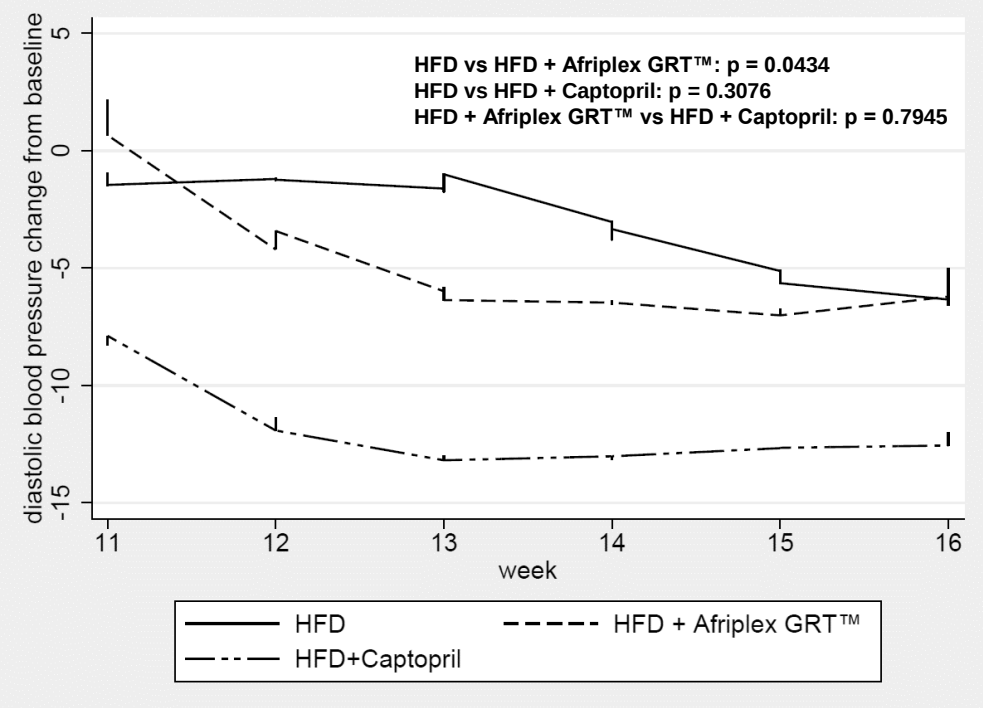

Figure 3.21: *Baseline adjusted diastolic blood pressure (mm Hg) of the HFD animals after treatment with Afriplex GRT™ and Captopril; n = 8-20 per group.*

3.2.4. Urine volume and chemical composition

3.2.4.1. Urine volume: Before and after treatment

Before treatment, the HFD animals excreted significantly less urine over 24 hours when compared to the control animals (4.3 ± 2.4 ml vs 8.1 ± 3.3 ml; $p < 0.05$) ***(Figure 3.19)***.

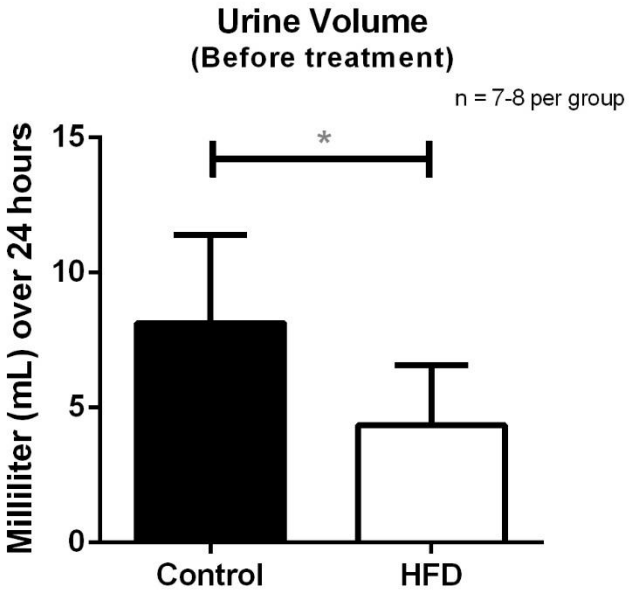

Figure 3.22: *Urine volume (ml) over a period of 24 hours of the control and HFD animals before treatment. * $p < 0.05$; n = 7-8 per group.*

After 16 weeks on the respective diets, the HFD animals still presented with significantly lower urine volumes when compared to the controls (4.8 ± 1.8 ml vs 8.7 ± 3.8 ml; $p < 0.05$). The control animals treated with Afriplex GRT™ had a significant increase in urine excretion when compared to the untreated control animals (12.3 ± 5.6 ml vs 8.7 ± 3.8 ml; $p < 0.05$). Afriplex GRT™ had no effect on the urine volume of the HFD animals. Treatment with Captopril significantly increased urine excretion when compared to the HFD untreated animals (7.6 ± 1.5 ml vs 4.8 ± 1.8 ml; $p < 0.05$) **(*Figure 3.20*)**.

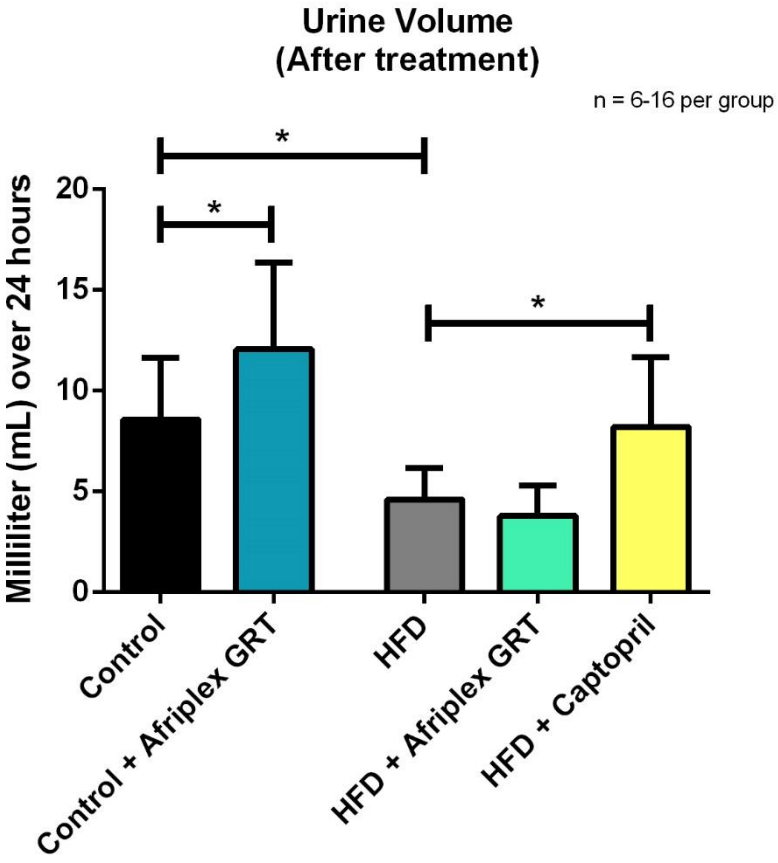

Figure 3.23: *Urine volume (ml)) over a period of 24 hours of the control and HFD untreated and treated animals. * $p < 0.05$; n = 6-16 per group.*

3.2.4.2. Urine parameters: Before and After treatment

(a) Bilirubin*:* The measurement of bilirubin in the urine is indicative of certain liver and bile diseases. Under normal conditions, no bilirubin is detected (negative)**,** and the slightest discoloration of the reagent suggests liver disease (+ or ++ or +++) (Test-it Urinalysis, 2010). *In healthy rats no bilirubin is present in the urine (negative) (Ferrets, 2014).*

Before and after treatment, all the groups tested negative for bilirubin **(*Table 3.7a & Table 3.8a*)**.

(b) Blood: The measurement of blood in the urine indicates urological or kidney diseases. *No blood (negative) is present in the urine of healthy rats (Ferrets, 2014).*

Before treatment, both the control and HFD animals tested negative for urinal blood. After treatment, 75 % of the control animals had no blood present in their urine. The remaining 25 %, had a slight increase in green coloration (+ca.5-10 Ery/µl), which is indicative of myoglobin and haemoglobin. The 25 % might be false positive results caused by the activities of microbial oxidase from urogenital tract infections. All other groups tested negative against blood in the urine **(*Table 3.7b & Table 3.8b*)**.

(c) Glucose: The measurement of glucose in the urine is used in the diagnosis and treatment of carbohydrate metabolism disorders such as hyperglycaemia and diabetes*. In healthy rats the urine glucose is either negative or trace (Ferrets, 2014).*

Before treatment, both the control and HFD animals had normal urinary glucose levels. After treatment the control, HFD and HFD + Captopril animals still had normal urinal glucose; whereas treatment with Afriplex GRT™ increased the amount of glucose excreted via the urine in 50 % of the control animals and in all the HFD animals **(*Table 3.7c & Table 3.8c*)**.

(d) Leukocytes: The measurement of leukocytes are indicative of kidney or urinary tract inflammation. Normally, healthy subjects do not contain any leukocytes and any positive results are considered as problematic. *Healthy rats usually present with a few leukocytes in their urine (Keeble and Meredith, 2009).*

Before treatment, all the control animals and 87.5 % of the HFD animals had roughly 25 leuko/ µl present in their urine. After treatment, 87.5 % of the control animals and 100 %

of the control + Afriplex GRT™ animals had small amounts (25 leuko/µl) of leukocytes in their urine. Half of the HFD animals (50 %) tested negative for urinal leukocytes, where the remaining 50 % presented with small amounts (25 leuko/µl) of leukocytes in their urine. All the HFD + Afriplex GRT™ and HFD + Captopril animals tested negative for urinal leukocytes **(*Table 3.7d & Table 3.8d*)**.

(e) Protein: The measurement of protein in the urine is indicative of renal diseases. In healthy subjects, no protein is detectable in the urine (Test-it Urinalysis, 2010). *In healthy rats the urine protein is less than 30 mg/dl (Ferrets, 2014).*

Prior to treatment, 75 % of the control and HFD animals had 100 mg/dl protein in their urine. After treatment, the majority control and HFD untreated and Afriplex GRT™ treated animals still presented with 100 mg/dl protein in their urine. From all the HFD + Captopril animals, 87.5 % presented with 30 mg/dl protein in their urine. False positive results can be ascribed to high alkalinity urine or urine containing quinine **(*Table 3.7e & Table 3.8e*)**.

(f) Ketones: The measurement of ketones (mg/dl) in the urine are indicative of acidosis or ketosis. The presence of ketones in the urine are typically associated with patients suffering from diabetes. Under normal conditions, urine specimens usually yield negative results, however, detectable ketone levels may be observed during physiological stress conditions such as fasting (Test-it Urinalysis, 2010). *In healthy rats no ketones are present in the urine (Ferrets, 2014).*

Before treatment, 87.5 % of the control animals and 75 % of the HFD animals had small amounts (trace) of ketones present in their urine. After treatment, 75 % of both the control treated and untreated animals, presented with small amounts (trace) of ketones in their urine. In 50 % of the HFD animals and 42.9 % of the HFD + Afriplex GRT™ animals, small amounts (trace) of ketones were also detected. The majority of remaining HFD Afriplex GRT™ treated (57.1 %) and untreated (37.5) animals tested negative against ketones. High concentrations of phenyl ketones could have caused a variation in colour, as seen in the control + Afriplex GRT™ (12.5 % (+)) and HFD group (12.5 % (+)). Since Captopril contained sulfhydryl groups which interfered with the reaction mechanism, it resulted in false-positive results and would therefore not be used **(*Table 3.7f & Table 3.8f*)**.

(g) Nitrite: The measurement of nitrite in the urine is indicative of urinary tract infections of bacterial origin. Even a slight pink coloration is indicative of significant bacteriuria (Test-it

Urinalysis, 2010). *No specific nitrite values have been reported in rats and therefore any pink coloration was considered as positive.*

Before treatment, all the control animals and 75 % of the HFD animals tested negatively for urinal nitrite. When comparing the groups after treatment, the majority animals tested negative for nitrite. False positive results, as seen in the HFD (12.5 % positive), HFD + Afriplex GRT™ (28.6 % positive) and HFD + Captopril (12.5 % positive) group, might be due to stale urine in which nitrite has formed by contamination, a diet low in nitrate content, high diuresis or bacteria not containing nitrate reductase **(*Table 3.7g & Table 3.8g*)**.

(h) Urobilinogen: The measurement of urobilinogen, a bile pigment degradation product of red cell haemoglobin, is indicative of liver diseases and haemolytic disorders. Under normal conditions, urinary urobilinogen concentrations ranges from 0.1-1.8 mg/dl whereas values higher than 2 mg/dl (35 µmol/l) is considered pathological (Test-it Urinalysis, 2010). *No specific urobilinogen values have been reported in rats, therefore the human parameters will be used as a guideline.*

Before treatment, 87.5 % of the control animals had 2 mg/dl urobilinogen in their urine and 87.5 % of the HFD animals had normal levels of urobilinogen. After treatment, more than half of the control and control + Afriplex GRT™ animals had 2 mg/dl urobilinogen present in their urine, whereas all the HFD, HFD + Afriplex GRT™ and HFD + Captopril animals still had normal urobilinogen levels **(*Table 3.7h & Table 3.8h*)**.

(i) pH: The measurement of the urinary pH is used to determine the acidity or alkalinity of the urine in response to different diets. Abnormal urinary pH values are associated with various renal/metabolic disorders, whereas persistently high pH values may be indicative of urinary tract infections. In healthy individuals, the pH varies between pH 5-6. *In healthy rats the pH varies between 5 and 7 (Ferrets, 2014).*

Before treatment, the urinal pH of the control animals was 9 where the majority of HFD animals had a pH of 5 or 9. After treatment, all the control Afriplex GRT™ treated, and untreated animals still had an unhealthy pH of 9, and all the HFD Afriplex GRT™ treated and untreated animals a healthy pH of 5. The majority of HFD + Captopril (37.5 %) animals presented with urinary pH readings of 6. Bacterial contamination may have been the cause of false results **(*Table 3.7i & Table 3.8i*)**.

Table 3.7: *Urine parameters: Before treatment; n = 8 per group. Neg = negative, pos = positive.*

(a) Bilirubin *(mg/dl)*

Control	HFD
neg	neg
neg	neg
neg	neg
neg	neg
neg	neg
neg	neg
neg	neg
neg	neg
100 % neg	**100 % neg**

(b) Blood *(Ery/µl)*

Control	HFD
neg	neg
neg	neg
neg	neg
neg	neg
neg	neg
neg	neg
neg	neg
neg	neg
100 % neg	**100 % neg**

(c) Glucose *(mg/dl)*

Control	HFD
normal	normal
normal	normal
normal	normal
normal	normal
normal	normal
normal	normal
normal	normal
normal	normal
100 % normal	**100 % normal**

(d) Leukocytes *(Leuko/µl)*

Control	HFD
25	neg
25	25
25	25
25	25
25	25
25	25
25	25
25	25
	12.5 % neg
100 % 25	**87.5 % 25**

(e) Protein *(mg/dl)*

Control	HFD
30	30
30	100
100	100
100	100
100	100
100	100
100	100
100	300
25 % 30	**12.5 % 30**
75 % 100	**75 % 100**
	12.5 % 300

(f) Ketones *(mg/dl)*

Control	HFD
trace	neg
trace	neg
trace	trace
trace	trace
trace	trace
trace	trace
trace	trace
(+)	trace
	25 % neg
87.5 % trace	**75 % trace**
12.5 % (+)	

(g) Nitrite *(mg/dl)*

Control	HFD
neg	neg
neg	neg
neg	pos
neg	pos
neg	pos
neg	pos
neg	pos
neg	pos
100 % neg	**75 % neg**
	25 % pos

(h) Urobilinogen *(mg/dl)*

Control	HFD
normal	normal
2(35)	normal
2(35)	normal
2(35)	normal
2(35)	normal
2(35)	normal
2(35)	normal
2(35)	2(35)
12.5 % normal	**87.5 % normal**
87.5 % 2(35)	**12.5 % 2(35)**

(i) pH

Control	HFD
9	5
9	5
9	5
9	6
9	8
9	9
9	9
9	9
	37.5 % pH 5
	12.5 % pH 6
	12.5 % pH 8
100 % pH 9	**37.5 % pH 9**

Table 3.8: *Urine parameters: After treatment with Afriplex GRT™ and Captopril; n = 7-8 per group. Neg = negative, pos = positive.*

(a) Bilirubin *(mg/dl)*

Control	Control + Afriplex GRT™	HFD	HFD + Afriplex GRT™	HFD + Captopril
neg	neg	neg	neg	neg
neg	neg	neg	neg	neg
neg	neg	neg	neg	neg
neg	neg	neg	neg	neg
neg	neg	neg	neg	neg
neg	neg	neg	neg	neg
neg	neg	neg	neg	neg
neg	neg	neg		neg
100 % neg	100 % neg	100 % neg	100 % neg	100 % neg

(b) Blood *(Ery/µl)*

Control	Control + Afriplex GRT™	HFD	HFD + Afriplex GRT™	HFD + Captopril
neg	neg	neg	neg	neg
neg	neg	neg	neg	neg
neg	neg	neg	neg	neg
neg	neg	neg	neg	neg
neg	neg	neg	neg	neg
neg	neg	neg	neg	neg
+ca. 5-10	neg	neg	neg	neg
+ca. 5-10	neg	neg		neg
75 % neg	100 % neg	100 % neg	100 % neg	100 % neg
25 % +ca. 5-10				

(c) Glucose *(mg/dl)*

Control	Control + Afriplex GRT™	HFD	HFD + Afriplex GRT™	HFD + Captopril
normal	normal	normal	normal	normal
normal	normal	normal	50 (2.8)	normal
normal	normal	normal	50 (2.8)	normal
normal	normal	normal	50 (2.8)	normal
normal	50 (2.8)	normal	50 (2.8)	normal
normal	50 (2.8)	normal	50 (2.8)	normal
normal	50 (2.8)	normal	50 (2.8)	normal
normal	50 (2.8)	normal		normal
100 % normal	50 % normal	100 % normal	14.3 % normal	100 % normal
	50 % 50 (2.8)		85.7 % 50 (2.8)	

(d) Leukocytes *(Leuko/µl)*

Control	Control + Afriplex GRT™	HFD	HFD + Afriplex GRT™	HFD + Captopril
neg	25	neg	neg	neg
25	25	neg	neg	neg
25	25	neg	neg	neg
25	25	neg	neg	neg
25	25	25	neg	neg
25	25	25	neg	neg
25	25	25	neg	neg
25	25	25		neg
12.5 % neg	100 % 25	50 % neg	100 % neg	100 % neg
87.5 % 25		50 % 25		

(e) Protein *(mg/dl)*

Control	Control + Afriplex GRT™	HFD	HFD + Afriplex GRT™	HFD + Captopril
neg	30	30	30	neg
neg	100	30	100	30
30	100	30	100	30
100	100	100	100	30
100	100	100	100	30
100	100	100	100	30
100	100	100	100	30
100	300	100		30
25 % neg				12.5 % neg
12.5 % 30	12.5 % 30	37.5 % 30	14.3 % 30	87.5 % 30
62.5 % 100	75 % 100	62.5 % 100	85.7 % 100	
	12.5 % 300			

(f) Ketones *(mg/dl)*

Control	Control + Afriplex GRT™	HFD	HFD + Afriplex GRT™	HFD + Captopril
neg	neg	neg	neg	(+)
neg	trace	neg	neg	(+)
trace	trace	neg	neg	(++)
trace	trace	trace	neg	(++)
trace	trace	trace	trace	(++)
trace	trace	trace	trace	(++)
trace	trace	trace	trace	(++)
trace	(+)	(+)		(++)
25 % neg	12.5 % neg	37.5 % neg	57.1 % neg	
75 % trace	75% trace	50 % trace	42.9 % trace	
		12.5 % (+)		
	12.5 % (+)			25 % (+)
				75 % (++)

(g) Nitrite *(mg/dl)*

Control	Control + Afriplex GRT™	HFD	HFD + Afriplex GRT™	HFD + Captopril
neg	neg	neg	neg	neg
neg	neg	neg	neg	neg
neg	neg	neg	neg	neg
neg	neg	neg	neg	neg
neg	neg	neg	neg	neg
neg	neg	neg	pos	neg
neg	neg	neg	pos	neg
neg	neg	pos		pos
100 % neg	100 % neg	87.5 % neg	71.4 % neg	87.5 % neg
		12.5 % pos	28.6 % pos	12.5 % pos

(h) Urobilinogen *(mg/dl)*

Control	Control + Afriplex GRT™	HFD	HFD + Afriplex GRT™	HFD + Captopril
normal	normal	normal	normal	normal
2 (35)	normal	normal	normal	normal
2 (35)	2 (35)	normal	normal	normal
2 (35)	2 (35)	normal	normal	normal
2 (35)	2 (35)	normal	normal	normal
2 (35)	2 (35)	normal	normal	normal
2 (35)	2 (35)	normal	normal	normal
2 (35)	2 (35)	normal		normal
12.5 % normal	25 % normal	100 % normal	100 % normal	100 % normal
87.5 % 2 (35)	75 % 2 (35)			

(i) pH

Control	Control + Afriplex GRT™	HFD	HFD + Afriplex GRT™	HFD + Captopril
9	9	5	5	5
9	9	5	5	5
9	9	5	5	6
9	9	5	5	6
9	9	5	5	6
9	9	5	5	7
9	9	5	5	8
9	9	5		8
100 % pH 9	100 % pH 9	100 % pH 5	100 % pH 5	25 % pH 5
				37.5 % pH 6
				12.5 % pH 7
				25 % pH 8

3.3. Vascular Endothelium

Assessment of the vascular endothelium entailed isometric tension studies and Western blotting.

3.3.1. Aortic ring isometric tension studies

The function of the endothelium in both the control and HFD Afriplex GRT™ treated and untreated animals was assessed by performing isometric tension studies. A 3-4 mm segment of each aortic ring (with PVAT intact) was exposed to cumulative Phe-induced vasoconstriction, followed by cumulative ACh-induced vasodilation. To determine contraction of the VSMCs via a different smooth muscle cell mechanism, several aortic rings were exposed to cumulative KCl-induced vasoconstriction. Endothelium-independent vasodilation was determined by exposing several aortic rings to cumulative Phe-induced vasoconstriction, followed by cumulative SNP-induced vasodilation.

3.3.1.1. Phe-induced vasoconstriction and Ach-induced vasodilation

Maximum Phe-induced contraction reached in the groups were as follows: **Control** 2.2 ± 0.2 g, **HFD** 2.1 ± 0.2 g, **control + Afriplex GRT™** 2.1 ± 0.1 g, **HFD + Afriplex GRT™** 2.1 ± 0.2 g and **HFD + Captopril** 2.1 ± 0.1 g.

Overall the HFD animals presented with a significant reduction in vascular contraction when compared to the control animals (**HFD vs control:** $p < 0.05$). In both groups, vascular contraction was not overall affected by Afriplex GRT™ treatment **(*Figure 3.21*)**. No significant differences were seen in LogEC50 values between the different groups ***(Table 3.9)***.

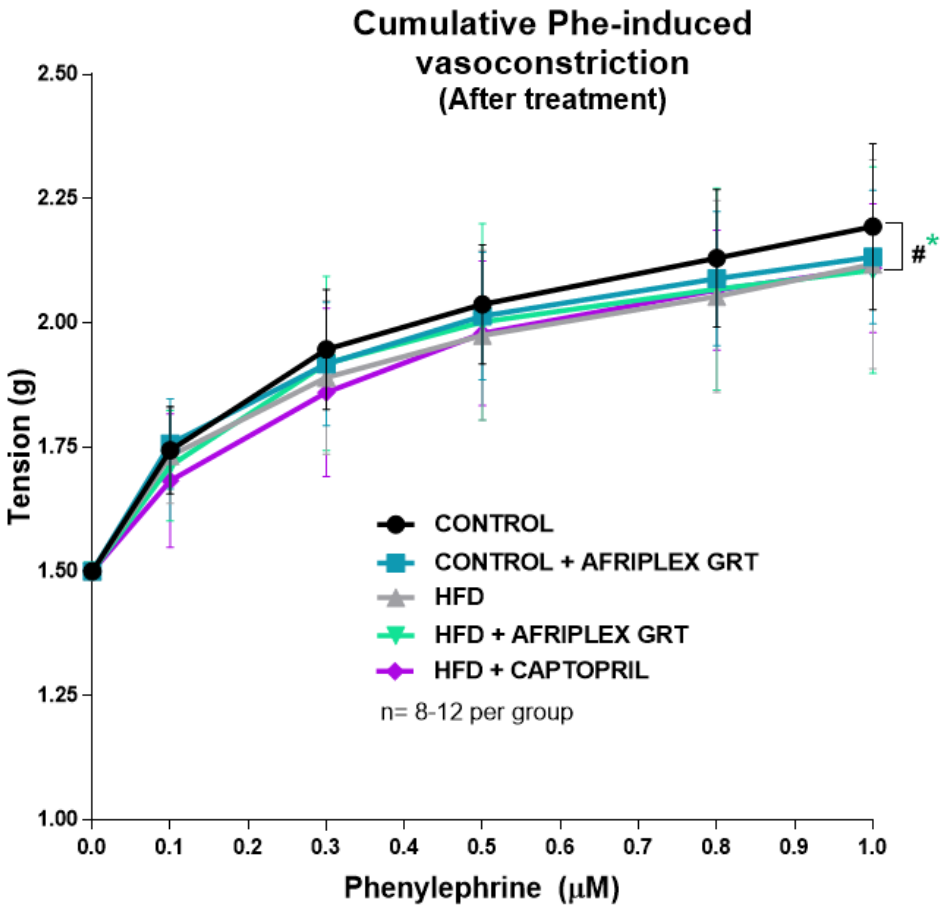

Figure 3.24: *Phe-induced vasoconstriction (tension) in the control and HFD untreated and Afriplex GRT™/Captopril treated groups. * p < 0.05; n = 8-12 per group.*
#: control vs HFD

Maximum ACh-induced relaxation reached in the groups were as follows: **Control** 83.4 ± 11 %, **HFD** 70.7 ± 16.3, **control + Afriplex GRT™** 79.9 ± 10.7 %, **HFD + Afriplex GRT™** 85.2 ± 22.1 % and **HFD + Captopril** 85.0 ± 18.2 %.

Overall, the HFD animals had a significant decrease in vascular relaxation when compared to the control animals (**HFD vs control:** $p < 0.0001$). Treatment with Afriplex GRT™ and Captopril significantly increased the overall vascular relaxation in the HFD animals, when compared to the HFD untreated animals (**HFD + Afriplex GRT™ vs HFD:** $p < 0.0001$, **HFD + Captopril vs HFD:** $p < 0.0001$) to reach a value similar to the controls (***Figure 3.22***). LogEC50 values significantly differed between the control and HFD animals (-7.0 ± 0.1 % vs -6.5 ± 0.1 %; $p = 0.0076$), HFD and HFD + Afriplex GRT™ animals (-6.5 ± 0.1 % vs -7.3 ± 0.2 %; $p = 0.0040$) and the HFD vs HFD + Captopril animals (-6.5 ± 0.1 % vs -7.2 ± 0.2 %; $p = 0.0005$) ***(Table 3.9)***.

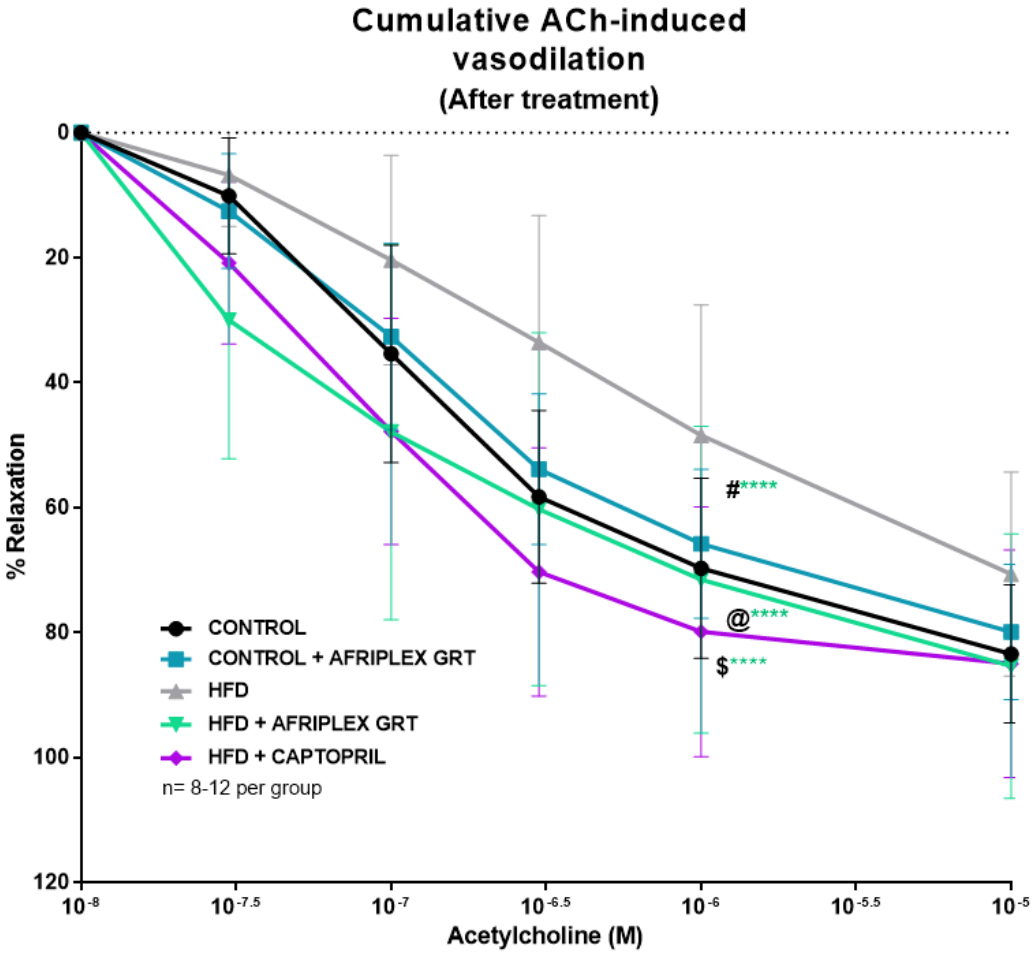

Figure 3.25: *Ach-induced vasodilation (% relaxation) in the control and HFD untreated and Afriplex GRT™/Captopril treated groups. **** $p < 0.0001$; n = 8-12 per group.*
*#: control vs HFD, @: HFD vs HFD + Afriplex GRT™, **$:** HFD vs HFD + Captopril*

Table 3.9: *LogEC50 values for different treatment groups. Phe was used to induce contraction and ACh to induce relaxation.*

		Control	Control + Afriplex GRT™	HFD	HFD + Afriplex GRT™	HFD + Captopril
Phe (g)	**LogEC50 ± SE**	-0.4 ± 0.3	-0.4 ± 0.4	-0.2 ± 0.5	-0.7 ± 0.5	-0.3 ± 0.4
Ach (%)	**LogEC50 ± SE**	-7.0 ± 0.1 **#**	-6.9 ± 0.1	-6.5 ± 0.1	-7.3 ± 0.2 **@**	-7.2 ± 0.2 **$**

Data are expressed as Mean ± SE; n = 8-12 per group

ACh: ***#:*** *control vs HFD p = 0.0076;* ***@:*** *HFD vs HFD + Afriplex GRT™ p = 0.0040;* ***$:*** *HFD vs HFD + Captopril p = 0.0005.*

3.3.1.2. Phe-induced vasoconstriction and SNP-induced vasodilation

Maximum Phe-induced contraction reached in the groups were as follows: **Control** 2.3 ± 0.1 g, **HFD** 2.2 ± 0.3 g, **control + Afriplex GRT™** 2.2 ± 0.2 g and **HFD + Afriplex GRT™** 2.2 ± 0.2 g.

Overall the HFD animals presented with a significant reduction in vascular contractility when compared to the control animals (**HFD vs control:** $p < 0.05$). In the control group, vascular contraction was overall significantly decreased by Afriplex GRT™ treatment (**Control + Afriplex GRT™ vs control:** $p < 0.01$) (***Figure 3.23***). No significant differences were seen in LogEC50 values between the different groups ***(Table 3.10)***.

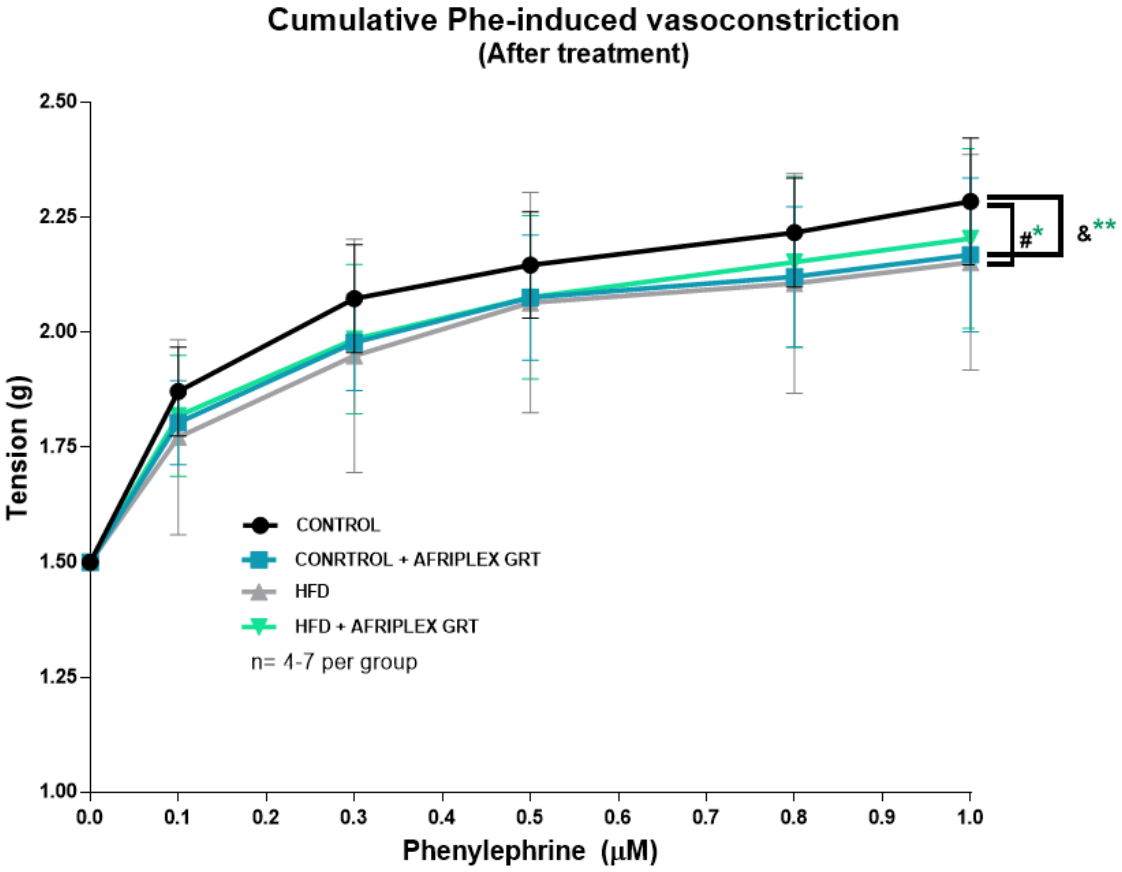

Figure 3.26: *Phe-induced vasoconstriction (tension) in the control and HFD untreated and Afriplex GRT™ treated groups. * p < 0.05, ** p < 0.01; n = 4-7 per group.*
#: *control vs HFD,* ***&*** *control vs control + Afriplex GRT™*

Maximum SNP-induced relaxation reached in the groups were as follows: **Control** 100 ± 14.9 %, **HFD** 116 ± 24.5 %, **control + Afriplex GRT™** 129 ± 18.7 % and **HFD + Afriplex GRT™** 116 ± 22.3 %.

Overall the HFD animals had a significant increase in vascular SNP relaxation when compared to the control animals (**HFD vs control:** $p < 0.05$). Treatment with Afriplex GRT™ overall significantly increased vascular SNP-induced relaxation in the control animals (**Control + Afriplex GRT™ vs control:** $p < 0.05$) and decreased the overall vascular SNP relaxation in the HFD animals (**HFD + Afriplex GRT™ vs HFD:** $p < 0.001$) when compared to their respective untreated groups (***Figure 3.24***). The LogEC50 value of the HFD animals differed significantly from the HFD + Afriplex™ group (-7.4 ± 0.2 % vs -6.7 ± 0.1 %; $p = 0.0001$) ***(Table 3.10)***.

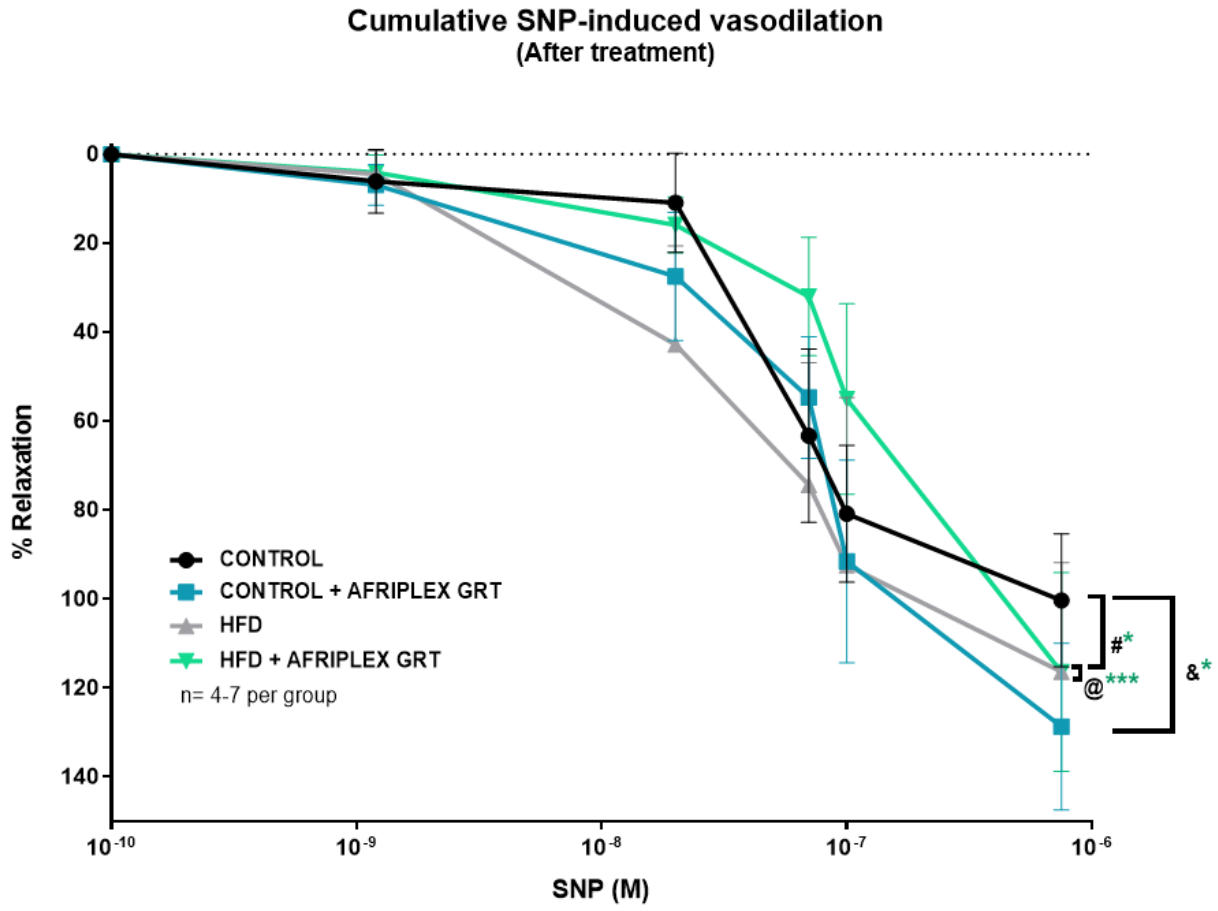

Figure 3.27: *SNP-induced vasodilation (% relaxation) in the control and HFD untreated and Afriplex GRT™ treated groups. * $p < 0.05$, *** $p < 0.001$; n = 4-7 per group.*

***#:** control vs HFD, **&:** control vs control + Afriplex GRT™, **@:** HFD vs HFD + Afriplex GRT*

Table 3.10: *LogEC50 values for different treatment groups. Phe was used to induce contraction and SNP to induce relaxation.*

		Control	Control + Afriplex GRT™	HFD	HFD + Afriplex GRT™
Phe (g)	**LogEC50 ± SE**	-0.5 ± 0.5	-0.6 ± 0.5	-0.6 ± 0.9	-0.3 ± 0.6
SNP (%)	**LogEC50 ± SE**	-7.0 ± 0.1	-7.0 ± 0.1	-7.4 ± 0.2	-6.7 ± 0.1 @

Data are expressed as Mean ± SE; n = 8-12 per group.

SNP: *@: HFD vs HFD + Afriplex GRT™ p = 0.0001.*

3.3.1.3. KCl-induced vasoconstriction

KCl-induced vasoconstriction was only performed on 2-3 animals per group since the aorta's were unable to relax after administration of two 75 mM KCl dosages.

Since we were only interested to determine whether contraction with KCl can achieve the same maximum contraction as with Phe, only a table comparing the maximum contraction of both these vasoconstrictors is illustrated. No significant differences were observed between any of the groups ***(Table 3.11)***.

Table 3.11: *KCl and Phe-induced vasoconstriction*

KCL and SNP-induced vasoconstriction (measured from 1.5 g)				
	Control	**Control + Afriplex GRT™**	**HFD**	**HFD + Afriplex GRT™**
KCl (g)	2.2 ± 0.4	2.0 ± 0.0	1.9 ± 0.0	1.9 ± 0.1
Phe (g)	2.1 ± 0.1	2.1 ± 0.2	2.1 ± 0.2	2.1 ± 0.1

Data are expressed as Mean ± SD; n = 2-12 per group.

3.3.2. Western blotting

To determine whether our functional data correlated with intracellular signalling pathways, Western blotting analyses were performed using 50 mg frozen aortic tissue of the control, control + Afriplex GRT™, HFD, HFD + Afriplex GRT™, and HFD + Captopril animals. The following signalling proteins, specifically involved in NO production, were analysed: AMPK, eNOS and PKB.

The subsequent data represents the total (T) protein expression, level of protein phosphorylation (P), and the phosphorylation: total expression ratio (P:T) of each protein. Blots are expressed as a ratio of the positive control, and the controls are expressed as 1.

3.3.2.1. AMPK

Analyses showed that the expression of T-AMPK was significantly lower in the HFD animals when compared to the control animals; $p < 0.0001$ **(*Figure 3.25*)**. Treatment with Afriplex GRT™ was effective in increasing the P-AMPK levels in both the control and HFD animals when respectively compared to their untreated counterparts; $p < 0.05$ **(*Figure 3.26*)**.

The AMPK P:T ratio was significantly higher in the HFD animals when compared to the control animals, $p < 0.001$ **(*Figure 3.27*)**. Control animals treated with Afriplex GRT™ presented with a significant increase in AMPK P:T ratio when compared to the control animals, $p < 0.05$; this result was obtained via an t-test which reduces the value of the result.

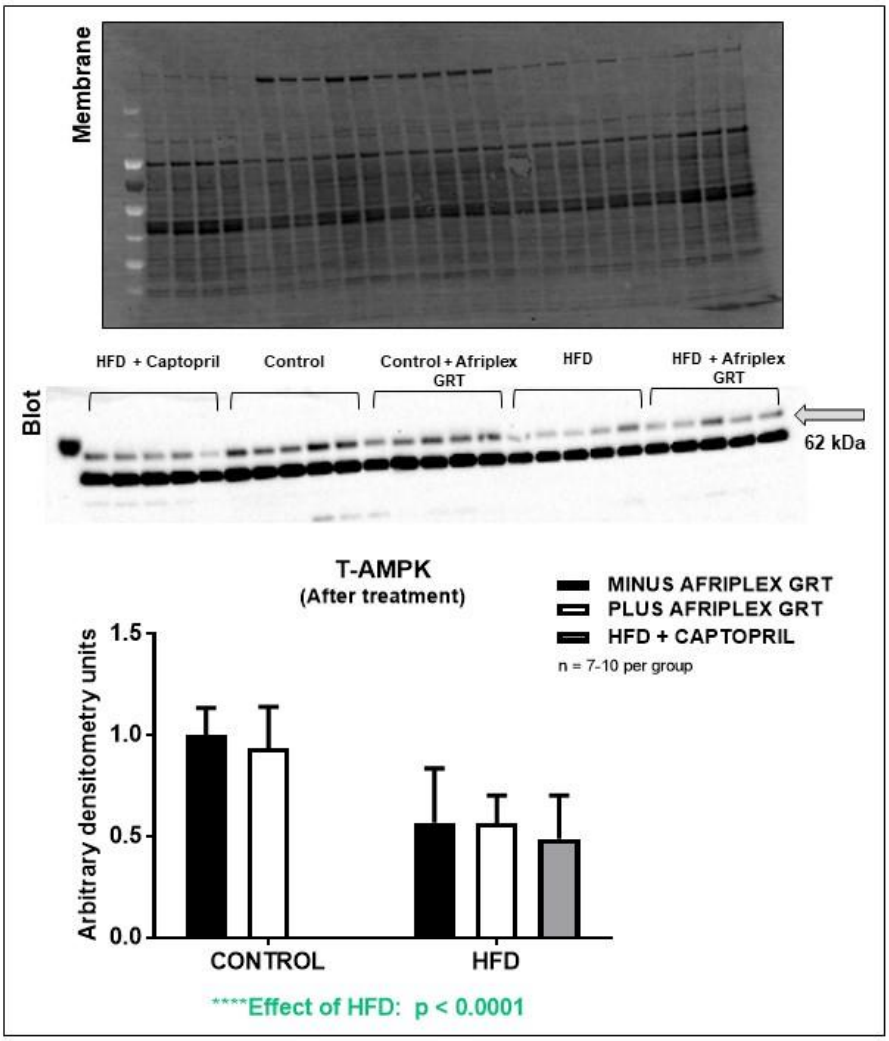

.

Figure 3.28: *T-AMPK expression (Arbitrary densitometry units) in the aortic tissue of the control and HFD Afriplex GRT™ treated and untreated animals, as well as the HFD + Captopril group. **** $p < 0.0001$; n = 7-10 per group.*

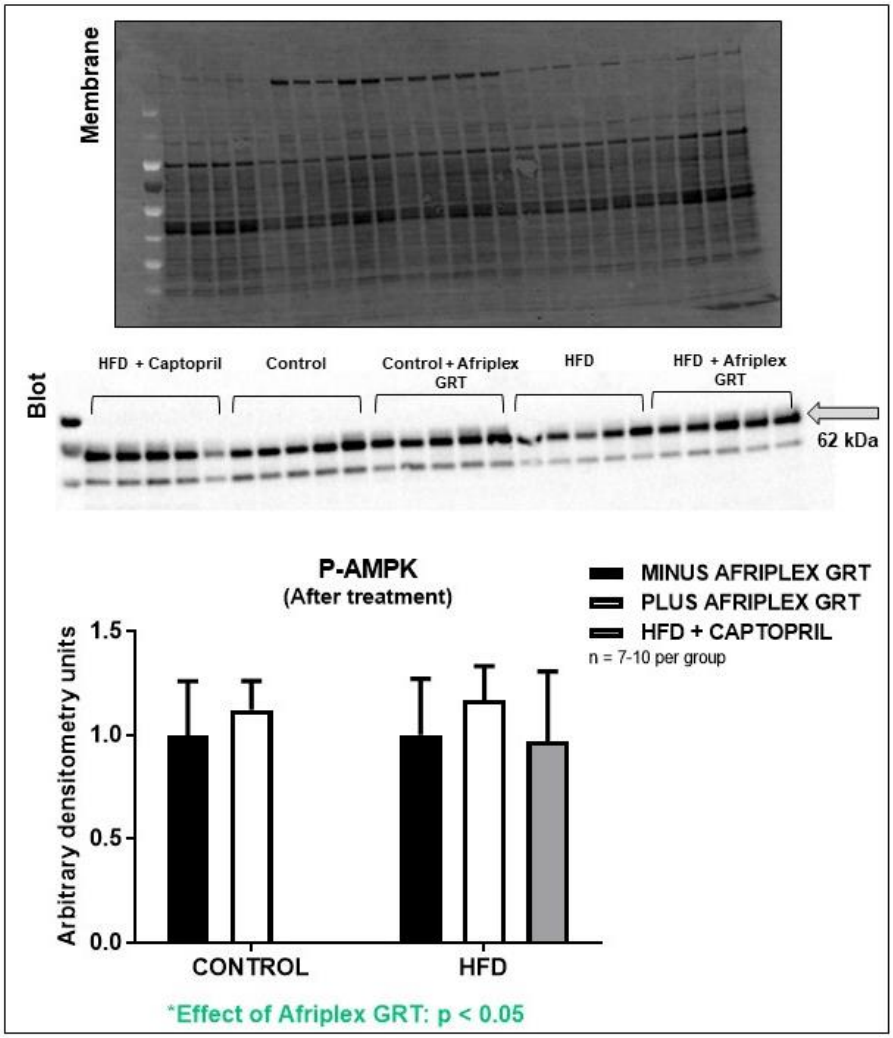

Figure 3.29: *P-AMPK levels (Arbitrary densitometry units) in the aortic tissue of the control and HFD Afriplex GRT™ treated and untreated animals, as well as the HFD + Captopril group. * p < 0.05; n = 7-10 per group.*

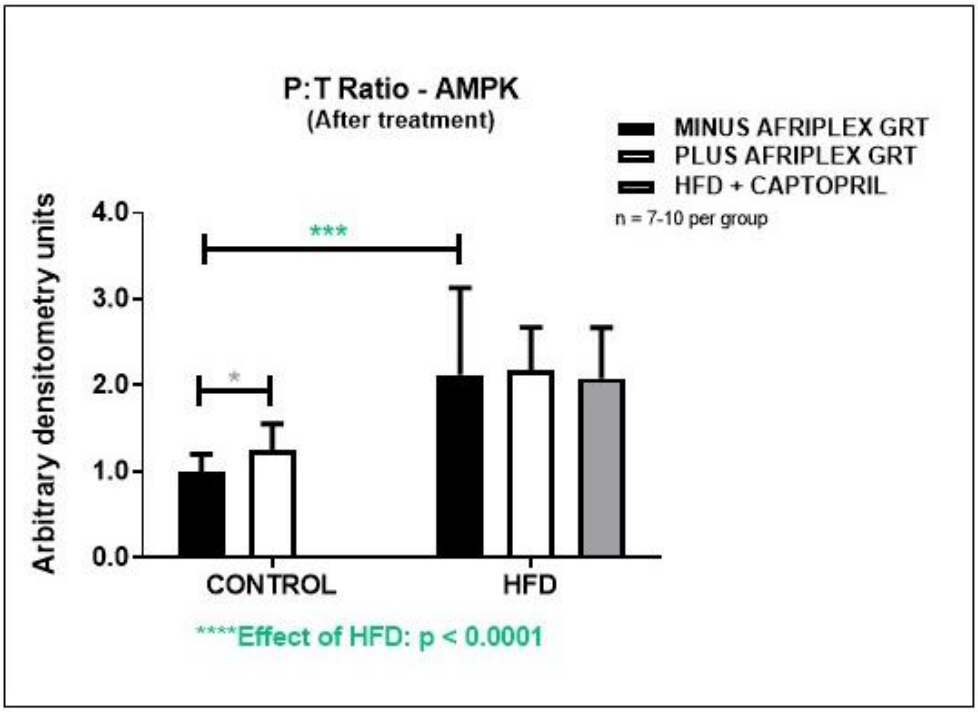

Figure 3.30: *AMPK P:T ratio (Arbitrary densitometry units) in the aortic tissue of the control and HFD Afriplex GRT™ treated and untreated animals, as well as the HFD + Captopril group. * p < 0.05, *** p < 0.001, **** p < 0.0001; n = 7-10 per group.*

3.3.2.2. eNOS

Analyses showed that the expression of eNOS was significantly upregulated in the HFD animals when compared to the control animals; $p < 0.01$ **(*Figure 3.28*)**. No significant differences were observed in the P-eNOS levels (***Figure 3.29).*** The eNOS P:T ratio was significantly lower in the HFD animals when compared to the controls; $p < 0.01$ **(*Figure 3.30)***.

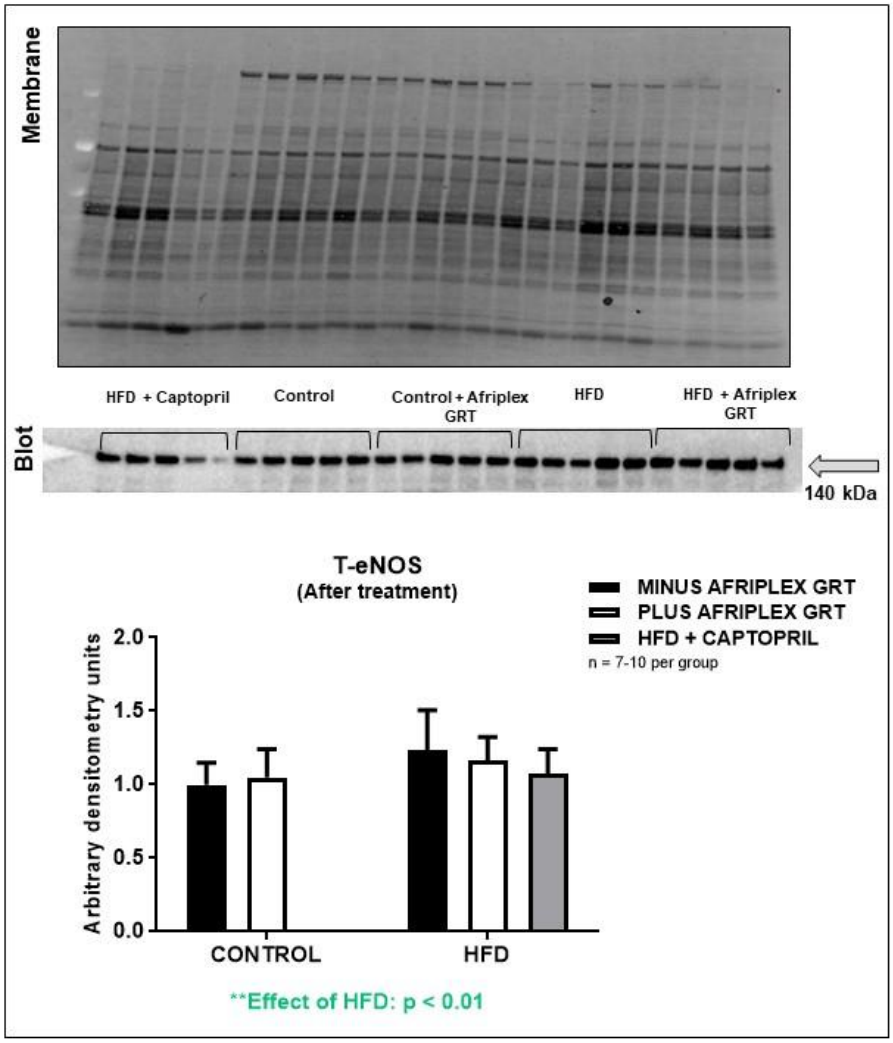

Figure 3 31: *T-eNOS expression (Arbitrary densitometry units) in the aortic tissue of the control and HFD Afriplex GRT™ treated and untreated animals, as well as the HFD + Captopril group. ** $p < 0.01$; n = 7-10 per group.*

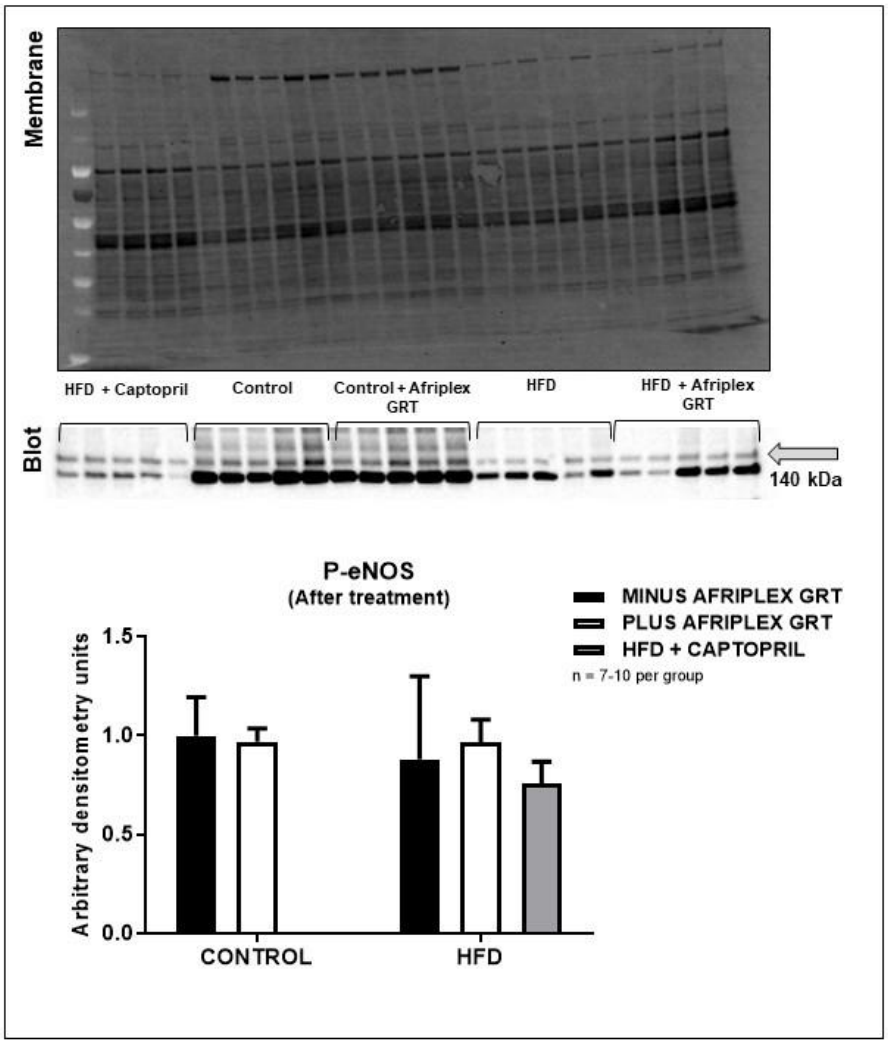

Figure 3.32: *P-eNOS levels (Arbitrary densitometry units) in the aortic tissue of the control and HFD Afriplex GRT™ treated and untreated animals, as well as the HFD + Captopril group. n = 7-10 per group.*

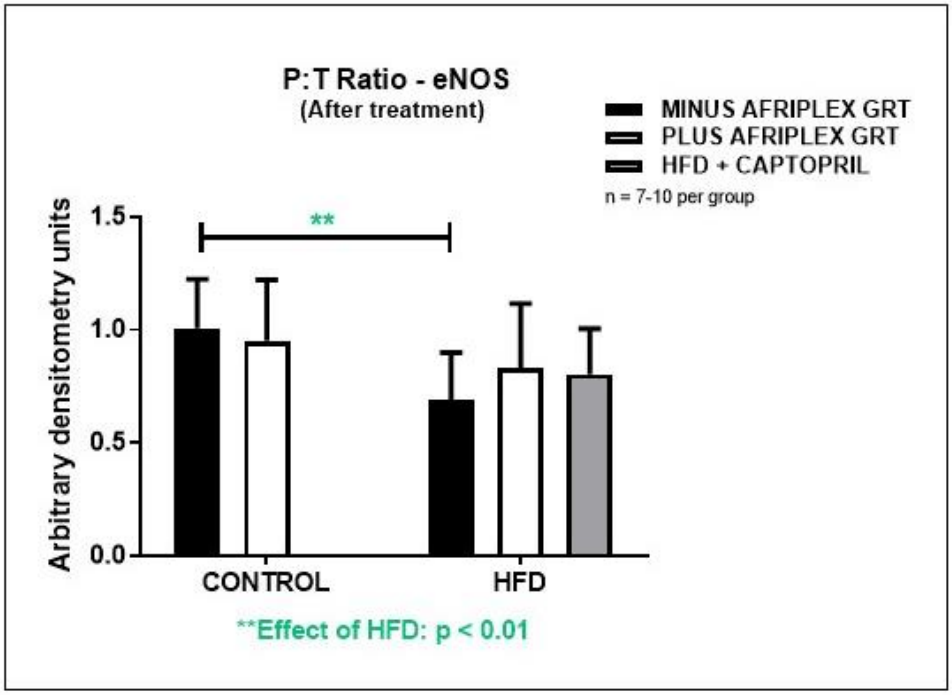

Figure 3.33: *eNOS P:T ratio (Arbitrary densitometry units) in the aortic tissue of the control and HFD Afriplex GRT™ treated and untreated animals, as well as the HFD + Captopril group. ** p < 0.01; n = 7-10 per group.*

3.3.2.3. PKB

The expression of PKB was significantly higher in the HFD animals treated with Afriplex GRT™ when compared to the HFD untreated animals; $p < 0.05$ **(*Figure 3.31*)**. The HFD animals had a significant decrease in PKB phosphorylation when compared to the controls; $p < 0.05$. Treatment with Afriplex GRT™ significantly increased the activation of PKB in both the control and HFD animals when compared to their respective untreated counterparts; $p < 0.05$ **(*Figure 3.32*)**.

The PKB P:T ratio of the HFD animals was significantly lower when compared to the controls; $p < 0.05$. Treatment with Afriplex GRT™ significantly increased the PKB P:T ratio in both the control and HFD animals when compared to their respective untreated counterparts; $p < 0.05$ **(*Figure 3.33)*.**

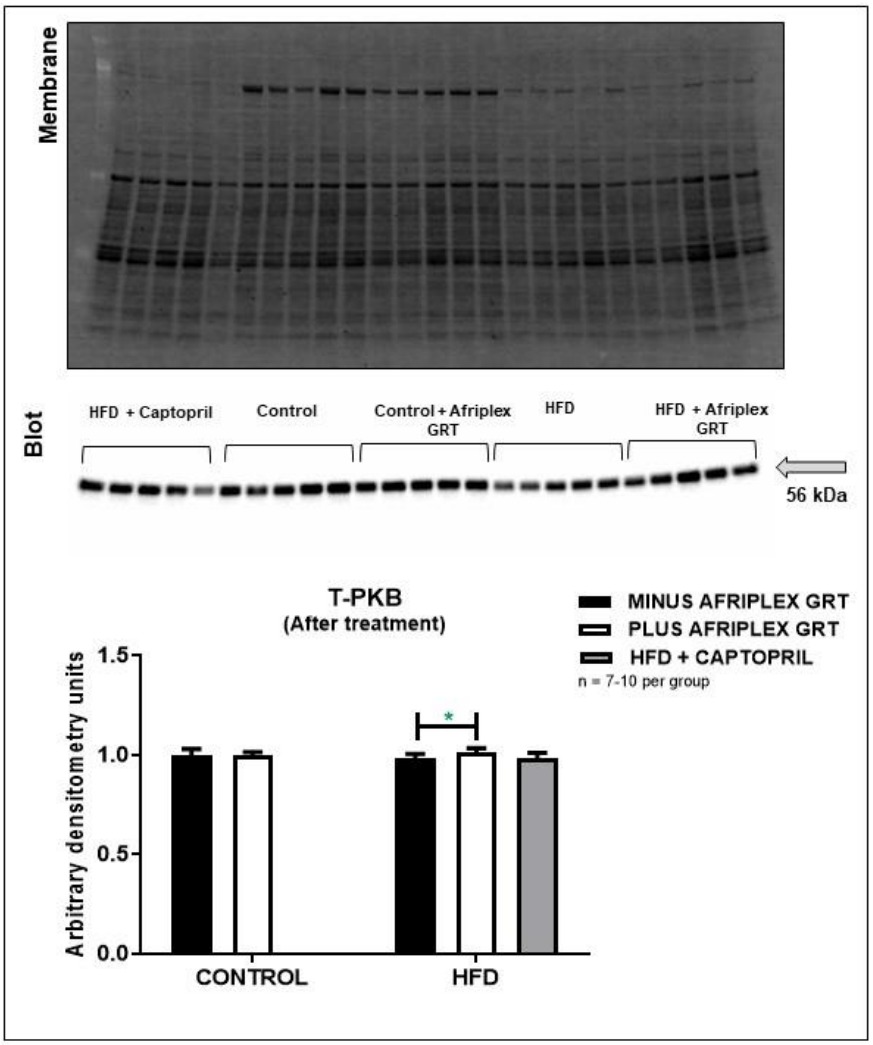

Figure 3.34: *T-PKB expression (Arbitrary densitometry units) in the aortic tissue of the control and HFD Afriplex GRT™ treated and untreated animals, as well as the HFD + Captopril group. * $p < 0.05$; n = 7-10 per group.*

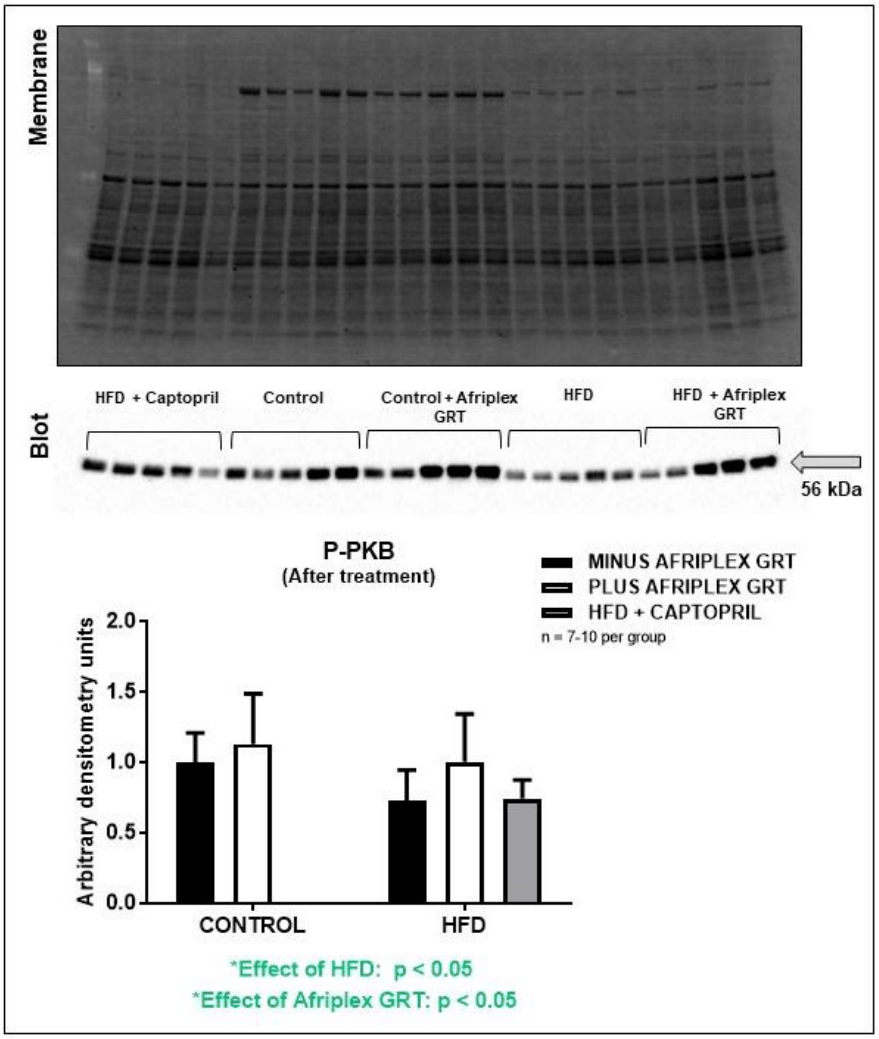

Figure 3.35: *P-PKB levels (Arbitrary densitometry units) in the aortic tissue of the control and HFD Afriplex GRT™ treated and untreated animals, as well as the HFD + Captopril group. * p < 0.05; n = 7-10 per group.*

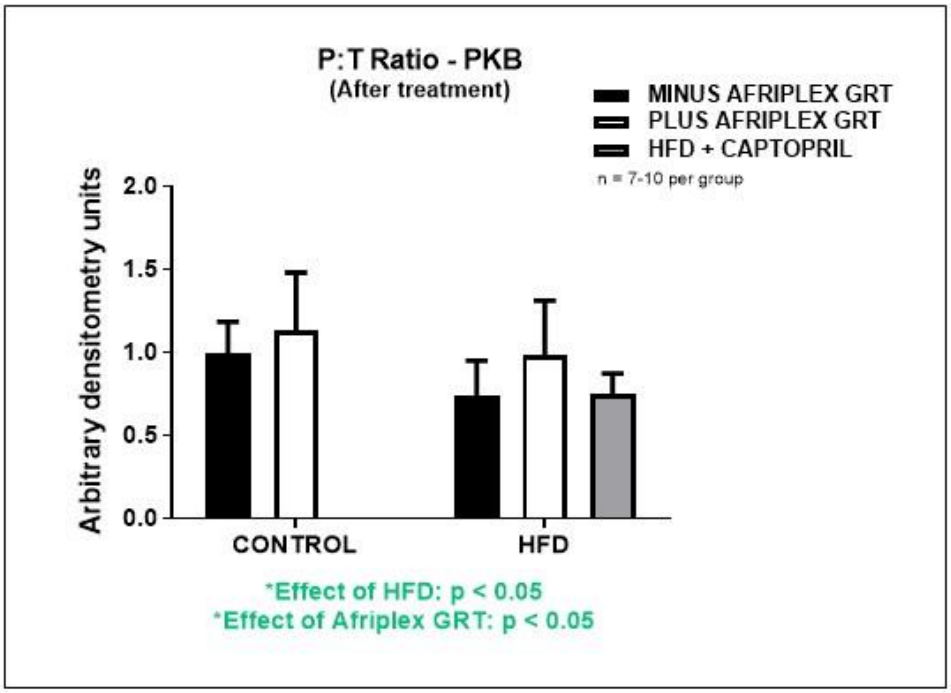

Figure 3.36: *PKB P:T ratio (Arbitrary densitometry units) in the aortic tissue of the control and HFD Afriplex GRT™ treated and untreated animals, as well as the HFD + Captopril group. * p < 0.05; n = 7-10 per group.*

3.4. AECs

The effect of Afriplex GRT™ on cellular apoptosis, cellular metabolic activity and NO production was measured using AECs treated with three different Afriplex GRT™ concentrations. The possibility of ACE-inhibitor actions was determined using AECs treated with either the same three Afriplex GRT™ concentrations, or with non-fasting serum (collected previously from the control and HFD untreated and treated animals).

After the 24-hour treatment period, the cells were treated with the relevant probes, and fluorescence/absorbance was measured using the FLUOstar Omega plate reader. Data are expressed as a ratio of the vehicle control (untreated cells).

3.4.1. DAF-2/DA: NO production

Untreated AECs (vehicle control) (100.0 ± 19 %) as well as those treated with 1 µg/ml (96.8 ± 15.2 %), 10 µg/ml (95.2 ± 12.9 %) and 100 µg/ml (88.4 ± 12.8 %) Afriplex GRT™ presented with significantly lower mean DAF-2/DA fluorescence when compared to the positive control (DEA) (412.7 ± 137.0 %). No significant differences in mean DAF-2/DA fluorescence were observed between the vehicle control and the 1 µg/ml, 10 µg/ml and 100 µg/ml Afriplex GRT™ treatment groups **(*Figure 3.34*)**.

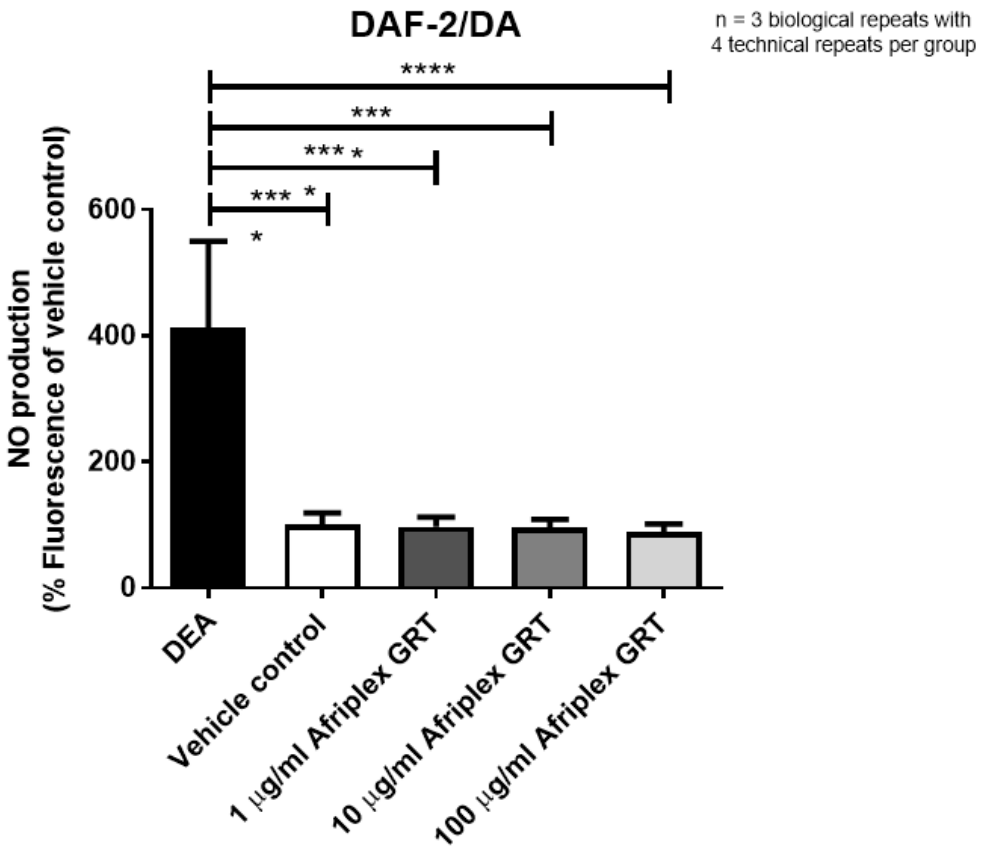

Figure 3.37: *The effect of 1 µg/ml, 10 µg/ml and 100 µg/ml Afriplex GRT™ on NO production measured by DAF-2/DA fluorescence. NO production expressed as % fluorescence of the vehicle control (untreated cells); Vehicle control fluorescence adjusted to 100 %. *** p < 0.0001; n = 3 biological repeats with 4 technical repeats per group*.

3.4.2. PI: Cell viability (Necrosis)

Untreated AECs (vehicle control) (100 ± 9.4 %) as well as those treated with 1 µg/ml (102 ± 6.7 %), 10 µg/ml (104.7 ± 6.9 %) and 100 µg/ml (98.9 ± 7.5 %) Afriplex GRT™ showed significantly lower mean PI fluorescence (necrosis) when compared to the positive control (distilled water) (211.3 ± 35.9 %); $p < 0.0001$. No significant differences in PI fluorescence were observed between the vehicle control and the 1 µg/ml, 10 µg/ml and 100 µg/ml Afriplex GRT™ treatment groups (***Figure 3.35***).

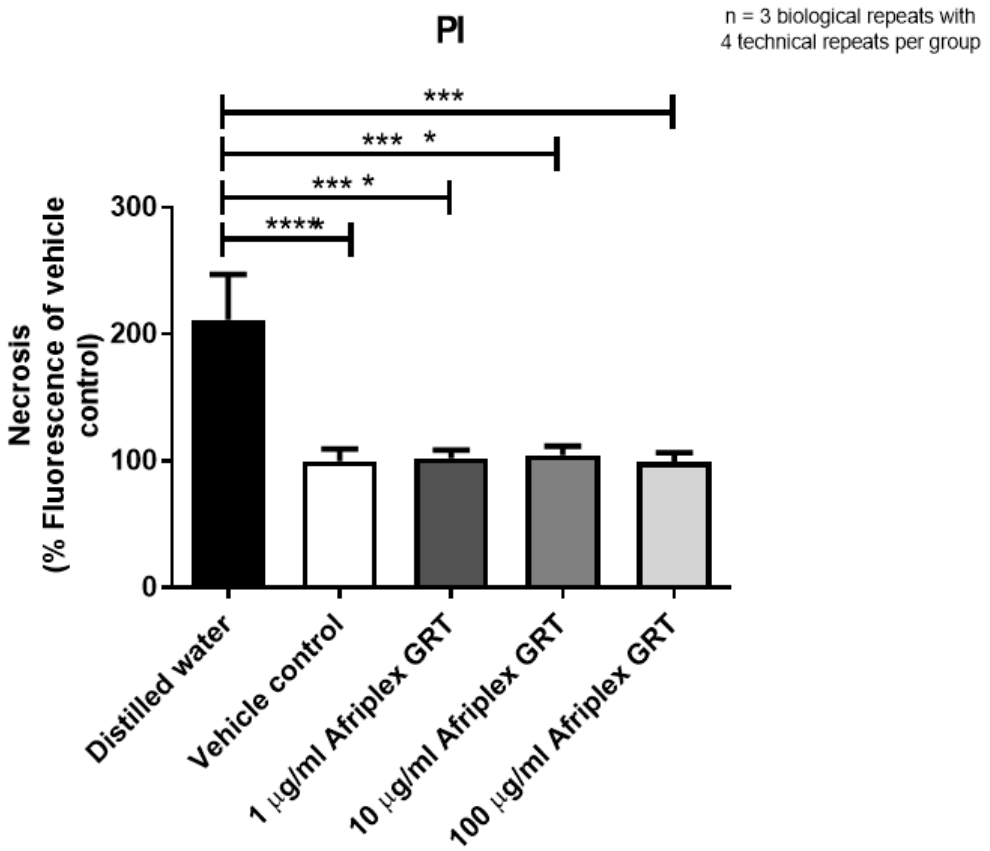

Figure 3.38: *The effect of 1 µg/ml, 10 µg/ml and 100 µg/ml Afriplex GRT™ on necrosis measured by PI fluorescence. Necrosis expressed as % fluorescence of the vehicle control (untreated cells); Vehicle control fluorescence adjusted to 100 %. **** $p < 0.0001$; n = 3 biological repeats with 4 technical repeats per group.*

3.4.3. MTT: Cellular metabolic activity

AECs treated with 100 µg/ml (179.5 ± 82.0 %) Afriplex GRT™ showed a significant increase in mean MTT absorbance (cellular metabolic activity) when compared to the vehicle control (untreated cells) (100.0 ± 18.9 %); $p < 0.001$. Treatment with 1 µg/ml and 10 µg/ml Afriplex GRT™ had no effect on mean MTT absorbance **(*Figure 3.36*)**.

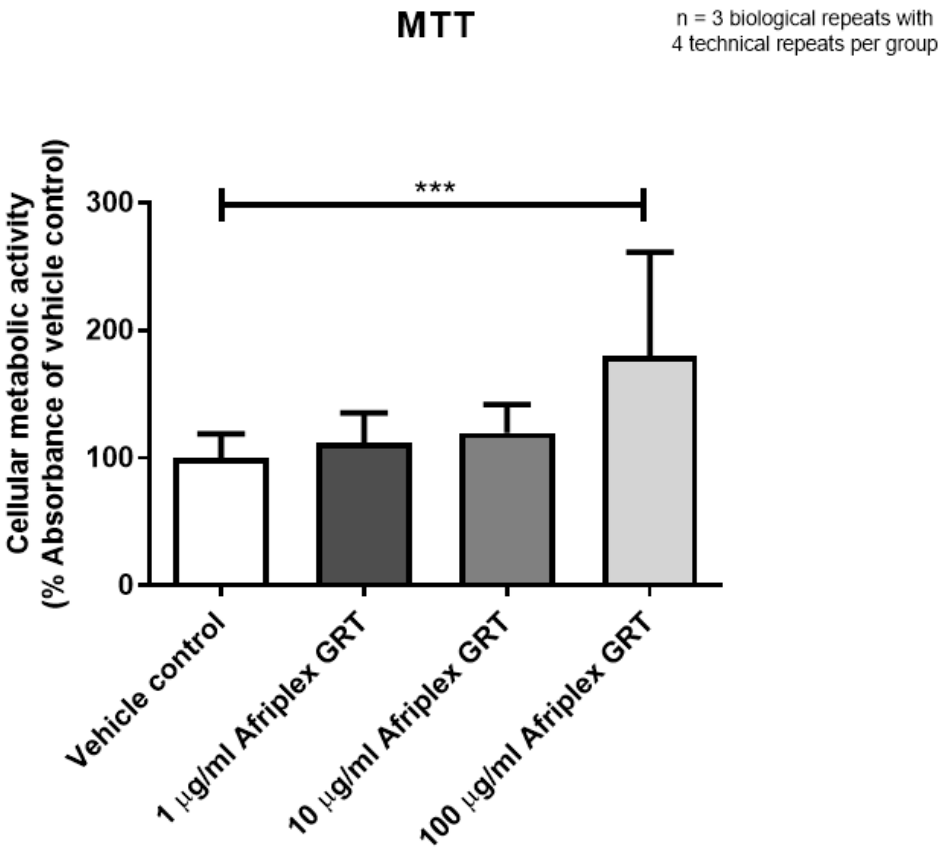

Figure 3.39: *The effect of 1 µg/ml, 10 µg/ml and 100 µg/ml Afriplex GRT™ on cellular metabolic activity measured by MTT absorbance. Cellular metabolic activity expressed as % absorbance of the vehicle control (untreated cells); Vehicle control fluorescence adjusted to 100 %. *** $p < 0.001$; n = 3 biological repeats with 4 technical repeats per group.*

3.4.4. FRET: ACE-inhibitor actions

FRET analyses using Afriplex GRT™ extract: AECs treated with LFK (155330.5 ± 52959.0 arbitrary units) presented with increased mean fluorescence when compared to the untreated AECs (vehicle control) (73975.2 ± 6060.7 arbitrary units); $p < 0.01$. LFK + Captopril (72298.3 ± 9476.5 arbitrary units) significantly lowered the fluorescence (increased ACE inhibitor activity) when compared to LFK treated AECs (155330.5 ± 52959.0 arbitrary units); $p < 0.01$.

Treatment with 1 µg/ml, 10 µg/ml and 100 µg/ml Afriplex GRT™ did not significantly differ from the LFK group. No significant differences were observed in the N-domain of the ACE enzyme **(*Figure 3.37*)**.

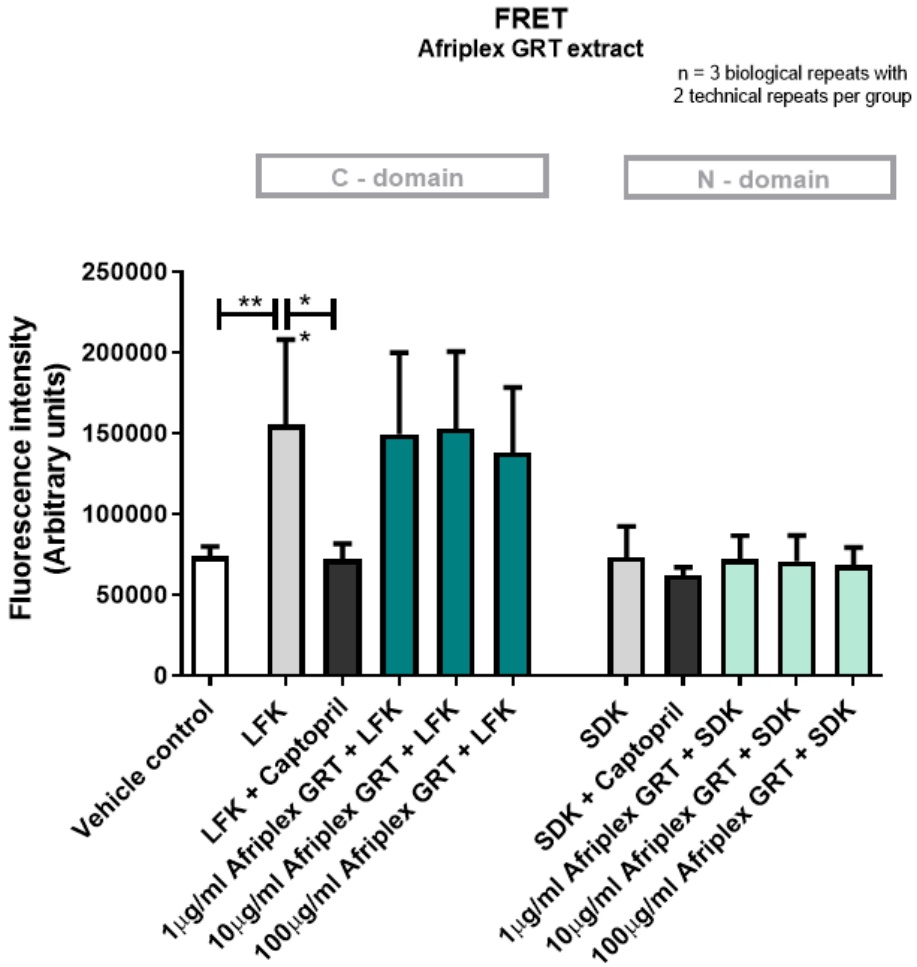

Figure 3.40: *The effect of 1 µg/ml, 10 µg/ml and 100 µg/ml Afriplex GRT™ on ACE activity (fluorescence intensity). LFK and SDK respectively refers to the probes for the C- and N-terminal of the ACE enzyme. Captopril was used as the positive control. ** $p < 0.01$; n = 3 biological repeats with 2 technical repeats per group.*

FRET analyses using non-fasting serum: AECs treated with LFK + Captopril (59104.2 ± 14812.4 arbitrary units) presented with decreased mean fluorescence (increased ACE inhibitor activity) when compared to the LFK treated AECs (117089.0 ± 25901 arbitrary units); $p < 0.01$. The control and HFD Afriplex GRT™ treated and untreated animals did not significantly differ from the LFK group. No significant differences were observed in the N-domain of the ACE enzyme **(Figure 3.38)**.

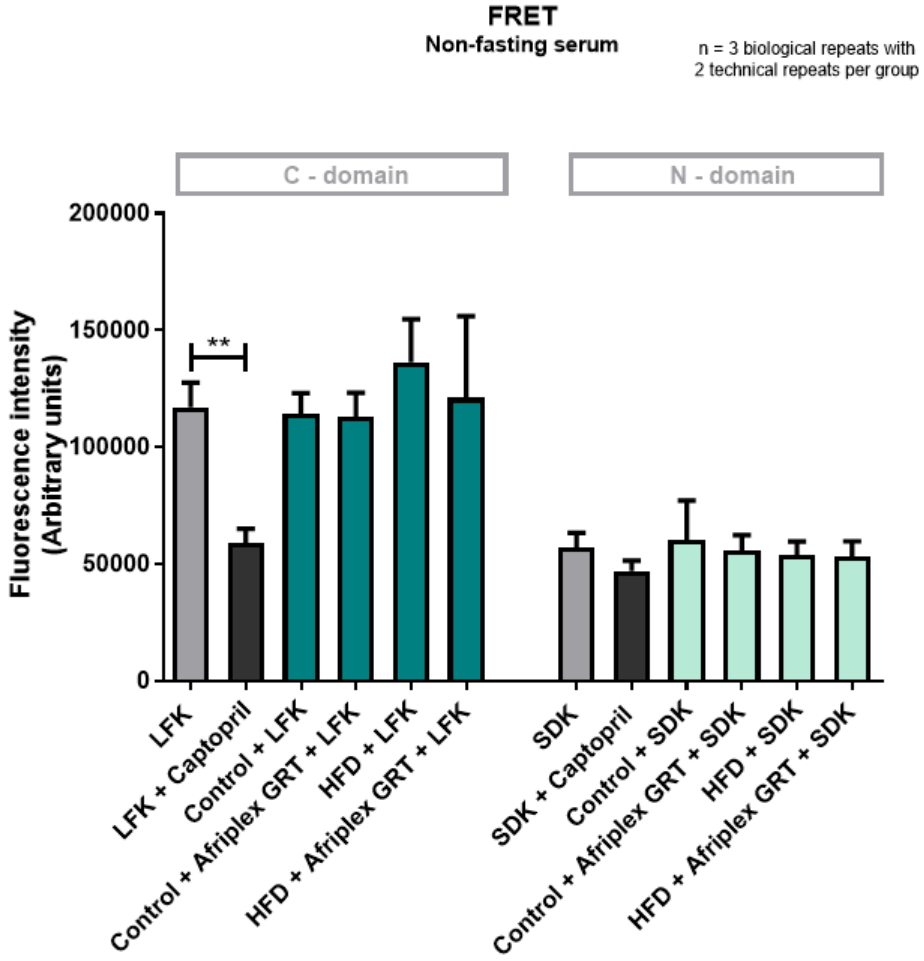

Figure 3.41: *The effect of control, control + Afriplex GRT™, HFD and HFD + Afriplex GRT™ non-fasting serum on ACE activity (fluorescence intensity). LFK and SDK respectively refers to the probes for the C- and N-terminal of the ACE enzyme. Captopril was used as the positive control. ** $p < 0.01$; n = 3 per group with 2 biological replicates per group.*

3.5. Biochemical analyses

Using commercially available ELISAs, Leptin, Adiponectin, Aldosterone and ET-1 levels of the control and HFD untreated and Afriplex GRT™ treated animals were measured using non-fasting serum.

3.5.1. Leptin

The HFD animals (4.1 ± 2.1 ng/ml) showed a significant increase in leptin levels when compared to the control group (2.4 ± 1.3 ng/ml); $p < 0.01$. Treatment with Afriplex GRT™ did not affect the leptin levels of either the control or the HFD animals **(*Figure 3.39*)**.

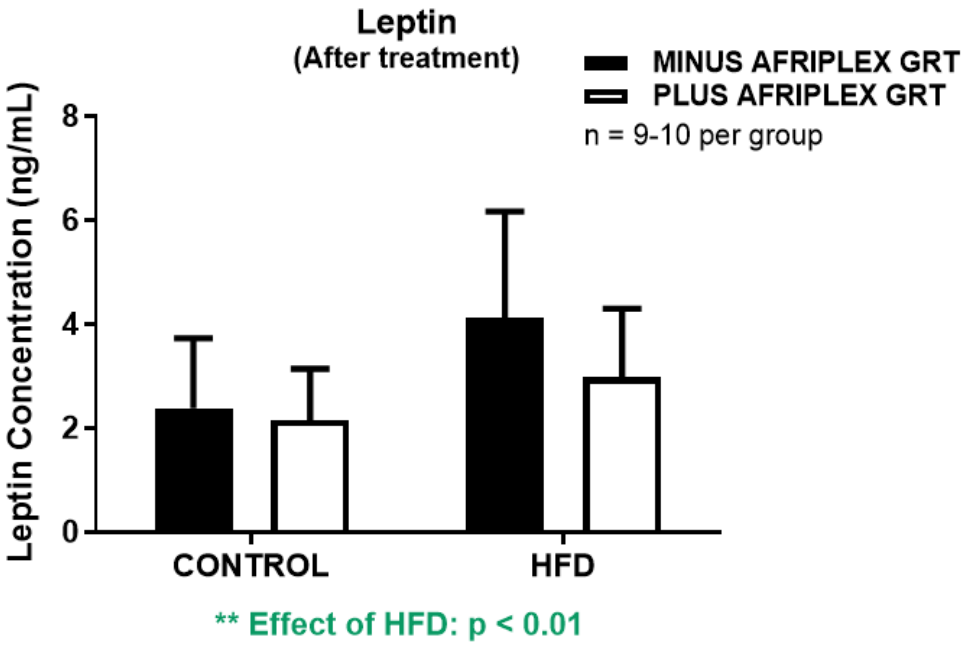

Figure 3.42: *Leptin levels (ng/ml) of the control and HFD untreated and Afriplex GRT™ treated animals. ** p < 0.01 (HFD vs control); n = 9-10 per group.*

3.5.2. Adiponectin

The HFD animals (28.3 ± 3.3 µg/ml) showed a significant increase in adiponectin levels when compared to the control group (21.8 ± 3.6 µg/ml; $p < 0.01$). Treatment with Afriplex GRT™ did not affect the adiponectin levels of both the control and HFD animals **(*Figure 3.40*)**.

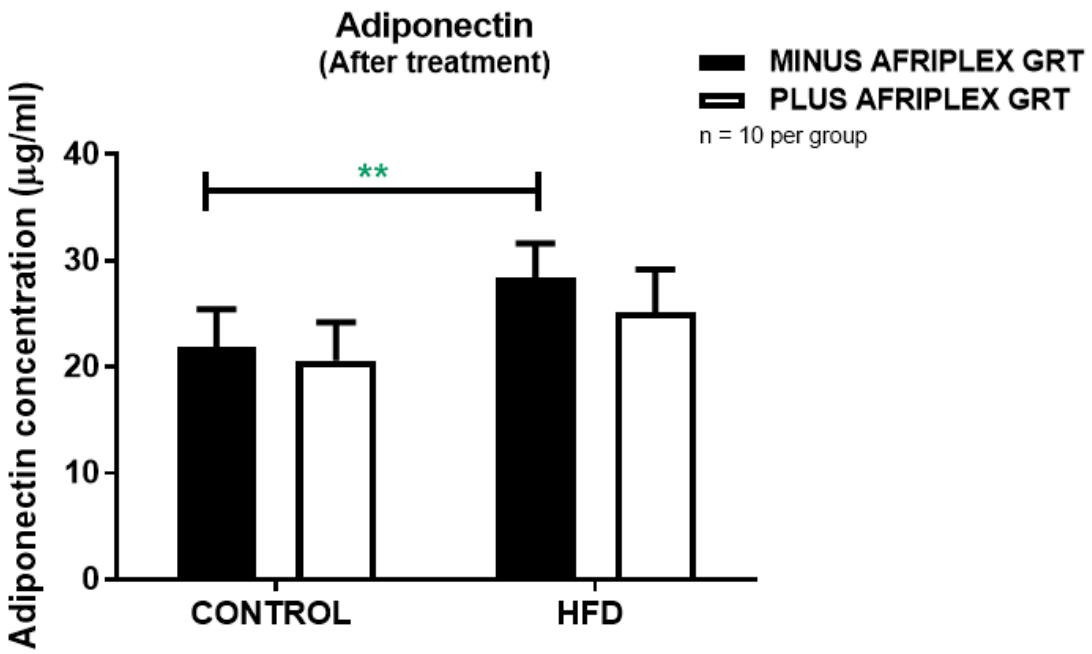

Figure 3.43: *Adiponectin levels (µg/ml) of the control and HFD untreated and Afriplex GRT™ treated animals. ** $p < 0.01$; n = 10 per group.*

3.5.3. Aldosterone

The Aldosterone assay failed the required minimum threshold. It is evident that the high-dilution samples did not allow the aldosterone count to be significant.

3.5.4. ET-1

Between the groups, no significant differences were observed in the ET-1 levels **(*Figure 3.41*)**.

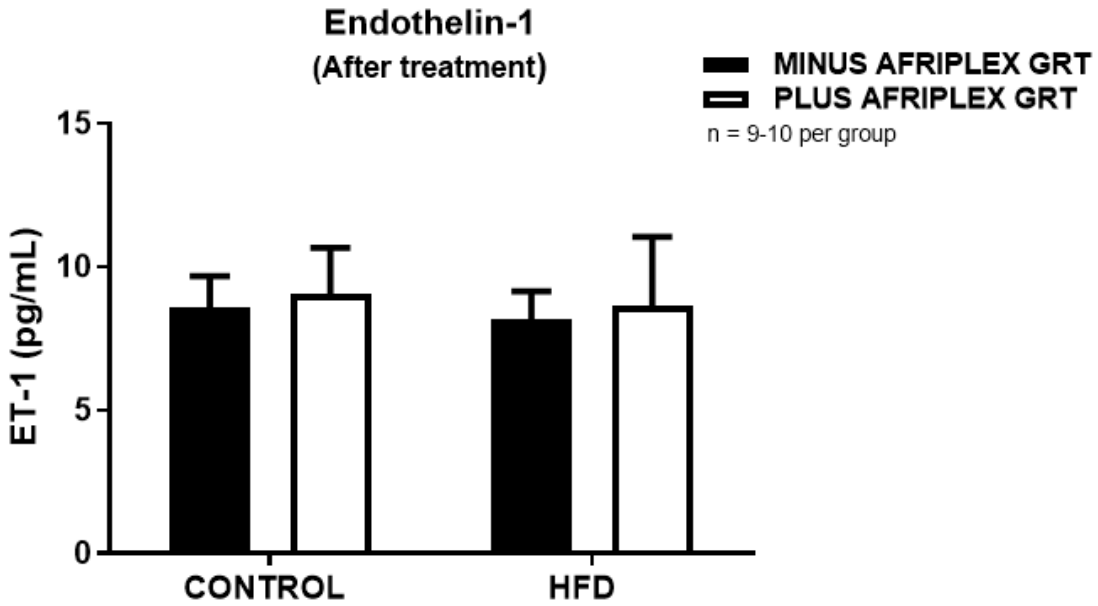

Figure 3.44: *ET-1 levels (pg/ml) in the control and HFD untreated and Afriplex GRT™ treated animals. n = 9-10 per group.*

CHAPTER 4: DISCUSSION

4.1. Summary of main findings

The main focus of the current study was to determine whether treatment with an unique green rooibos extract, Afriplex GRT™, has the potential to ameliorate obesity-induced hypertension. Animals were fed an HFD to induce insulin resistance, vascular dysfunction and hypertension.

As expected, the HFD was coupled to the development of **insulin resistance**, as these animals presented with increased body weight gain, IP-fat weight, leptin levels, decreased glucose clearance and downregulated AMPK expression and PKB activation. Furthermore, the HFD was also coupled to the development of increased vascular dysfunction and elevated blood pressure, as these animals presented with reduced vascular contraction and vascular relaxation, urine excretion, eNOS activation according to the P:T ratio and increased systolic and diastolic blood pressure.

HFD animals treated with Afriplex GRT™ showed improved **insulin sensitivity**, **decreased blood pressure** and **improved vascular function,** as these animals had lower body weights, increased glucose clearance and AMPK/PKB activation, improved vascular relaxation and decreased systolic and diastolic blood pressure. Interestingly, and the most profound finding of the current study was that treatment with Afriplex GRT™ also increased glucose excretion via the urine which is indicative of SGLT2 inhibition. We speculate that the associated health benefits of Afriplex GRT™ can amongst other, be mainly ascribed to SGLT2 inhibition.

In the following sections, each parameter measured in the current study will be discussed in detail.

4.2. Biometric data and insulin sensitivity

4.2.1. Food and water intake

Food intake: During the 16-week period, the HFD animals presented with a significant increase in food intake when compared to the age-matched chow fed controls **(*Figure 3.1*)**. This observation can be attributed to the moisture and sweetness of the HFD food being very palatable. According to a previous study, the consumption of a diet high in fructose decreases hypothalamic satiety consequently increasing hunger and the desire for food (Luo *et al.*, 2015).

HFD animals treated with Afriplex GRT™ showed a significant decrease in food intake, suggesting that Afriplex GRT™ might act as an appetite suppressant **(*Figure 3.1*)**. The flavonoids, aspalathin

and nothofagin present in rooibos, are believed to specifically reduce the stress hormone, cortisol, which is known to increase comfort eating (Schloms *et al.*, 2012).

Treatment with Captopril significantly decreased food consumption in the HFD animals when compared to the HFD untreated animals **(*Figure 3.1*)**, correlating with previous research where treatment with Captopril in rats resulted in RAS suppression and consequently reduced food intake (Eghoghosoa *et al.*, 2010). In another study, rats treated daily with 50 mg/kg Captopril presented with a significant decrease in their appetite for sodium (via food). This result can be ascribed to the high Captopril dosage which is able to cross the blood-brain barrier, consequently inhibiting ACE activity in the brain (Elfont, Epstein and Fitzsimons, 1984).

Water intake: During the 16-week period, the HFD animals drank significantly less water when compared to the age-matched chow fed controls **(*Figure 3.2)*.** This result can be ascribed to the HFD food being moister in comparison to the normal dry rat chow (Guelinckx *et al.*, 2016).

Treatment with Afriplex GRT™ increased water intake in the control animals and decreased water intake in the HFD animals **(*Figure 3.2*)**, hence, changes in water intake are most probably unlikely to be due to a specific effect of Afriplex GRT™. The consumption of herbal teas are known to induce diuresis (Taylor, 2017) as shown in the control Afriplex GRT™ animals who presented with an increase in fluid loss through the urine **(*Figure 3.20*)**. We speculate that treatment with Afriplex GRT™ in the control animals increased thirst, and to compensate for the increased water consumption, the kidneys stimulated the excretion of water as urine. The decrease in water intake in the HFD + Afriplex GRT™ animals had no effect on their urine output **(*Figure 3.20*)**. The further decrease in water intake may have caused dehydration in these animals. Dehydration in rats is associated with dull coat and eyes, thinner body appearance and inactivity (Hunt, 2018). Each animal in the current study was monitored daily and none of these dehydration markers were observed.

HFD animals treated with Captopril drank significantly more water when compared HFD untreated animals **(*Figure 3.2)***. This result correlates with their increase in fluid loss through the urine **(*Figure 3.20*)**. This finding also corresponds with a previous study which showed that the inhibition of angiotensin II formation via Captopril increased fluid loss and water consumption in rats (Gardiner and Bennett, 1983).

4.2.2. Body weight

Before the HFD was administered (week 0), all the animals had the same initial body weight **(*Figure 3.4*)**. Prior to treatment and after treatment the HFD animals presented with a significant increase in body weight **(*Figure 3.3*)**, specifically from Week 7-15, when compared to the age-matched control animals **(*Figure 3.4*)**. This could be explained by the constant consumption of high kilojoule foods, which is typically associated with an increase in body weight due to the imbalance between energy intake and energy expenditure (Goedecke, Jennings and Lambert, 2006; Hall and Guo, 2017)

In the HFD and control animals, treatment with Afriplex GRT™ significantly decreased body weight when compared to HFD and control untreated animals **(*Figure 3.3*)**. For the HFD animals, this result can be ascribed to the decrease in food consumption in response to treatment with Afriplex GRT™ **(*Figure 3.1*),** or due to the inhibition of adipogenesis (Choi *et al.*, 2006). According to previous research, the phenolic compounds present in rooibos are closely associated to the anti-obesogenic potential of rooibos. Among all the polyphenols, rutin has been shown to be the most effective in suppressing adipocyte differentiation (Choi *et al.*, 2006) by downregulating the mRNA expression of the peroxisome proliferator-activated receptor-gamma (PPAR-γ) (Sanderson *et al.*, 2014). PPAR-γ is a key regulator of preadipocyte to mature adipocyte differentiation (Muller *et al.*, 2017).
For the control animals, this result does not correspond with previous studies where treatment with unfermented rooibos and GRE have been shown to have no effect on the body weight of control chow fed animals (Canda, Oguntibeju and Marnewick, 2014; Van Der Merwe *et al.*, 2015), therefore we speculate that the polyphenols present in Afriplex GRT™ also altered adipocyte differentiation in these animals. An increase in water consumption is associated with weight loss (Sciamanna *et al.*, 2011) and therefore we speculate that the increased water intake in these animals ***(Figure 3.2)*** could have resulted in decreased body weight gain.

The HFD + Captopril animals presented with a significant decrease in body weight **(*Figure 3.3*)** specifically from one week after treatment until the end of the treatment regimen **(*Figure 3.4*)**. The decrease in the overall body weight correlates with the decrease in food intake **(*Figure 3.1*)** and IP-fat accumulation **(*Figure 3.5 a-b*)** in these animals. According to previous research, the chronic intake of Captopril in rats increased angiotensin I (1-7) levels, which are known to stimulate the breakdown of triglycerides into glycerol and FFA (lipolysis) by binding to the Mas receptor (Oh *et al.*, 2012).

4.2.3. IP-fat weight

An increase in IP-fat mass is associated with the consumption of more calories than physiologically needed (Manabe, Matsumura and Fushiki, 2010), or according to the carbohydrate-insulin model, the consumption of processed high-glycemic carbohydrates (Ludwig and Ebbeling, 2018).

Correlating with the significant increase in body weight **(*Figure 3.3)***, the HFD animals presented with a significant increase in IP-fat accumulation when compared to the age-matched chow fed controls **(*Figure 3.5 a-b*)**, thus indicating that the HFD animals stored the excess calories consumed in the form of abdominal fat.

Since treatment with Afriplex GRT™ decreased the body weight **(*Figure 3.3)*** in the control and HFD animals, we expected a significant decrease in IP-fat accumulation; however, this was not the case. Treatment with Afriplex GRT™ had no effect on the IP-fat weight in either the control and HFD animals **(*Figure 3.5 a-b*)** and we therefore speculate that the reduction in body weight is linked to subcutaneous fat loss rather than the measured IP-fat loss.

The HFD + Captopril animals presented with reduced IP-fat mass (***Figure 3.5 a-b)***, when compared to the HFD untreated animals. This reduction in IP-fat can be linked to the reduction in body weight (***Figure 3.3)***. As mentioned in *Chapter 4, Section 4.2.2.*, Captopril increases the breakdown of fat, which may explain the reduced IP-fat weight observed in the Captopril-treated HFD animals (Oh *et al.*, 2012).

4.2.4. Liver weight

The HFD animals presented with a significant increase in liver weight when compared to the age-matched chow fed controls ***(Figure 3.6a-b)***. This finding is consistent with previous research showing a significant increase in the liver weight of HFD-fed rats, when compared to control rats (Milagro, Campión and Martínez, 2006; Picchi *et al.*, 2011).

Obesity is associated with increased FFA release from the adipose tissue, resulting in elevated FFA uptake and accumulation in the skeletal muscle and liver. Due to excess fat build-up in the liver, also known as NAFLD, the total liver weight increases (Fabbrini, Sullivan and Klein, 2010). NAFLD is closely associated with cardiometabolic abnormalities, including type II diabetes, coronary heart disease and the metabolic syndrome (Marchesini *et al.*, 2003). In addition, NAFLD also increases the risk of developing dyslipidemia and hypertension (Adams *et al.*, 2005). When

left untreated, NAFLD can progress to severe liver disease, including liver failure or liver cancer (DeWeerdt, 2017).

Two-way ANOVA multiple comparison analyses showed that only the HFD animals treated with Afriplex GRT™ had a significant decrease in liver weight, whereas the overall effect of Afriplex GRT™ treatment was significant in both the control and HFD animals ***(Figure 3.6a)***. Consistent with our control data, previous research showed that the consumption of a GRE for 90 days significantly decreased the liver weight of control Fischer rats (Van Der Merwe *et al.*, 2015).
Since the majority of NAFLD cases are obesity/insulin resistant related, lifestyle modifications mainly include weight loss and insulin sensitivity improvement (Lam and Younossi, 2010; Nseir, Hellou and Assy, 2014). As mentioned previously, certain polyphenols present in rooibos inhibit adipogenesis. We therefore speculate that the decrease in liver weight of the HFD Afriplex GRT™ treated animals were due to the reduction in their body weights ***(Figure 3.3)***. The liver weight to total body weight ratio showed no significant differences in response to treatment with Afriplex GRT™ (***(Figure 3.6b)***.

In addition, previous studies also found that treatment with pure aspalathin (Kawano *et al.*, 2009) and GRE (Kamakura *et al.*, 2015) significantly improved glucose homeostasis and insulin sensitivity. Since improved glucose homeostasis/insulin sensitivity, as seen in both the control and HFD Afriplex GRT™ treated OGTT results ***(Figure 3.8)***, can reverse NAFLD, it might also be a possible cause for the decreased liver weights.

4.2.5. Glucose clearance and insulin sensitivity

Obesity is associated with the accumulation of excess fat in the adipocytes. As a result, FFA release into the plasma is elevated and the anti-lipolytic activity of insulin is decreased. Raising plasma FFAs increase insulin resistance in the skeletal muscle, liver and endothelial cells (Boden, 2008). Insulin resistance results in hyperglycemia, defined as an excessive amount of circulating blood glucose due to the imbalance between glucose intake (food consumption) or glucose production (hepatic glucose production during fasting) and the insulin-stimulated glucose uptake in target tissues (Lee and Halter, 2017).

Blood glucose levels, determined after a stable overnight fast, served as an important marker for the identification of glucose homeostasis. According to the American Diabetes Association, a fasting blood glucose level less than 5.6 mmol/L is considered as normal, 5.6 to 6.9 mmol/L as prediabetic and 7 mmol/L and higher as diabetic. When performing an OGTT, a glucose level less than 7.8 mmol/L 120 min postprandial is considered normal and more than 11.1 mmol/L as diabetic

(American Diabetes Association, 2014). A study performed by Wang et al. (2010) estimated the normal range of fasting blood glucose in Wistar rats as 3.95 +/- 1.31 mmol/L and 5.65 +/- 1.63 mmol/L 120 min postprandial (Wang *et al.*, 2010). Our blood glucose values were higher than those proposed by Wang et al. but correlated with the values proposed by the American Diabetes Association for humans. However, it must be considered that the age of the animals may have an effect on the fasting blood glucose levels.

After an oral glucose (or sucrose) load, an early response in clearance of glucose from the circulation is elicited by the release of incretin hormones (GLP-1 and gastric inhibitory polypeptide (GIP)). After about 15-20 min, the release of insulin from the pancreatic β–cells, results in clearance of glucose by means of stimulating the uptake into the insulin sensitive tissues with the skeletal muscle responsible for the majority of removal of plasma glucose. Mostly, the curves do not display these biphasic events in the intervals that glucose is determined in animal studies (Ghezzi *et al.*, 2012).

In week 10 and week 16 respectively, the baseline fasting glucose levels of the control animals were within the normal blood glucose range, as specified by the American Diabetes Association, whereas the baseline blood glucose levels of the HFD animals were only 0.3 mmol/L lower than the prediabetic mark in week 10 but equal to pre-diabetic levels at 16 weeks of age **(*Table 3.1*)**. In addition, OGTT data showed that the HFD animals exhibited lower glucose clearance in week 10 and week 16 when compared to the age-matched controls as indicated by a significantly higher plasma glucose level 15 min after ingestion of the sucrose **(*Figure 3.7a, 3.8a*)**. HFD animals were therefore glucose intolerant and it can be speculated that the incretin response in these animals were also compromised.

The HFD animals presented with significantly higher baseline fasting glucose levels after 16 weeks when compared to the age-matched chow fed controls **(*Figure 3.10*)**. Treatment with Afriplex GRT™ had no effect on the fasting blood glucose levels in either the control or HFD animals; however according to the OGTT's, the overall glucose clearance of both groups was significantly improved with Afriplex GRT™ treatment **(*Figure 3.8a*)**.

Previous research linked hypoglycemic effects to treatment with aspalathin and GRE respectively. Treatment with aspalathin i*n vivo* significantly increased AMPK phosphorylation, which in turn enhanced GLUT4 vesicle translocation and glucose uptake. Aspalathin also reduced the expression of hepatic genes related to lipogenesis (fat formation) and gluconeogenesis (glucose generation) (Son *et al.*, 2013) and inhibited the α-glucosidase (degrades glycogen to glucose) (Sasaki, Nishida and Shimada, 2018). In a different study, treatment with aspalathin *in vitro*

showed increased glucose uptake in myotubes (muscle cells) and increased secretion of insulin from the pancreas (Kamakura *et al.*, 2015).
Treatment with GRE has been shown to suppress the elevation of blood glucose levels, by preventing glucose absorption from the gastrointestinal system (Mikami *et al.*, 2015). In addition, *in vitro* treatment with GRE has also been documented to promote glucose uptake via AMPK stimulation (insulin-independent) or via PKB stimulation (insulin-dependent). Interestingly, treatment with GRE has been shown to be more effective in activating AMPK and glucose uptake than aspalathin, as GRE contains additional polyphenols such as rutin (Muller *et al.*, 2012) and isoorientin (Sezik *et al.*, 2005) which are speculated to synergistically contribute to the glucose lowering capabilities of GRE.

Since both our control and HFD animals presented with increased AMPK phosphorylation in the vasculature in response to treatment with Afriplex GRT™ **(*Figure 3.26*)**, we speculate that this may also be the case in the other insulin sensitive tissues – liver, skeletal muscle, heart and fat depots. Afriplex GRT™, as previously described for aspalathin, may therefore act via the AMPK pathway to decrease plasma glucose levels by increasing peripheral glucose uptake. This would therefore also indicate improvement of insulin resistance and the prediabetic state.

As mentioned above, obesity is associated with high circulating plasma glucose levels. As a result, insulin secretion from the pancreas is elevated to compensate for and decrease the elevated glucose levels. Due to the increased demand on the pancreas and the high FFA levels present, β-cell failure in the pancreas can develop, resulting in decreased insulin secretion, increased glucose levels and consequently, type II diabetes (Kahn, Hull and Utzschneider, 2006).
After 16 weeks, the HFD animals presented with a significant decrease in fasting insulin levels when compared to the age-matched chow fed controls **(*Figure 3.11*)**. We speculate that the HFD animals already had pancreatic β-cell damage which restricted their insulin secretion. This phenomenon that the HFD animals presented with decreased insulin levels, rather than the expected increase, has been observed in other diet-induced obesity animal studies specifically conducted in our laboratory.

Treatment with Afriplex GRT™ significantly decreased the fasting insulin levels in both the control and HFD animals **(*Figure 3.11*)**. This finding correlates with the baseline fasting glucose data obtained after 16 weeks, where treatment with Afriplex GRT™ had no significant effect **(*Figure 3.10)***. However, due to the decrease in insulin levels and the overall improved glucose clearance in both the control and HFD Afriplex GRT™ treated groups ***(Figure 3.8a)***, we speculate that this improvement was not insulin-dependent and involved the activation of the AMPK insulin-independent pathway. Since both the control and HFD animals treated with Afriplex GRT™

excreted more glucose via the urine when compared to the untreated groups ***(Table 3.8c)***, we further speculate that the demand for insulin secretion from the pancreas might have been decreased.

In addition, the HOMA-IR was calculated to determine the presence of insulin resistance in both the control and HFD Afriplex GRT™ treated and untreated animals. The HOMA-IR value increases proportionally to the degree of insulin resistance. Interestingly, both the control and HFD animals presented with a high HOMA-IR value, suggesting insulin resistance ***(Figure 3.12)***. In the control animals, this result suggests that the control animals at this age, were also becoming insulin resistant. According to previous research, ageing in control rats (Week 5 -16 of age) is associated with an increase in visceral adiposity together with the accumulation of senescent cells with an inflammatory phenotype. As a result, the high circulating levels of pro-inflammatory cytokines interferes with normal insulin signalling (Goodman et al., 1983).

Treatment with Afriplex GRT™ in both the control and HFD animals decreased the HOMA-IR values when compared to the respective untreated controls **(*Figure 3.12*)**. This result is indicative of improved insulin sensitivity and is suggested to be linked to the increased glucose excretion via the urine ***(Table 3.8c)*** which decreased the demand for insulin secretion ***(Figure 3.11)*** from the pancreas.

At sacrifice, the HFD animals had increased non-fasting glucose levels wh en compared to the age-matched controls ***(Figure 3.9)***, underscoring the conclusion that the HFD animals were insulin resistant. Treatment with Afriplex GRT™ was unable to decrease circulating non-fasting glucose levels despite the improved overall glucose clearance in both the control and HFD animals indicated by the OGTTs ***(Figure 3.8a).*** This may be because these values were taken at different points after ingestion of food, as the animals were not sacrificed at the same time of day.

4.3. Blood pressure and urine analyses

4.3.1. Blood pressure

The pathogenesis of obesity-related hypertension is speculated to be closely associated with (a) activation of the sympathetic nervous system and the RAS resulting in arterial vasoconstriction and sodium retention, (b) excessive intra-vascular and intra-abdominal fat which triggers inflammation and consequently endothelial dysfunction (Jiang *et al.*, 2016) and physical compression of the kidneys due to the excessive fat accumulated around the kidneys (Hall *et al.*, 2015). Obesity-related hypertension is also linked to the (c) overexpression of RAS components

such as angiotensin II (Saiki *et al.*, 2009), (d) elevated leptin levels (Cassis *et al.*, 2004) and (e) reduced adiponectin levels (Ran *et al.*, 2006). These changes enhance the activation of the sympathetic nervous system consequently increasing blood pressure.

From these contributing factors, we managed to determine the body weight, IP-fat weight, leptin, adiponectin, and the endothelial function (aortic ring studies) of the animals.

Before treatment, the HFD animals presented with significantly higher systolic and diastolic blood pressure readings when compared to the age-matched chow fed controls ***(Table 3.2 & Figure 3.13-3.14)***. Thus, the main purpose of inducing hypertension using the specific HFD, was accomplished. This finding is consistent with a previous study conducted in our laboratory where rats consuming the same HFD also developed hypertension (Huisamen *et al.*, 2013). It is important to note that the rats in the current study specifically had hypertension stage 1 according to ***Table 1.2***.

We speculate that the HFD animals presented with increased blood pressure due to their increased body weights ***(Figure 3.3)*** and IP-fat accumulation **(*Figure 3.5a-b)*** which in turn could have resulted in renal compression, or due to their elevated leptin levels **(*Figure 3.39)*** which could have increased sympathetic activation as shown by their reduced endothelium-dependent vasorelaxation **(*Figure 3.22)***. Previous studies showed that activation of the sympathetic system may increase the release of NO from eNOS, consequently attenuating vasoconstrictor responses, however since obesity is normally associated with eNOS dysfunction and cardiovascular risk, vascular resistance and blood pressure is elevated during sympathetic stimulation (Shabeeh *et al.*, 2013). Upregulation of RAS components in response to obesity could not be successfully determined because of the very low plasma levels. To answer this question, another set of animals may be investigated in future.

Treatment with Afriplex GRT™ had no overall effect on the systolic and diastolic blood pressure of the control animals ***(Figure 3.15-3.16)***; correlating with their unchanged IP-fat weight **(*Figure 3.5a-b)*** and leptin levels **(*Figure 3.39)***. HFD animals treated with Afriplex GRT™ presented with a significant decrease in systolic and diastolic blood pressure, when compared to the HFD untreated animals ***(Figure 3.15 & Figure 3.17-3.18)***. We speculate that this result can be ascribed to the decrease in body weight ***(Figure 3.3)***, which could have reduced the release of FFAs into circulation, thereby decreasing inflammation, improving endothelial reactivity and increasing NO-induced vasorelaxation. Aortic isometric tension studies showed that treatment with Afriplex GRT™ significantly improved endothelium-dependent vasodilation in the HFD animals, suggesting improved NO availability ***(Figure 3.22)***. Since our eNOS data showed no significant differences in response to treatment with Afriplex GRT™, we speculate that the improved vasodilation seen in these animals were most probably due to the anti-oxidant potential of Afriplex

GRT™ to increase SOD, CAT and glutathione peroxidase activity (data not shown - experiments were performed by another student as part of her M.Sc.) (Maqeda, 2018), consequently decreasing ROS, oxidative stress and endothelial dysfunction.
Previously reported data showed that treatment with rooibos resulted in ACE activity inhibition consequently decreasing blood pressure levels (Persson *et al.*, 2010), however according to our FRET analyses, treatment with Afriplex GRT™ had no ACE inhibitor capabilities ***(Figure 3.37-3.38)***.

Although the mean blood pressure values of the Captopril treated animals were almost two times lower than the HFD + Afriplex GRT™ group, the standard deviation values were very high and treatment with this anti-hypertensive drug was unable to significantly reduce systolic and diastolic blood pressure as expected ***(Figure 3.17-3.18)***. According to previous data, the ability of Captopril to inhibit ACE can either be an immediate or late response (Tarazi, Bravo and Fouad, 1981). In another study, individuals became resistant to Captopril after an immediate response (Fallo, Maragno and Mantero, 1985). We therefore speculate that the period (6 weeks) of Captopril treatment was either not long enough to significantly reduce the blood pressure, or that the animals became Captopril resistant specifically after week 14 where the blood pressure values started to slightly increase again ***(Table 3.5-3.6)***. In addition, the blood pressure values of the Captopril animals were not reduced in response to their decreased body weight and IP-fat weight ***(Figure 3.3, 3.5)***, suggesting that a decrease in body weight and IP-fat weight in the HFD animals in response to treatment with Afriplex GRT™ or Captopril, might not be the cause for blood pressure lowering.

4.3.2. Urine volume

Hypertension is associated with increased blood flow resulting in shear stress. Eventually, excessive stretching can damage the blood vessels throughout the body and also those in the kidneys. When the blood vessels in the kidneys are damaged, a reduction in waste and body fluid removal via urinary excretion is observed, which, as a result, further elevates the blood pressure (NIDDK, 2014).

Before and after treatment, the HFD animals secreted significantly less urine when compared to the age-matched chow fed controls ***(Figure 3.19-3.20)***. This result is consistent with previous research where rats consuming the same HFD as in the current study, also presented with water retention (Huisamen *et al.*, 2013). Water retention in the HFD animals correlates with their decrease in water consumption ***(Figure 3.2)*** and to their obesity-induced hypertensive stage 1 profiles ***(Figure 3.13-3.14)*** which could have damaged the blood vessels in the kidneys,

consequently restricting body fluid removal. Since these rats are obese, increased RAS activation could have resulted in increased sodium reabsorption in the kidneys, and consequently fluid retention; however, these markers were not determined.

Treatment with Afriplex GRT™ significantly increased the amount of urine secreted by the control animals when compared to the age-matched chow fed controls ***(Figure 3.20)***. This result correlates with the increased water consumption in these animals ***(Figure 3.2)***. In the HFD animals, treatment with Afriplex GRT™ did not have a diuretic effect, and we therefore speculate that the decreased blood pressure values in these animals involved a more complex mechanism. Taken together, the effect of Afriplex GRT™ on the urine volume was specific to the control animals.

As expected, treatment with Captopril significantly increased the excretion of urine in the HFD animals, when compared to the HFD untreated animals ***(Figure 3.20)***. This result correlates with the increase in water consumption observed in these animals ***(Figure 3.2)***. Consistent with our data, a previous study reported that the administration of Captopril to diabetic Brattleboro rats significantly increased fluid intake and urine output (Gardiner and Bennett, 1983). In addition, the administration of Captopril to Wistar rats consuming the same HFD as in the current study, significantly increased the urine volume (Huisamen *et al.*, 2013).

4.3.3. Urine parameters

Before treatment: The control and HFD animals tested negative against bilirubin and presented with urobilinogen levels considered as normal thus indicating that no liver or bile diseases were present in these animals ***(Table 3.7a, 3.7h)***.

As expected, the majority of the control and HFD animals presented with no blood in their urine and little leukocyte levels, thereby suggesting that kidney and urological diseases/inflammation were not present ***(Table 3.7b, 3.7d)***. Protein levels in the majority control and HFD animals were above the normal standard and therefore suggest the presence of renal diseases ***(Table 3.7e)***. Since blood and leukocyte levels were not indicative of any renal diseases, we assume that the higher than normal protein levels were not associated with renal diseases in these animals.

Obesity is usually associated with the presence of glucose in the urine, a condition known as glucosuria. According to the American Heart Association, the exact point when glucose spilling occur varies by organism and depends on the kidney function. Glucosuria is not necessarily linked

to obesity, as lean individuals previously also showed glucose spilling (American Diabetes Association, 2018).

In both the control and HFD group, the majority animals had no glucose and ketones present in their urine ***(Table 3.7c, 3.7f)***. This result shows that these animals were not suffering from carbohydrate metabolism disorders and diabetes. Ketone production is usually associated with type I diabetes where the body initiates the burning of fat, because glucose delivery to the cells are restricted.

The majority control and HFD animals tested negative against nitrite, which confirms that these animals did not have urinary tract infections ***(Table 3.7g)***. Interestingly, the urinary pH of the control animals was very basic (pH=9), and the majority of HFD animals had either the same basic urinary pH (pH=9) or an acidic urinary pH (pH=5) ***(Table 3.7i)***. In healthy rats the pH varies between 5 and 7 (Ferrets, 2014), thus according to our results, the increased pH in the control and half of the HFD animals is indicative of urinary tract infections, however, nitrite measurements contradict this observation.

After treatment: The control and HFD animals tested negative for urinary bilirubin and presented with urobilinogen levels below the pathological mark. Treatment with Afriplex GRT™ and Captopril had no effect on the bilirubin and urobilinogen levels in the control and HFD animals, indicating that no liver or bile diseases were initiated ***(Table 3.8a, 3.8h)***.

The majority control and HFD animals presented with no blood in their urine and acceptable leukocyte levels, thereby suggesting that kidney and urological diseases/inflammation were not present. Treatment with Afriplex GRT™ or Captopril did not change these parameters, indicating that kidney and urological diseases/inflammation were not initiated in response to treatment with Afriplex GRT™ or Captopril ***(Table 3.8b, 3.8d)***. Protein levels in the majority control and HFD animals were the same, but still above the normal standard, as before treatment. Treatment with Afriplex GRT™ had no effect on the protein levels in the majority control and HFD animals. The high protein level present in the Afriplex GRT™ treated and untreated groups could be indicative of renal diseases ***(Table 3.8e)***; however, since blood and leukocyte levels contradicted this result, we assume that the higher than normal protein levels were not associated with renal diseases in these animals. Interestingly, treatment with Captopril decreased the urinary protein levels in the HFD animals to an acceptable normal level which is indicative of ACE inhibition, contradicting the blood pressure results ***(Figure 3.17-3.18)***. When Captopril inhibits ACE, it reduces the glomerular filtration rate and consequently the amount of protein filtered in the nephrons, resulting in reduced proteinuria (Bansal, 2015).

In both the control and HFD group, the majority animals had no glucose and no or little ketones present in their urine ***(Table 3.8c, f)***, indicating the absence of carbohydrate metabolism disorders and diabetes. Treatment with Afriplex GRT™ did not affect the ketone levels in the control and HFD animals, but interestingly, increased urinary glucose in half of the control animals and in all the HFD animals. The excretion of glucose in the urine is closely associated with inhibition of the SGLT2 transporter, thereby suggesting that Afriplex GRT™ might act as an SGLT2 inhibitor. Confirming this suggestion, a previous study reported that aspalathin can inhibit SGLT2 (Sasaki, Nishida and Shimada, 2018). SGLT2 is predominantly expressed in the renal proximal tubules of the kidneys, and to a lesser extent in the liver, muscle, heart (Wright, Loo and Hirayama, 2011), and pancreatic α-cells (Bonner *et al.*, 2015). Since glucose is mainly reabsorbed by the kidney via the SGLT2, inhibition of SGLT2 offers an insulin-independent novel mechanism for the treatment of type II diabetes. In humans, the inhibition of the SGLT2 have been shown to initiate glucose excretion in the urine, consequently inducing weight loss and hypoglycaemia (Whaley *et al.*, 2012). SGLT2 inhibition also increases the activation of AMPK (Hawley *et al.*, 2016, Xu *et al.*, 2017), consequently initiating glucose uptake from the circulation in to peripheral tissues. We speculate that the decrease in body weight and improved glucose clearance in both the control and HFD animals can be ascribed to the inhibition of the SGLT2 by Afriplex GRT™ ***(Figure 3.3, 3.8)***.
Treatment with Captopril had no effect on urinary glucose levels, however it did increase urinary ketone levels. This is most probably a false-positive result, as Captopril is secreted in the urine as a free-sulfhydryl compound. In the alkaline urine, this free-sulfhydryl compound reacts with a purple colour which is similar to that of ketone bodies in the nitroprusside dipstick test (Csako and Elin, 1993).

The control and HFD Afriplex GRT™/Captopril treated and untreated animals tested negative against nitrite, which confirms that these animals did not have urinary tract infections ***(Table 3.8g)***. The urinary pH of the control animals was very basic (pH=9) where the pH of the HFD animals was acidic (pH=5). The pH levels in both the control and HFD animals were unaffected by treatment with Afriplex GRT™ ***(Table 3.7i)***. In healthy rats the urinary pH varies between 5 and 7 (Ferrets, 2014), indicating that the HFD and HFD + Afriplex GRT™ animals had a normal pH. with no urinary tract infections. Interestingly, the control and control + Afriplex GRT™ animals presented with a higher urinary pH which is indicative of urinary tract infections; however, nitrite measurements contradict this observation. SGLT2 inhibition is linked to the additional growth of genital microorganisms thereby increasing the risk for urinary tract infections (Liu *et al.*, 2017). Thus, if Afriplex GRT™ acted as a SGLT2 inhibitor as speculated, we expected the control + Afriplex GRT™ animals to develop a urinary tract infection as these animals urinated more when compared to the HFD + Afriplex GRT™ animals ***(Figure 3.20)***.

In the majority HFD animals, treatment with Captopril changed the pH from 5 to 6, which is still in the normal pH range and therefore not indicative of urinary tract infections. This result also correlates with the urinary nitrite data of the Captopril treated animals.

4.4. Vascular endothelium

4.4.1. Aortic ring isometric tension studies

Endothelial dysfunction refers to decreased bioavailability of vasodilators (predominantly NO) and/or increased EDCF (Lerman and Burnett, 1992) ***(Table 1.1)***. This imbalance results in impaired endothelium-dependent vasodilation and increased vasoconstriction, a known functional characteristic of endothelial dysfunction (Hadi, Carr and Al Suwaidi, 2005). In addition, an unbalanced endothelial-derived vasodilator/vasoconstrictor ratio results in hypertension (Rubanyi, 1991).

After the 16-week feeding period, the aortic rings from both the control and HFD untreated and treated animals were isolated and used for isometric aortic ring studies. The aortic rings of the HFD animals were less responsive to Phe (decreased vasoconstriction) and ACh (decreased relaxation) administration when compared to the age-matched controls ***(Table 3.9, Figure 3.21-3.23)***. This finding supports previous reports where Phe-induced contraction and ACh-induced relaxation was significantly reduced in rats suffering from pulmonary hypertension. The exact cause of changes in contraction and relaxation is unclear but it is speculated to be closely related to pulmonary VSMC growth/proliferation and vascular remodelling. It is also suggested that the increase in vascular wall thickness, due to vascular remodelling, decreases the sensitivity to vasodilator and vasoconstrictor stimuli, as the VSMCs switch from a contractile to proliferative phenotype (Mam *et al.*, 2010).

Obesity has also been shown to impair eNOS expression/activity, increase O_2•- production (eNOS uncoupling), and release vasoconstrictor factors such as ET-1 and Angiotensin II. Furthermore, obesity is associated with decreased endothelial progenitor cells, resulting in decreased endothelial cell regeneration. Together these changes reduce NO production and impairs vasodilation (Toda and Okamura, 2013). In the current study, we only determined eNOS expression/activity and ET-1 levels. Consumption of the HFD increased the expression of eNOS, decreased the P:T eNOS ratio ***(Figure 3.28 & Figure 3.30)*** and had no effect on the ET-1 levels ***(Figure 3.41)***, thus suggesting that the impaired vasodilation is not ET-1 related and might rather be due to the decrease in eNOS activation. As the HFD animals presented with increased eNOS expression, we would have expected improved vasodilation; however, the amount of eNOS

proteins activated as well as SOD levels (data not shown - experiments were performed by another student as part of her M.Sc. (Maqeda, 2018)) were significantly decreased, consequently reducing NO availability for relaxation.

Since we previously observed in our laboratory that the fat surrounding the aorta (PVAT) signals to the underlying tissue, we conducted our isometric tension studies using aortas with PVAT. Accordingly, the PVAT must also be taken into consideration when analysing and interpreting our results. The PVAT acts as an active endocrine organ releasing inflammatory cytokines, adipokines and additional factors influencing vascular tone (Gollasch and Dubrovska, 2004; Gao, 2007; Fernández-Alfonso, Gil-Ortega and Somoza, 2009). Under normal physiological conditions, the PVAT releases vasodilatory agents, including adiponectin (Fésüs *et al.*, 2007), leptin (Gálvez-Prieto *et al.*, 2012), adipocyte-derived relaxing factor (ADRF), H_2O_2 (Gao *et al.*, 2006) and NO (Gil-Ortega *et al.*, 2010). These anticontractile agents are crucial for maintenance of vascular resistance (Gollasch and Dubrovska, 2004; Gao, 2007; Fernández-Alfonso, Gil-Ortega and Somoza, 2009). In obesity, the increase in PVAT throughout the vasculature (Iacobellis *et al.*, 2003; Somoza *et al.*, 2007; Greenstein *et al.*, 2009; Ma *et al.*, 2010) triggers both structural and functional changes in PVAT which results in endothelial dysfunction and vascular damage. Obesity is also associated with altered adipokine expression, causing an unbalanced endothelial-derived vasodilator/vasoconstrictor ratio in favour of vasoconstrictor and pro-inflammatory substances (Fernández-Alfonso *et al.*, 2013).

In addition, insulin resistance and diabetes mellitus have been shown to augment obesity-induced endothelial dysfunction (Toda and Okamura, 2013). According to previous cell culture studies, insulin stimulates NO formation, and high circulating glucose levels inhibit NO formation (Aljada *et al.*, 2000; Schnyder *et al.*, 2002). Insulin-induced signal transduction in the endothelium entails the activation of PI3K which in turn phosphorylates the PKB and eNOS protein complex to form NO. The presence of high glucose concentrations averts the formation of the enzymatic complexes (Schnyder *et al.*, 2002).

When taking above mentioned into consideration, we speculate that in our HFD animals, leptin resistance ***(Figure 3.39)*** could have resulted in increased glucose levels ***(Figure 3.9)*** due to uncontrolled food intake ***(Figure 3.1)***. The high circulating glucose levels most probably reduced the formation of NO by decreasing PKB ***(Figure 3.32-3.33)*** and eNOS ***(Figure 3.30)*** activation.

In the first 12 control animals, treatment with Afriplex GRT™ had no significant effect on Phe-induced vasoconstriction ***(Figure 3.21)***, whereas in the second 7 control + Afriplex GRT™ animals, Phe-induced vasoconstriction was significantly reduced ***(Figure 3.23)*** when compared to the age-matched untreated controls. This reduction suggests that VSMCs switched from a contractile to proliferative phenotype, thereby decreasing its sensitivity to Phe. VSMC proliferation

mainly develops in response to insulin resistance where NO production is reduced and therefore unable to inhibit VSMC proliferation. This result does not correlate with the increased AMPK ***(Figure 3.26-27)*** and PKB ***(Figure 3.32-33)*** activation as well as the unchanged blood pressure data ***(Figure 3.15-16***) in these 7 animals, thus creating uncertainty about its reliability. These observations should therefore be repeated in future. Phe-induced vasoconstriction in the HFD animals was unaffected by treatment with Afriplex GRT™ ***(Figure 3.21 & Figure 3.23)***.

Treatment with Afriplex GRT™ in the control animals had no effect on ACh-induced vasodilation. However, in the HFD animals treated with Afriplex GRT™, ACh-induced vasodilation was significantly increased when compared to the delayed vasodilation in the HFD untreated animals ***(Table 3.9, Figure 3.22)***, suggesting improved NO production. Previous research showed that the polyphenolic compounds present in rooibos are able to inhibit ACE activity, which in turn increases NO production and decreases blood pressure (Persson *et al.*, 2006, 2010). According to our FRET analysis ***(Figure 3.37),*** Afriplex GRT™ had no ACE inhibitor potential, and therefore a different mechanism must have been involved to increase endothelium-dependent vasorelaxation. We speculate that the improved glucose clearance in the HFD animals treated with Afriplex GRT™ ***(Figure 3.8a)*** increased the activation of the PI3K-dependent pathway as seen by the increase in T-PKB expression and phosphorylation ***(Figure 3.31-33)***. Activated PKB results in increased eNOS activation and consequently NO generation (Ritchie *et al.*, 2004). Another speculated mechanism for the improved relaxation in response to treatment with Afriplex GRT™ can be ascribed to the anti-oxidative stress potential of Afriplex GRT™. The antioxidant effects of Afriplex GRT™ was determined using the same animals; however as mentioned, these experiments were performed by another student as part of her M.Sc. Data obtained showed that Afriplex GRT™ improved CAT, SOD, and glutathione peroxidase, consequently decreasing ROS, oxidative stress and endothelial dysfunction. Afriplex GRT™ also decreased lipid peroxidation, measured by the thiobarbituric acid reactive substance (TBARS) assay (Maqeda, 2018).

As expected, HFD animals treated with the anti-hypertensive drug, Captopril, presented with a significant increase in vascular relaxation in response to ACh administration, when compared to the delayed vasodilation in the HFD untreated animals ***(Table 3.9, Figure 3.22)***. Captopril inhibits the conversion of angiotensin I to angiotensin II, consequently averting NO production (Odaka and Mizuochi, 2000). We therefore speculate that the pro-relaxation effects of Captopril might be due to the activation of bradykinin by Captopril, which in turn activates EDHF and PGI_2. EDHF passes through the VSMC layer, consequently stimulating the ion channels which results in hyperpolarization followed by relaxation. PGI_2 increases AMP levels, consequently inducing relaxation (Gauthier, Cepura and Campbell, 2013). According to our blood pressure analyses ***(Figure 3.17-3.18)***, Captopril at the dose and time of treatment, did not lower blood pressure;

whereas in our *in vitro* FRET analyses ***(Figure 3.37-3.38)*** ACE inhibition was detected. As we previously obtained positive results on lowering blood pressure with Captopril at the dose given, it is difficult to speculate why the blood pressure of the animals was not significantly lowered as we have no information on the levels of the RAS intermediates from the current study. Currently, the data indicates that the blood pressure in these animals was not elevated because of elevated activation of the RAS. This is a shortcoming in our results and should be investigated in future studies.

To determine whether the differences in ACh-induced relaxation were caused by responses of the vascular smooth muscle to NO, we used the endothelium-independent nitrodilator SNP, a known NO donor. Once NO is released in response to SNP (or endothelial-dependently via eNOS), it enters the vascular smooth muscle cells, activates guanylate cyclase which in turn increases the cGMP levels. Elevated cGMP increases calcium uptake, consequently inducing vasodilation (Cogolludo *et al.*, 2001).

SNP-induced endothelium-independent vasodilation was significantly increased in the HFD animals when compared to the age-matched controls ***(Figure 3.24)***. This result is not consistent with the ACh-induced endothelium-dependent vasodilation where these animals presented with impaired relaxation (decreased NO) ***(Figure 3.22)***. We speculate that there was likely to be some endothelium-dependent impairment, possibly related to the eNOS-NO biosynthesis pathway of the endothelial cells, which was partially (as we used vascular tissue and not only endothelial tissue) supported by the P:T eNOS ratio ***(Figure 3.30)***.

Treatment with Afriplex GRT™ significantly increased SNP-induced vascular relaxation in the control animals ***(Figure 3.24)***, indicating that the VSMCs were more responsive to NO when treated with Afriplex GRT™. In the HFD animals, treatment with Afriplex GRT™ delayed the SNP-induced vascular relaxation process, however the maximum relaxation reached did not significantly differ from that in the HFD animals ***(Table 3.10, Figure 3.24)***. This result contradicts the ACh-induced vasodilation results where treatment with Afriplex GRT™ significantly increased vascular relaxation in the HFD animals ***(Figure 3.22)***. We speculate that Afriplex GRT™ increased NO production via eNOS, but the VSMCs were less responsive to its actions due to presence of obesity-induced oxidative stress in these animals. Previous studies reported that oxidative stress results in loss of the prosthetic haem group of guanylate cyclase, consequently averting its activation by NO (Thoonen *et al.*, 2015). More studies will have to be conducted to elucidate the oxidative stress levels in these animals.

Another method of VSMC contraction was also performed in a few animals using KCl, however experimentation was terminated since the aortic rings hypercontracted and were unable to relax after KCl administration. KCl initiates contraction in VSMC by depolarizing the VSMC membrane which in turn, stimulates the opening of the calcium voltage channels. As a result, extracellular calcium enters the VSMCs and contraction is initiated (Karaki, Urakawa and Kutsky, 1984). No significant differences in response to KCl-induced constriction were observed between the groups ***(Table 3.11)***. Maximum VSMC contraction with KCl correlated with Phe-induced vasoconstriction suggesting that differences caused in the Phe-induced vasoconstriction is closely associated with contraction in the VSMCs. As treatment with KCl resulted in the same maximum contraction as Phe, we are uncertain why the aortas were unable to relax. We speculate that the addition of KCl to the aorta in the organ bath caused a chemical reaction, which increased the temperature of the buffer surrounding the aorta, consequently initiating hypercontraction.

4.4.2. Western blotting

Western blotting was performed using the aortic tissue of both the control and HFD untreated and treated animals to determine the expression and activation of AMPK, eNOS and PKB.

AMPK, an insulin-independent signalling protein, is activated in response to nutrient starvation (particularly glucose) and hypoxia (Mihaylova and Shaw, 2011; Hardie, Ross and Hawley, 2012). Once activated, AMPK stimulates fatty acid oxidation (Carling, Zammit and Hardie, 1987), glucose uptake (Ruderman *et al.*, 2013) and also NO production via eNOS (Hu *et al.*, 2008; Chen *et al.*, 2009).

Obesity is associated with increased insulin resistance and decreased AMPK levels which in turn, results in the development of hypertension (Ruderman *et al.*, 2013). This result is consistent with our findings as the HFD animals were obese ***(Figure 3.2)***, insulin resistant ***(Figure 3.11)***, presented with lower T-AMPK expression ***(Figure 3.25)*** and increased blood pressure levels ***(Figure 3.15, 3.17-3.18)*** when compared to the age-matched controls. Decreased T-AMPK expression results in increased fatty acid synthesis, glucose levels and impaired NO production, reducing vascular vasodilation as shown in the isometric tension studies ***(Figure 3.22)***. The HFD animals presented with an increased P:T AMPK ratio when compared to the age-matched controls. This result is misleading since T-AMPK levels were decreased. We therefore assume that all of the AMPK proteins, although low in expression, were phosphorylated.

Treatment with Afriplex GRT™ significantly increased the phosphorylation of AMPK in the HFD animals when compared to the HFD untreated animals ***(Figure 3.26)***. In the control group,

treatment with Afriplex GRT™ increased AMPK phosphorylation and the P:T AMPK ratio ***(Figure 3.26-3.27)*** . The effect of Afriplex GRT™ are thus not specific to the HFD. We speculate that Afriplex GRT™ may have upregulated glucose uptake via the AMPK pathway, however the exact mechanism remains unclear. Our finding supports that of previous studies where treatment with aspalathin *in vivo* (Son *et al.*, 2013) or aspalathin-rich GRE *in vitro* (Kamakura *et al.*, 2015) significantly increased AMPK phosphorylation, and in turn enhanced GLUT4 vesicle translocation and glucose uptake.

Active AMPK is linked to the phosphorylation of eNOS on Ser 1179 (Hu *et al.*, 2008) and Ser 633 (Chen *et al.*, 2009), and therefore we expected the activation of eNOS in the HFD animals to be decreased and, in turn, increased in response to treatment with Afriplex GRT™. Unexpectedly, T-eNOS expression was significantly increased in the HFD animals when compared to the age-matched controls; whereas, the P:T ratio was significantly decreased ***(Figure 3.28, 3.30)***. Thus, the total amount of eNOS was increased, but only a small amount was actually activated, correlating with impaired vasodilation in these animals ***(Figure 3.22)***. We also speculate that a reduction in NO bioavailability (as shown by reduced Ach-induced vasodilation) could be linked to the decrease in SOD enzyme activity (data not shown - experiments were performed by another student as part of her M.Sc. (Maqeda, 2018)), which contributes to a decrease in NO bioavailability via eNOS uncoupling.

Since the control animals treated with Afriplex GRT™ presented with increased P-AMPK levels ***(Figure 3.26)***, increased glucose clearance ***(Figure 3.8a)*** and unaffected vasodilation and blood pressure ***(Figure 3.15-3.16, 3.22)***, we assume that in these animals, AMPK activation only induced glucose uptake via GLUT 4, and did not increase the eNOS expression ***(Figure 3.28)*** for NO production. This is a positive finding as the induction of hypotension in normal control animals, would have pointed to a detrimental effect of the product.

In the HFD animals, activation of PKB and the P:T PKB ratio was significantly decreased when compared to the age-matched controls ***(Figure 3.32-3.33)***. As the HFD animals presented with decreased glucose clearance ***(Figure 3.8a)*** and insulin sensitivity ***(Figure 3.11)*** when compared to the age-matched controls, we assume that this finding indicates a state of insulin resistance in the HFD animals. Furthermore, since PKB is a potent upstream activator of eNOS, the downregulation of P:T PKB in the HFD animals also correlates with the eNOS data where these animals presented with decreased P:T eNOS ***(Figure 3.30)***.

Treatment with Afriplex GRT™ in the HFD animals increased the T-PKB expression, phosphorylation and P:T PKB ratio ***(Figure 3.31-3.33)***. In the control animals, treatment with

Afriplex GRT™ only increased PKB phosphorylation and the P:T PKB ratio. We speculate that the improved glucose clearance in the HFD and control animals treated with Afriplex GRT™ ***(Figure 3.8a)*** are indicative of the increased activation of the PI3K-dependent pathway as confirmed by the increase in activation of the downstream PKB signalling molecule. Activated PKB is known to increase eNOS activation and consequently NO generation (Ritchie *et al.*, 2004); however our eNOS data does not significantly correlate with this result.

Treatment with Captopril showed no significant differences in AMPK, eNOS and PKB expression and phosphorylation, suggesting that Captopril does not have any effect on the insulin-dependent or insulin-independent pathway. This result correlates with the blood pressure data where Captopril was unable to decrease blood pressure. Interestingly, Captopril showed improved endothelium-dependent vasodilation ***(Figure 3.22)***, which suggests that relaxation was not linked to the vasodilator, NO, but rather to a different vasodilator such as EDHF and PGI_2 (described in *Chapter 4, Section 4.4.1*).

4.5. AECs

The effect of Afriplex GRT™ on NO production (DAF-2/DA assay), cellular apoptosis (PI assay) and cellular metabolic activity (MTT assay) was measured using AECs treated with three different Afriplex GRT™ concentrations. The possibility of ACE-inhibitor activity was determined using AECs treated with either the same three Afriplex GRT™ concentrations, or with non-fasting serum (collected previously from the control and HFD untreated and treated animals).

Treatment with Afriplex GRT™ had no significant effect on NO production or cellular apoptosis, when compared to the untreated vehicle control ***(Figure 3.34-3.35)***, indicating that Afriplex GRT™ did not induce apoptosis and was also unable to generate NO - contradicting the increased vasodilation result in the HFD + Afriplex GRT™ animals ***(Figure 3.22)***. Since only our HFD animals, and not the control animals, presented with improved vasodilation in response to treatment with Afriplex GRT™ ***(Figure 3.22)***, we speculate that Afriplex GRT™ was able to improve the metabolic status of the HFD with the changes in vascular patency and lowering of blood pressure as a result of that.

A previous study reported that treatment with rooibos inhibits apoptosis, which can be ascribed to the flavonol content of this South African herbal tea (Pantsi *et al.*, 2011). Up to a concentration of 100 μg/mL, Afriplex GRT™ showed no signs of cytotoxicity on AES's in culture.

The highest dosage of Afriplex GRT™ treatment significantly increased cellular metabolic activity in the AECs, in other words, cell proliferation, when compared to the vehicle control ***(Figure 3.36)***. Increased cell proliferation (angiogenesis) is associated with increased VEGF levels. VEGF is a key regulator of vascular permeability (Lal *et al.*, 2001). Furthermore, vasodilation is also associated with increased vascular permeability (Baskurt, Yalcin and Meiselman, 2004). We therefore speculate that treatment with Afriplex GRT™ initiates vasodilation (in HFD animals), which in turn might affect VEGF levels to increase vascular permeability.

We were not able to detect any ACE inhibitor activity in the serially diluted Afriplex GRT™ extract ***(Figure 3.37)*** or an elevation in ACE activity in the serum collected from control and HFD Afriplex GRT™ treated and untreated animals ***(Figure 3.38)***. The mechanism whereby Afriplex GRT™ lowers blood pressure and increases endothelium-dependent relaxation in HFD animals is therefore not ACE related.

4.6. Biochemical analyses

4.6.1. Leptin

Leptin is a polypeptide hormone, produced by adipocytes and responsible for controlling food intake. In response to energy consumption, leptin binds to its receptor (LEPR) in the hypothalamus, consequently inhibiting food intake and increasing energy expenditure (Myers *et al.*, 2010).

Although obesity is associated with high levels of circulating leptin, these individuals are usually unresponsive to the respiratory and metabolic effects of leptin (Berger and Polotsky, 2018). In lean subjects, normal circulating leptin levels are relatively low (5-10 ng/ml) (Sinha *et al.*, 1996), whereas an increase in body fat mass of 30 % can increase leptin levels to approximately 98 ng/ml (Ostlund *et al.*, 1996).

In obese subjects, high circulating leptin levels are unable to decrease appetite (satiety) and increase energy expenditure, a phenomenon known as leptin resistance (Berger and Polotsky, 2018). The development of leptin resistance can be ascribed to three possible mechanisms including the inability of circulating leptin to cross the blood-brain barrier, downregulation of the cell surface LEPR receptor and/or the inhibition of the leptin-LRPR signalling pathway (Myers, Cowley and Münzberg, 2008).

According to previous *in vivo* research, leptin is associated with the activation of PI3K in the hypothalamus (Niswender *et al.*, 2001), which in turn, activates renal sympathetic nerve activity to increase arterial pressure (Harlan and Rahmouni, 2013).

Although the circulating leptin levels of the control animals in the current study were below the normal 5 ng/ml, consumption of the HFD increased leptin secretion from adipocytes (leptin resistance) ***(Figure 3.39)***. This result is consistent with previous research where rats whom consumed a HFD presented with increased leptin levels when compared to rats fed a standard diet (Lozano *et al.*, 2016). In the current study, the increase in leptin levels was expected as these animals presented with increased body weight ***(Figure 3.3)***, IP-fat weight ***(Figure 3.5a-b)*** and blood pressure levels ***(Figure 3.13-3.14)***. The expansion of the adipose tissue most probably increased the production and release of leptin into circulation, consequently activating the renal sympathetic nerve activity to increase the blood pressure. The three mechanisms related to leptin resistance development were not determined in the current study, and therefore no conclusions can be made.

Treatment with Afriplex GRT™ was unable to significantly decrease the elevated leptin levels in the HFD animals. This result is consistent with the unaffected IP-fat weight ***(Figure 3.5a-b)***. Interestingly, these animals presented with reduced blood pressure values ***(Figure 3.15, 3.17-3.18)***, suggesting that blood pressure regulation was not leptin related.

4.6.2. Adiponectin

Adiponectin is the most abundant cytokine secreted by adipocytes and plays an important role in the modulation of lipid and glucose metabolism in insulin sensitive tissues (Chandran *et al.*, 2003).

Adiponectin exerts its actions by increasing autophosphorylation of the insulin receptor in the skeletal muscle (Yamauchi *et al.*, 2001), activating the AMPK pathway in the liver and skeletal muscle (Yamauchi *et al.*, 2002), upregulating genes encoding proteins involved in fatty acid transport and oxidation in the skeletal muscle and downregulating the expression of proteins involved in fatty acid transport in the liver (Yamauchi *et al.*, 2001). Together these actions regulate energy expenditure and glucose and lipid metabolism.

Adiponectin levels are normally decreased in subjects suffering from obesity, insulin resistance, high blood pressure and coronary heart disease. Specifically of interest for the current study,

adiponectin has also been shown to directly stimulate NO production in endothelial cells via the PI3K-dependent pathway involving eNOS and AMPK phosphorylation (Han *et al.*, 2007).
Interestingly, the HFD animals presented with increased circulating adiponectin levels when compared to the age-matched chow fed controls ***(Figure 3.40)***. This result does not correlate with previous research indicating that obesity is associated with decreased adiponectin levels. According to former studies, adiponectin levels are increased in autoimmune and chronic inflammatory diseases which are not necessarily related to obesity. These diseases include type 1 diabetes, chronic heart failure and diastolic heart dysfunction (Iacobellis *et al.*, 2006). It might therefore be that the increase in blood pressure in the HFD animals ***(Figure 3.13-3.14)***, caused diastolic heart dysfunction resulting in increased circulating adiponectin levels. Furthermore, due to the speculated pancreatic β-cell dysfunction in these animals **(*Figure 3.8a*)**, this might also be a reason for the increase in adiponectin levels.

Furthermore, the elevated adiponectin levels correlated with the increased P:T AMPK ratio **(*Figure 3.27*)** in the HFD animals, suggesting that AMPK was most probably activated as a compensatory mechanism to reduce elevated circulating glucose levels, but was unable to activate eNOS **(*Figure 3.30)*** for NO generation.

Treatment with Afriplex GRT™ had no effect on the adiponectin levels, suggesting that the improved glucose clearance ***(Figure 3.8a)*** in both the control and HFD Afriplex GRT™ treated animals was not adiponectin related, but rather involved a different mechanism. The improved vasorelaxation observed in the HFD + Afriplex GRT™ animals ***(Figure 3.22)*** is also not adiponectin related, since adiponectin levels were unaffected by Afriplex GRT™ treatment.

4.6.3. ET-1

ET-1 is a well-known potent endogenous vasoconstrictor, which is released in response to low shear stress or via angiotensin II (Yanagisawa *et al.*, 1988; Hynynen and Khalil, 2006). Binding of ET-1 to the ETA or the ETB_2 receptors elevates intracellular Ca^{2+} (Hynynen and Khalil, 2006; Lima *et al.*, 2011), whereas binding to ETB_1 receptors stimulate NO production (Kedzierski and Yanagisawa, 2001).

Individuals suffering from obesity and the metabolic syndrome present with elevated ET-1 levels and decreased NO levels (Campia *et al.*, 2014), thus suggesting the ETB_2 receptors are upregulated and the ETB_1 receptors are downregulated, consequently resulting in augmented vasoconstriction (Böhm and Pernow, 2007).

No significant differences between the treated and untreated groups were observed in our ET-1 assay ***(Figure 3.42)***. Reduced ACh-induced vasorelaxation in the HFD and increased vasorelaxation in the HFD + Afriplex GRT™ treated animals ***(Figure 3.22)*** can therefore not be linked to ET-1.

4.7. General discussion and conclusion

Obesity, particularly the excess fat accumulated under the skin or around the organs, is a major risk factor for type II diabetes and cardiovascular diseases. As proposed, the HFD used in the current study successfully induced obesity in male Wistar rats. This result is supported by an increase in body weight, leptin levels, IP-fat weight and liver weight. Together these obesity-induced changes resulted in insulin resistance (increased glucose and decreased insulin levels), endothelial dysfunction (decreased endothelium-dependent vasodilation) and hypertension. Furthermore, the HFD downregulated AMPK expression, but interestingly increased AMPK phosphorylation, indicating that the insulin-independent pathway was activated probably as a compensatory mechanism to reduce elevated glucose levels. Adiponectin is a known AMPK stimulator, and therefore elevated adiponectin levels in the HFD animals might have been responsible for AMPK activation. The HFD caused a decrease in PKB activation, suggesting that activation of the insulin-dependent pathway was impaired. Lastly, the HFD upregulated eNOS expression, but decreased its activation and consequently NO production, correlating with the impaired vasodilation in these animals. The decrease in eNOS activation also relates to the decrease in PKB activation, as PKB can directly phosphorylate eNOS.

The novelty of this study laid in determining whether treatment with an unique green rooibos extract, Afriplex GRT™, had the potential to ameliorate obesity-induced hypertension. In this regard, the study had a positive outcome. We herewith propose four possible mechanisms that might have been involved in the anti-hypertensive effects of Afriplex GRT™.

(i) The first speculated mechanism whereby Afriplex GRT™ decreased the blood pressure in the HFD animals was by reducing food intake, body weight, and liver weight. Together these anti-obesogenic effects resulted in improved insulin sensitivity as shown by the increase in glucose clearance and the increase in PKB phosphorylation. Since PKB activation and vascular vasodilation were increased in response to Afriplex GRT™ treatment, we expected an increase in eNOS activation; however, this was not the case. We are therefore not convinced that the anti-obesogenic potential of Afriplex GRT™ is the key mechanism responsible for reduced blood pressure although it may have been partly responsible.

(ii) The second speculated mechanism involved the AMPK insulin-independent pathway. AMPK is known to stimulate fatty acid oxidation, glucose uptake and NO production via eNOS. Treatment with Afriplex GRT™ in the HFD animals had no effect on AMPK expression but did increase AMPK activation. If the same elevated activation of AMPK was also in skeletal muscle, it may have impacted on peripheral glucose utilization and the state of insulin resistance. However, in the aortic tissue with PVAT, activated AMPK was unable to significantly increase eNOS phosphorylation for NO generation. Improved vasodilation was shown in these animals, suggesting that eNOS was activated in response to Afriplex GRT™ treatment, however we are not able to make such a conclusion. Thus, the insulin-independent pathway might have been involved in decreasing lipid accumulation and glucose levels which could have contributed to the anti-hypertensive activity of Afriplex GRT™.

(iii) The third speculated mechanism whereby Afriplex GRT™ could have alleviated hypertension was the possibility of ACE inhibitor activity. According to our FRET analyses, Afriplex GRT™ did not act as an ACE inhibitor. Modulation of the RAS at this level is therefore not associated with the anti-hypertensive actions of Afriplex GRT™.

(iv) The last speculated mechanism is the possibility that Afriplex GRT™ could have acted as a SGLT2 inhibitor in the kidneys. Urine analyses showed that treatment with Afriplex GRT™ increased glucose excretion in the urine of the HFD animals, which suggests SGLT2 inhibition. The suggested inhibition of SGLT2 was most probably responsible for the decrease in body weight and improved glucose clearance (Whaley *et al.*, 2012). In addition, a previous study reported that sodium- glucose co-transporter-1 (SGLT1) inhibition decreased the absorption of glucose over the brush border membrane in the intestine (Gorboulev *et al*., 2012). We therefore speculate that SGLT1 in the digestive system could also have been inhibited via Afriplex GRT™, which in turn, could have decreased the absorption of glucose from the ingested food, consequently contributing to glucose lowering.

Taken together, we suggest that in the HFD animals, treatment with Afriplex GRT™ reduces body weight, consequently improving insulin sensitivity. It also activates the insulin-independent AMPK and insulin-dependent PI3K-dependent pathways, resulting in increased glucose uptake from circulation. Activated AMPK and PKB may result in the activation of eNOS, which may increase NO production and subsequently improve vasodilation. It is furthermore also suggested that Afriplex GRT™ exerts its effects in another insulin-independent manner via the inhibition of SGLT2 in the kidneys. SGLT2 inhibition may have resulted in weight loss and improved glucose clearance. Thus, Afriplex GRT™ exerts its anti-hypertensive effects via insulin-dependent and insulin-independent mechanisms.

Summarized effect of the HFD (indicated in black) and treatment with Afriplex GRT™ (indicated in red) on blood pressure regulation.

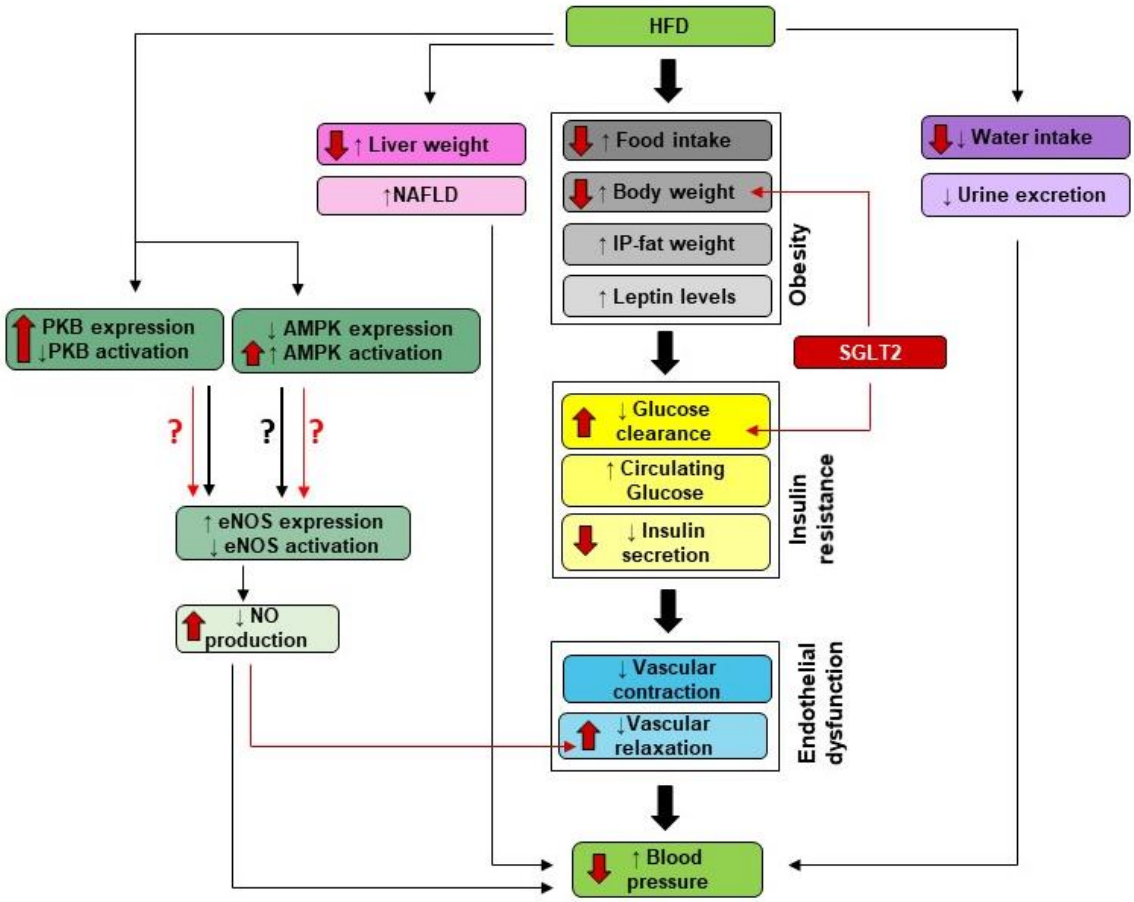

Figure 4.1: *Summarized effect of HFD and Afriplex GRT™ on blood pressure regulation and composed using Microsoft PowerPoint.*

Conclusion: The HFD was coupled to the development of obesity and insulin resistance as these animals presented with increased body weight, liver weight, leptin levels as well as decreased insulin levels and glucose clearance after an oral sucrose bolus. Obesity-induced insulin resistance resulted in a model of hypertension, confirmed by the presence of reduced vascular contraction, vascular relaxation and NO generation. Treatment with Afriplex GRT™ decreased body weight, liver weight, and improved glucose clearance possibly via activation of the insulin-independent (AMPK) and insulin-dependent (PI3K) pathways. In addition, enhanced glucose secretion in the urine indicated SGLT2 inhibition. Lowering of plasma glucose by this route could have resulted in the positive effects on weight gain and glucose homeostasis and consequently blood pressure lowering.

CHAPTER 5: LIMITATIONS AND FUTURE RESEARCH

In the current study, the speculated effects of Afriplex GRT™ to reduce blood pressure switched unexpectedly from RAS inhibition to SGLT2 inhibition; however, we are still unable to confirm this result due to several limitations.

- Firstly, an angiotensin II assay should be performed to confirm the absence of ACE inhibitor activity in Afriplex GRT™ as shown in the FRET analyses. In addition, aldosterone and ET-1 ELISAs should be repeated to confirm that treatment with Afriplex GRT™ did not influenced the RAS system to improve vascular relaxation and alleviate hypertension.

- Since we only used aorta's with PVAT for isometric tension studies and protein expression/activation determination, it would have been of much value to determine the effect of Afriplex GRT™ on aorta's without signalling from the PVAT; however, this would have doubled the number of animals used for experimentation. In addition, *ex vivo* experimentation may be performed on aortic tissue to determine whether the activation of PKB and AMPK in response to Afriplex GRT™ does increase NO production via eNOS. This can be done using various inhibitors of PKB, AMPK as well as eNOS.

- The inhibition of SGLT2 in the kidneys in response to treatment with Afriplex GRT™ should be investigated using SGLT2 knockout animals.

- One of the major limitations of the current study was the inability of the well-known ACE inhibitor, Captopril, to lower blood pressure. We speculate that this result could have been due to not using freshly-ordered Captopril stock for experimentation.

- Since the consumption of herbal teas are closely associated with liver toxicity, livers should be assessed to determine whether Afriplex GRT™ caused liver toxicity, although the observed changes in liver weight does not argue for this. In addition, livers and serum should be analysed for HDL, LDL, triglycerides, very low-density lipoprotein (VLDL) and total cholesterol levels to determine the antioxidant potential of Afriplex GRT™ on these lipoproteins and the associated cardiovascular benefits.

- Kidneys should be assessed for increased renal compression in response to the consumption of the HFD, and to determine whether Afriplex GRT™ can alleviate renal compression, and consequently blood pressure.

- Since AEC experiments were limited to healthy endothelial cells, it was not representative of the HFD animals. We are specifically interested in the effect of Afriplex GRT™ on HFD animals, and therefore an obesogenic AEC model will be of good value. Cell density was not physically determined before seeding and protein content was not determined after experimentation, which is another limitation of the current study since these are important parameters for normalising the data obtained.

- The n-value of the HOMA-IR, KCl-contraction and SNP-relaxation studies should be enlarged for consistency in the results.

- Antioxidant enzymes such as SOD and CAT should be measured in response to treatment with Afriplex GRT™.

- The antioxidant effects of Afriplex GRT™ in the kidneys, aorta and pancreas should be determined.

OUTPUTS DURING THE COURSE OF THE STUDY (2016-2018):

Presentations:

- University of Stellenbosch Academic Year Day 2016.
- Biomedical Science Year Day 2017 and won the second price in the poster presentation section.

Publications:

- I completed a one draft academic publication as first author, and one as co-author, which awaits acceptance.
- The following article (where I was a co-author), was recently published online: ‘Revisiting the Cardiotoxic effect of Chloroquine’ (Blignaut *et al.*, 2019).

REFERENCES

Achan, V. *et al.* (2003) 'Asymmetric Dimethylarginine Causes Hypertension and Cardiac Dysfunction in Humans and Is Actively Metabolized by Dimethylarginine Dimethylaminohydrolase', *Arteriosclerosis, Thrombosis, and Vascular Biology*, 23(8), pp. 1455–1459.

Adams, L. A. *et al.* (2005) 'The natural history of nonalcoholic fatty liver disease: a population-based cohort study.', *Gastroenterology*, 129(1), pp. 113–121.

Ailhaud, G. (1999) 'Cross Talk between Adipocytes and Their Precursors: Relationships with Adipose Tissue Development and Blood Pressure', *Annals of the New York Academy of Sciences*. Wiley/Blackwell (10.1111), 892, pp. 127–133.

Ailhaud, G. *et al.* (2000) 'Angiotensinogen, angiotensin II and adipose tissue development.', *International Journal of Obesity and related metabolic disorders : Journal of the International Association for the Study of Obesity*, 24(Suppl 4), pp. S33–S35.

Alderton, W. K., Cooper, C. E. and Knowles, R. G. (2001) 'Nitric oxide synthases: structure, function and inhibition.', *The Biochemical Journal*, 357(Pt 3), pp. 593–615.

Alessi, D. R. *et al.* (1996) 'Mechanism of activation of protein kinase B by insulin and IGF-1.', *The EMBO journal*. European Molecular Biology Organization, 15(23), pp. 6541–6551.

Alheid, U., Frölich, J. C. and Förstermann, U. (1987) 'Endothelium-derived relaxing factor from cultured human endothelial cells inhibits aggregation of human platelets.', *Thrombosis Research*, 47(5), pp. 561–571.

Aljada, A. *et al.* (2000) 'Insulin Inhibits the Expression of Intercellular Adhesion Molecule-1 by Human Aortic Endothelial Cells through Stimulation of Nitric Oxide [1]', *The Journal of Clinical Endocrinology & Metabolism*, 85(7), pp. 2572–2575.

Almeida, A. P. *et al.* (2000) 'Angiotensin-(1-7) potentiates the coronary vasodilatatory effect of bradykinin in the isolated rat heart.', *Brazilian Journal of Medical and Biological Research*, 33(6), pp. 709–713.

AlphaLaboratories (2018) *Double Staining Calcein-AM Propidium Iodide Kit Cell Analysis Simultaneous Viable and Dead Cell Stain Cellstain® Dojindo Laboratories Wako - Research Reagents*. Available at: https://www.alphalabs.co.uk/341-07381.

American Diabetes Association (2014) *Diagnosing Diabetes and Learning About Prediabetes: American Diabetes Association®*. Available at: http://www.diabetes.org/are-you-at-risk/prediabetes/.

American Diabetes Association (2018) *When does glucose spilling (glucosuria) occur? | Diabetes Complications - Sharecare*. Available at: https://www.sharecare.com/health/diabetes-complications/when-does-glucose-spilling-glucosuria-occur.

American Heart Association (2017) *Understanding Blood Pressure*, *American Heart Association*. Available at: http://www.heart.org/HEARTORG/Conditions/HighBloodPressure/KnowYourNumbers/Understanding-Blood-Pressure-Readings.

Anai, M. *et al.* (1998) 'Different subcellular distribution and regulation of expression of insulin receptor substrate (IRS)-3 from those of IRS-1 and IRS-2.', *The Journal of Biological Chemistry*. American Society for Biochemistry and Molecular Biology, 273(45), pp. 29686–92.

Anderson, T. J. *et al.* (1995) 'Systemic nature of endothelial dysfunction in atherosclerosis.', *The American Journal of Cardiology*, 75(6), p. 71B–74B.

Anderson, T. J. (1999) 'Assessment and treatment of endothelial dysfunction in humans.', *Journal of the American College of Cardiology*, 34(3), pp. 631–638.

Andrews, A. M. *et al.* (2010) 'Direct, real-time measurement of shear stress-induced nitric oxide produced from endothelial cells in vitro', *Nitric Oxide*, 23(4), pp. 335–342.

Angiotensinogen | definition of angiotensinogen by Medical dictionary (2012) *Segen's Medical Dictionary*. Available at: https://medical-dictionary.thefreedictionary.com/angiotensinogen.

Appeldoorn, M. M. *et al.* (2009) 'Some Phenolic Compounds Increase the Nitric Oxide Level in Endothelial Cells in Vitro', *Journal of Agricultural and Food Chemistry*, 57(17), pp. 7693–7699.

Arndt, H., Smith, C. W. and Granger, D. N. (1993) 'Leukocyte-endothelial cell adhesion in spontaneously hypertensive and normotensive rats', *Hypertension*, 21(5), pp. 667–673.

Arner, P. and Spalding, K. L. (2010) 'Fat cell turnover in humans', *Biochemical and Biophysical Research Communications*, 396(1), pp. 101–104.

Arts, I. C. *et al.* (2001) 'Dietary catechins in relation to coronary heart disease death among postmenopausal women.', *Epidemiology*, 12(6), pp. 668–675.

Arts, I. C. and Hollman, P. C. (2005) 'Polyphenols and disease risk in epidemiologic studies', *The American Journal of Clinical Nutrition*, 81(1), p. 317S–325S.

Ayeleso, A., Brooks, N. and Oguntibeju, O. (2014) 'Modulation of antioxidant status in streptozotocin-induced diabetic male wistar rats following intake of red palm oil and/or rooibos', *Asian Pacific Journal of Tropical Medicine*, 7(7), pp. 536–544.

Bae, S. W. *et al.* (2003) 'Rapid increase in endothelial nitric oxide production by bradykinin is mediated by protein kinase A signaling pathway', *Biochemical and Biophysical Research Communications*. Academic Press, 306(4), pp. 981–987.

Bagchi, K. and Puri, S. (1998) 'Free radicals and antioxidants in health and disease', *Eastern Mediterranean Health Journal*, 4(2), pp. 350–360.

Baleta, A. and Mitchell, F. (2014) 'Diabetes and Obesity in South Africa.', *The Lancet Diabetes Endocrinol.*, 2(9), pp. 687–688.

Bansal, N. (2015) *What is the mechanism behind reduction of proteinuria by ACE inhibitors? - Quora*. Available at: https://www.quora.com/What-is-the-mechanism-behind-reduction-of-proteinuria-by-ACE-inhibitors-1.

Baskurt, O. K., Yalcin, O. and Meiselman, H. J. (2004) 'Hemorheology and vascular control mechanisms.', *Clinical Hemorheology and Microcirculation*, 30(3–4), pp. 169–178.

Bazzoni, G. and Dejana, E. (2004) 'Endothelial Cell-to-Cell Junctions: Molecular Organization and Role in Vascular Homeostasis', *Physiological Reviews*, 84(3), pp. 869–901.

Beckman, C. H. (2000) 'Phenolic-storing cells: keys to programmed cell death and periderm formation in wilt disease resistance and in general defence responses in plants?', *Physiological and Molecular Plant Pathology*. Academic Press, 57(3), pp. 101–110.

Beelders, T. (2011) 'HPLC method development for the characterisation of the flavonoid and phenolic acid composition of Rooibos (Aspalathus Linearis) infusions', MSc Thesis(December), pp. 1–50.

Bennett, M. R., Sinha, S. and Owens, G. K. (2016) 'Vascular Smooth Muscle Cells in Atherosclerosis', *Circulation Research*, 118(4), pp. 692–702.

Berger, S. and Polotsky, V. Y. (2018) 'Leptin and Leptin Resistance in the Pathogenesis of Obstructive Sleep Apnea: A Possible Link to Oxidative Stress and Cardiovascular Complications', *Oxidative Medicine and Cellular Longevity*. Hindawi, 2018, pp. 1–8.

Bergheanu, S. C., Bodde, M. C. and Jukema, J. W. (2017) 'Pathophysiology and treatment of atherosclerosis', *Netherlands Heart Journal*. Bohn Stafleu van Loghum, 25(4), pp. 231–242.

Bertrand, L. *et al.* (2008) 'Insulin signalling in the heart', *European Society of Cardiology*, 79, pp. 238–245.

Beta-Blockers: Function and Effects | MU Science Blog (2010). Available at: https://marianuniversityscienceblog.wordpress.com/2010/10/15/beta-blockers-function-and-effects/.

Bevan, P. (2001) 'Insulin signalling', *Journal of Cell Science*, 114(8), pp. 1429–1430.

Bindom, S. M. *et al.* (2010) 'Angiotensin I-converting enzyme type 2 (ACE2) gene therapy improves glycemic control in diabetic mice.', *Diabetes*. American Diabetes Association, 59(10), pp. 2540–2548.

Blignaut, M. *et al.* (2019) 'Revisiting the Cardiotoxic Effect of Chloroquine', *Cardiovascular Drugs and Therapy*.

Bloomgarden, Z. T. (2006) 'Third Annual World Congress on the Insulin Resistance Syndrome: associated conditions.', *Diabetes care*, 29(9), pp. 2165–2174.

Boden, G. (2008) 'Obesity and free fatty acids.', *Endocrinology and Metabolism Clinics of North America*. NIH Public Access, 37(3), pp. 635–639.

Böhm, F. and Pernow, J. (2007) 'The importance of endothelin-1 for vascular dysfunction in cardiovascular disease', *Cardiovascular Research*, 76(1), pp. 8–18.

Bonetti, P. O., Lerman, L. O. and Lerman, A. (2003) 'Endothelial dysfunction: a marker of atherosclerotic risk.', *Arteriosclerosis, Thrombosis, and Vascular Biology*, 23(2), pp. 168–175.

Bonner, C. *et al.* (2015) 'Inhibition of the glucose transporter SGLT2 with dapagliflozin in pancreatic alpha cells triggers glucagon secretion', *Nature Medicine*, 21(5), pp. 512–517.

Boo, Y. C., Sorescu, G., *et al.* (2002) 'Shear Stress Stimulates Phosphorylation of Endothelial Nitric-oxide Synthase at Ser ^{1179} by Akt-independent Mechanisms', *Journal of Biological Chemistry*, 277(5), pp. 3388–3396.

Boo, Y. C., Hwang, J., *et al.* (2002) 'Shear stress stimulates phosphorylation of eNOS at Ser ^{635} by a protein kinase A-dependent mechanism', *American Journal of Physiology-Heart and Circulatory Physiology*, 283(5), pp. H1819–H1828.

Booth, R. E., Johnson, J. P. and Stockand, J. D. (2002) 'Aldosterone', *Advances in Physiology Education*, 26(1), pp. 8–20.

Borggreve, S. E., de Vries, R. and Dullaart, R. P. F. (2003) 'Alterations in high-density lipoprotein metabolism and reverse cholesterol transport in insulin resistance and type 2 diabetes mellitus: role of lipolytic enzymes, lecithin:cholesterol acyltransferase and lipid transfer proteins', *European Journal of Clinical Investigation*. Blackwell Publishing Ltd., 33(12), pp. 1051–1069.

Bozulic, L. and Hemmings, B. A. (2009) 'PIKKing on PKB: regulation of PKB activity by phosphorylation', *Current Opinion in Cell Biology*, 21(2), pp. 256–261.

Bradford, M. M. (1976) 'A rapid and sensitive method for the quantitation of microgram quantities of protein utilizing the principle of protein-dye binding.', *Analytical Biochemistry*, 72, pp. 248–254.

Bratanova-Tochkova, T. *et al.* (2002) 'Triggering and augmentation mechanisms, granule pools, and biphasic insulin secretion.', *Diabetes*, 51(Suppl 1), pp. S83–S90.

Brotman, D. J. (2002) 'Effects of counterregulatory hormones in a high-glycemic index diet.', *JAMA*, 288(6), p. 695.

Broyles, S. T. *et al.* (2015) 'The epidemiological transition and the global childhood obesity epidemic.', *International Journal of Obesity Supplements*. Nature Publishing Group, 5(Suppl 2), pp. S3–S8.

Burks, D. J. and White, M. F. (2001) 'IRS proteins and beta-cell function.', *Diabetes*, 50(Suppl 1), pp. S140–S145.

Cacicedo, J. M. *et al.* (2004) 'AMPK inhibits fatty acid-induced increases in NF-κB transactivation in cultured human umbilical vein endothelial cells', *Biochemical and Biophysical Research Communications*, 324(4), pp. 1204–1209. doi: 10.1016/j.bbrc.2004.09.177.

Cai, H. and Harrison, D. G. (2000) 'Endothelial dysfunction in cardiovascular diseases: The role of oxidant stress', *Circulation Research*, 87(10), pp. 840–844.

Campia, U. *et al.* (2014) 'The vascular endothelin system in obesity and type 2 diabetes: Pathophysiology and therapeutic implications', *Life Sciences*, 118(2), pp. 149–155.

Canda, B. D., Oguntibeju, O. O. and Marnewick, J. L. (2014) 'Effects of consumption of rooibos (Aspalathus linearis) and a rooibos-derived commercial supplement on hepatic tissue injury by tert -butyl hydroperoxide in wistar rats', *Oxidative Medicine and Cellular Longevity*. Hindawi Publishing Corporation, 2014, p. 716832.

Canner, D. *et al.* (2013) *The Structure of PI3K*, *Proteopedia*. Available at: http://proteopedia.org/wiki/index.php/The_Structure_of_PI3K.

Carling, D., Zammit, V. A. and Hardie, D. G. (1987) 'A common bicyclic protein kinase cascade inactivates the regulatory enzymes of fatty acid and cholesterol biosynthesis.', *FEBS letters*, 223(2), pp. 217–222.

Carmona, A. K. *et al.* (2006) 'A continuous fluorescence resonance energy transfer angiotensin I-converting enzyme assay', *Nature Protocols*, 1(4), pp. 1971–1976.

Cassis, L. A. *et al.* (2004) 'Differential Effects of Local *Versus* Systemic Angiotensin II in the Regulation of Leptin Release from Adipocytes', *Endocrinology*, 145(1), pp. 169–174.

Cazzolli, R. *et al.* (2001) 'A role for protein phosphatase 2A-like activity, but not atypical protein kinase Czeta, in the inhibition of protein kinase B/Akt and glycogen synthesis by palmitate.', *Diabetes*, 50(10), pp. 2210–2218.

Chandran, M. *et al.* (2003) 'Adiponectin: More Than Just Another Fat Cell Hormone?', *Diabetes Care*. American Diabetes Association, 26(8), pp. 2442–2450.

Cheeseman, K. H. and Slater, T. F. (1993) 'An introduction to free radical biochemistry.', *British Medical Bulletin*, 49(3), pp. 481–493.

Chen, Z. *et al.* (2009) 'AMP-Activated Protein Kinase Functionally Phosphorylates Endothelial Nitric Oxide Synthase Ser633', *Circulation Research*, 104(4), pp. 496–505.

Chen, Z. P. *et al.* (1999) 'AMP-activated protein kinase phosphorylation of endothelial NO synthase.', *FEBS letters*, 443(3), pp. 285–9.

Chiang, S.-H. *et al.* (2001) 'Insulin-stimulated GLUT4 translocation requires the CAP-dependent activation of TC10', *Nature*, 410(6831), pp. 944–948.

Cho, J. and Park, J. (2008) 'Contribution of Natural Inhibitors to the Understanding of the PI3K/PDK1/PKB Pathway in the Insulin-mediated Intracellular Signaling Cascade', *International Journal of Molecular Sciences*. Molecular Diversity Preservation International, 9(11), pp. 2217–2230.

Chobanian, A. V. *et al.* (2003) 'Seventh Report of the Joint National Committee on Prevention, Detection, Evaluation, and Treatment of High Blood Pressure', *Hypertension*, 42(6), pp. 1206–1252.

Choi, I. *et al.* (2006) 'Anti-adipogenic activity of rutin in 3T3-L1 cells and mice fed with high-fat diet', *BioFactors*. Wiley-Blackwell, 26(4), pp. 273–281.

Choo, C. Y. *et al.* (2012) 'Vitexin and isovitexin from the Leaves of Ficus deltoidea with in-vivo α-glucosidase inhibition', *Journal of Ethnopharmacology*, 142(3), pp. 776–781.

Chung, K.-T. *et al.* (1998) 'Tannins and Human Health: A Review', *Critical Reviews in Food Science and Nutrition*, 38(6), pp. 421–464.

Cogolludo, A. L. *et al.* (2001) 'Mechanisms involved in SNP-induced relaxation and [Ca+]i reduction in piglet pulmonary and systemic arteries.', *British Journal of Pharmacology*. Wiley-Blackwell, 132(4), pp. 959–967.

Cooke, J. P. (2002) 'Nitric Oxide and Angiogenesis', *Circulation*, 105(18), pp. 2133–2135.

Coppo, R. and Amore, A. (2000) 'Importance of the bradykinin–nitric oxide synthase system in the hypersensitivity reactions of chronic haemodialysis patients', *Nephrology Dialysis Transplantation*. Oxford University Press, 15(9), pp. 1288–1290.

Corder, R. *et al.* (2001) 'Health: Endothelin-1 synthesis reduced by red wine', *Nature*, 414(6866), pp. 863–864.

Cornier, M.-A. *et al.* (2008) 'The Metabolic Syndrome', *Endocrine Reviews*. Oxford University Press, 29(7), pp. 777–822.

Csako, G. and Elin, R. J. (1993) 'Unrecognized False-Positive Ketones From Drugs Containing Free-Sulfhydryl Group(s)', *JAMA: The Journal of the American Medical Association*. American Medical Association, 269(13), p. 1634.

Cushman, D. and Ondetti, M. (1980) 'Inhibitors of angiotensin-converting enzyme.', *Progress in Medicinal Chemistry.*, 17, pp. 42–104.

Czech, M. P. *et al.* (2013) 'Insulin signalling mechanisms for triacylglycerol storage.', *Diabetologia*. NIH Public Access, 56(5), pp. 949–964.

Danser, A. H., Batenburg, W. W. and van Esch, J. H. M. (2007) 'Prorenin and the (pro)renin receptor--an update', *Nephrology Dialysis Transplantation*. Oxford University Press, 22(5), pp. 1288–1292.

Danser, A. H. J. *et al.* (1989) 'Renin, Prorenin, and Immunoreactive Renin in Vitreous Fluid From Eyes With and Without Diabetic Retinopathy', *The Journal of Clinical Endocrinology & Metabolism*, 68(1), pp. 160–167.

Danser, A. H. J. and Deinum, J. (2005) 'Renin, Prorenin and the Putative (Pro)renin Receptor', *Hypertension*, 46(5), pp. 1069–1076.

Davidson, S. M. and Duchen, M. R. (2007) 'Endothelial Mitochondria: Contributing to Vascular Function and Disease', *Circulation Research*, 100(8), pp. 1128–1141.

Davis, B. J. *et al.* (2006) 'Activation of the AMP-activated kinase by antidiabetes drug metformin stimulates nitric oxide synthesis in vivo by promoting the association of heat shock protein 90 and endothelial nitric oxide synthase.', *Diabetes*, 55(2), pp. 496–505.

Dearth, R. K. *et al.* (2007) 'Oncogenic Transformation by the Signaling Adaptor Proteins Insulin Receptor Substrate (IRS)-1 and IRS-2', *Cell Cycle*, 6(6), pp. 705–713.

DeFronzo, R. A. (2004) 'Dysfunctional fat cells, lipotoxicity and type 2 diabetes.', *International Journal of Clinical Practice.*, (143), pp. 9–21.

de Gasparo, M. *et al.* (2000) 'International union of pharmacology. XXIII. The angiotensin II receptors.', *Pharmacological Reviews*, 52(3), pp. 415–472.

de Groot, H. and Rauen, U. (1998) 'Tissue injury by reactive oxygen species and the protective effects of flavonoids.', *Fundamental & Clinical Pharmacology*, 12(3), pp. 249–255.

Denton, R. and Tavaré, J. (1997) 'Molecular basis of insulin action on intracellular metabolism.', in *International Textbook of Diabetes Mellitus (2nd ed) John Wiley & Sons, New York.*, pp. 469–488.

Deprez, J. *et al.* (2000) 'Partial purification and characterization of a wortmannin-sensitive and insulin-stimulated protein kinase that activates heart 6-phosphofructo-2-kinase.', *The Biochemical Journal*. Portland Press Ltd, 347(Pt 1), pp. 305–312.

Desch, S. *et al.* (2010) 'Effect of Cocoa Products on Blood Pressure: Systematic Review and Meta-Analysis', *American Journal of Hypertension*, 23(1), pp. 97–103.

DeWeerdt, S. (2017) 'Disease progression: Divergent paths', *Nature*, 551(7681).

Diabetes, Heart Disease, and Stroke | *NIDDK* (2017). Available at: https://www.niddk.nih.gov/health-information/diabetes/overview/preventing-problems/heart-disease-stroke.

Dimmeler, S. *et al.* (1999) 'Activation of nitric oxide synthase in endothelial cells by Akt-dependent phosphorylation', *Nature*, 399(6736), pp. 601–605.

Dimmeler, S. and Zeiher, A. M. (1999) 'Nitric oxide–an endothelial cell survival factor', *Cell Death & Differentiation*, 6(10), pp. 964–968.

Dinitto, J. and Lambright, D. (2006) 'Membrane and juxtamembrane targeting by PH and PTB domains', *Biochimica et Biophysica Acta (BBA) - Molecular and Cell Biology of Lipids*, 1761(8), pp. 850–867.

de Dios, S. T., Sobey, C. G. and Drummond, G. R. (2010) 'Oxidative stress and endothelial dysfunction', in *Endothelial Dysfunction and Inflammation*. Springer Basel, pp. 37–64.

Duckitt, K. and Harrington, D. (2005) 'Risk factors for pre-eclampsia at antenatal booking: systematic review of controlled studies', *BMJ*, 330(7491), p. 565.

Dyck, D. J., Steinberg, G. and Bonen, A. (2001) 'Insulin increases FA uptake and esterification but reduces lipid utilization in isolated contracting muscle', *American Journal of Physiology-Endocrinology and Metabolism*, 281(3), pp. E600–E607.

Dzau, V., Burt, D. and Pratt, R. (1988) 'Molecular biology of the renin-angiotensin system.', *American Journal of Physiology*, 255(4 Pt 2), pp. F563–F573.

Eghoghosoa, A. R. *et al.* (2010) 'Effect of Angiotensin I-Converting Enzyme Inhibitor, Captopril on Body Weight, Food and Water Consumption in Oral Contraceptive-Treated Rats', *Research Journal of Medical Sciences*, 4(3), pp. 166–169.

Ehlers, M. R. W. *et al.* (2012) 'Shedding the load of hypertension: The proteolytic processing of angiotensin-converting enzyme', *South African medical journal*. Medical Association of South Africa, 102(6), pp. 461–464.

Ehlers, M. and Riordan, J. (1990) 'Angiotensin-converting enzyme: Biochemistry and molecular Biology.', *Hypertension Pathophysiology, Diagnosis and Management*, pp. 1217–1231.

Ehrhart-Bornstein, M. *et al.* (2003) 'Human adipocytes secrete mineralocorticoid-releasing factors.', *Proceedings of the National Academy of Sciences of the United States of America*. National Academy of Sciences, 100(24), pp. 14211–14216.

Elfont, R. M., Epstein, A. N. and Fitzsimons, J. T. (1984) 'Involvement of the renin-angiotensin system in captopril-induced sodium appetite in the rat.', *The Journal of Physiology*. Wiley/Blackwell (10.1111), 354(1), pp. 11–27.

Endo, T. *et al.* (1992) 'Regulation of endothelin-1 synthesis in cultured guinea pig airway epithelial cells by various cytokines.', *Biochemical and Biophysical Research Communications*, 186(3), pp. 1594–1599.

Erlund, I. *et al.* (2008) 'Favorable effects of berry consumption on platelet function, blood pressure, and HDL cholesterol', *The American Journal of Clinical Nutrition*, 87(2), pp. 323–331.

Evans, A. M. *et al.* (2005) 'Does AMP-activated protein kinase couple inhibition of mitochondrial oxidative phosphorylation by hypoxia to calcium signaling in O2-sensing cells?', *The Journal of Biological Chemistry*. American Society for Biochemistry and Molecular Biology, 280(50), pp. 41504–41511.

Fabbrini, E., Sullivan, S. and Klein, S. (2010) 'Obesity and Nonalcoholic Fatty Liver Disease: Biochemical, Metabolic and Clinical Implications', *Hepatology (Baltimore, Md.)*. NIH Public Access, 51(2), p. 679.

Facchinetti, V. *et al.* (2008) 'The mammalian target of rapamycin complex 2 controls folding and stability of Akt and protein kinase C', *The EMBO Journal*, 27(14), pp. 1932–1943.

Fallo, F., Maragno, I. and Mantero, F. (1985) 'Resistance to captopril in hypertension of coarctation of the aorta', *International Journal of Cardiology*. Elsevier, 9(1), pp. 111–113.

Fan, L. . *et al.* (2009) 'α1D- adrenergic receptor in sensitivity is associated with alterations in its expression and distribution in cultured vascular myocytes.', *Acta Pharmacologica Sinica*, 30(12), pp. 1585–1590.

Fantin, V. R. *et al.* (1999) 'Cloning, Tissue Expression, and Chromosomal Location of the Mouse Insulin Receptor Substrate 4 Gene [1]', *Endocrinology*. Oxford University Press, 140(3), pp. 1329–1337.

Fernandes, A. A. H. *et al.* (2010) 'Influence of rutin treatment on biochemical alterations in experimental diabetes', *Biomedicine & Pharmacotherapy*, 64(3), pp. 214–219.

Fernández-Alfonso, M. S. *et al.* (2013) 'Mechanisms of perivascular adipose tissue dysfunction in obesity.', *International Journal of Endocrinology*. Hindawi, 2013, p. 402053.

Fernández-Alfonso, M. S., Gil-Ortega, M. and Somoza, B. (2009) 'Role of Perivascular Adipose Tissue in Vascular Function', in *Advances in Vascular Medicine*. London: Springer London, pp. 175–186.

Ferrario, C. M. and Schiavone, M. T. (1989) 'The renin angiotensin system: importance in physiology and pathology', *Cleveland Clinic Journal of Medicine*, 56, pp. 439–446.

Ferreira, D. *et al.* (1995) 'Rooibos tea as a likely health food supplement.', *Fundamental Foods for Health*, pp. 77–88.

Ferrets (2014) 'Rabbits and Rodents', in *Quesenberry and Carpenter*. 2nd Editio.

Fésüs, G. *et al.* (2007) 'Adiponectin is a novel humoral vasodilator', *Cardiovascular Research*, 75(4), pp. 719–727.

Fielding, C. J. and Fielding, P. E. (1995) 'Molecular physiology of reverse cholesterol transport.', *Journal of Lipid Research*. American Society for Biochemistry and Molecular Biology, 36(2), pp. 211–228.

Fitzpatrick, D. F. *et al.* (1995) 'Endothelium-dependent vasorelaxation caused by various plant extracts.', *Journal of Cardiovascular P45harmacology*, 26(1), pp. 90–95.

Fleming, I. and Busse, R. (2003) 'Molecular mechanisms involved in the regulation of the endothelial nitric oxide synthase', *American Journal of Physiology-Regulatory, Integrative and Comparative Physiology*, 284(1), pp. R1–R12.

Foëx, P. and Sear, J. (2004) 'Hypertension: pathophysiology and treatment', *Continuing Education in Anaesthesia Critical Care & Pain*. Oxford University Press, 4(3), pp. 71–75.

Forslund, T., Kouvonen, I. and Fyhrquist, F. (1984) 'Tissue distribution of angiotensin converting enzyme in the rat: effect of captopril treatment.', *Acta Pharmacologica et Toxicologica*, 54(2), pp. 124–128.

Förstermann, U. *et al.* (1986) 'Stimulation of soluble guanylate cyclase by an acetylcholine-induced endothelium-derived factor from rabbit and canine arteries', *Circulation Research*, 58(4), pp. 531–538.

Förstermann, U. (2008) 'Oxidative stress in vascular disease: causes, defense mechanisms and potential therapies', *Nature Clinical Practice Cardiovascular Medicine*, 5(6), pp. 338–349.

Förstermann, U. and Münzel, T. (2006) 'Endothelial Nitric Oxide Synthase in Vascular Disease: From Marvel to Menace', *Circulation*, 113(13), pp. 1708–1714.

Förstermann, U. and Sessa, W. C. (2012) 'Nitric oxide synthases: regulation and function.', *European Heart Journal*. Oxford University Press, 33(7), pp. 829–837.

Fraga, C. G. *et al.* (2010) 'Basic biochemical mechanisms behind the health benefits of polyphenols', *Molecular Aspects of Medicine*, 31(6), pp. 435–445.

Freedman, J. E. *et al.* (2001) 'Select flavonoids and whole juice from purple grapes inhibit platelet function and enhance nitric oxide release.', *Circulation*, 103(23), pp. 2792–2798.

Fridovich, I. (1975) 'Superoxide Dismutases', *Annual Review of Biochemistry*, 44(1), pp. 147–159.

Fuchs, S. *et al.* (2008) 'Angiotensin-Converting Enzyme C-Terminal Catalytic Domain Is the Main Site of Angiotensin I Cleavage In Vivo', *Hypertension*, 51(2), pp. 267–274.

Fuentes, R. *et al.* (2000) 'Hypertension in developing economies: a review of population-based studies carried out from 1980 to 1998.', *Journal of Hypertension*, 18(5), pp. 521–529.

Fukasawa, R., Kanda, A. and Hara, S. (2009) 'Anti-oxidative Effects of Rooibos Tea Extract on Autoxidation and Thermal Oxidation of Lipids', *Journal of Oleo Science*. Japan Oil Chemists' Society, 58(6), pp. 275–283.

Gallagher, S. (2005) 'The Challenges of Obesity and Skin Integrity', *Nursing Clinics of North America*, 40(2), pp. 325–335.

Gálvez-Prieto, B. *et al.* (2012) 'Anticontractile Effect of Perivascular Adipose Tissue and Leptin are Reduced in Hypertension', *Frontiers in Pharmacology*, 3, p. 103.

Gao, T., Furnari, F. and Newton, A. C. (2005) 'PHLPP: A Phosphatase that Directly Dephosphorylates Akt, Promotes Apoptosis, and Suppresses Tumor Growth', *Molecular Cell*. Cell Press, 18(1), pp. 13–24.

Gao, Y. J. *et al.* (2006) 'Perivascular adipose tissue promotes vasoconstriction: the role of superoxide anion', *Cardiovasc Res*, 71(2), pp. 363–373.

Gardiner, S. M. and Bennett, T. (1983) 'The effects of captopril on blood pressure, urinary water and electrolyte excretion and drinking behaviour in Brattleboro rats.', *Clinical Science*, 65(6), pp. 589–597.

Garg, U. C. and Hassid, A. (1989) 'Nitric oxide-generating vasodilators and 8-bromo-cyclic guanosine monophosphate inhibit mitogenesis and proliferation of cultured rat vascular smooth muscle cells.', *The Journal of Clinical Ivestigation*. American Society for Clinical Investigation, 83(5), pp. 1774–1777.

Garrow, J. S. (1988) 'Obesity and related diseases.', *London: Churchill Livingstone*, pp. 1–16.

Gauthier, K. M., Cepura, C. J. and Campbell, W. B. (2013) 'ACE inhibition enhances bradykinin relaxations through nitric oxide and B1 receptor activation in bovine coronary arteries.', *Biological Chemistry*. NIH Public Access, 394(9), pp. 1205–1212.

Gelderblom, W. C. A. *et al.* (2017) 'Rooibos (Aspalathus linearis), honeybush (Cyclopia intermedia) and cancer bush (Sutherlandia frutescens subsp. microphylla) protect against tobacco-specific mutagenesis in vitro', *South African Journal of Botany*, 110, pp. 194–200.

Ghezzi, A. *et al.* (2012) 'Metabolic syndrome markers in wistar rats of different ages', *Diabetology & Metabolic Syndrome*. BioMed Central, 4(1), p. 16.

Giese, N. (2009) *Cell pathway on overdrive prevents cancer response to dietary restriction*. PhysOrg.com. Available at: http://www.physorg.com/news.

Gil-Ortega, M. *et al.* (2010) 'Adaptative Nitric Oxide Overproduction in Perivascular Adipose Tissue during Early Diet-Induced Obesity', *Endocrinology*. Oxford University Press, 151(7), pp. 3299–3306.

Giles, T. D. *et al.* (2005) 'Expanding the definition and classification of hypertension.', *Journal of Cinical Hypertension*, 7(9), pp. 505–512.

Giles, T. D. *et al.* (2009) 'Definition and Classification of Hypertension: An Update', *The Journal of Clinical Hypertension*. Wiley/Blackwell (10.1111), 11(11), pp. 611–614.

Giorgino, F., Laviola, L. and Eriksson, J. W. (2005) 'Regional differences of insulin action in adipose tissue: insights from in vivo and in vitro studies', *Acta Physiologica Scandinavica*, 183(1), pp. 13–30.

Giovannone, B. *et al.* (2000) 'Insulin receptor substrate (IRS) transduction system: distinct and overlapping signaling potential.', *Diabetes/metabolism research and reviews*, 16(6), pp. 434–41.

Godsland, I. F. (2009) 'Insulin resistance and hyperinsulinaemia in the development and progression of cancer.', *Clinical science (London, England : 1979)*. Portland Press Limited, 118(5), pp. 315–32.

Goedecke, J. H., Jennings, C. L. and Lambert, E. V. (2006) 'Obesity in South Africa. Chronic Diseases of Lifestyle in South Africa since 1995-2002.', in *Medical Research Council*, pp. 65–79.

Gollasch, M. and Dubrovska, G. (2004) 'Paracrine role for periadventitial adipose tissue in the regulation of arterial tone', *Trends in Pharmacological Sciences*, 25(12), pp. 647–653.

Gómez-Olivé, F. X. *et al.* (2013) 'Self-reported health and health care use in an ageing population in the Agincourt sub-district of rural South Africa.', *Global health action*. Taylor & Francis, 6, p. 19305.

Gomez, R. *et al.* (1990) 'Molecular biology of the renal renin-angiotensin system.', *Kidney International Supplement*, 38, pp. S18–S23.

Goodfriend, T. L. *et al.* (2004) 'Epoxy-Keto Derivative of Linoleic Acid Stimulates Aldosterone Secretion', *Hypertension*, 43(2), pp. 358–363.

Goodfriend, T. L. (2006) 'Aldosterone - A Hormone of Cardiovascular Adaptation and Maladaptation', *The Journal of Clinical Hypertension*. Wiley/Blackwell (10.1111), 8(2), pp. 133–139.

Goodfriend, T. L. and Calhoun, D. A. (2004) 'Resistant Hypertension, Obesity, Sleep Apnea, and Aldosterone: Theory and Therapy', *Hypertension*, 43(3), pp. 518–524.

Goodman, M. N. *et al.* (1983) 'Glucose uptake and insulin sensitivity in rat muscle: changes during 3-96 weeks of age', *American Journal of Physiology-Endocrinology and Metabolism*, 244(1), pp. E93–E100.

Graf, B. A., Milbury, P. E. and Blumberg, J. B. (2005) 'Flavonols, Flavones, Flavanones, and Human Health: Epidemiological Evidence', *Journal of Medicinal Food*, 8(3), pp. 281–290.

Grant, R. (2014) *Mitochondrial reduction of MTT to blue formazan product - Wikimedia Commons*. Available at: https://commons.wikimedia.org/wiki/File:MTT_reaction.png.

Grassi, D. *et al.* (2005) 'Cocoa Reduces Blood Pressure and Insulin Resistance and Improves Endothelium-Dependent Vasodilation in Hypertensives', *Hypertension*, 46(2), pp. 398–405.

Grassi, D. *et al.* (2009) 'Black tea consumption dose-dependently improves flow-mediated dilation in healthy males', *Journal of Hypertension*, 27(4), pp. 774–781.

Greenstein, A. S. *et al.* (2009) 'Local inflammation and hypoxia abolish the protective anticontractile properties of perivascular fat in obese patients', *Circulation*, 119(12), pp. 1661–1670.

Griendling, K. K., Murphy, T. J. and Alexander, R. W. (1993) 'Molecular biology of the renin-angiotensin system.', *Circulation*. American Heart Association, Inc., 87(6), pp. 1816–1828.

Gu, L. *et al.* (1998) 'Absence of monocyte chemoattractant protein-1 reduces atherosclerosis in low density lipoprotein receptor-deficient mice.', *Molecular cell*, 2(2), pp. 275–281.

Guelinckx, I. *et al.* (2016) 'Contribution of Water from Food and Fluids to Total Water Intake: Analysis of a French and UK Population Surveys.', *Nutrients*. Multidisciplinary Digital Publishing Institute (MDPI), 8(10).

Guo, S. (2014) 'Insulin signaling, resistance, and the metabolic syndrome: insights from mouse models into disease mechanisms.', *The Journal of Rndocrinology*. BioScientifica, 220(2), pp. T1–T23.

Gupta-Malhotra, M. *et al.* (2015) 'Essential hypertension vs. secondary hypertension among children.', *American Journal of Hypertension*. Oxford University Press, 28(1), pp. 73–80.

Haar, E. Vander *et al.* (2007) 'Insulin signalling to mTOR mediated by the Akt/PKB substrate PRAS40', *Nature Cell Biology*, 9(3), pp. 316–323.

Hadi, H. A. R., Carr, C. S. and Al Suwaidi, J. (2005) 'Endothelial dysfunction: cardiovascular risk factors, therapy, and outcome.', *Vascular Health and Risk Management*. Dove Press, 1(3), pp. 183–198.

Hall, J. E. (2003) 'The Kidney, Hypertension, and Obesity', *Hypertension*, 41(3), pp. 625–633.

Hall, J. E. *et al.* (2015) 'Obesity-Induced Hypertension: Interaction of Neurohumoral and Renal Mechanisms', *Circulation Research*, 116(6), pp. 991–1006.

Hall, J. M. (1997) 'Bradykinin receptors.', *General pharmacology*, 28(1), pp. 1–6.

Hall, K. D. and Guo, J. (2017) 'Obesity Energetics: Body Weight Regulation and the Effects of Diet Composition.', *Gastroenterology*. NIH Public Access, 152(7), p. 1718–1727.

Halliwell, B. (1995) 'How to characterize an antioxidant: an update.', *Biochemical Society symposium*, 61, pp. 73–101.

Hammarstedt, A., Graham, T. E. and Kahn, B. B. (2012) 'Adipose tissue dysregulation and reduced insulin sensitivity in non-obese individuals with enlarged abdominal adipose cells', *Diabetology & Metabolic Syndrome*, 4(1), p. 42.

Han, S. H. *et al.* (2007) 'Adiponectin and Cardiovascular Disease: Response to Therapeutic Interventions', *Journal of the American College of Cardiology*. Elsevier, 49(5), pp. 531–538.

Hardie, D. G., Ross, F. A. and Hawley, S. A. (2012) 'AMPK: a nutrient and energy sensor that maintains energy homeostasis', *Nature Reviews Molecular Cell Biology*, 13(4), pp. 251–262.

Hardy, O. T., Czech, M. P. and Corvera, S. (2012) 'What causes the insulin resistance underlying obesity?', *Current opinion in Endocrinology, Diabetes, and Obesity*. NIH Public Access, 19(2), pp. 81–87.

Harlan, S. M. and Rahmouni, K. (2013) 'PI3K signaling: A key pathway in the control of sympathetic traffic and arterial pressure by leptin', *Molecular Metabolism*. Elsevier, 2(2), pp. 69–73.

Hattori, Y. *et al.* (2006) 'Metformin Inhibits Cytokine-Induced Nuclear Factor B Activation Via AMP-Activated Protein Kinase Activation in Vascular Endothelial Cells', *Hypertension*, 47(6), pp. 1183–1188.

Hawley, S. A. *et al.* (2016) 'The Na^+ /Glucose Cotransporter Inhibitor Canagliflozin Activates AMPK by Inhibiting Mitochondrial Function and Increasing Cellular AMP Levels', *Diabetes*, 65(9), pp. 2784–2794.

Heinrich, T., Willenberg, I. and Glomb, M. A. (2012) 'Chemistry of Color Formation during Rooibos Fermentation', *Journal of Agricultural and Food Chemistry*. American Chemical Society, 60(20), pp. 5221–5228.

Heiss, C. *et al.* (2003) 'Vascular Effects of Cocoa Rich in Flavan-3-ols', *JAMA: The Journal of the American Medical Association*, 290(8), pp. 1030–1031.

Heiss, C. *et al.* (2005) 'Acute Consumption of Flavanol-Rich Cocoa and the Reversal of Endothelial Dysfunction in Smokers', *Journal of the American College of Cardiology*, 46(7), pp. 1276–1283.

Heiss, C. *et al.* (2007) 'Sustained Increase in Flow-Mediated Dilation After Daily Intake of High-Flavanol Cocoa Drink Over 1 Week', *Journal of Cardiovascular Pharmacology*, 49(2), pp. 74–80.

Hemmings, B. A. and Restuccia, D. F. (2012) 'PI3K-PKB/Akt pathway.', *Cold Spring Harbor Perspectives in Biology*. Cold Spring Harbor Laboratory Press, 4(9), p. a011189.

Herrmann, H. C. and Dzau, V. J. (1983) 'The feedback regulation of angiotensinogen production by components of the renin-angiotensin system.', *Circulation Research*. American Heart Association, Inc., 52(3), pp. 328–334.

Hertog, M. G. *et al.* (1993) 'Dietary antioxidant flavonoids and risk of coronary heart disease: the Zutphen Elderly Study.', *Lancet*, 342(8878), pp. 1007–1011.

Hertog, M. G. *et al.* (1995) 'Flavonoid intake and long-term risk of coronary heart disease and cancer in the seven countries study.', *Archives of Internal Medicine*, 155(4), pp. 381–386.

Hertog, M. G., Feskens, E. J. and Kromhout, D. (1997) 'Antioxidant flavonols and coronary heart disease risk', *The Lancet*, 349(9053), p. 699.

Higashi, Y. *et al.* (2014) 'Oxidative stress and endothelial dysfunction: Clinical evidence and therapeutic implications', *Trends in Cardiovascular Medicine*, 24(4), pp. 165–169.

Higman, D. J. *et al.* (1996) 'Smoking impairs the activity of endothelial nitric oxide synthase in saphenous vein.', *Arteriosclerosis, Thrombosis, and Vascular Biology*, 16(4), pp. 546–552.

Higuchi, S. *et al.* (2007) 'Angiotensin II signal transduction through the AT_1 receptor: novel insights into mechanisms and pathophysiology', *Clinical Science*, 112(8), pp. 417–428.

Hillis, W. E. and Inoue, T. (1967) 'The polyphenols of Nothofagus species-II.: The heartwood of Nothofagus fusca', *Phytochemistry*. Pergamon, 6(1), pp. 59–67.

Hoedemaeker, F. J. *et al.* (1999) 'Crystal structure of the C-terminal SH2 domain of the p85α regulatory subunit of phosphoinositide 3-kinase: an SH2 domain mimicking its own substrate', *Journal of Molecular Biology*, 292(4), pp. 763–770.

Hogan, M., Cerami, A. and Bucala, R. (1992) 'Advanced glycosylation endproducts block the antiproliferative effect of nitric oxide. Role in the vascular and renal complications of diabetes mellitus.', *The Journal of Clinical Investigation*. American Society for Clinical Investigation, 90(3), pp. 1110–1115.

Hogg, N. *et al.* (1993) 'Inhibition of low-density lipoprotein oxidation by nitric oxide. Potential role in atherogenesis.', *FEBS letters*, 334(2), pp. 170–174.

Hooper, L. *et al.* (2008) 'Flavonoids, flavonoid-rich foods, and cardiovascular risk: a meta-analysis of randomized controlled trials', *The American Journal of Clinical Nutrition*, 88(1), pp. 38–50.

Horton, R. *et al.* (2006) *Principles of Biochemistry | Pearson*. 4th Edition. Available at: https://www.pearson.com/us/higher-education/product/Horton-Principles-of-Biochemistry-4th-Edition/.

Hu, Z. *et al.* (2008) 'Bidirectional Actions of Hydrogen Peroxide on Endothelial Nitric-oxide Synthase Phosphorylation and Function', *Journal of Biological Chemistry*, 283(37), pp. 25256–25263.

Huang, H. and Tindall, D. J. (2011) 'Regulation of FOXO protein stability via ubiquitination and proteasome degradation', *Biochimica et Biophysica Acta (BBA) - Molecular Cell Research*. Elsevier, 1813(11), pp. 1961–1964.

Huang, P. L. *et al.* (1995) 'Hypertension in mice lacking the gene for endothelial nitric oxide synthase', *Nature*, 377(6546), pp. 239–242.

Huang, S. M., Wu, C. H. and Yen, G. C. (2006) 'Effects of flavonoids on the expression of the pro-inflammatory response in human monocytes induced by ligation of the receptor for AGEs', *Molecular Nutrition & Food Research*, 50(12), pp. 1129–1139.

Huisamen, B. *et al.* (2013) 'Cardioprotective and anti-hypertensive effects of Prosopis glandulosa in rat models of pre-diabetes.', *Cardiovascular Journal of Africa*, 24(2), pp. 10–16.

Hunt, K. (2018) *Signs of Dehydration in Fancy Rats | Animals - mom.me*. Available at: https://animals.mom.me/signs-dehydration-fancy-rats-1322.html.

Hussain, S. . (2009) *An Introduction to Fluorescence Resonance Energy Transfer (FRET)*. Available at: http://www.geocities.com/sa_h153/.

Hynynen, M. M. and Khalil, R. A. (2006) 'The vascular endothelin system in hypertension-recent patents and discoveries.', *Recent patents on cardiovascular drug discovery*, 1(1), pp. 95–108.

Iacobellis, G. *et al.* (2003) 'Echocardiographic epicardial adipose tissue is related to anthropometric and clinical parameters of metabolic syndrome: a new indicator of cardiovascular risk', *Journal of Clinical Endocrinology and Metabolism*, 88(11), pp. 5163–5168.

Iacobellis, G. *et al.* (2006) 'Left Ventricular Mass and +276 G/G Single Nucleotide Polymorphism of the Adiponectin Gene in Uncomplicated Obesity', *Obesity*, 14(3), pp. 368–372.

Ibekwe, R. (2015) 'Modifiable Risk factors of Hypertension and Socio-demographic Profile in Oghara, Delta State; Prevalence and Correlates.', *Annals of Medical and Health Sciences Research*, 5(1), pp. 71–77.

Ido, Y., Carling, D. and Ruderman, N. (2002) 'Hyperglycemia-induced apoptosis in human umbilical vein endothelial cells: inhibition by the AMP-activated protein kinase activation.', *Diabetes*, 51(1), pp. 159–167.

Ignarro, L. J. *et al.* (1986) 'Activation of purified soluble guanylate cyclase by endothelium-derived relaxing factor from intrapulmonary artery and vein: stimulation by acetylcholine, bradykinin and arachidonic acid.', *The Journal of Pharmacology and Experimental Therapeutics*, 237(3), pp. 893–900.

Ignarro, L. J. *et al.* (1999) 'Nitric oxide as a signaling molecule in the vascular system: an overview.', *Journal of Cardiovascular Pharmacology*, 34(6), pp. 879–886.

Ignarro, L. J. and Napoli, C. (2004) 'Novel features of nitric oxide, endothelial nitric oxide synthase, and atherosclerosis.', *Current Atherosclerosis Reports*, 6(4), pp. 281–287.

Ikenoue, T. *et al.* (2008) 'Essential function of TORC2 in PKC and Akt turn motif phosphorylation, maturation and signalling', *The EMBO Journal*, 27(14), pp. 1919–1931.

Inoue, G. *et al.* (1998) 'Dynamics of insulin signaling in 3T3-L1 adipocytes. Differential compartmentalization and trafficking of insulin receptor substrate (IRS)-1 and IRS-2.', *The Journal of Biological Chemistry*. American Society for Biochemistry and Molecular Biology, 273(19), pp. 11548–11555.

Jiang, S.-Z. *et al.* (2016) 'Obesity and hypertension.', *Experimental and Therapeutic Medicine*. Spandidos Publications, 12(4), pp. 2395–2399.

Johanning, J. M. *et al.* (2001) 'Inhibition of inducible nitric oxide synthase limits nitric oxide production and experimental aneurysm expansion', *Journal of Vascular Surgery*. Mosby, 33(3), pp. 579–586.

Joubert, E. (1996) 'HPLC quantification of the dihydrochalcones, aspalathin and nothofagin in rooibos tea (Aspalathus linearis) as affected by processing', *Food Chemistry*. Elsevier, 55(4), pp. 403–411.

Joubert, E. *et al.* (2008) 'South African herbal teas: Aspalathus linearis, Cyclopia spp. and Athrixia phylicoides-A review', *Journal of Ethnopharmacology*, 119(3), pp. 376–412.

Joubert, E. and De Beer, D. (2011) 'Rooibos (Aspalathus linearis) beyond the farm gate: From herbal tea to potential phytopharmaceutical', *South African Journal of Botany*, 77, pp. 869–886.

Joyner, M. J., Charkoudian, N. and Wallin, B. G. (2010) 'Sympathetic Nervous System and Blood Pressure in Humans: Individualized Patterns of Regulation and Their Implications', *Hypertension*, 56(1), pp. 10–16.

Kahn, S. E., Hull, R. L. and Utzschneider, K. M. (2006) 'Mechanisms linking obesity to insulin resistance and type 2 diabetes', *Nature*, 444(7121), pp. 840–846.

Kalupahana, N. S. and Moustaid-Moussa, N. (2011) 'The renin-angiotensin system: a link between obesity, inflammation and insulin resistance', *Obesity Reviews*. Blackwell Publishing Ltd, 13(2), pp. 136–149.

Kalupahana, N. S. and Moustaid-Moussa, N. (2012) 'The adipose tissue renin-angiotensin system and metabolic disorders: a review of molecular mechanisms', *Critical Reviews in Biochemistry and Molecular Biology*, 47(4), pp. 379–390.

Kamakura, R. *et al.* (2015) 'Antidiabetic effect of green rooibos (Aspalathus linearis) extract in cultured cells and type 2 diabetic model KK-Ay mice', *Cytotechnology*. Springer Netherlands, 67(4), pp. 699–710.

Kamalakkannan, N. and Prince, P. S. M. (2006) 'Antihyperglycaemic and Antioxidant Effect of Rutin, a Polyphenolic Flavonoid, in Streptozotocin-Induced Diabetic Wistar Rats', *Basic Clinical Pharmacology and Toxicology*, 98(1), pp. 97–103.

Karaki, H., Urakawa, N. and Kutsky, P. (1984) 'Potassium-induced contraction in smooth muscle.', *Nihon Heikatsukin Gakkai zasshi*, 20(6), pp. 427–444.

Kawanabe, Y. and Nauli, S. M. (2011) 'Endothelin', *Cellular and Molecular Life Sciences*, 68(2), pp. 195–203.

Kawano, A. *et al.* (2009) 'Hypoglycemic effect of aspalathin, a rooibos tea component from Aspalathus linearis, in type 2 diabetic model db/db mice', *Phytomedicine*, 16(5), pp. 437–443.

Kearney, P. M. *et al.* (2005) 'Global burden of hypertension: analysis of worldwide data', *The Lancet*, 365(9455), pp. 217–223.

Kedzierski, R. M. and Yanagisawa, M. (2001) 'Endothelin system: The Double-Edged Sword in Health and Disease', *Annual Review of Pharmacology and Toxicology*, 41(1), pp. 851–876.

Keeble, E. J. and Meredith, A. (2009) *BSAVA manual of rodents and ferrets*. British Small Animal Veterinary Association. Available at: https://www.wiley.com/en-us/BSAVA+Manual+of+Rodents+and+Ferrets-p-9781905319084.

Keevil, J. G. *et al.* (2000) 'Grape Juice, But Not Orange Juice or Grapefruit Juice, Inhibits Human Platelet Aggregation', *The Journal of Nutrition*, 130(1), pp. 53–56.

Kellogg, D. L. *et al.* (2005) 'Acetylcholine-induced vasodilation is mediated by nitric oxide and prostaglandins in human skin', *Journal of Applied Physiology*, 98(2), pp. 629–632.

Khan, A. and Pessin, J. (2002) 'Insulin regulation of glucose uptake: a complex interplay of intracellular signalling pathways', *Diabetologia*. Springer-Verlag, 45(11), pp. 1475–1483.

Khan, W. *et al.* (1993) 'Selective regulation of protein kinase C isoenzymes by oleic acid in human platelets.', *Journal of Biological Chemistry*, 268, pp. 5063–5068.

Kido, Y., Nakae, J. and Accili, D. (2001) 'The Insulin Receptor and Its Cellular Targets [1]', *The Journal of Clinical Endocrinology & Metabolism*, 86(3), pp. 972–979.

Kierszenbaum, A. L. (2007) *Histology and cell biology: an introduction to pathology.*, *Mosby Elsevier*.

Kim, J. M. *et al.* (2010) 'Kaempferol modulates pro-inflammatory NF-κB activation by suppressing advanced glycation endproducts-induced NADPH oxidase', *AGE*, 32(2), pp. 197–208.

King, G. L., Park, K. and Li, Q. (2016) 'Selective Insulin Resistance and the Development of Cardiovascular Diseases in Diabetes: The 2015 Edwin Bierman Award Lecture.', *Diabetes*. American Diabetes Association, 65(6), pp. 1462–1471.

Klabunde, R. E. (2017) *CV Pharmacology | Diuretics*. Available at: http://www.cvpharmacology.com/diuretic/diuretics.

Knekt, P. *et al.* (1996) 'Flavonoid intake and coronary mortality in Finland: a cohort study.', *BMJ (Clinical research ed.)*, 312(7029), pp. 478–481.

Koeppen, B. ., Smit, C. . J. . and Roux, D. . (1962) 'The flavone C-glycosides and the flavonol O-glycosides of Aspalathus acuminatus (Rooibos tea).', *Biochemical Journal*. Portland Press Limited, 83(3), pp. 507–511.

Koeppen, B. H. and Roux, D. G. (1965) 'Aspalathin : a novel C-glycosylflavonoid from aspalathus linearis.', *Tetrahedron Letters*. Pergamon, 6(39), pp. 3497–3503.

Kolluru, G. K. *et al.* (2010) 'Shear stress promotes nitric oxide production in endothelial cells by sub-cellular delocalization of eNOS: A basis for shear stress mediated angiogenesis', *Nitric Oxide*, 22(4), pp. 304–315..

Kolluru, G. K., Siamwala, J. H. and Chatterjee, S. (2010) 'eNOS phosphorylation in health and disease', *Biochimie*, 92(9), pp. 1186–1198.

Korkina, L. G. *et al.* (2009) 'Plant polyphenols and tumors: from mechanisms to therapies, prevention, and protection against toxicity of anti-cancer treatments.', *Current Medicinal Chemistry*, 16(30), pp. 3943–3965.

Kostyuk, V. A. *et al.* (2001) 'Influence of Metal Ions on Flavonoid Protection against Asbestos-Induced Cell Injury', *Archives of Biochemistry and Biophysics*. Academic Press, 385(1), pp. 129–137.

Kowalczyk, A. *et al.* (2015) 'The role of endothelin-1 and endothelin receptor antagonists in inflammatory response and sepsis.', *Archivum Immunologiae et Therapiae Experimentalis*. Springer, 63(1), pp. 41–52.

Krafczyk, N. *et al.* (2009) 'Oxidation of the Dihydrochalcone Aspalathin Leads to Dimerization', *Journal of Agricultural and Food Chemistry*. American Chemical Society, 57(15), pp. 6838–6843.

Krafczyk, N. and Glomb, M. A. (2008) 'Characterization of Phenolic Compounds in Rooibos Tea', *Journal of Agricultural and Food Chemistry*. American Chemical Society, 56(9), pp. 3368–3376.

Krop, M. and Danser, A. H. (2008) 'Circulating versus tissue renin-angiotensin system: On the origin of (pro)renin', *Current Hypertension Reports*. Current Science Inc., 10(2), pp. 112–118.

Kubes, P., Suzuki, M. and Granger, D. N. (1991) 'Nitric oxide: an endogenous modulator of leukocyte adhesion.', *Proceedings of the National Academy of Sciences of the United States of America*. National Academy of Sciences, 88(11), pp. 4651–4655.

Kuchan, M. J. and Frangos, J. A. (1994) 'Role of calcium and calmodulin in flow-induced nitric oxide production in endothelial cells', *American Journal of Physiology-Cell Physiology*, 266(3), pp. C628–C636.

Kukidome, D. *et al.* (2006) 'Activation of AMP-activated protein kinase reduces hyperglycemia-induced mitochondrial reactive oxygen species production and promotes mitochondrial biogenesis in human umbilical vein endothelial cells.', *Diabetes*, 55(1), pp. 120–127.

Kulkarni, R. N. *et al.* (1999) 'Altered function of insulin receptor substrate-1–deficient mouse islets and cultured β-cell lines', *Journal of Clinical Investigation*, 104(12), pp. R69–R75.

Kwok, C.-Y. *et al.* (2010) 'Consumption of dried fruit of Crataegus pinnatifida (hawthorn) suppresses high-cholesterol diet-induced hypercholesterolemia in rats', *Journal of Functional Foods*, 2(3), pp. 179–186.

Laemmli, U. K. (1970) 'Cleavage of Structural Proteins during the Assembly of the Head of Bacteriophage T4', *Nature*. Nature Publishing Group, 227(5259), pp. 680–685.

Lal, B. K. *et al.* (2001) 'VEGF Increases Permeability of the Endothelial Cell Monolayer by Activation of PKB/akt, Endothelial Nitric-Oxide Synthase, and MAP Kinase Pathways', *Microvascular Research*. Academic Press, 62(3), pp. 252–262.

Lam, B. and Younossi, Z. M. (2010) 'Treatment options for nonalcoholic fatty liver disease.', *Therapeutic advances in gastroenterology*. SAGE Publications, 3(2), pp. 121–137.

Lavan, B. E. *et al.* (1997) 'A novel 160-kDa phosphotyrosine protein in insulin-treated embryonic kidney cells is a new member of the insulin receptor substrate family.', *The Journal of Biological Chemistry*. American Society for Biochemistry and Molecular Biology, 272(34), pp. 21403–21407.

Lavan, B. E., Lane, W. S. and Lienhard, G. E. (1997) 'The 60-kDa phosphotyrosine protein in insulin-treated adipocytes is a new member of the insulin receptor substrate family.', *The Journal of Biological Chemistry*. American Society for Biochemistry and Molecular Biology, 272(17), pp. 11439–11443.

Lazar, D. F. and Saltiel, A. R. (2006) 'Lipid phosphatases as drug discovery targets for type 2 diabetes', *Nature Reviews Drug Discovery*, 5(4), pp. 333–342.

Leckie, B. J., Birnie, G. and Carachi, R. (1994) 'Renin in Wilms' tumor: prorenin as an indicator.', *The Journal of Clinical Endocrinology & Metabolism*, 79(6), pp. 1742–1746.

Lee, D. G. *et al.* (2016) 'Effect of rutin from tartary buckwheat sprout on serum glucose-lowering in animal model of type 2 diabetes', *Acta Pharmaceutica*, 66(2), pp. 297–302.

Lee, J. (2013) 'Adipose tissue macrophages in the development of obesity-induced inflammation, insulin resistance and type 2 Diabetes', *Archives of Pharmacal Research*, 36(2), pp. 208–222.

Lee, P. G. and Halter, J. B. (2017) 'The Pathophysiology of Hyperglycemia in Older Adults: Clinical Considerations.', *Diabetes Care*. American Diabetes Association, 40(4), pp. 444–452.

Leikert, J. F. *et al.* (2002) 'Red wine polyphenols enhance endothelial nitric oxide synthase expression and subsequent nitric oxide release from endothelial cells.', *Circulation*, 106(13), pp. 1614–1617.

Lemarié, C. A. and Schiffrin, E. L. (2010) 'The angiotensin II type 2 receptor in cardiovascular disease', *Journal of the Renin-Angiotensin-Aldosterone System*, 11(1), pp. 19–31.

Lerman, A. and Burnett, J. C. (1992) 'Intact and altered endothelium in regulation of vasomotion.', *Circulation*, 86(6 (Suppl), pp. 312–319.

Levine, M. *et al.* (1999) 'Criteria and recommendations for vitamin C intake.', *JAMA*, 281(15), pp. 1415–1423.

Li, H. *et al.* (2003) 'Histamine Upregulates Gene Expression of Endothelial Nitric Oxide Synthase in Human Vascular Endothelial Cells', *Circulation*, 107(18), pp. 2348–2354.

Library of Science & Medical Illustrations (2018). Available at: http://www.somersault1824.com/science-illustrations/.

Lim, S. S. *et al.* (2012) 'A comparative risk assessment of burden of disease and injury attributable to 67 risk factors and risk factor clusters in 21 regions, 1990-2010: A systematic analysis for the Global Burden of Disease Study 2010', *The Lancet*, 380(9859), pp. 2224–2260.

Lima, V. V. *et al.* (2011) '*O* -GlcNAcylation: a novel pathway contributing to the effects of endothelin in the vasculature', *American Journal of Physiology-Regulatory, Integrative and Comparative Physiology*, 300(2), pp. R236–R250.

Lin, M. I. *et al.* (2003) 'Phosphorylation of threonine 497 in endothelial nitric-oxide synthase coordinates the coupling of L-arginine metabolism to efficient nitric oxide production.', *The Journal of Biological Chemistry*. American Society for Biochemistry and Molecular Biology, 278(45), pp. 44719–44726.

Liu, J. *et al.* (2017) 'Effects of SGLT2 inhibitors on UTIs and genital infections in type 2 diabetes mellitus: a systematic review and meta-analysis.', *Scientific reports*. Nature Publishing Group, 7(1), p. 2824.

Liu, T.-J. *et al.* (2007) 'Bidirectional regulation of upstream IGF-I/insulin receptor signaling and downstream FOXO1 in cardiomyocytes', *Journal of Endocrinology*, 192(1), pp. 149–158.

Liu, T. *et al.* (1999) 'The Isoprostanes: Novel Prostaglandin-Like Products of the Free Radical-Catalyzed Peroxidation of Arachidonic Acid', *Journal of Biomedical Science*, 6(4), pp. 226–235.

Liyasova, M. S., Ma, K. and Lipkowitz, S. (2015) 'Molecular pathways: cbl proteins in tumorigenesis and antitumor immunity-opportunities for cancer treatment.', *Clinical cancer research : an official journal of the American Association for Cancer Research*. American Association for Cancer Research, 21(8), pp. 1789–1794.

Lloyd-Sherlock, P. *et al.* (2014) 'Hypertension among older adults in low- and middle-income countries: prevalence, awareness and control', *International Journal of Epidemiology*, 43(1), pp. 116–128.

Lobo, V. *et al.* (2010) 'Free radicals, antioxidants and functional foods: Impact on human health.', *Pharmacognosy Reviews*. Wolters Kluwer -- Medknow Publications, 4(8), pp. 118–126.

Lohmeier, T. E. *et al.* (2000) 'Baroreflexes prevent neurally induced sodium retention in angiotensin hypertension', *American Journal of Physiology-Regulatory, Integrative and Comparative Physiology*. American Physiological SocietyBethesda, MD , 279(4), pp. R1437–R1448.

De Lonlay, P. and Saudubray, J. M. (2012) 'Persistent hyperinsulinaemic hypoglycaemia', *Inborn Metabolic Diseases*, pp. 167–174.

Lorenz, M. *et al.* (2004) 'A Constituent of Green Tea, Epigallocatechin-3-gallate, Activates Endothelial Nitric Oxide Synthase by a Phosphatidylinositol-3-OH-kinase-, cAMP-dependent Protein Kinase-, and Akt-dependent Pathway and Leads to Endothelial-dependent Vasorelaxation', *Journal of Biological Chemistry*, 279(7), pp. 6190–6195.

Lozano, I. *et al.* (2016) 'High-fructose and high-fat diet-induced disorders in rats: impact on diabetes risk, hepatic and vascular complications', *Nutrition & Metabolism*, 13(1), p. 15.

Ludwig, D. S. and Ebbeling, C. B. (2018) 'The Carbohydrate-Insulin Model of Obesity', *JAMA Internal Medicine*, 178(8), p. 1098.

Luetscher, J. A. *et al.* (1985) 'Increased Plasma Inactive Renin in Diabetes Mellitus', *New England Journal of Medicine*, 312(22), pp. 1412–1417.

Luiken, J. *et al.* (2002) 'Insulin stimulates long-chain fatty acid utilization by rat cardiac myocytes through cellular redistribution of FAT/CD36.', *Diabetes*, 51(10), pp. 3113–3119.

Luo, H. *et al.* (2014) 'Medicinal chemistry The Tyrosine Phosphatase SHP2: A Key Molecule Linked both Type 2 Diabetes and Cancers?', *Medicinal Chemistry*, 4(4), pp. 435–438.

Luo, S. *et al.* (2015) 'Differential effects of fructose versus glucose on brain and appetitive responses to food cues and decisions for food rewards.', *Proceedings of the National Academy of Sciences of the United States of America*. National Academy of Sciences, 112(20), pp. 6509–6514.

Lusis, A. J. (2000) 'Atherosclerosis.', *Nature*, 407(6801), pp. 233–241.

Ma, L. *et al.* (2010) 'Perivascular fat-mediated vascular dysfunction and remodeling through the AMPK/mTOR pathway in high-fat diet-induced obese rats', *Hypertension Research*, 33(5), pp. 446–453.

Madamanchi, N. R., Vendrov, A. and Runge, M. S. (2005) 'Oxidative stress and vascular disease.', *Arteriosclerosis, Thrombosis, and Vascular biology*. American Heart Association, Inc., 25(1), pp. 29–38.

Mam, V. *et al.* (2010) 'Impaired vasoconstriction and nitric oxide-mediated relaxation in pulmonary arteries of hypoxia- and monocrotaline-induced pulmonary hypertensive rats.', *The Journal of Pharmacology and Experimental Therapeutics*. American Society for Pharmacology and Experimental Therapeutics, 332(2), pp. 455–462.

Manabe, Y., Matsumura, S. and Fushiki, T. (2010) *Preference for High-Fat Food in Animals*, *Fat Detection: Taste, Texture, and Post Ingestive Effects*. CRC Press/Taylor & Francis. Available at: http://www.ncbi.nlm.nih.gov/pubmed/21452473.

Mandelker, D. *et al.* (2009) 'A frequent kinase domain mutation that changes the interaction between PI3Kalpha and the membrane.', *Proceedings of the National Academy of Sciences of the United States of America*, 106(40), pp. 16996–17001.

Mannaioni, P. F. *et al.* (1997) 'Interaction between histamine and nitric oxide in rat mast cells and in isolated guinea pig hearts.', *International archives of allergy and immunology*. Karger Publishers, 113(1–3), pp. 297–299.

Mao, T. K. *et al.* (2002) 'Modulation of TNF-alpha secretion in peripheral blood mononuclear cells by cocoa flavanols and procyanidins.', *Developmental Immunology*, 9(3), pp. 135–141.

Maqeda, Z. (2018) 'Investigating the Modulating Effects of Afriplex GRT TM Extract on Vascular Function and Antioxidant Status in Obese Wistar Rats', MSc Thesis.

Marais, C. *et al.* (2000) '(S)- and (R)-eriodictyol-6-C-beta-D-glucopyranoside, novel keys to the fermentation of rooibos (Aspalathus linearis).', *Phytochemistry*, 55(1), pp. 43–49.

Marchesini, G. *et al.* (2003) 'Nonalcoholic fatty liver, steatohepatitis, and the metabolic syndrome', *Hepatology*, 37(4), pp. 917–923.

Mardilovich, K., Pankratz, S. L. and Shaw, L. M. (2009) 'Expression and function of the insulin receptor substrate proteins in cancer', *Cell Communication and Signaling*. BioMed Central, 7(1), p. 14.

Marnewick, J. *et al.* (2005) 'Inhibition of tumour promotion in mouse skin by extracts of rooibos (Aspalathus linearis) and honeybush (Cyclopia intermedia), unique South African herbal teas', *Cancer Letters*, 224(2), pp. 193–202.

Marnewick, J. L. *et al.* (2009) 'Chemoprotective properties of rooibos (Aspalathus linearis), honeybush (Cyclopia intermedia) herbal and green and black (Camellia sinensis) teas against cancer promotion induced by fumonisin B1 in rat liver', *Food and Chemical Toxicology*, 47(1), pp. 220–229.

Marnewick, J. L. *et al.* (2011) 'Effects of rooibos (Aspalathus linearis) on oxidative stress and biochemical parameters in adults at risk for cardiovascular disease', *Journal of Ethnopharmacology*. Elsevier Ireland Ltd, 133(1), pp. 46–52.

Martin, T. L., Mufson, E. J. and Mesulam, M. M. (1984) 'The light side of horseradish peroxidase histochemistry.', *The Journal of Histochemistry and Cytochemistry : Official Journal of the Histochemistry Society*, 32(7), p. 793.

Mas, M. (2009) 'A Close Look at the Endothelium: Its Role in the Regulation of Vasomotor Tone', *European Urology, Supplements*, 8(2), pp. 48–57.

Massiéra, F. *et al.* (2001) 'Adipose angiotensinogen is involved in adipose tissue growth and blood pressure regulation', *The FASEB Journal*, 15(14), pp. 2727–2729.

Mathur, S. *et al.* (2002) 'Cocoa Products Decrease Low Density Lipoprotein Oxidative Susceptibility but Do Not Affect Biomarkers of Inflammation in Humans', *The Journal of Nutrition*, 132(12), pp. 3663–3667.

Matthews, D. R. *et al.* (1985) 'Homeostasis model assessment: insulin resistance and β-cell function from fasting plasma glucose and insulin concentrations in man', *Diabetologia*. Springer-Verlag, 28(7), pp. 412–419.

Mazibuko, S. E. *et al.* (2015) 'Aspalathin improves glucose and lipid metabolism in 3T3-L1 adipocytes exposed to palmitate', *Molecular Nutrition & Food Research*, 59(11), pp. 2199–2208.

McKay, D. L. and Blumberg, J. B. (2007) 'A review of the bioactivity of south African herbal teas: rooibos (Aspalathus linearis) and honeybush (Cyclopia intermedia)', *Phytotherapy Research*, 21(1), pp. 1–16.

Miao, B. *et al.* (2010) 'Small molecule inhibition of phosphatidylinositol-3,4,5-triphosphate (PIP3) binding to pleckstrin homology domains.', *Proceedings of the National Academy of Sciences of the United States of America*, 107(46), pp. 20126–20131.

Mihaylova, M. M. and Shaw, R. J. (2011) 'The AMPK signalling pathway coordinates cell growth, autophagy and metabolism', *Nature Cell Biology*, 13(9), pp. 1016–1023.

Mikami, N. *et al.* (2015) 'Aspalathin, Suppress Elevation of Blood Glucose Levels in Mice and Inhibit α-amylase and α-glucosidase Activities in vitro', *Food Science and Technology Research*, 21(2), pp. 231–240.

Milagro, F. I., Campión, J. and Martínez, J. A. (2006) 'Weight Gain Induced by High-Fat Feeding Involves Increased Liver Oxidative Stress*', *Obesity*, 14(7), pp. 1118–1123.

Mink, P. J. *et al.* (2007) 'Flavonoid intake and cardiovascular disease mortality: a prospective study in postmenopausal women', *The American Journal of Clinical Nutrition*, 85(3), pp. 895–909.

Mondillo, C. *et al.* (2009) 'Involvement of Nitric Oxide Synthase in the Mechanism of Histamine-Induced Inhibition of Leydig Cell Steroidogenesis via Histamine Receptor Subtypes in Sprague-Dawley Rats1', *Biology of Reproduction*. Oxford University Press, 80(1), pp. 144–152.

Montani, J. . and van Vliet, B. . (2004) 'General Physiology and Pathophysiology of the Renin – Angiotensin System', *Handbook of Experimental Pharmacology*, 163, pp. 3–29.

Mora, A. *et al.* (2003) 'Deficiency of PDK1 in cardiac muscle results in heart failure and increased sensitivity to hypoxia', *The EMBO Journal*, 22(18), pp. 4666–4676.

Motte, S., McEntee, K. and Naeije, R. (2006) 'Endothelin receptor antagonists', *Pharmacology & Therapeutics*, 110(3), pp. 386–414.

Moulian, N. *et al.* (2001) 'In vivo and in vitro apoptosis of human thymocytes are associated with nitrotyrosine formation.', *Blood*. American Society of Hematology, 97(11), pp. 3521–3530.

Mudau, M. *et al.* (2012) 'Endothelial dysfunction: the early predictor of atherosclerosis.', *Cardiovascular Journal of Africa*. Clinics Cardive Publishing (Pty) Ltd., 23(4), pp. 222–231.

Muller, C. J. F. *et al.* (2012) 'Acute assessment of an aspalathin-enriched green rooibos (Aspalathus linearis) extract with hypoglycemic potential', *Phytomedicine*. Elsevier GmbH., 20(1), pp. 32–39.

Muller, C. J. F. *et al.* (2017) 'Potential of rooibos, its major C-glucosyl flavonoids, and Z-2-(β-D-glucopyranosyloxy)-3-phenylpropenoic acid in prevention of metabolic syndrome', *Critical Reviews in Food Science and Nutrition*, 58(2), pp. 227–246.

Myers, M. G. *et al.* (2010) 'Obesity and leptin resistance: distinguishing cause from effect.', *Trends in endocrinology and metabolism: TEM*. NIH Public Access, 21(11), pp. 643–651.

Myers, M. G., Cowley, M. A. and Münzberg, H. (2008) 'Mechanisms of Leptin Action and Leptin Resistance', *Annual Review of Physiology*. Annual Reviews , 70(1), pp. 537–556.

Nagarathnam, D. *et al.* (1998) 'Design and synthesis of novel alpha1aadrenoceptor-selective dihydropyridine antagonists for the treatment of benign prostatic hyperplasia.', *Journal of Medicinal Chemistry*. American Chemical Society, 41(26), pp. 5320–5333.

Nakachi, K. *et al.* (2000) 'Preventive effects of drinking green tea on cancer and cardiovascular disease: epidemiological evidence for multiple targeting prevention.', *BioFactors (Oxford, England)*, 13(1–4), pp. 49–54.

Nakaki, T., Nakayama, M. and Kato, R. (1990) 'Inhibition by nitric oxide and nitric oxide-producing vasodilators of DNA synthesis in vascular smooth muscle cells.', *European Journal of Pharmacology*, 189(6), pp. 347–353.

Naseem, K. M. (2005) 'The role of nitric oxide in cardiovascular diseases', *Molecular Aspects of Medicine*, 26, pp. 33–65.

Nature (2006) *Nature Reviews*, *Molecular Cell Biology*.

Naumnik, B. and Myśliwiec, M. (2010) 'Renal consequences of obesity.', *Medical science monitor : international medical journal of experimental and clinical research*, 16(8), pp. RA163-RA170.

Navab, M. *et al.* (1996) 'The Yin and Yang of oxidation in the development of the fatty streak. A review based on the 1994 George Lyman Duff Memorial Lecture.', *Arteriosclerosis, Thrombosis, and Vascular Biology*, 16(7), pp. 831–842.

Navar, L. G. (2014) 'Physiology: hemodynamics, endothelial function, renin-angiotensin-aldosterone system, sympathetic nervous system.', *Journal of the American Society of Hypertension : JASH*. NIH Public Access, 8(7), pp. 519–524.

NIDDK (2014) *High Blood Pressure & Kidney Disease*. Available at: https://www.niddk.nih.gov/health-information/kidney-disease/high-blood-pressure.

Niswender, K. D. *et al.* (2001) 'Key enzyme in leptin-induced anorexia', *Nature*. Nature Publishing Group, 413(6858), pp. 794–795.

Nseir, W., Hellou, E. and Assy, N. (2014) 'Role of diet and lifestyle changes in nonalcoholic fatty liver disease.', *World Journal of Gastroenterology*. Baishideng Publishing Group Inc, 20(28), pp. 9338–4934.

Nunokawa, Y. and Tanaka, S. (1992) 'Interferon-γ inhibits proliferation of rat vascular smooth muscle cells by nitric oxide generation', *Biochemical and Biophysical Research Communications*. Academic Press, 188(1), pp. 409–415.

Nurdiana, S. *et al.* (2017) 'Changes in pancreatic histology, insulin secretion and oxidative status in diabetic rats following treatment with Ficus deltoidea and vitexin', *BMC Complementary and Alternative Medicine*, 17(1), p. 290.

Oakhill, J. S. *et al.* (2011) 'AMPK Is a Direct Adenylate Charge-Regulated Protein Kinase', *Science*, 332(6036), pp. 1433–1435.

Odaka, C. and Mizuochi, T. (2000) 'Angiotensin-converting enzyme inhibitor captopril prevents activation-induced apoptosis by interfering with T cell activation signals.', *Clinical and Experimental Immunology*. Wiley-Blackwell, 121(3), pp. 515–522.

Ogihara, T. *et al.* (1997) 'Insulin Receptor Substrate (IRS)-2 Is Dephosphorylated More Rapidly than IRS-1 via Its Association with Phosphatidylinositol 3-Kinase in Skeletal Muscle Cells*', *The Journal of Biological Chemistry*, 272(19), pp. 12868–12873.

Oh, Y. B. *et al.* (2012) 'Captopril intake decreases body weight gain via angiotensin-(1–7)', *Peptides*, 37(1), pp. 79–85.

Ohkita, M. *et al.* (2012) 'Pathophysiological roles of endothelin receptors in cardiovascular diseases.', *Journal of Pharmacological Sciences*, 119(4), pp. 302–313.

Oishi, K., Zheng, B. and Kuo, J. (1990) 'Inhibition of Na,K-ATPase and Sodium Pump by Protein Kinase C Regulators Sphingosine, Lysophosphatidylcholine, and Oleic Acid', *The Journal of Biological Chemistry*, 265(1), pp. 70–75.

Okamoto, Y. *et al.* (2002) 'Adiponectin reduces atherosclerosis in apolipoprotein E-deficient mice.', *Circulation*, 106(22), pp. 2767–2770.

Ordway, R. W., Singer, J. J. and Walsh, J. V (1991) 'Direct regulation of ion channels by fatty acids.', *Trends in Neurosciences*, 14(3), pp. 96–100.

Osaki, M., Oshimura, M. and Ito, H. (2004) 'PI3K-Akt pathway: its functions and alterations in human cancer.', *Apoptosis : An International Journal on Programmed Cell Death*, 9(6), pp. 667–676.

Osegbe, I., Okpara, H. and Azinge, E. (2016) 'Relationship between serum leptin and insulin resistance among obese Nigerian women.', *Annals of African Medicine*, 15(1), pp. 14–19.

Ostlund, R. E. *et al.* (1996) 'Relation between plasma leptin concentration and body fat, gender, diet, age, and metabolic covariates.', *The Journal of Clinical Endocrinology & Metabolism*. Oxford University Press, 81(11), pp. 3909–3913.

Oteiza, P. I. *et al.* (2005) 'Flavonoid-membrane interactions: A protective role of flavonoids at the membrane surface?', *Clinical and Developmental Immunology*, 12(1), pp. 19–25.

Otsu, M. *et al.* (1991) 'Characterization of two 85 kd proteins that associate with receptor tyrosine kinases, middle-T/pp60c-src complexes, and PI3-kinase.', *Cell*, 65(1), pp. 91–104.

Paizis, G. *et al.* (2005) 'Chronic liver injury in rats and humans upregulates the novel enzyme angiotensin converting enzyme 2.', *Gut*. BMJ Publishing Group, 54(12), pp. 1790–1796.

Panchal, S. K. *et al.* (2011) 'Rutin Attenuates Metabolic Changes, Nonalcoholic Steatohepatitis, and Cardiovascular Remodeling in High-Carbohydrate, High-Fat Diet-Fed Rats', *The Journal of Nutrition*, 141(6), pp. 1062–1069.

Panche, A. N., Diwan, A. D. and Chandra, S. R. (2016) 'Flavonoids: an overview.', *Journal of Nutritional Science*. Cambridge University Press, 5, p. e47.

Pandey, K. B. and Rizvi, S. I. (2009) 'Plant polyphenols as dietary antioxidants in human health and disease.', *Oxidative Medicine and Cellular Longevity*. Hindawi Limited, 2(5), pp. 270–278.

Pantsi, W. G. *et al.* (2011) 'Rooibos (Aspalathus linearis) offers cardiac protection against ischaemia/reperfusion in the isolated perfused rat heart', *Phytomedicine*, 18(14), pp. 1220–1228.

Papamichael, C. *et al.* (2004) 'Red wine's antioxidants counteract acute endothelial dysfunction caused by cigarette smoking in healthy nonsmokers.', *American Heart Journal*, 147(2), p. E5.

Park, K. H. and Park, W. J. (2015) 'Endothelial Dysfunction: Clinical Implications in Cardiovascular Disease and Therapeutic Approaches.', *Journal of Korean Medical Science*. Korean Academy of Medical Sciences, 30(9), pp. 1213–1225.

Parsons, M. E. and Ganellin, C. R. (2009) 'Histamine and its receptors', *British Journal of Pharmacology*, 147(S1), pp. S127–S135.

Patravale, V. *et al.* (2012) 'Nanotoxicology: evaluating toxicity potential of drug-nanoparticles', *Nanoparticulate Drug Delivery*. Woodhead Publishing, pp. 123–155.

Pearson, D. A. *et al.* (2002) 'The effects of flavanol-rich cocoa and aspirin on ex vivo platelet function.', *Thrombosis Research*, 106(4–5), pp. 191–197.

Peltzer, K. and Phaswana-Mafuya, N. (2013) 'Hypertension and associated factors in older adults in South Africa : cardiovascular topics', *Cardiovascular Journal Of Africa*, 24(3), pp. 66–71.

Peppa, M. and Raptis, S. A. (2008) 'Advanced glycation end products and cardiovascular disease.', *Current Diabetes Reviews*, 4(2), pp. 92–100.

Persson, I. A. L. *et al.* (2010) 'Effects of green tea, black tea and Rooibos tea on angiotensin-converting enzyme and nitric oxide in healthy volunteers', *Public Health Nutrition*, 13(5), p. 730.

Persson, I. A. L. *et al.* (2006) 'Tea flavanols inhibit angiotensin-converting enzyme activity and increase nitric oxide production in human endothelial cells', *Journal of Pharmacy and Pharmacology*, 58(8), pp. 1139–1144.

Persson, P. B. (2003) 'Renin: origin, secretion and synthesis.', *The Journal of Physiology*. Wiley-Blackwell, 552(Pt 3), pp. 667–671.

Pessin, J. E. and Saltiel, A. R. (2000) 'Signaling pathways in insulin action: molecular targets of insulin resistance', *Journal of Clinical Investigation*, 106(2), pp. 165–169.

Peterson, J. *et al.* (2010) 'Dietary lignans: physiology and potential for cardiovascular disease risk reduction.', *Nutrition reviews*. NIH Public Access, 68(10), pp. 571–603.

Piascik, M. T. and Perez, D. M. (2001) 'Alpha1-adrenergic receptors: new insights and directions.', *The Journal of Pharmacology and Experimental Therapeutics*, 298(2), pp. 403–410.

Picchi, M. G. *et al.* (2011) 'A high-fat diet as a model of fatty liver disease in rats', *Acta Cirurgica Brasileira*, 26(Suppl 2), pp. 25–30.

Pignatelli, P. *et al.* (2000) 'The flavonoids quercetin and catechin synergistically inhibit platelet function by antagonizing the intracellular production of hydrogen peroxide', *The American Journal of Clinical Nutrition*, 72(5), pp. 1150–1155.

Pivovarova, O. *et al.* (2016) 'Insulin-degrading enzyme: new therapeutic target for diabetes and Alzheimer's disease?', *Annals of Medicine*, 48(8), pp. 614–624.

Poirier, P. *et al.* (2006) 'Obesity and Cardiovascular Disease: Pathophysiology, Evaluation, and Effect of Weight Loss: An Update of the 1997 American Heart Association Scientific Statement on Obesity and Heart Disease From the Obesity Committee of the Council on Nutrition, Physical Activity, and Metabolism', *Circulation*, 113(6), pp. 898–918.

Pries, A. R., Secomb, T. W. and Gaehtgens, P. (2000) 'The endothelial surface layer', *Pflügers Archiv - European Journal of Physiology*, 440(5), pp. 653–666.

Prince, P. S. M. and Kannan, N. K. (2006) 'Protective effect of rutin on lipids, lipoproteins, lipid metabolizing enzymes and glycoproteins in streptozotocin-induced diabetic rats', *Journal of Pharmacy and Pharmacology*, 58(10), pp. 1373–1383.

Privett, K., Kunert, M. . and Lombard, J. . (2004) 'Vascular phenotypes: high throughput characterization of vascular reactivity in rats conditioned on 0.4% and 4.0% NaCl diet. User manual for vascular tension studies.', *Medical College of Wisconsin*.

Puar, T. H. K. *et al.* (2016) 'Secondary hypertension in adults.', *Singapore Medical Journal*. Singapore Medical Association, 57(5), pp. 228–232.

Pupo, A. S. and Minneman, K. P. (2001) 'Adrenergic pharmacology: focus on the central nervous system.', *CNS Spectrums*, 6(8), pp. 656–662.

Qu, B. H. *et al.* (1999) 'Insulin receptor substrate-4 enhances insulin-like growth factor-I-induced cell proliferation.', *The Journal of Biological Chemistry*. American Society for Biochemistry and Molecular Biology, 274(44), pp. 31179–31184.

Quintero, M. *et al.* (2006) 'Mitochondria as signaling organelles in the vascular endothelium', *Proceedings of the National Academy of Sciences*, 103(14), pp. 5379–5384.

Rabe, C., Joubert, E. and Ferrema, D. (1994) 'Phenolic metabolites from Rooibos (Aspalathus Linearis)', *Phytochemistry*, 35(6), pp. 1559–1565.

Racioppi, L. and Means, A. R. (2012) 'Calcium/Calmodulin-dependent Protein Kinase Kinase 2: Roles in Signaling and Pathophysiology', *Journal of Biological Chemistry*, 287(38), pp. 31658–31665.

Rad, A. (2006) *Renin-angiotensin-aldosterone system.png - Wikimedia Commons*. Available at: https://commons.wikimedia.org/wiki/File:Renin-angiotensin-aldosterone_system.png.

Radi, R. (2013) 'Peroxynitrite, a stealthy biological oxidant.', *The Journal of Biological Chemistry*. American Society for Biochemistry and Molecular Biology, 288(37), pp. 26464–26472.

Rahmouni, K. *et al.* (2005) 'Obesity-Associated Hypertension: New Insights Into Mechanisms', *Hypertension*, 45(1), pp. 9–14.

Rajavashisth, T. B. *et al.* (1990) 'Induction of endothelial cell expression of granulocyte and macrophage colony-stimulating factors by modified low-density lipoproteins', *Nature*. Nature Publishing Group, 344(6263), pp. 254–257.

Ramalingam, L. *et al.* (2017) 'The renin angiotensin system, oxidative stress and mitochondrial function in obesity and insulin resistance', *Biochimica et Biophysica Acta (BBA) - Molecular Basis of Disease*. Elsevier, 1863(5), pp. 1106–1114.

Ran, J. *et al.* (2006) 'Angiotensin II infusion decreases plasma adiponectin level via its type 1 receptor in rats: an implication for hypertension-related insulin resistance', *Metabolism*, 55(4), pp. 478–488.

Rapoport, R. M., Draznin, M. B. and Murad, F. (1983) 'Endothelium-dependent relaxation in rat aorta may be mediated through cyclic GMP-dependent protein phosphorylation', *Nature*. Nature Publishing Group, 306(5939), pp. 174–176.

Rask-Madsen, C. and Kahn, C. R. (2012) 'Tissue-Specific Insulin Signaling, Metabolic Syndrome, and Cardiovascular Disease', *Arteriosclerosis, Thrombosis, and Vascular Biology*, 32(9), pp. 2052–2059.

Reaven, G. (2004) 'The metabolic syndrome or the insulin resistance syndrome? Different names, different concepts, and different goals', *Endocrinology and Metabolism Clinics of North America*, 33(2), pp. 283–303.

Reddy, K. G. *et al.* (1994) 'Evidence that selective endothelial dysfunction may occur in the absence of angiographic or ultrasound atherosclerosis in patients with risk factors for atherosclerosis.', *Journal of the American College of Cardiology*, 23(4), pp. 833–843.

Rein, D., Paglieroni, T. G., *et al.* (2000 a) 'Cocoa and Wine Polyphenols Modulate Platelet Activation and Function', *The Journal of Nutrition*. Oxford University Press, 130(8), p. 2120S–2126S.

Rein, D., Paglieroni, T. G., *et al.* (2000 b) 'Cocoa inhibits platelet activation and function.', *The American Journal of Clinical Nutrition*. American Society for Nutrition, 72(1), pp. 30–35.

Rein, D., Lotito, S., *et al.* (2000) 'Epicatechin in Human Plasma: In Vivo Determination and Effect of Chocolate Consumption on Plasma Oxidation Status', *The Journal of Nutrition*, 130(8), p. 2109S–2114S.

Reitsma, S. *et al.* (2007) 'The endothelial glycocalyx: composition, functions, and visualization.', *Pflugers Archiv : European journal of physiology*. Springer, 454(3), pp. 345–59.

Rena, G. *et al.* (1999) 'Phosphorylation of the transcription factor forkhead family member FKHR by protein kinase B.', *The Journal of Biological Chemistry*. American Society for Biochemistry and Molecular Biology, 274(24), pp. 17179–17183.

Renaud, S. and de Lorgeril, M. (1992) 'Wine, alcohol, platelets, and the French paradox for coronary heart disease.', *Lancet (London, England)*, 339(8808), pp. 1523–1526.

Riccardi, C. and Nicoletti, I. (2006) 'Analysis of apoptosis by propidium iodide staining and flow cytometry', *Nature Protocols*, 1(3), pp. 1458–1461.

Rider, M. H. *et al.* (2004) '6-Phosphofructo-2-kinase/fructose-2,6-bisphosphatase: head-to-head with a bifunctional enzyme that controls glycolysis', *Biochem. J*, 381, pp. 561–579.

Rider, M. and Hue, L. (1984) 'Activation of rat heart phosphofructokinase-2 by insulin in vivo.', *FEBS Lett.*, 176, pp. 484–488.

Ritchie, S. A. *et al.* (2004) 'The role of insulin and the adipocytokines in regulation of vascular endothelial function', *Clinical Science*. Portland Press Limited, 107(6), pp. 519–532.

Rocchini, A. P., Yang, J. Q. and Gokee, A. (2004) 'Hypertension and Insulin Resistance Are Not Directly Related in Obese Dogs', *Hypertension*, 43, pp. 1011–1016.

Rolfe, M. *et al.* (2005) 'Activation of protein synthesis in cardiomyocytes by the hypertrophic agent phenylephrine requires the activation of ERK and involves phosphorylation of tuberous sclerosis complex 2 (TSC2)', *Biochemical Journal*, 388(3), pp. 973–984.

Rondinone, C. M. *et al.* (1997) 'Insulin receptor substrate (IRS) 1 is reduced and IRS-2 is the main docking protein for phosphatidylinositol 3-kinase in adipocytes from subjects with non-insulin-dependent diabetes mellitus.', *Proceedings of the National Academy of Sciences of the United States of America*, 94(8), pp. 4171–4175.

Rubanyi, G. M. (1991) 'Endothelium-derived relaxing and contracting factors', *Journal of Cellular Biochemistry*. Wiley-Blackwell, 46(1), pp. 27–36.

Rubanyi, G. M., Romero, J. C. and Vanhoutte, P. M. (1986) 'Flow-induced release of endothelium-derived relaxing factor', *American Journal of Physiology-Heart and Circulatory Physiology*, 250(6), pp. H1145–H1149.

Rubbo, H. *et al.* (1994) 'Nitric oxide regulation of superoxide and peroxynitrite-dependent lipid peroxidation. Formation of novel nitrogen-containing oxidized lipid derivatives.', *The Journal of Biological Chemistry*, 269(42), pp. 26066–26075.

Rubbo, H., Darley-Usmar, V. and Freeman, B. A. (1996) 'Nitric Oxide Regulation of Tissue Free Radical Injury', *Chemical Research in Toxicology*, 9(5), pp. 809–820.

Rubin, L. J. *et al.* (2005) 'Metabolic activation of AMP kinase in vascular smooth muscle', *Journal of Applied Physiology*, 98(1), pp. 296–306.

Ruderman, N. B. *et al.* (2003) 'Malonyl-CoA and AMP-activated protein kinase (AMPK): possible links between insulin resistance in muscle and early endothelial cell damage in diabetes.', *Biochemical Society Transactions*, 31(Pt 1), pp. 202–206.

Ruderman, N. B. *et al.* (2013) 'AMPK, insulin resistance, and the metabolic syndrome.', *The Journal of Clinical Investigation*. American Society for Clinical Investigation, 123(7), pp. 2764–2772.

Rudic, R. D. *et al.* (1998) 'Direct evidence for the importance of endothelium-derived nitric oxide in vascular remodeling.', *The Journal of Clinical Investigation*. American Society for Clinical Investigation, 101(4), pp. 731–736.

Russell, F. D. and Hamilton, K. D. (2014) 'Nutrient deprivation increases vulnerability of endothelial cells to proinflammatory insults', *Free Radical Biology and Medicine*, 67, pp. 408–415.

Russo, A. *et al.* (2018) 'Advances in the genetics of hypertension: The effect of rare variants', *International Journal of Molecular Sciences*, 19(3), pp. 1–21.

Sadhukhan, R. *et al.* (1998) 'The distal ectodomain of angiotensin-converting enzyme regulates its cleavage-secretion from the cell surface.', *Proceedings of the National Academy of Sciences of the United States of America*. National Academy of Sciences, 95(1), pp. 138–143.

Saiki, A. *et al.* (2009) 'Circulating angiotensin II is associated with body fat accumulation and insulin resistance in obese subjects with type 2 diabetes mellitus', *Metabolism*, 58(5), pp. 708–713.

Sakakura, K. *et al.* (2013) 'Pathophysiology of Atherosclerosis Plaque Progression', *Heart, Lung and Circulation*, 22(6), pp. 399–411.

Saltiel, A. R. *et al.* (2000) 'CAP defines a second signalling pathway required for insulin-stimulated glucose transport.', *Nature*, 407(6801), pp. 202–207.

Salvetti, A. *et al.* (1993) 'The inter-relationship between insulin resistance and hypertension.', *Drugs*, 46(Suppl 2), pp. 149–159.

Sanderson, M. *et al.* (2014) 'Effects of fermented rooibos (Aspalathus linearis) on adipocyte differentiation', *Phytomedicine*, 21(2), pp. 109–117.

Santos, R. A. S. *et al.* (2003) 'Angiotensin-(1-7) is an endogenous ligand for the G protein-coupled receptor Mas.', *Proceedings of the National Academy of Sciences of the United States of America*. National Academy of Sciences, 100(14), pp. 8258–8263.

Sapsford, K. E., Berti, L. and Medintz, I. L. (2006) 'Materials for Fluorescence Resonance Energy Transfer Analysis: Beyond Traditional Donor–Acceptor Combinations', *Angewandte Chemie International Edition*, 45(28), pp. 4562–4589.

Sasaki, K. *et al.* (1991) 'Cloning and expression of a complementary DNA encoding a bovine adrenal angiotensin II type-1 receptor', *Nature*, 351(6323), pp. 230–233.

Sasaki, M., Nishida, N. and Shimada, M. (2018) 'A Beneficial Role of Rooibos in Diabetes Mellitus: A Systematic Review and Meta-Analysis', *Molecules*. Multidisciplinary Digital Publishing Institute, 23(4), p. 839.

Sawka-Verhelle, D. *et al.* (1996) 'Insulin receptor substrate-2 binds to the insulin receptor through its phosphotyrosine-binding domain and through a newly identified domain comprising amino acids 591-786.', *The Journal of Biological Chemistry*, 271(11), pp. 5980–5983.

Scheid, M. P. and Woodgett, J. R. (2003) 'Unravelling the activation mechanisms of protein kinase B/Akt.', *FEBS letters*, 546(1), pp. 108–112.

Schlaich, M. P. *et al.* (2009) 'Renal Denervation as a Therapeutic Approach for Hypertension: Novel Implications for an Old Concept', *Hypertension*, 54(6), pp. 1195–1201.

Schloms, L. *et al.* (2012) 'The influence of Aspalathus linearis (Rooibos) and dihydrochalcones on adrenal steroidogenesis: Quantification of steroid intermediates and end products in H295R cells', *The Journal of Steroid Biochemistry and Molecular Biology*, 128(3–5), pp. 128–138.

Schmieder, R. E. *et al.* (2007) 'Renin-angiotensin system and cardiovascular risk', *The Lancet*. Elsevier, 369(9568), pp. 1208–1219.

Schmitt, C. A. and Dirsch, V. M. (2009) 'Modulation of endothelial nitric oxide by plant-derived products', *Nitric Oxide*, 21(2), pp. 77–91.

Schnyder, B. *et al.* (2002) 'Rapid effects of glucose on the insulin signaling of endothelial NO generation and epithelial Na transport', *American Journal of Physiology-Endocrinology and Metabolism*, 282(1), pp. E87–E94.

Schramm, D. D. *et al.* (2003) 'Food effects on the absorption and pharmacokinetics of cocoa flavanols.', *Life sciences*, 73(7), pp. 857–869.

Schramm, D. D. and German, J. B. (1998) 'Potential effects of flavonoids on the etiology of vascular disease', *The Journal of Nutritional Biochemistry*. Elsevier Inc., 9(10), pp. 560–566.

Schroeter, H. *et al.* (2006) '(-)-Epicatechin mediates beneficial effects of flavanol-rich cocoa on vascular function in humans', *Proceedings of the National Academy of Sciences*, 103(4), pp. 1024–1029.

Schulz, H., Joubert, E. and Schütze, W. (2003) 'Quantification of quality parameters for reliable evaluation of green rooibos (Aspalathus linearis)', *European Food Research Technology*, 216, pp. 539–543.

Sciamanna, C. N. *et al.* (2011) 'Practices Associated with Weight Loss Versus Weight-Loss Maintenance', *American Journal of Preventive Medicine*, 41(2), pp. 159-166.

Segura, J. and Ruilope, L. M. (2007) 'Obesity, essential hypertension and renin–angiotensin system', *Public Health Nutrition*, 10(10A), pp. 1151–1155.

Sessa, W. C. (2004) 'eNOS at a glance', *Journal of Cell Science*, 117(12), pp. 2427–2429.

Sesti, G. *et al.* (2001) 'Defects of the insulin receptor substrate (IRS) system in human metabolic disorders', *The FASEB Journal*, 15(12), pp. 2099–2111.

Sezik, E. *et al.* (2005) 'Hypoglycaemic activity of Gentiana olivieri and isolation of the active constituent through bioassay- directed fractionation techniques', *Life Sciences*, 76(11), pp. 1223–1238.

Shabeeh, H. *et al.* (2013) 'Sympathetic activation increases NO release from eNOS but neither eNOS nor nNOS play an essential role in exercise hyperemia in the human forearm.', *American journal of physiology. Heart and circulatory physiology*. American Physiological Society, 304(9), pp. H1225-H1230.

Shaikh, N., Dadachanji, R. and Mukherjee, S. (2014) 'Genetic Markers of Polycystic Ovary Syndrome: Emphasis on Insulin Resistance', *International Journal of Medical Genetics*. Hindawi, 2014, pp. 1–10.

Shesely, E. G. *et al.* (1996) 'Elevated blood pressures in mice lacking endothelial nitric oxide synthase.', *Proceedings of the National Academy of Sciences of the United States of America*, 93(23), pp. 13176–13181.

Shi, H., Noguchi, N. and Niki, E. (1999) 'Comparative study on dynamics of antioxidative action of alpha-tocopheryl hydroquinone, ubiquinol, and alpha-tocopherol against lipid peroxidation.', *Free Radical Biology & Medicine*, 27(3–4), pp. 334–346.

Shimamura, N. *et al.* (2006) 'Phytoestrogens from Aspalathus linearis.', *Biological & Pharmaceutical Bulletin*, 29(6), pp. 1271–1274.

Sigma-Aldrich (2018a) *4,5-Diaminofluorescein diacetate solution*| *Sigma-Aldrich*. Available at: https://www.sigmaaldrich.com/catalog/product/sigma/.

Sigma-Aldrich (2018b) *Propidium iodide* | *Sigma-Aldrich*. Available at: https://www.sigmaaldrich.com/catalog/product/sigma/.

Sinha, M. K. *et al.* (1996) 'Evidence of free and bound leptin in human circulation: Studies in lean and obese subjects and during short-term fasting', *Journal of Clinical Investigation*, 98(6), pp. 1277–1282.

Skurk, T. *et al.* (2007) 'Relationship between Adipocyte Size and Adipokine Expression and Secretion', *The Journal of Clinical Endocrinology & Metabolism*, 92(3), pp. 1023–1033.

Smith-Hall, J. *et al.* (1997) 'The 60 kDa Insulin Receptor Substrate Functions Like an IRS Protein (pp60IRS3) in Adipose Cells', *Biochemistry*. American Chemical Society, 36(27), pp. 8304–8310.

Smith, U. (2002) 'Impaired ("diabetic") insulin signaling and action occur in fat cells long before glucose intolerance—is insulin resistance initiated in the adipose tissue?', *International Journal of Obesity*. Nature Publishing Group, 26(7), pp. 897–904.

Snijman, P. W. *et al.* (2007) 'The antimutagenic activity of the major flavonoids of rooibos (Aspalathus linearis): Some dose-response effects on mutagen activation-flavonoid interactions', *Mutation Research/Genetic Toxicology and Environmental Mutagenesis*, 631(2), pp. 111–123.

Soleimani, M. (2015) 'Insulin resistance and hypertension: new insights', *Kidney International*, 87, pp. 497–499.

Somoza, B. *et al.* (2007) 'Induction of cardiac uncoupling protein-2 expression and adenosine 5′-monophosphate-activated protein kinase phosphorylation during early states of diet-induced obesity in mice', *Endocrinology*, 148(3), pp. 924–931.

Son, M. J. *et al.* (2013) 'Aspalathin improves hyperglycemia and glucose intolerance in obese diabetic ob/ob mice', *European Journal of Nutrition*, 52(6), pp. 1607–1619.

Soria, B. *et al.* (2004) 'Novel players in pancreatic islet signaling: from membrane receptors to nuclear channels.', *Diabetes*, 53(Suppl 1), pp. S86–S91.

Southgate, K. and Newby, A. C. (1990) 'Serum-induced proliferation of rabbit aortic smooth muscle cells from the contractile state is inhibited by 8-Br-CAMP but not 8-Br-cGMP', *Atherosclerosis*. Elsevier, 82(1–2), pp. 113–123.

Spencer, J. P. E. *et al.* (2008) 'Biomarkers of the intake of dietary polyphenols: strengths, limitations and application in nutrition research', *British Journal of Nutrition*, 99(1), pp. 12–22.

Stahmann, N. *et al.* (2006) 'Thrombin Activates AMP-Activated Protein Kinase in Endothelial Cells via a Pathway Involving Ca2+/Calmodulin-Dependent Protein Kinase Kinase', *Molecular and Cellular Biology*, 26(16), pp. 5933–5945.

Steffen, Y. *et al.* (2008) 'Mono-O-methylated flavanols and other flavonoids as inhibitors of endothelial NADPH oxidase', *Archives of Biochemistry and Biophysics*, 469(2), pp. 209–219.

Steffen, Y., Schewe, T. and Sies, H. (2007) '(–)-Epicatechin elevates nitric oxide in endothelial cells via inhibition of NADPH oxidase', *Biochemical and Biophysical Research Communications*, 359(3), pp. 828–833.

Stein, J. H. *et al.* (1999) 'Purple grape juice improves endothelial function and reduces the susceptibility of LDL cholesterol to oxidation in patients with coronary artery disease.', *Circulation*, 100(10), pp. 1050–1055.

Steyn, K. *et al.* (2001) 'Hypertension in South African adults: results from the Demographic and Health Survey, 1998.', *Journal of h=Hypertension*, 19(10), pp. 1717–1725.

Stoclet, J.-C. *et al.* (2004) 'Vascular protection by dietary polyphenols', *European Journal of Pharmacology*, 500(1–3), pp. 299–313.

Stroes, E. *et al.* (1997) 'Tetrahydrobiopterin restores endothelial function in hypercholesterolemia.', *The Journal of Clinical Investigation*. American Society for Clinical Investigation, 99(1), pp. 41–46.

Strumpf, E. (2004) 'The Obesity Epidemic in the United States: Causes and Extent, Risks and Solutions', *Issue Brief (The Commonwealth Fund)*, 713, pp. 1–6.

Sun, X. J. *et al.* (1991) 'Structure of the insulin receptor substrate IRS-1 defines a unique signal transduction protein', *Nature*, 352(6330), pp. 73–77.

Sun, X. J. *et al.* (1995) 'Role of IRS-2 in insulin and cytokine signalling', *Nature*, 377(6545), pp. 173–177.

Sun, X. J. *et al.* (1997) 'The IRS-2 Gene on Murine Chromosome 8 Encodes a Unique Signaling Adapter for Insulin and Cytokine Action', *Molecular Endocrinology*. Oxford University Press, 11(2), pp. 251–262.

Symonowicz, M. and Kolanek, M. (2012) 'Biotechnology and Food Sciences Flavonoids and their properties to form chelate complexes', *Biotechnology Food Science*, 76(1), pp. 35–41.

Tanaka, S. *et al.* (1994) 'C3G, a guanine nucleotide-releasing protein expressed ubiquitously, binds to the Src homology 3 domains of CRK and GRB2/ASH proteins.', *Proceedings of the National Academy of Sciences of the United States of America*. National Academy of Sciences, 91(8), pp. 3443–3447.

Taniguchi, C., Emanuelli, B. and Kahn, C. (2006) 'Critical nodes in signalling pathways: insights into insulin action.', *Nature Reviews: Molecular Cell Biology*, 7, pp. 85–96.

Tarazi, R. C., Bravo, E. L. and Fouad, F. M. (1981) 'Late Resistance to Captopril', in *Frontiers in Hypertension Research*. Springer New York, pp. 522–526.

Tarbell, J. M. and Pahakis, M. Y. (2006) 'Mechanotransduction and the glycocalyx', *Journal of Internal Medicine*, 259(4), pp. 339–350.

Taubert, D., Roesen, R. and Schömig, E. (2007) 'Effect of Cocoa and Tea Intake on Blood Pressure', *Archives of Internal Medicine*, 167(7), p. 626.

Taylor, G. (2017) *Can Herbal Tea Dehydrate You? | LIVESTRONG.COM*. Available at: https://www.livestrong.com/article/542050-can-herbal-tea-dehydrate-you/.

Test-it Urinalysis (2010) *Test-it™ URINALYSIS*. Available at: https://www.viaglobalhealth.com/wp-content/uploads/2016/04/Test-it-Urine-Instructions-21-10-10-v1.

Thom, S. (1997) 'Arterial structural modifications in hypertension: Effects of treatment', *European Heart Journal*, 18(Suppl E), pp. E2–E4.

Thoonen, R. *et al.* (2015) 'Cardiovascular and pharmacological implications of haem-deficient NO-unresponsive soluble guanylate cyclase knock-in mice', *Nature Communications*. Nature Publishing Group, 6(1), p. 8482.

Thorogood, M. *et al.* (2007) 'A cross-sectional study of vascular risk factors in a rural South African population: data from the Southern African Stroke Prevention Initiative (SASPI)', *BMC Public Health*, 7(1), p. 326.

Toda, N. and Okamura, T. (2013) 'Obesity impairs vasodilatation and blood flow increase mediated by endothelial nitric oxide: An overview', *The Journal of Clinical Pharmacology*. Wiley-Blackwell, 53(12), pp. 1228–1239.

Torday, J. S. (2015) 'Homeostasis as the Mechanism of Evolution', *Biology*. Multidisciplinary Digital Publishing Institute, 4(3), pp. 573–590.

Tsuruzoe, K. *et al.* (2001) 'Insulin Receptor Substrate 3 (IRS-3) and IRS-4 Impair IRS-1- and IRS-2-Mediated Signaling', *Molecular and Cellular Biology*, 21(1), pp. 26–38.

Uchida, T., Myers, M. G. and White, M. F. (2000) 'IRS-4 mediates protein kinase B signaling during insulin stimulation without promoting antiapoptosis.', *Molecular and cellular biology*. American Society for Microbiology, 20(1), pp. 126–138.

Ulicná, O. *et al.* (2006) 'Rooibos tea (Aspalathus linearis) partially prevents oxidative stress in streptozotocin-induced diabetic rats.', *Physiological Research*, 55(2), pp. 157–164.

Valentijn, K. M. *et al.* (2011) 'Functional architecture of Weibel-Palade bodies.', *Blood*. American Society of Hematology, 117(19), pp. 5033–5043.

Valko, M. *et al.* (2006) 'Free radicals, metals and antioxidants in oxidative stress-induced cancer', *Chemico-Biological Interactions*, 160(1), pp. 1–40.

van der Heide, L. P., Ramakers, G. M. J. and Smidt, M. P. (2006) 'Insulin signaling in the central nervous system: Learning to survive', *Progress in Neurobiology*, 79(4), pp. 205–221.

Van Der Merwe, J. D. *et al.* (2015) 'Short-term and sub-chronic dietary exposure to aspalathin-enriched green rooibos (Aspalathus linearis) extract affects rat liver function and antioxidant status', *Molecules*, 20(12), pp. 22674–22690.

van Esch, J. H. M. *et al.* (2005) 'Selective Angiotensin-Converting Enzyme C-Domain Inhibition Is Sufficient to Prevent Angiotensin I-Induced Vasoconstriction', *Hypertension*, 45(1), pp. 120–125.

van Niekerk, C. and Viljoen, A. (2008) 'Indigenous South African medicinal plants part 11 : Aspalathus linearis ('Rooibos') : medicinal plants', *SA Pharmaceutical Journal*. MIMS, 75(10), pp. 41–42.

van Wyk, B.-E. and Verdoorn, G. H. (1989) 'Alkaloids of the genera Aspalathus, Rafnia and Wiborgia (Fabaceae-Crotalarieae)', *South African Journal of Botany*. Elsevier, 55(5), pp. 520–522.

Vanhaesebroeck, B. and Alessi, D. R. (2000) 'The PI3K-PDK1 connection: more than just a road to PKB.', *The Biochemical Journal*, 346(Pt 3), pp. 561–576.

Vasan, R. S. *et al.* (2002) 'Residual lifetime risk for developing hypertension in middle-aged women and men: The Framingham Heart Study.', *JAMA*, 287(8), pp. 1003–1010.

Vauzour, D. *et al.* (2010) 'Polyphenols and Human Health: Prevention of Disease and Mechanisms of Action', *Nutrients*. Molecular Diversity Preservation International, 2(11), pp. 1106–1131.

Virtue, S. and Vidal-Puig, A. (2010) 'Adipose tissue expandability, lipotoxicity and the Metabolic Syndrome - An allostatic perspective', *Biochimica et Biophysica Acta (BBA) - Molecular and Cell Biology of Lipids*, 1801(3), pp. 338–349.

von Willebrand, M. *et al.* (1998) 'Modification of phosphatidylinositol 3-kinase SH2 domain binding properties by Abl- or Lck-mediated tyrosine phosphorylation at Tyr-688.', *The Journal of Biological Chemistry*, 273(7), pp. 3994–4000.

Wada, A. *et al.* (2005) 'New Twist on Neuronal Insulin Receptor Signaling in Health, Disease, and Therapeutics', *Journal of Pharmacological*, 99, pp. 128–143.

Walch, L., Brink, C. and Norel, X. (2000) 'The muscarinic receptor subtypes in human blood vessels.', *Therapie*, 56(3), pp. 223–226.

Wallerath, T. *et al.* (2002) 'Resveratrol, a polyphenolic phytoalexin present in red wine, enhances expression and activity of endothelial nitric oxide synthase.', *Circulation*, 106(13), pp. 1652–1658.

Wan, Y. *et al.* (2001) 'Effects of cocoa powder and dark chocolate on LDL oxidative susceptibility and prostaglandin concentrations in humans', *The American Journal of Clinical Nutrition*, 74(5), pp. 596–602.

Wang-Polagruto, J. F. *et al.* (2006) 'Chronic consumption of flavanol-rich cocoa improves endothelial function and decreases vascular cell adhesion molecule in hypercholesterolemic postmenopausal women.', *Journal of Cardiovascular Pharmacology*, 47(Suppl 2), pp. S177-S186; S206-S209.

Wang, Z. *et al.* (2010) 'Estimation of the normal range of blood glucose in rats.', *Journal of Hygiene Research*, 39(2), pp. 133–137, 142.

Warner, F. J. *et al.* (2005) 'Angiotensin-converting Enzyme 2 (ACE2), But Not ACE, Is Preferentially Localized to the Apical Surface of Polarized Kidney Cells', *Journal of Biological Chemistry*, 280(47), pp. 39353–39362.

Weibel, E. R. and Palade, G. E. (1964) 'New Cytoplasmic Components in Arterial Endothelia.', *The Journal of Cell Biology*. Rockefeller University Press, 23(1), pp. 101–112.

Weiss, M., Steiner, D. F. and Philipson, L. H. (2000) *Insulin Biosynthesis, Secretion, Structure, and Structure-Activity Relationships*, *Endotext*.

Whaley, J. M. *et al.* (2012) 'Targeting the kidney and glucose excretion with dapagliflozin: preclinical and clinical evidence for SGLT2 inhibition as a new option for treatment of type 2 diabetes mellitus.', *Diabetes, Metabolic syndrome and Obesity : Targets and Therapy*, 5, pp. 135–148.

Whelton, P. K. *et al.* (2018) '2017 ACC/AHA/AAPA/ABC/ACPM/AGS/APhA/ASH/ASPC/NMA/PCNA Guideline for the Prevention, Detection, Evaluation, and Management of High Blood Pressure in Adults: A Report of the American College of Cardiology/American Heart Association Task Force on Clinical Practice Guidelines', *Hypertension*, 71(6), pp. e13–e115.

White, M. F. (1997) 'The insulin signalling system and the IRS proteins.', *Diabetologia*, 40(Suppl 2), pp. S2–S17.

WHO :: Global Database on Body Mass Index (2018). Available at: http://apps.who.int/bmi/index.jsp?introPage=intro_3.html.

'WHO | Obesity and overweight' (2018) *WHO*. World Health Organization. Available at: http://www.who.int/mediacentre/factsheets/fs311/en/.

WHO | World Health Organization (2015). Available at: http://gamapserver.who.int/gho/interactive_charts/ncd/risk_factors/blood_pressure_prevalence/atlas.html.

Widlansky, M. E. *et al.* (2007) 'Acute EGCG supplementation reverses endothelial dysfunction in patients with coronary artery disease.', *Journal of the American College of Nutrition*, 26(2), pp. 95–102.

Wilcox, G. (2005) 'Insulin and insulin resistance.', *The Clinical Biochemist. Reviews*. The Australian Association of Clinical Biochemists, 26(2), pp. 19–39.

Withers, D. J. and White, M. (2000) 'Perspective: The Insulin Signaling System-A Common Link in the Pathogenesis of Type 2 Diabetes', *Endocrinology*. Oxford University Press, 141(6), pp. 1917–1921.

Wolever, T. M. (1990) 'The glycemic index.', *World Review of Nutrition and Dietetics*, 62, pp. 120–185.

Wong, M. K. S. (2016) 'Renin', in *Handbook of Hormones*. Elsevier, pp. 255–258.

Wong, S. L. *et al.* (2009) 'Cyclooxygenase-2-derived prostaglandin F2alpha mediates endothelium-dependent contractions in the aortae of hamsters with increased impact during aging.', *Circulation Research*. American Heart Association, Inc., 104(2), pp. 228–235.

World Health Organization (2015) *WHO | Questions & Answers on hypertension*, *World Health Organization*. World Health Organization. Available at: http://www.who.int/features/qa/82/en/.

World Health Organization (2017) *Cardiovascular diseases (CVDs)*. Available at: http://www.who.int/news-room/fact-sheets/detail/cardiovascular-diseases-(cvds).

Wright, E. M., Loo, D. D. F. and Hirayama, B. A. (2011) 'Biology of Human Sodium Glucose Transporters', *Physiological Reviews*, 91(2), pp. 733–794.

Wymann, M. P. and Pirola, L. (1998) 'Structure and function of phosphoinositide 3-kinases.', *Biochimica et biophysica acta*, 1436(1–2), pp. 127–50.

Xavier, F. E. *et al.* (2003) 'Time-dependent hyperreactivity to phenylephrine in aorta from untreated diabetic rats: role of prostanoids and calcium mobilization', *Vascular Pharmacology*, 40, pp. 67–76.

Xiao, B. *et al.* (2011) 'Structure of mammalian AMPK and its regulation by ADP.', *Nature*. Europe PMC Funders, 472(7342), pp. 230–233.

Xu, L. *et al.* (2017) 'SGLT2 Inhibition by Empagliflozin Promotes Fat Utilization and Browning and Attenuates Inflammation and Insulin Resistance by Polarizing M2 Macrophages in Diet-induced Obese Mice', *EBioMedicine*. Elsevier, 20, pp. 137–149.

Xu, P., Jacobs, A. R. and Taylor, S. I. (1999) 'Interaction of insulin receptor substrate 3 with insulin receptor, insulin receptor-related receptor, insulin-like growth factor-1 receptor, and downstream signaling proteins.', *The Journal of Biological Chemistry*, 274(21), pp. 15262–15270.

Xu, Q. and Si, L.-Y. (2010) 'Protective effects of AMP-activated protein kinase in the cardiovascular system.', *Journal of Cellular and Molecular Medicine*. Wiley-Blackwell, 14(11), pp. 2604–2613.

Yamauchi, T. *et al.* (2001) 'The fat-derived hormone adiponectin reverses insulin resistance associated with both lipoatrophy and obesity', *Nature Medicine*, 7(8), pp. 941–946.

Yamauchi, T. *et al.* (2002) 'Adiponectin stimulates glucose utilization and fatty-acid oxidation by activating AMP-activated protein kinase', *Nature Medicine*, 8(11), pp. 1288–1295.

Yanagisawa, M. *et al.* (1988) 'A novel potent vasoconstrictor peptide produced by vascular endothelial cells', *Nature*, 332(6163), pp. 411–415.

Yanagita, T. *et al.* (2013) 'Neuronal Insulin Receptor Signaling: A Potential Target for the Treatment of Cognitive and Mood Disorders', *In Tech*, 11, pp. 264–287.

Yiannikouris, F. *et al.* (2012) 'Adipocyte-specific deficiency of angiotensinogen decreases plasma angiotensinogen concentration and systolic blood pressure in mice', *American Journal of Physiology-Regulatory, Integrative and Comparative Physiology*, 302(2), pp. R244–R251.

Yochum, L. *et al.* (1999) 'Dietary flavonoid intake and risk of cardiovascular disease in postmenopausal women.', *American Journal of Epidemiology*, 149(10), pp. 943–949.

Young, I. S. and Woodside, J. V (2001) 'Antioxidants in health and disease.', *Journal of Clinical Pathology*, 54(3), pp. 176–186.

Yuan, X. *et al.* (2017) 'Rutin ameliorates obesity through brown fat activation', *The FASEB Journal*, 31(1), pp. 333–345.

Yvan-Charvet, L. and Quignard-Boulangé, A. (2011) 'Role of adipose tissue renin–angiotensin system in metabolic and inflammatory diseases associated with obesity', *Kidney International*, 79(2), pp. 162–168.

Zeiher, A. M. *et al.* (1995) 'Nitric oxide modulates the expression of monocyte chemoattractant protein 1 in cultured human endothelial cells.', *Circulation Research*, 76(6), pp. 980–986.

Zhao, Y., Vanhoutte, P. M. and Leung, S. W. S. (2015) 'Vascular nitric oxide: Beyond eNOS', *Journal of Pharmacological Sciences*. Elsevier, 56(129), pp. 83–94.

Zhong, H. and Minneman, K. (1999) 'Alpha1-adrenoceptor subtypes.', *European Journal of Pharmacology*, 375, pp. 261–276.

Zhou, L. *et al.* (1999) 'Action of Insulin Receptor Substrate-3 (IRS-3) and IRS-4 to Stimulate Translocation of GLUT4 in Rat Adipose Cells', *Molecular Endocrinology*, 13(3), pp. 505–514.

Zhou, X. and He, P. (2011) 'Improved measurements of intracellular nitric oxide in intact microvessels using 4,5-diaminofluorescein diacetate.', *American Journal of Physiology. Heart and Circulatory Physiology*. American Physiological Society, 301(1), pp. H108–H114.

Zou, M. H. *et al.* (2004) 'Activation of the AMP-activated Protein Kinase by the Anti-diabetic Drug Metformin in Vivo', *Journal of Biological Chemistry*, 279(42), pp. 43940–43951.